

UNIVERSITÀ DELLA CALABRIA



UNIVERSITA' DELLA CALABRIA

Dipartimento di Ingegneria Informatica, Modellistica, Elettronica e Sistemistica

Dottorato di Ricerca in
Scienza Della Vita

CICLO
XXXII

TITOLO TESI

Renewable Energy Driven low cost membrane for water purification and Reclamation

Settore Scientifico Disciplinare ING –IND/24

Coordinatore: Ch.mo Prof. Maria Carmela Cerra

Firma _____

Supervisore/Tutor: Ch.mo Prof. Vincenza Calabro

Firma _____

Dottorando: Dott./ssa DEBOLINA MUKHERJEE

Firma _____

UNIVERSITÀ DELLA CALABRIA



UNIVERSITA' DELLA CALABRIA

Dipartimento di Ingegneria Informatica, Modellistica, Elettronica e Sistemistica

Dottorato di Ricerca in
Scienza Della Vita

CICLO

XXXII

TITOLO TESI

Renewable Energy Driven low cost membrane for water purification and Reclamation

Settore Scientifico Disciplinare ING –IND/24

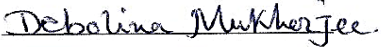
Coordinatore: Ch.mo Prof. Maria Carmela Cerra

Firma 

Supervisore/Tutor: Ch.mo Prof. Vincenza Calabro

Firma 

Dottorando: Dott./ssa DEBOLINA MUKHERJEE

Firma 

INDEX

Acknowledgement	iv
Abstract	vi
Acronyms and Abbreviations	viii

Part 1

Background

Chapter 1

Introduction	1
1.1 Thesis Objectives	1
1.2 Thesis Structure	2

Chapter 2

Membrane Technology, low cost materials and Application	6
Introduction to Membrane Technology	6
2.1 Membrane and its function	6
2.2 Different membrane processes	7
2.3 The membrane transport mechanisms	9
2.4 Materials and structures of synthetic membranes	10
2.5 Symmetric and asymmetric membranes	11
2.6 Porous Membranes	12
2.7 Homogeneous dense membranes	15
2.8 Membrane Types and Configurations Membrane	15
2.9 Membrane Process Challenges	16
2.10 Low-Cost Ceramic Membranes	17
2.11 Materials	17
2.12 Natural Materials	18
2.13 Other Clays	22
2.14 Membrane Applications	25
2.14.1 Application in Food Industry	26
2.14.2 Application in Chemical and Biochemical Industry	28
2.14.3 Other Applications	29
Summery	
Rereferces	30

Chapter 3		
	Wastewater sources and renewable energy driven membrane separation	37
	3.0 Wastewater	37
	3.1 Heavy metals and inorganic species	41
	3.2 Parameters of wastewater significance in membrane	42
	3.3 Conventional water treatment	45
	3.4 Membrane Based water treatment	47
	3.5 Renewable energy driven water treatment	47
	3.6 Role of Membrane Technology in Sustainable Water Generation	48
	3.7 Other Membrane Processes	50
	3.8 Hybrid Membranes Process	51
	References	53
Chapter 4	Published Manuscript	57
Chapter 5	Published Manuscript	83
Chapter 6	Published Manuscript	140
Chapter 7		
	Membrane Fabrication and Experimental set up	
	7.0 Membrane fabrication plan	143
	7.1 Materials	144
	7.2 Membrane Fabrication	147
	7.2.1 Ceramic membrane fabrication (Phase I)	147
	7.2.2 Ceramic membranes fabrication (Phase II)	148
	7.2.3 Ceramic membrane fabrication (Phase III)	153
	7.3 Characterization	154
	7.3.1 Membrane (Phase I)	154
	7.3.2 Membrane (Phase II)	155
	7.3.3 Membrane (Phase III)	156
	7.4 Operating Procedure and set up	157
	7.5 Permeate product characterization	162
	References	163
Chapter 8		
	Results and discussions	165

8.1	Membrane Characterizations	165
Phase I		
8.1.1	SEM Analysis	165
8.1.2	XRD analysis	166
8.1.3	Mean pore size analysis	168
8.1.4	mechanical strength	168
8.1.5	TGA	169
8.2	Effect of Organic Solvent on Partition Coefficient	169
8.3	Effect of Amine Extractant on the Removal of Acetic Acid	170
8.4	Removal of Acetic Acid with Temperature	172
8.5	Calculation of the Overall Mass-Transfer Coefficient	174
Phase II		
8.6	Characterization of Active Carbon	176
8.7	Geopolymers Characterization	180
8.8	Dead end membrane separation of MB	186
8.9	Photodegradation studies	187
8.10	Kinetic Study	188
Phase III		
8.11	Membrane synthesis and characterization	194
8.11.1	Morphology and pore size distribution	195
8.11.2	Permeability tests	199
8.11.3	Characterization of wastewater	200
8.11.4	Ultrafiltration tests	200

Part II

Concluding remarks and future directions

Chapter 9

Concluding remarks and future Directions	204
Appendix	206
Other Publication	206

This thesis is dedicated to my family

*Without all of yours support, encouragement
and inspiration it would never have been accomplished.*

Acknowledgement

First of all, I would like to thank Department of DIMES, University of Calabria, for the opportunity of making the research that is the core of this thesis. I am grateful to my advisor Prof. Vincenza Calabro for continuously inspiring me to approach new problems, overcome challenges and for allowing me the freedom to pursue the independent research. Words are very poor to express my gratefulness. Your presence consists of an example to me.

It was Prof. Calabro's unwavering support and faith in my work that helped me to successfully complete my research and made this challenging journey a smooth and memorable one. Prof. Calabro have served as a true mentor – as much in my academic activities, as in the non-academic ones.

A special thanks to Prof. Stefano Curcio for her support during my time at UNICAL. I am so grateful to him for his advices, understanding and behaviors to me during the difficult and sometime unfortunate days of my life here in Italy. He made me complete this thesis. I also would like to thanks Prof, Jaya Sikder from NIT Durgapur for hosting me during my first phase of mobility and Prof. Raja Ben Amar from University of Sfax during the last phase.

I extend sincere thanks to Prof. Maria Carmela Cerra for her coordinations, suggestions and valuable advice before and during my doctoral work. I especially want to thank the current and former lab members like Ralf, Maria, Gerardo, Catia, Francesco for their company and helping hands all the time. I am sorry if I missed someone.

At UNICAL I was fortunate to meet many people from different cultural background and from different parts of the world. Thanks to all of you. I learned to appreciate my fellow Europeans, their habits and their food, and learned more about the Italians in the many trips to, what are considered to be, Italian tourist attractions.

I would like to express my deep thanks to many people that made possible the realization of this work. I am particularly thankful to Dr. Sebastiano Candamano for his continuous and altruistic technical support all these years.

My deep and sincere thanks go to the people that always supported me all these years: Many thanks go to all my friends in India, Germany, Greece, Tunisia, Spain, Norway, US and off course Cosenza for reminding me there is life out of work.

Finally, I would like to thank those without whom I would never be able to accomplish anything. My parents, brothers and sisters, in laws, Sudip and off course my two naughty boys Soubhit (Enrico) and Sourish (Stefano) you've been through many sacrifices and you've sustained many things in order to support me continuously all these years. Words cannot express your contribution neither I can describe your patience and dedication. Thank you very much for standing by me all this time.

For anyone maybe not mentioned, it was not intended. My thanks go to everyone I met last three years. Finally Grazie dio , my god.

Abstract

Industrial wastewater is the aqueous discard that results from substances having been dissolved or suspended in water, typically during the use of water in an industrial manufacturing process or the cleaning activities that take place along with that process. The wastewater treatment describes the processes used for treating wastewater that is produced by industries as an undesirable by-product. After treatment, the treated industrial wastewater may be reused or released to a sanitary sewer or to a surface water in the environment. Inorganic effluents are produced from various industries, including textile, electroplating, paints and stainless steel manufacturing which leads to alarming the concern to the environmental issues. These inorganic micro-pollutants are generally toxic and non-biodegradable in the environment. The majority of the inorganic micro-pollutants consist of metal ion carrying charge and this fact can be used to separate them using membranes with comparatively bigger pore size and having charge on their surface. In fact, the development of nanofiltration membranes has improved the economy of the process because they perform comparable separation at much lower pressure as compared to the reverse osmosis membranes. Therefore, the necessity of obtaining higher performance with lower cost lead to development of charged membranes for ultrafiltration to separate metal ions from industrial effluents. These membranes are gaining popularity in wastewater treatment due to their capability for electrostatic interactions between a charged membrane and metal ions, even when wide pore membranes are used.

Solar energy is also being use to minimize the cose in some cases. Sunlight may provide heat for evaporative desalination processes, or for some indirect methods, convert to electricity to power a membrane process. Solar derivatives have been studied and in some cases implemented in small and medium scale plants around the world. Production data shows that MSF solar distillation has an output capacity of 6-60 L/m²/day versus the 3-4 L/m²/day standard output of a solar still which is why it is one of the major source of energy to treatment of the wastewater for pure water production. Ceramic membranes have been exploited in different fields. However, in the development of these ceramic membranes, expensive commercial ceramic

supports such as, alumina, titania and zirconia are used, contributing significantly to cost of production of these membranes. Despite this shortcoming, ceramic membranes, employed as UF membranes, have been extensively used for concentrating and purifying macromolecular species in aqueous solutions. Especially, membranes with single or multiple separative layers are made by depositing the active layers on macroporous supports resulting in asymmetric membrane materials with varied pore size.

The present study describes the preparation, characterization and performance evaluation of three different types of ceramic membranes prepared using low cost material as support including utilization of renewable energy for the water treatment and reclamation. These fabricated membranes were employed to treat two effluent discharges from the industry and other possibility will also explored.

ACRONYMS AND ABBREVIATIONS:

AC	Alternating current
AD	Adsorption distillation
AEM	Anion exchange membrane
AFM	Atomic force microscopy
ATR-FTIR	Attenuated total Reflectance Fourier transform Infrared Spectroscopy
BOD	Biological oxygen demand g O ₂ L ⁻¹
CA	Cellulose acetate
CAC	Critical aggregation concentration
CG-MD	Coarse-grained molecular dynamics
CIP	Clean-In-Place
CM	Center of mass
CMC	Critical micelle concentration
COD	Chemical oxygen demand g O ₂ L ⁻¹
CP	Concentration polarization
CSLM	Confocal scanning laser microscopy
CTAB	Hexadecyltrimethylammonium bromide
CEM	Cation exchange membrane
DC	Direct current
DPD	Dissipative Particle Dynamics
EDS	Energy-Dispersive X-ray Spectroscopy
EIS	Electrochemical impedance spectroscopy
ELSD	Evaporative light scattering detector
ESCA	Spectroscopy for chemical analysis
ED	Electrodialysis
EDR	Electrodialysis reversal
FO	Forward osmosis
FH	Flory-Huggins
HPLC	High performance liquid chromatography
IR	Infrared Spectroscopy
kWh	Kilowatt hour
L/day	Litres per day
LPH	Litres per hour

mCDI	Membrane capacitive deionization
MD	Membrane distillation
MED	Multiple-effect distillation
mg/L	milligrams per litre
MSF	Multi-stage flash distillation
MD	Molecular dynamics simulation
MEUF	Micellar-enhanced ultrafiltration
MF	Microfiltration
MP	Membrane potential
MSD	Mean square displacement
MWCO	Molecular weight cut-off
NF	Nanofiltration
NP	Polyoxyethylene nonylphenyl ether
NVT	Constant particle number, volume, and temperature
Nm	Nanometre
Ppm	Parts per million
Psi	Pounds per square inch
PV	Photovoltaic
PA	Polyamide
PES	Polyethersulfone
PFOS	Perfluorooctane sulfonate
PVC	Polyvinyl chloride
PVDF	Poly(vinylidene fluoride)
RDF	Radial distribution function
RO	Reverse osmosis
RO	Reverse osmosis
SSD	Solar still distillation
SBE	Backscattered electrons
SDBS	Sodium dodecyl benzene sulfonate
SDS	Sodium dodecyl sulfate
SE	Secondary electrons
SEM	Scanning electron microscope
SHS	Sodium hexyl sulfate,
SNS	Sodium nonyl sulfate,
TDBNC	Tetradecylbenzylammonium chloride

TEM	Transmission electron microscope
TFC	Thin film composite
TMP	Transmembrane pressure bar
TOC	Total organic carbon g O ₂ L ⁻¹ TOF-
TDS	Total dissolved solids
Ti	Titanium
UV	Ultraviolet
UF	Ultrafiltration
VCD	Vapour compression distillation
XPS	X-ray Photoelectron Spectroscopy
ZLD	Zero liquid discharge

Part I
Background

CHAPTER 1

INTRODUCTION

This thesis corresponds to the introduction of this PhD thesis document in which all the work carried out to achieve the planned objectives in detailed. Thereby, the aim of this chapter is to first describe the main objective of this PhD thesis in section 1.1. Then, the thesis structure are presented in Section 1.2. Finally, in section 1.3 a brief outline of the structure of this thesis is presented, which provides a summary of every chapter.

1.1 Thesis Objectives

Keeping the mentioned issues in previous section in mind, the general objectives of this thesis is to find a low cost membrane material for the treatment of industrial wastewater without using conventional energy whereas use of renewable energy. In this regard the complete work is divided into different parts to fulfil. The general objectives are stated below:

- 1) Literature review on membrane and utilization of renewable energy in membrane separation
 - a) Membrane Materials, configuration and application
 - b) Use of Renewable energy in membrane science
 - c) Summary of renewable energy based membrane water treatment
- 2) Synthesize of Kaolin ceramic membrane
 - a) Membrane Characterization
 - b) Treatment of wastewater from explosive manufacturing.
 - c) Optimize the operating conditions
- 3) Synthesize **O**live-based **A**ctivated carbon as **B**iosorbent (OAB) for dye.
 - a) Active carbon characterization

- 4) Synthesize and characterize geopolymer-13X-OAB ceramic composite.
 - a) Optimize the appropriate amount of OAB additive
 - b) Perform routine characterization to the composite
 - c) Apply the as-synthesized 13X-OAB for cationic dye adsorption
 - d) Application of artificial solar heat for photodegradation
- 5) Fabricate low cost natural Turkish zeolite membrane
 - a) Perform routine characterization to the composite
 - b) Apply the as-synthesized membrane for dye adsorption

1.2 Thesis Structure

The structure of this thesis is described in this section introducing the different parts and chapters. Thereby, a short description of contents and its related published papers are also provided wherever relevant.

Apart from Chapter 1 , where the introduction, motivation and general objectives of the thesis and in Chapter 2 and where the state of the art on Membrane technologies, New low cost materials and their applications. In Chapter 3 the discussions about different sources of waste water and renewable energy driven membrane based treatment is considered in this thesis. This PhD thesis is divided into two parts related to different mentioned objectives as follows:

Part I entitled ***Contributions*** contains the following chapters

- *Chapter 4 : Renewable energy based desalination*
- *Chapter 5 : Industrial water pollution and membrane treatment*
- *Chapter 6 : Renewable energy used in membrane reactor*
- *Chapter 7 : New membrane fabrication*
- *Chapter 8 : Results and discussions*

Part II entitled ***Conclusion and future research*** contains the following chapter:

Chapter 9 Concluding Remarks and future direction

Chapter 2

This chapter mainly focuses on the state of the study of membrane technology. Different membrane materials, their configuration and characteristic has been discussed. Not only that the separation mechanism and their transport mechanism has also been discussed. Different membrane process and application of different configuration in different industry has also been documented.

Chapter 3

Chapter 3 is based on the renewable energy technology and different types of waste water sources. The contamination of water bodies from different industrial processes has been summarized. The effect of the pollution on marine life as well as their impact on environment has also been summarized. Different parametric study of different types of wastewater has also been documents in this chapter. In this chapter we also discussed the use of renewable energy for different applications. Different type of renewable energy has also been summarized. Membrane and membrane based photocatalytic activities has also been review.

Chapter 4

This chapter based on a book chapter published after rigorous study the state of the art of renewable energy based desalination. Energy is needed to produce fresh water; thus water-energy nexus is a crucial area of interest. when considering the impact of fresh water production on sustainability. So the concept of renewable energy arises and considered in this chapter. A lot of fossil-based energy is consumed for water production worldwide, leading to considerable environmental impacts. As a result, schemes that can produce vast amounts of energy in a sustainable manner and ensure simultaneous production of fresh water are summarized and described in this book chapter.

Chapter 5

In this chapter various source of industries and their pollutants has been discussed. Pollution from the industries are increasing day by day. This resulted in serious pollution problems in the water bodies and caused negative effects to the eco-system and human's life. There are many types of industrial wastewater pollutants based on different industries and each sector produces its own particular combination of pollutants from the processes. The technology for the treatment of industrial wastewater must be designed more specifically for the particular type of pollutants produced. Membrane has made important contributions to the welfare of people with positive quality of life more than the majority of all other disciplines. In this chapter most of the industrial pollutants and their membrane based treatment mechanisms are

described. This chapter is based on another book chapter published as a state of the art study on the said topics.

Chapter 6

Pharmaceutical waste is one of the major threats to our environment that adversely affects the aquatic life with considerable changes in the ecosystem. Pharmaceutical waste is entering the environment with or without any modification of parent compounds after their intake and excretion by living bodies. Pharmaceutical compounds such as antibiotics, steroids and hormones are being disposed in water bodies globally. However, several groups of researchers have proven that different pharmaceutical compounds, mainly antibiotics, can neither be removed during wastewater treatment nor be biodegraded in the environment due to their antibacterial properties. In this chapter 6 we focused on the photocatalytic process and study the efficiency of this process to remove contaminants from waste stream. Assessment of the process efficiency necessitates optimisation of the process conditions has also been discussed in this book chapter.

Chapter 7

Nowadays, the use of organic membranes is more developed but ceramic membranes presents a number of advantages, such as better thermal, chemical and mechanical resistance unfortunately these membranes are too expensive to consider economic applications in depollution control which needs high fluxes and low costs to treat great volumes of wastewater. To overcome this drawback, many researches were devoted to the preparation of new membranes with high permeate flux for the treatment of large volumes of effluent. In this chapter the fabrication of three different ceramic membranes with high flux will be evaluated. In the first phase the membrane prepared in India during my stage will be discussed. Followed by the phase I started my laboratory activity here in Italy at DIMES. We also explored the possibility to use natural adsorbent for the membrane fabrication which can not only improve the mechanical strength but also adsorption capacity of reactive dye. Application of solar radiation as a source of renewable energy was also investigated in this period. In the final phase I again spent few months in Tunisia for the study of low cost ceramic membrane fabrication by clay materials.

Chapter 8

The fabricated membrane in previous chapter has been characterized for further application. SEM, EDX, FTIR, Mechanical strength were done. Not only that the membrane was

then characterises with pure water to measure the flux and permeability. The fabricated membrane was then applied for the treatment of different wastewater. Adsorption of dye was measured and kinetic was studied. Application of artificial solar light was also investigated in this chapter and discussed.

Chapter 9

Concluding remarks and future prospects of this research will be summarized followed by appendix. The appendix will contain another two of my publications which is somehow during my PhD but out of the topic of this thesis.

CHAPTER 2

MEMBRANE TECHNOLOGY, LOW COST MATERIALS AND APPLICATIONS

Introduction to Membrane Technology

In this chapter the basic principles that govern membrane and in principals are reported. First, the discussion will focus on the membrane, its characteristic, morphological structure, etc. Then, membranes fabrication and general aspects of membrane application will be discussed.

2.1 Membrane and its function

A precise and complete definition of a membrane that covers all its aspects is rather difficult, even when the discussion is limited to synthetic structures as in this outline. Various definitions have been reported in the literature, most of them focusing on the selective properties of the membrane. For example, Lonsdale defined a synthetic membrane as an interphase that separates two phases and restricts the transport of various components in a specific manner [Lonsdale 1982]. In new membrane processes, such as membrane contactors, the membrane is a non-selective barrier that separates and contacts the two adjacent phases. Therefore, in the most general sense we can define a membrane as a selective or non-selective barrier that separates and/or contacts two adjacent phases and allows or promotes the exchange of matter, energy, and information between the phases in a specific or non-specific manner. Separation of a mixture in a membrane process is the result of different transport rates of different components through the membrane. The transport rate of a component through a membrane is determined by driving forces such as concentration, pressure, temperature, and electrical potential gradients, and the concentration and mobility of the component in the membrane matrix.

A membrane can be homogeneous or heterogeneous, symmetric or asymmetric in structure. It may be solid or liquid and may consist of organic or inorganic materials. It may be neutral or it may carry positive or negative charges, or functional groups with specific binding or complexing abilities. Its thickness can be less than 100 nm to more than a millimeter. The electrical resistance may vary from more than 1,000,000 ohm cm² to less than one ohm cm². The term "membrane", therefore, includes a great variety of materials and structures, and a membrane can often be better described by its function rather than by its

structure. Some materials, such as protective coatings, or packaging materials, show typical membrane properties, and are in fact membranes. Most materials functioning as membranes have one characteristic property in common: they restrict the passage of different components in a very specific manner. In some cases, a hydrophobic polymeric membrane may allow the passage of water as vapour phase but not as liquid phase, as for example in membrane distillation. In other cases, e.g. membrane contactors, the porous structure of the membrane material functions as a barrier that keeps in contact two adjacent phases between which a mass transfer occurs, and separates them at the same time. In both cases the membrane has no direct effect on the transport of various components and is non-selective. The concept of a selective and non-selective membrane is illustrated in Figure 2.1 which shows in a) a membrane which is highly selective and capable of separating, e.g. two enantiomers and b) a membrane that acts as a barrier between two phases and avoids the mixing of the phases but has no effect on the transport of different components from one phase to the other.

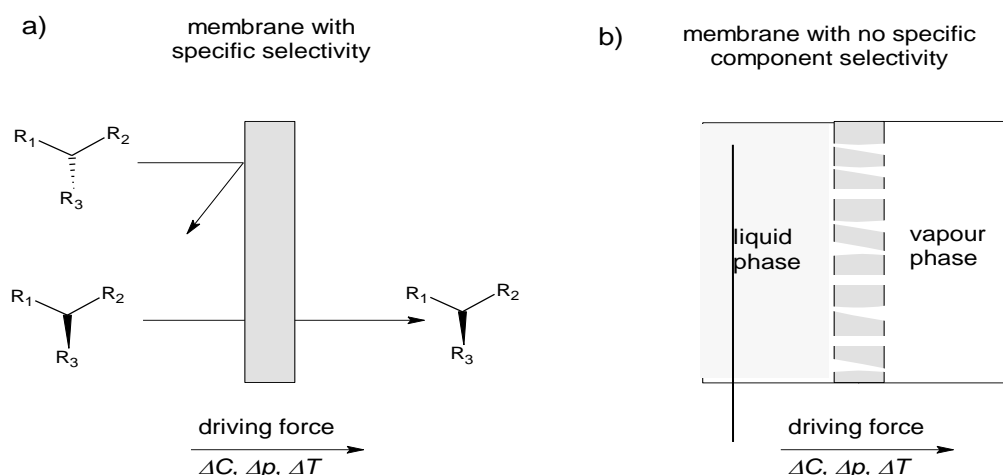


Fig. 2.1. a) Membrane which is selective for the transport of different components such as two enantiomers and b) Membrane which separates a liquid and a vapour phase and allows passage of vapour molecules but is not selective for the transport of different components.

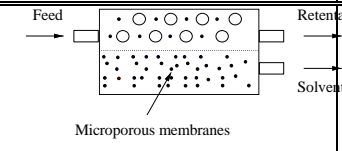
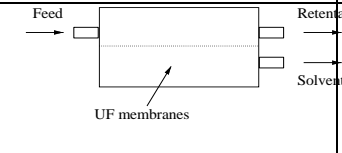
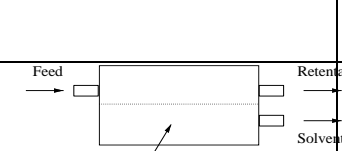
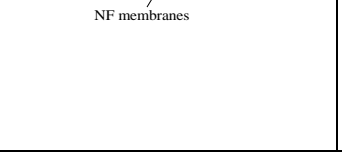
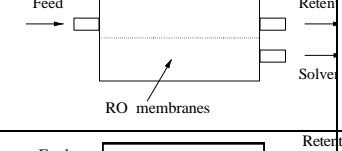
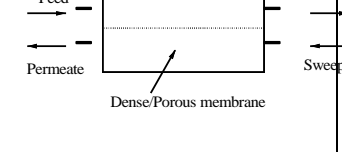
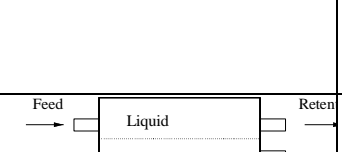
2.2 Different membrane processes

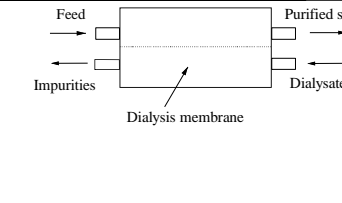
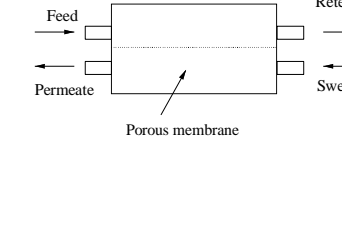
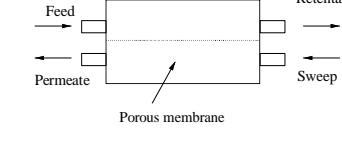
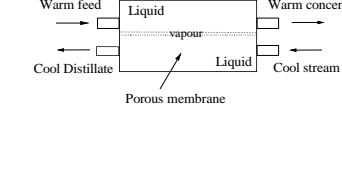
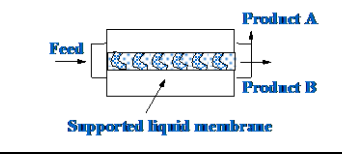
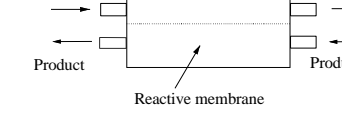
Membrane processes can be grouped according to the applied driving forces into:

- (1) hydrostatic pressure driven processes such as reverse osmosis, nano-, ultra- and microfiltration or gas separation, pervaporation;
- (2) concentration gradient or chemical potential driven processes such as dialysis, Donnan dialysis, pervaporation, and membrane contactors, such as membrane based solvent extraction, membrane scrubbers and strippers, osmotic distillation;
- (3) electrical potential driven processes such as electrodialysis; and
- (4) temperature difference driven membrane processes such as membrane distillation.

The molecular mixture which will be separated is referred to as feed, the mixture containing the components retained by the membrane is called the retentate and the mixture composed of the components that have permeated the membrane is referred to as permeate (or filtrate in micro- and ultrafiltration). Table 2.1. lists the basic properties of membrane operations.

Table 2.1. Basic concepts of different membrane operations

Process	Concept	Driving Force	Mode of transport	Species Passed	Species Retained
Microfiltration (MF)		pressure difference 100 - 500 kPa	size exclusion convection	solvent (water) and dissolved solutes	suspended solids, fine particulars, some colloids
Ultrafiltration (UF)		pressure difference 100 - 800 kPa	size exclusion convection	solvent (water) and Low molecular weight solutes (<1000 Da)	macrosolutes and colloids
Nanofiltration (NF)		pressure difference 0.3 - 3 MPa	size exclusion solution diffusion Donnan exclusion	solvent (water), low molecular weight solutes, monovalent ions	molecular weight compounds > 200 Da multivalent ions
Reverse Osmosis (RO)		pressure difference 1 - 10 MPa	solution diffusion mechanism	solvent (water)	dissolved and suspended solids
Gas Separation (GS)		pressure Difference 0.1 - 10 MPa	solution diffusion mechanism	gas molecules having Low molecular weight or high solubility-diffusivity	gas molecules having high molecular weight or low solubility-diffusivity
Pervaporation (PV)		chemical potential or concentration difference	solution diffusion mechanism	high permeable solute or solvents	less permeable solute or solvents
Electrodialysis (ED)		electrical potential difference 1 - 2 V / cell pair	Donnan exclusion	solutes (ions) Small quantity of solvent	non-ionic and macromolecular species

Dialysis (D)		concentration difference	diffusion	solute (ions and low MW organics) Small solvent quantity	dissolved and suspended solids with MW > 1000 Da
Membrane contactors (MC)		chemical potential, concentration difference; temperature difference	diffusion	compounds soluble in the extraction solvent; volatiles	compounds non soluble in the extraction solvent; Non volatiles
Membrane based solvent extraction (MBSX)		chemical potential or Concentration difference	diffusion partition	compounds soluble in the extraction solvent	compounds non soluble in the extraction solvent
Membrane Distillation (MD)		temperature difference	diffusion	volatiles	non volatiles
Supported liquid membranes (SLM)		concentration difference	diffusion	ions, low MW organics	ions, less permeable organics
Membrane reactors (MR)		various	various	permeable product	non permeable reagents

2.3 The membrane transport mechanisms

The mechanism by which certain components are transported through a membrane can also be very different. In some membranes, for example, the transport is based on viscous flow of a mixture through individual pores in the membrane caused by a hydrostatic pressure difference between the two phases separated by the membrane. This type of transport is referred to as *viscous flow*. The components that permeate through the membrane are transported by convective flow through micropores under a gradient pressure as driving force and the separation occurs because of size exclusion as indicated in Figure 2.2 a). Darcy's Law describes this type of transport. It is the dominant form of mass transport in micro- and ultrafiltration but also occurs in other membrane processes.

If the transport through a membrane is based on the solution and diffusion of individual molecules in the non-porous membrane matrix due to a concentration or chemical potential gradient the transport is referred to as *diffusion*. The separation occurs because of different solubility and diffusivity of components into the membrane material as indicated in Figure 2.2 b). The Fick's Law describes this type of transport. The diffusion of molecules through homogeneous dense membranes occurs through the free volume elements, or empty spaces between polymer chains caused by thermal motion of the polymer molecules, which fluctuate in position and volume on the same time scale as the molecule permeates. The transition between fluctuating free volumes and individual permanent pores is controversial. In general, it is considered in the range of 5-10 Å in diameter.

This form of mass transport is dominant in reverse osmosis, gas separation, pervaporation or dialysis but it may occur in other processes too. If an electrical potential gradient across the membrane is applied to achieve the desired transport of certain components through the membrane the transport is referred to as *migration*. Migration occurs in electro dialysis and related processes and is limited to the transport of components carrying electrical charges such as ions.

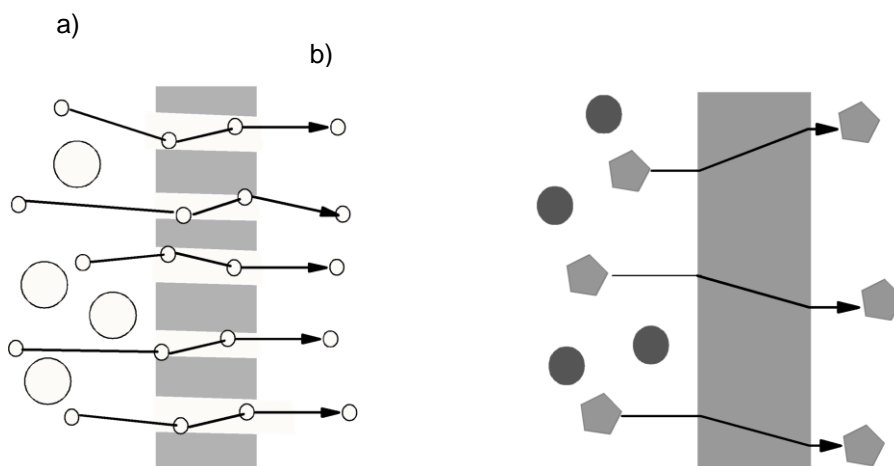


Fig. 2.2. a) The sieving mechanism of a porous membrane and b) The solution diffusion mechanism in a non-porous membrane.

2.4 Materials and structures of synthetic membranes

Synthetic membranes show a large variety in their physical structure and the materials they are made from. Based on their structure they can be classified in four groups:

- porous membranes,
- homogeneous solid membranes,
- solid membranes carrying electrical charges,
- liquid or solid films containing selective carriers.

Furthermore, the structure of membranes may be symmetric, i.e. the structure is identical over the entire cross-section of the membrane or it may be asymmetric, i.e. the structure varies over the cross-section of the membrane.

The materials used for the preparation of membranes can be polymers, ceramics, glass, metals or liquids. The materials may be neutral or carry electrical charges, i.e. fixed ions. The membrane conformation can be flat, tubular or a hollow fiber. The schematic drawing of Figure 2.3 illustrates the morphology, materials and configuration of some technically relevant synthetic membranes.

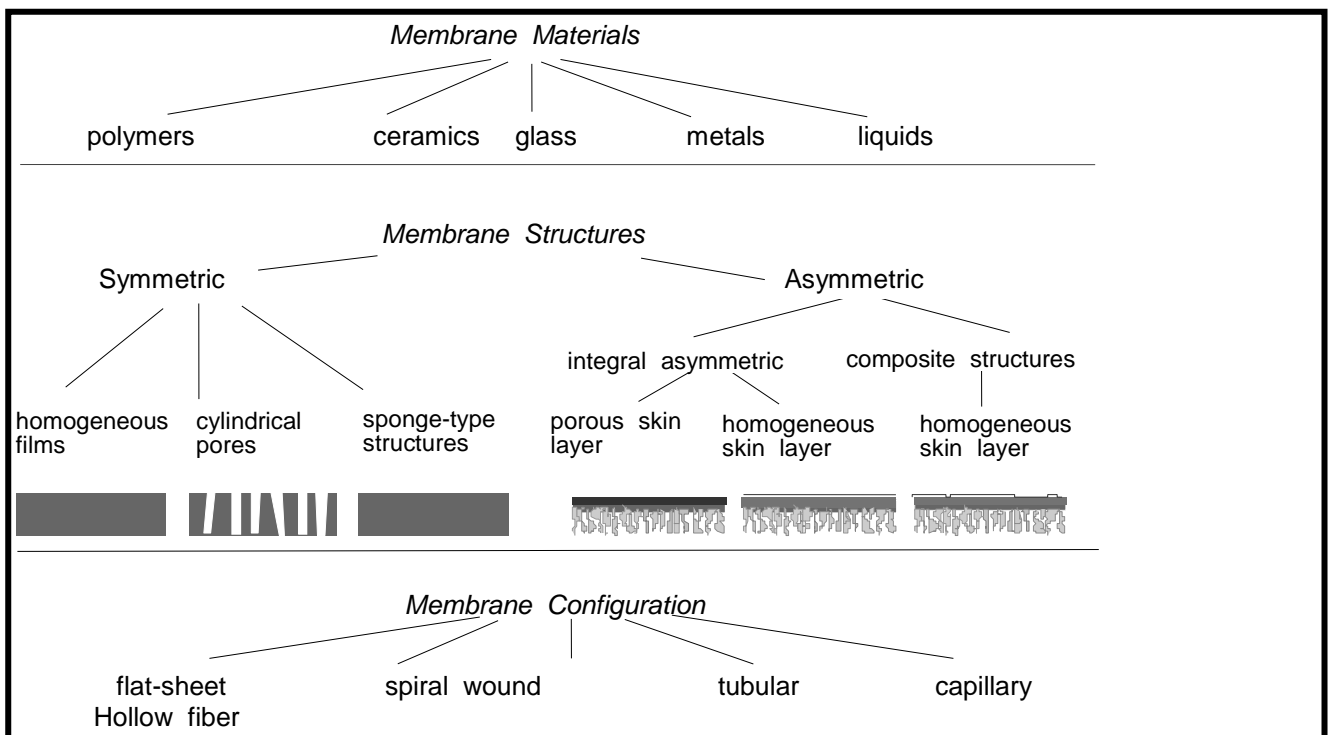


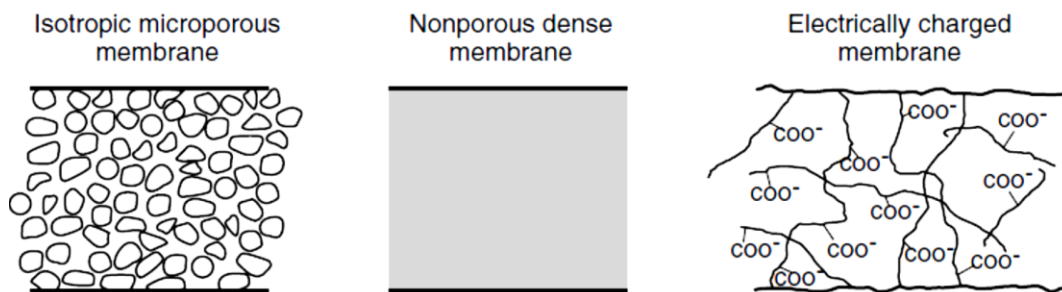
Fig. 2.3 Schematic drawing illustrating the various materials, structures and configuration of technically relevant synthetic membranes.

2.5 Symmetric and asymmetric membranes

As indicated earlier synthetic membranes may have a symmetric or an asymmetric structure. In a symmetric membrane (in Fig 2.4) the structure and the transport properties are identical over the entire cross-section and the thickness of the entire membrane determines the flux. Symmetric membranes are used today mainly in dialysis and electrodialysis. In asymmetric membranes structural as well as transport properties vary over the membrane cross-section. An asymmetric membrane consists of a 0.1 to 1 μm thick "skin" layer on a highly porous 100 to 200 μm thick substructure. The skin represents the actual selective barrier of the asymmetric membrane. Its separation characteristics are determined by the nature of the material or the size of pores in the skin-layer. The mass flux is determined mainly by the "skin" thickness. The

porous sub-layer serves only as a support for the mostly thin and fragile skin and has little effect on the separation characteristics or the mass transfer rate of the membrane. Asymmetric membranes are used primarily in pressure driven membrane processes such as reverse osmosis, ultrafiltration, or gas and vapor separation, since here the unique properties of asymmetric membranes, i.e. high fluxes and good mechanical stability can best be utilized. Two techniques are used to prepare asymmetric membranes: one utilizes the phase inversion process which leads to an integral structure with the skin and the support structure made from the same material in a single process, and the other resembles a composite structure where a thin barrier layer is deposited on a porous substructure in a two step process. In this case barrier and support structures are generally made from different materials.

Symmetrical membranes



Anisotropic membranes

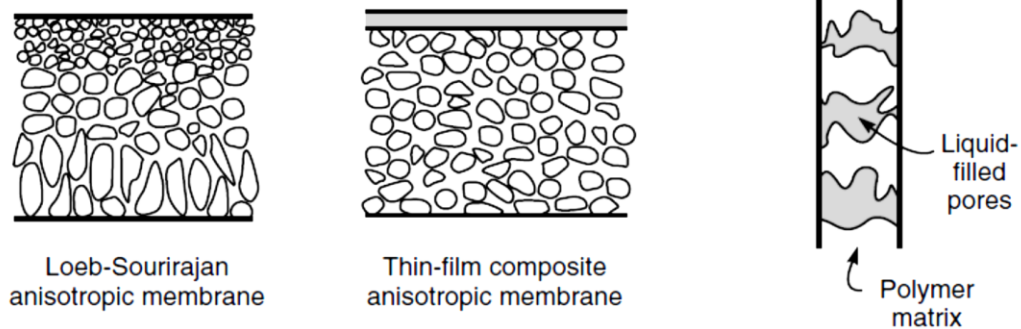


Fig 2.4 : Schematic diagrams of the principal types of membranes

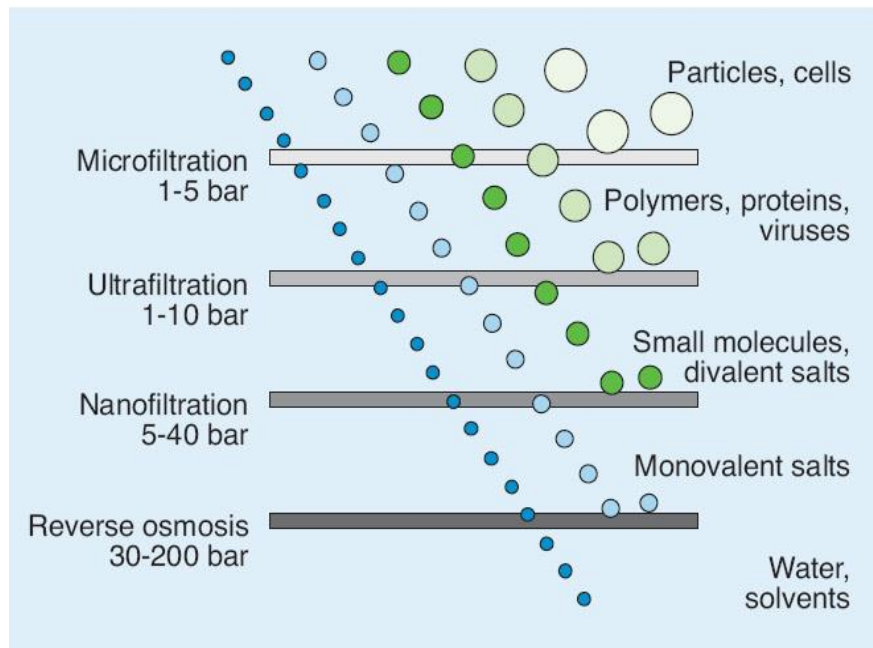
2.6 Porous membranes

A porous structure represents a very simple form of a membrane, which closely resembles the conventional fiber filter as far as the mode of separation is concerned. These membranes consist

of a solid matrix with defined holes or pores which have diameters ranging from less than 1 nm to more than 10 μm . The macromolecular size of the species to be separated plays an important role in determining the pore size of the membrane to be utilized and the related membrane process. Porous membranes with average pore diameters larger than 50 nm are classified as macroporous, and those with average pore diameters in the intermediate range between 2 and 50 nm are classified as mesoporous. Membranes with average pore diameters between 0.1 and 2 nm are classified as microporous. Dense membranes have no individual permanent pores, but the separation occurs through fluctuating free volumes. The schematic representation of such classification is illustrated in Figure 2.5.

Membrane type	non-porous	micro-porous	meso-porous	porous	
Membrane process	reverse osmosis gas separation pervaporation	nanofiltration	ultrafiltration	microfiltration	
Pore or particle size [m]	10^{-10}	10^{-9}	10^{-8}	10^{-7}	10^{-6} 10^{-5} 10^{-4}
Separated components	gases vapours soluble salts	sugars	proteins	viruses	bacteria emulsions colloids

a



b

Fig. 2.5 . Schematic classification of membranes, related processes and separated components

In pressure driven membrane processes the separation of the various components is achieved by a sieving mechanism with the pore diameters and the particle sizes being the determining parameters. In thermally driven membrane processes the separation is based on the principle of phase equilibrium and the non-wet ability of membrane pores is the determining parameter. Porous membranes can be made from various materials such as ceramics, graphite, metal or metal oxides, and various polymers. Their structure may be symmetric, i.e. the pore diameters do not vary over the membrane cross-section, or they can be asymmetric, i.e. the pore diameters increase from one side of the membrane to the other typically by a factor of 10 to 1000. The techniques for the preparation of porous membranes can be rather different and include simple pressing and sintering of polymer or ceramic powders, irradiation and leaching of templates as well as phase inversion and polymer precipitation procedures or sol-gel conversion techniques. Porous membranes are used to separate components that differ markedly in size or molecular weight in processes such as micro- and ultrafiltration or dialysis [Cheryan, 1998].

2.7 Homogeneous dense membranes

A homogeneous membrane is merely a dense film through which a mixture of molecules is transported by a pressure, a concentration, or an electrical potential gradient. The separation of the various components of a mixture is directly related to their transport rates within the membrane phase, which is determined by their diffusivities and concentrations in the membrane matrix. Therefore, homogeneous membranes are referred to as solution-diffusion type membranes [Merten, 1966]. They can be prepared from polymers, metals, metal alloys or, in some cases, ceramics which may also carry positive or negative electrical charges. Since the mass transport in homogeneous membranes is based on diffusion their permeabilities are rather low. Homogeneous membranes are used mainly to separate components which are similar in size but have different chemical nature in processes such as reverse osmosis, gas and vapor separation, and pervaporation [Raymond et al., 1992]. In these processes asymmetric membrane structures are used which consist of a thin homogeneous skin supported by a porous substructure. Some of the well known polymer used to prepare different membranes has been tabled in table 2.2.

Table 2.2 : Polymeric membrane materials (Judd, 2006; Mulder, 1996)

Material	Abbreviation	Applications
Polyvinylidene difluoride	PVDF	MF, UF
Polyethylsulphone	PES	UF, RO
Polyethylene	PE	MF, UF
Polypropylene	PP	MF, UF

2.8 Membrane Types and Configurations

Membranes usually are classified as isotropic or anisotropic. Isotropic membranes show a uniform composition and physical structure in cross-section, while anisotropic membranes are not uniform in cross-section. They generally are formed from differently structured layers and different materials.

Types of membranes in general use include tubular, hollow-fiber, and flat-sheet. These types are applied in different configurations, such as within a frame, like the flat-sheet membranes used in Fluence's Smart Packaged NIROBOX™ solution, or spirally wound, such as those

used in membrane aerated biofilm reactor (MABR) technologies like Fluence's Aspiral™ Smart Packaged wastewater treatment plants.

The ideal properties of water treatment membrane configurations are:

Compactness

Low tangential flow resistance

Uniform velocity distribution without dead regions

High retentate-side turbulence to minimize fouling and help mass transfer

Easy maintenance and cleaning

Low unit cost

Reverse osmosis (RO), in contrast, relies on pressure to force water through a membrane, thus separating water from impurities. A 2018 survey of industry professionals on the effectiveness of water reuse technologies placed RO among the top-ranked. While RO is frequently used for desalination, it also is used for wastewater treatment and water reuse, as well as for removal of trace phosphates, calcium, heavy metals, and other substances.

Microfiltration and Ultrafiltration

In membrane technologies based on blocking particles — including microfiltration and ultrafiltration — pore size is important because it determines the size of the particles and microorganisms that can pass through the barrier. The small-pored membranes used in ultrafiltration block proteins, fatty acids, macromolecules, bacteria, protozoa, viruses, and suspended solids.

2.9 Membrane Process Challenges

The effectiveness of membrane treatment often depends on the condition of the membrane. For example, for reverse osmosis technologies to operate efficiently the membrane must be impeccably maintained or it can be fouled with scale or biofilms, a perennial problem. Fouling can reduce effectiveness and increase energy consumption. Much research is devoted to engineering membranes to resist fouling through specialized coatings or other treatments, such as changing the charge of the membrane material.

In the mid-2010s, researchers in Israel developed an important chemical-free process to prevent membrane fouling in RO desalination. The process prevents membrane fouling,

lowers chemical costs, and makes desalination eco-friendlier. Pre-treatment with a two-stage, granular rapid bio flocculation filter (RBF), a first-stage bioflocculator (BF), and a mixed-media bed filter (MBF), prevents fouling agents from reaching the membrane. This and other improvements to seawater reverse osmosis (SWRO) have made the process much more cost-efficient, which in turn has led to explosive global growth in SWRO and water treatment. But the cost of membrane is always a problem and has to be addressed globally.

2.10 Low-Cost Ceramic Membranes

Over the past few years, the use of low-cost raw materials as ceramic membrane precursors has been attracting increasing attention. Studies have shown that worldwide, more than 2.5 billion people have limited access to clean water, predominantly in regions of lower economic development. Low-cost ceramic membranes have the potential to provide a high volume filtration capacity that would facilitate the provision of clean and reliable water in poorer regions of the world. To address large-scale water treatment challenges, there is a growing interest in the fabrication and application of low-cost ceramic membranes based on naturally occurring raw materials and waste products.

2.11 Materials

A variety of low-cost alternatives to conventional materials like alumina or zirconia have been examined for use in water filtration. Those low-cost materials are either natural minerals (clays, zeolite, quartz, apatite) or waste from industrial production (ash). Based on the literature surveyed in this work, a breakdown of materials studied for the fabrication of low-cost membranes is shown in Figure 2.6.

This figure demonstrates that clays are the most widely studied raw material for such applications, with fly-ash further playing a prominent role in this field. Materials used as low-cost precursors in the fabrication of inorganic filtration membranes are predominantly based on unprocessed sources of alumina and silica. Obtaining high levels of performance while avoiding high processing costs remains a significant challenge in this field. Here we present a survey of the types of raw materials and processes that can be used in the design of water filtration systems and address the challenges that remain in implementing such materials in cost-effective ways.

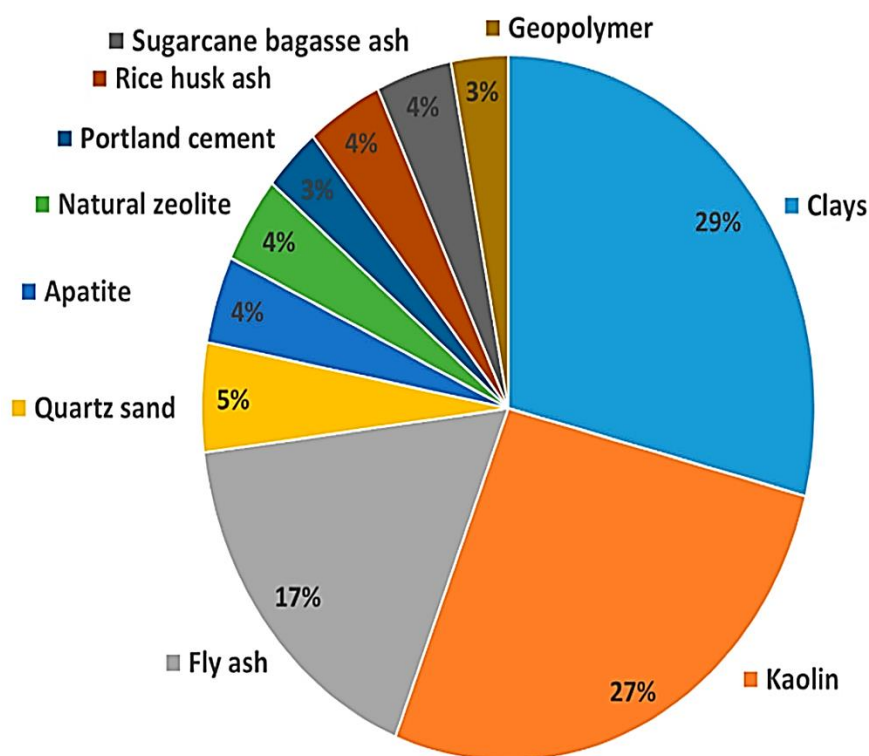


Fig 2.6. Representation of different raw materials in studies of low-cost inorganic filtration membranes (Abdullayev, A 2019)

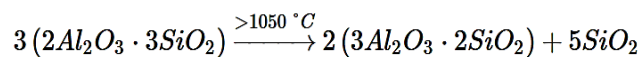
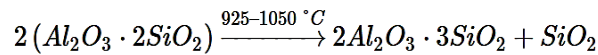
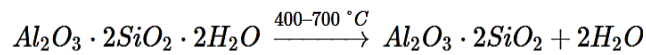
2.12 Natural Minerals

With an emphasis on their implementation in water treatment membranes, here we review the use of widely available low-cost natural minerals composed of silica, alumina, silicates/aluminosilicates, and phosphates. These materials—such as clays, natural zeolites, apatites, quartz sand, and natural pozzolan—are obtained from natural sources and are implemented in membrane fabrication with no further processing steps besides crushing and grinding.

Kaolin

There are numerous clay types on Earth distinguished by different chemical, mechanical, and physical characteristics. Predominant clay minerals include kaolinite, montmorillonite, and illite. Naturally occurring clays have non-identical compositions that depend on localized formation conditions. Clays are widely available across the globe and require only minimal processing for membrane preparation. Hence, there have been significant efforts made towards the preparation of low-cost ceramic membranes using different types of clays. Kaolin, the most widely found clay type, of which kaolinite is the main mineral form, is particularly suitable for membrane fabrication, owing to the pore structures and mechanical properties that can be

achieved following thermal processing. Consequently, kaolin plays a central role in emerging low-cost membrane technology and merits a separate discussion. Kaolin ($\text{Al}_2\text{Si}_2\text{O}_5(\text{OH})_4$) is a type of widely occurring clay that has been studied as the basis of components in inorganic membranes, including support layers, microfiltration (MF) layers, and ultrafiltration (UF) layers. Hubadillah et al. discussed kaolin membranes in detail in their recently published review paper, focused on the fabrication and application of kaolin-based low-cost membranes. In particular, the lower thermal processing temperatures of kaolin, when compared with most conventional oxide ceramics and the morphology of decomposition products, namely spinel and mullite, are of key importance in the development of new membranes. The thermal decomposition of kaolin and the formation of aluminosilicate phases is described in part by the reactions below:



Kaolin membranes have been studied both as composites and single-component systems. Kaolin membranes without any reactive additives presented only mullite ($3\text{Al}_2\text{O}_3 \cdot 2\text{SiO}_2$) and cristobalite (SiO_2) phases following processing at temperatures higher than 1200°C . The use of yet higher temperatures further enhances mechanical strength through the formation of needle-like mullite structures, i.e., mullite whiskers, and densification of membranes. However, it is possible to obtain different phase assemblages by including a various solid-state inorganic component with the propensity to react at high temperatures. For example, if an alumina source, like bauxite or pure alumina, is added, then cristobalite, formed during the metakaolin to spinel and spinel to mullite transformation steps, will react with alumina to yield an increased mullite content. Various processes have used calcium and magnesium sources, such as naturally occurring calcite and limestone (CaCO_3), dolomite (CaMgCO_3) [17], and commercial calcium carbonate [11], to obtain additional phases to mullite, such as anorthite ($\text{CaAl}_2\text{Si}_2\text{O}_8$) and cordierite ($(\text{Mg,Fe})_2\text{Al}_4\text{Si}_5\text{O}_{18}$), which both influence membrane performance and form at relatively low temperatures compared to mullite. Fabrication of membranes for water filtration applications using kaolin with or without additives is summarized in Table 2.3. Earlier research efforts employed significant levels of additives in fabrication processes. Those additives not only take part in phase formation but through gas evolution, can further serve as pore formers. As a few examples, calcium carbonate assists pore formation through CO_2 produced in decomposition,

while quartz increases mechanical and thermal stability, and feldspar acts as a sintering aid, forming a fluxed glassy phase at low temperatures. Additionally, the inclusion of ball clay provides plasticity and strength to the green body in the early processing stages. It should be noted that a large number of constituents often involved in processing results in difficulties to identify the effects of each component on the final properties of the membrane. In more recent research, fewer additives are employed, and the use of kaolin raw materials solely with organic pore formers has emerged as a promising approach.

As a soft clay, the particle size of kaolin clay is sufficiently small for membrane fabrication. Nevertheless, further decreases in particle size can readily be achieved by milling. Most commonly, kaolin particles used in water purification membranes are between 15 μm and 1 μm , with sintering temperatures ranging between 850°C and 1550°C, with most processes using temperatures higher than 1150°C, selected according to composition and desired pore size. Higher temperatures result in improved mechanical strength at the expense of reduced overall porosity. The mechanical strength of kaolin-based membranes is governed by porosity and mineralogy, which are determined by additives and sintering temperature. However, the comparison of the mechanical strength of different membranes fabricated using kaolin, with or without additives, is rendered complex owing to the diversity of mechanical testing methods and sample geometries. It should be noted that, in general, while a three-point bending test is more appropriate for facilitating comparative analysis, mechanical stability tests should be designed according to the membrane shape (configuration). To summarize, kaolin is cheaply available almost all over the world and can be applied in membrane technology as support or filtration layer. Fine powders can be produced from relatively soft kaolin, which is important for obtaining small pore sizes and high mechanical stability.

Table 2.3. Low-cost membranes prepared using kaolin as a main raw material.

Materials Mixed with Kaolin	Shaping Technique	Sintering Temperature, °C	Porosity, %	Pore Size, μm	Flexural Strength, MPa	Application
Quartz, sodium carbonate, calcium carbonate, and boric acid	Paste casting	850–1000	33–42	0.55–0.81	3–8	MF
Quartz, calcium carbonate, sodium carbonate, boric acid, and sodium metasilicate	Pressing	900	35–39	0.72–1.69	7–11	MF of mosambi juice
Quartz, calcium carbonate, sodium carbonate, boric acid, and sodium metasilicate	Pressing	900	30–37	2–3	-	MF of oil-in-water emulsions
Quartz, ball clay, pyrophyllite, and feldspar	Extrusion	950	53	0.31	12	MF of oil in water emulsion
Quartz and calcium carbonate	Pressing	900–1000	30	1.3	34	MF of oil and bacteria
Limestone	Extrusion	800–1100	48	7	30	Support layer
Lime	Extrusion	800–1100	47	8	30–53	Support layer
Feldspar, sodium metasilicate nanohydrate, and boric acid	Pressing	850	29	0.93	8.7	MF
Dolomite	Pressing and Extrusion	1000–1300	37–56	1.6–48	6–15	Support layer
	Extrusion	1100–1300	44.6	4.7	47.6	Support layer
Calcium carbonate	Extrusion	1250	52	4	23	Support layer
	Extrusion	1150–1300	42–50	4–8	67–77	Support layer
Calcite	Extrusion	1150	50	4	28	Support layer
	Pressing and extrusion	1300 and 1100–1250	49	3	87	Support layer
Bentonite, talc, sodium borate, and carbon black	Pressing	1000	34	0.65–1.25	58	MF of oil-in-water emulsion
Bauxite	Pressing	1300–1600	31	0.15–0.8	100 *	MF
Ball clay, quartz, alumina, and calcium carbonate	Paste casting	1100–1400	35–46	0.1–1	20–60	MF
Ball clay, feldspar, calcium carbonate, and pyrophyllite	Pressing	800–1000	44	1.01	28	Support layer
Alumina and aluminum hydroxide	Pressing	1300–1550	46	1.3	-	Support layer
Without reactive additives	Support: extrusion; MF layer: slip casting	Support: 1000–1250; MF layer: 1050	46–60	0.9–1.4	4–24	MF
	Extrusion	1150	49	1.2	5.8	Solid particle removal from water
	Extrusion	1200–1500	-	0.32	221	Arsenic removal and oil removal
	Extrusion	1100–1250	27	0.76	28	MF of cuttlefish effluent
	Extrusion	1200–1500	32–57	0.53–4.25	15–35	MF of oil-in-water emulsion
	Extrusion	1200–1500	-	0.4–0.5	70	MF of wastewater (oil and dye)
	Pressing	1050–1100	43	0.5	20	MF
	Support: pressing; UF: dip coating	Support: 900–1100; UF layer: 850–900	Support 30–41; UF 27	Support 1.4–6.3; UF 0.09	-	UF
Pressing	950	30	0.1	60	MF	

2.13 Other Clays

Further to kaolin, a broad variety of alternative clay types are also of interest towards low-cost filtration membranes. These clays include sepiolite, ball clay, bentonite, and attapulgite. The application of clays in water filtration has a long history. However, earlier studies are related to water filtration by clay media in bed filtration systems rather than as filtration membranes and are therefore beyond the scope of this review.

The chemical composition of clay material according to the origin, particle property (clay composed of powder particles or fibrous clay, like attapulgite), and particle size of clays are diverse and do not follow any trend in membrane fabrication from clays. It is worth mentioning that membranes with pore sizes as small as 3 nm, and flexural strength values up to 69 MPa are successfully achieved by cordierite membrane prepared from sepiolite clay.

Membrane preparation using attapulgite or palygorskite clay is a promising approach. Attapulgite is one of the most important naturally available fibrous clays with many attractive properties, such as a large specific surface area, excellent mechanical strength, high adsorptive capacity along with high chemical and thermal stability. Moreover, membranes can be prepared from attapulgite without the need for high-temperature sintering. Because of their fibrous composition, attapulgite-based membranes have competitive mechanical and filtration properties exhibiting pore sizes of around 12 nm and porosity above 60%, which makes them competitive with conventional membranes in UF applications. Additionally, by adding long-chain polymers, such as polyvinyl alcohol (PVA), it is possible to obtain flexible fibrous membranes, as shown in Figure 2.7.

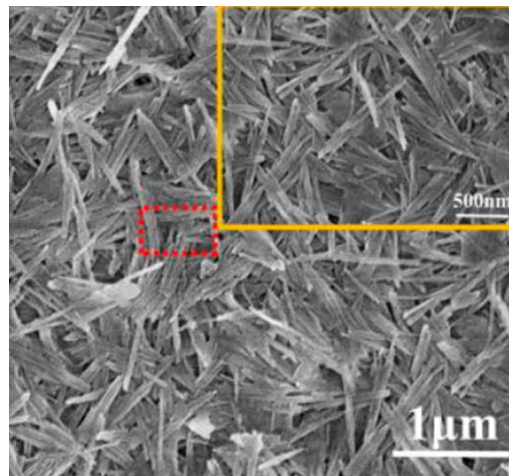


Fig 2.7 : SEM image of the membrane surface. Flexible membranes have been fabricated using fibrous attapulgite clay and sintering-free method

Zeolite Minerals

Naturally occurring zeolite minerals are mainly composed of hydrated aluminosilicates having a nominal composition of $[(\text{SiO}_2)(\text{AlO}_2)_x]\text{M}\cdot y\text{H}_2\text{O}$. These natural materials exhibit a three-

dimensional framework structure with nanoscale porosity. Zeolites occur in many types of rocks but are most common in volcanoclastic sediments, and the largest and purest deposits are altered vitric tuffs. They have a wide range of applications, such as in construction, water treatment, agriculture, catalysis, as well as medical applications. There are many types of synthetic zeolites, which can be obtained by hydrothermal or other applicable methods. However, here we focus only on naturally available zeolite materials, which can be sourced cheaply in large quantities and are thus of more direct relevance towards low-cost water filtration systems. Fabrication of membranes from natural zeolites involves steps of grinding, shaping, and sintering to obtain robust bulk materials of the desired aluminosilicate phases. An early study by Roque-Malherbe et al. used natural zeolite to fabricate porous support layers for membranes. Subsequently, multi-layer ceramic microfiltration membranes were produced using different particle sizes of ground zeolites. Obtained membranes have shown pore sizes between 0.3 μm and 1.1 μm .

Apatite

Apatites, having the nominal form $\text{Ca}_5(\text{PO}_4)_3(\text{F},\text{Cl},\text{OH})$, are naturally occurring materials that have a wide range of applications in biomedical, chemical, pharmaceutical, environmental, and geological fields. As an example, apatite particles can be used to remove divalent heavy or radioactive metals from water by cation exchange process, where Ca^{2+} exchanges with target metal ions, such as lead ion. There have been several studies related to the application of apatite in environmental technology to treat a variety of aqueous wastes and contaminated soils. Apatites are not only able to efficiently adsorb metal contaminants but are also effective in the removal of anionic and cationic dyes by adsorption. Apatite-based membranes are predominantly applied on support layers of other materials, e.g., alumina support layer covered with apatite filtration layer; therefore, mechanical strength is seldom discussed. Only Masmoudi et al. reported the preparation of flat support layers using apatite, with obtained materials exhibiting a flexural strength up to 30 MPa after sintering at a temperature of 1210 °C. This mechanical strength is comparable to other low-cost material-based membranes.

Quartz Sand

Natural quartz sand is a sedimentary rock that consists of crystalline silicon dioxide in the form of quartz (SiO_2). It is highly resistant to both mechanical and chemical weathering. Hence, quartz is among the most abundant and widely distributed minerals found at Earth's surface. Geological processes have occasionally deposited sands that are composed of almost 100% quartz grains. These deposits have been identified and produced as sources of high purity silica sand. These sands are of particular value in the glassmaking industry. Sand has a long history in water purification applications, having been used since 1829 for the production of slow sand filters (SSF), an earlier industrial water treatment process. As the name refers, this water

cleaning method is slow and has many drawbacks, that is why nowadays slow sand filters mainly exist in developing countries. Based on a survey of related literature, it can be concluded that on the basis of naturally and cheaply available quartz sands, it is feasible to prepare support, microfiltration, and ultrafiltration layers for water treatment membranes. However, further detailed research is necessary to fully understand the effect of sintering temperature, particle size, additives on pore structure, and mechanical properties of membranes

Natural Pozzolan

The term pozzolan is used generically to define materials, which have constituents that at ambient temperature combine with lime in the presence of water to form permanently insoluble and stable compounds that behave like cement, and that is why natural occurring pozzolan minerals are mainly used in cement industry. Rather than forming a cement, Achiou et al. sintered pozzolan material at 950 °C, to obtain microfiltration membranes with porosity around 30% and pore size 2–3 μm, which were successfully applied for treating wastewater from textile industries. Results thus far have been promising, motivating the further investigation of pozzolan-based membranes. Nevertheless, in all published work on this topic, a sintering temperature of 950 °C has been used. Nevertheless, in all published work on this topic, a sintering temperature of 950 °C has been used. Phase change behavior with temperature should be investigated to see if more durable and valuable phases occur at higher temperatures or how porosity and pore size distribution change with thermal treatment and densification.

Waste Materials (Ashes)

Utilization of waste materials and by-products from different industries is a key focal point in research towards sustainable materials development. Coal-fired power plants and agricultural industries often produce large volumes of ash as by-products, which pose a significant environmental problem if they are not handled appropriately. However, these so-called waste materials, which include significant silica content, offer various pathways for valorization. Fly ash, rice husk ash, and sugarcane bagasse ash are produced in high volumes worldwide, and they can be used as raw materials for technological applications, including membrane technology.

Fly Ash

Being a by-product of coal combustion, fly ash is among the most abundant waste materials produced and, despite being implemented in various industries, including concrete and paving, its safe disposal remains problematic. The use of fly ash as a raw material in membrane fabrication offers a pathway towards low-cost water treatment solutions. The spherical particle geometries, as shown in Figure 2.8, are lying between 1 and 100 microns in diameter, and the silica-rich

composition of readily available fly-ash is conducive to the fabrication of porous materials containing phases of cordierite, mullite, and anorthite, according to the additives used. The mineralogical composition of membranes prepared from fly ash exhibits tremendous variation, depending not only on the composition of the raw material but also on the sintering temperatures and additives used.

In the absence of additives, the phases formed in fly ash derived membranes are dependent only on sintering Temperature

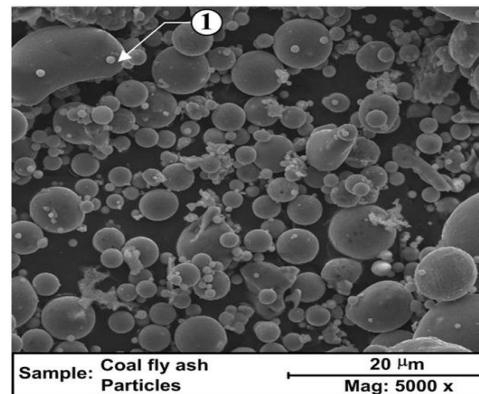


Fig 2.8: SEM image of typical fly ash composed of mainly spherical particles and 1- some irregularly shaped grains(Golewski, G.L. Improvement of fracture toughness of green concrete as a result of addition of coal fly ash. Characterization of fly ash microstructure. Mater. Charact. **2017**, 134, 335–346.)

Cement

Most of the research efforts towards low-cost ceramic membranes have used naturally available minerals in conjunction with high-temperature processing steps, which generally incurs significant energy costs. To further decrease the costs of ceramic membranes, there is interest in developing sintering-free preparation routes.

Sintering aims to give mechanical strength to membrane green bodies through fusion and densification. Ordinary Portland cement and geopolymer cement achieve mechanical strength without sintering. In this thesis, membranes fabricated using geopolymers, a newer kind of cement will be explored. Since this material is very high in resistance and locally available I started to think about using this geopolymers and modifying it to some extent.

2.14 Membrane Applications

Membrane products are well known for producing potable water in municipal plants and seawater desalination. However, what is not appreciated is how much membrane technology is used in industrial applications around the world. Membranes achieve separations without a phase change and the absence of applying heat can be advantageous to some applications. The ability to remove water from a process stream or effluent has shown to be an effective way of concentrating valuable components of an aqueous stream. At times the membrane facility may

not be large compared to a municipal plant but the value to the system and process may be critical for overall economic viability. Sometimes, the water available to an industrial facility may not meet the requirements of the application and membranes can be used to improve the quality so that the process can be run. Or perhaps the discharge from the processes is too great and a reduction step is needed that can be facilitated by membranes. At times, the concentration of the solution may not be desirable and an easy, efficient means of adjusting the concentration may be in order by using membranes. Finally, application of membrane includes are following :

- ✓ Food and Beverage:
 - Bottled Water
 - Beer, wine, and alcoholic beverages
 - Fruit juices and maple syrup
 - Milk and cheese
- ✓ Industrial Processes
 - Clarification of biochemical processes
 - Petroleum refining
 - Paint, adhesive, and solvent recovery
- ✓ High purity applications such as
 - semiconductor,
 - boiler feed and power industry
- ✓ Mining and Metal Processes
 - Plating processes and waste reduction
 - Gold and uranium recovery
 - Recovery of precious metals
- ✓ Landfill leachate reduction

2.14.1 Application in Food Industry

Membrane processes employ a barrier layer that allows water to permeate or pass through it but rejects or retards other components from going along with that filtrate. In the case of microfiltration and ultrafiltration, distinct pores in the polymer allow for water to flow through the barrier but retard/reject the passage of species larger than the pores. Reverse osmosis barrier layers do not have distinct pores but do allow water to diffuse through the barrier layer and reject most of the dissolved ions in the mixture. Since heat is not used to effect the separations, the components in the mixture are less likely to suffer thermal degradation. Membranes are replacing diatomaceous earth filtration (DE), multimedia filtration, centrifugation, extraction, rotary vacuum filters, evaporation and distillation and other unit operations that have been used to make products. Cold sterilization of beverages, pharmaceuticals and milk take advantage of the membrane systems. Most of the membrane products commercially available have a polymeric barrier layer however ceramic membranes with distinct pores have been used in demanding conditions and are finding use in new applications. Ceramic membranes have pore sizes that classify them as microfiltration and ultrafiltration filters. Membrane Applications, The range of applications that currently take advantage of membranes is impressive and continues to grow. Some of these are discussed below:

Food and Beverage Bottled water:

Since the feed water may vary from site to site, the bottled water industry has embraced membrane technology. Some purified bottled water manufacturers want to produce a reproducible product no matter what the feed source and as such they treat the local water to remove almost all of the constituents and then add back a package of ingredients to give a recognizable taste and feel to that particular brand of bottled water. Similarly, bottled water producers utilize membranes for their barrier properties to exclude bacteria and microorganisms. Soft drink manufacturers need safe clean water free of microorganisms and make up water is treated with membranes at a number of soft drink facilities.

Beer production:

During the production of beer, brew masters around the world are particularly specific about the consistency and quality of the water that they use for the manufacture of beer. Membrane facilities are able to take locally available water sources and treat them to acceptable ionic content including hardness and alkalinity for use. In addition, membranes are used for continuous beer stabilization to improve operating efficiency of the brewery and continuous clarification and final filtration of the beer.

Wine:

Membranes have been used for wine clarification and the avoidance of filter aids such as diatomaceous earth (DE) eliminates a disposal issue and loss of wine that would have been associated with the spent aid. Removal of suspended solids, yeast and bacteria and automation of the filtration process reduces losses, improve economics and minimizes labor when producing wine.

Fruit juice:

Fruit juice manufacturers take advantage of membrane technology in a number of ways. Concentration of natural juices can be achieved in which water is removed as permeate and the concentrated juice is left behind. Since no heat is applied there is no degradation of the many complex juice sugars and flavor components. Color can be controlled and even enhanced during the concentration step. Produced juice can be purified and clarified by removal of fine particles from juice which clarifies the mixture and gives it a haze-free property that allows for longer shelf life. Since bacteria and microorganisms are excluded in membrane processes, the juice is less likely to spoil and will remain safe to drink for longer periods of time. Fruit solids can be recovered in some cases and bitterness components removed by appropriate use of membranes.

Removal of limonin and polyphenols has been done in a number of fruit juices including orange, grapefruit, tangerine and many more. Apple juice clarification and concentration as well as removal of biological species that are thermal resistant have been accomplished with membrane systems.

Dairy applications

The dairy industry has embraced membranes for many years. An obvious use is the concentration of milk and whey to reduce shipping costs, produce condensed milk or provide concentrated milk for cheese production. Membranes are being used on sweet/acid whey concentration before evaporation or spray-drying. Removal of bacteria and spores from milk aids shelf life and product stability. Acids and caustic are used to clean the equipment at dairies and membranes are being used to clarify the cleaning solutions by removing suspended and dissolved solids to allow reuse of the solutions. Cheese manufacturing produced whey that was a troublesome by-product however membrane technology has allowed for use of this material via partial demineralization and concentration. Separation of casein from whey products allow for cheese production and whey protein concentration.

2.14.2 Application in Chemical and Biochemical Industry

Enzymes are important to industrial processes and they improve the speed or efficiency of biochemical reactions. Advancements in enzyme production have been facilitated by the use of microfiltration. The cells that generated the enzymes are rejected by the barrier layer of membranes but the enzymes can pass through the pores. Prior methods of centrifugation and filtration were hard on the enzymes and limited productivity.

Separation of sugars such as dextrose and maltose from fibrous and undesirable proteins while purifying the mixture can be done with membranes. Clarification of the process stream after saccharification has been done in different facilities. Gelatin, egg whites, soy protein and other natural products can be improved using microfiltration and ultrafiltration.

Wet corn milling grinds the corn and then membranes have been used for removal of the mud for dextrose clarification, cell and biomass removal, protein, peptide and enzyme recovery, purification of dextrose, and maltose clarification. Methanol removal from organic mixtures has been achieved by taking advantage of the hydrophilic nature and low molecular weight of that alcohol. Extraction of valuable volatiles, dehydration of organic solvents, aroma extraction can be done. Natural essential oils and flavors can be enriched and improved via membrane fractionation and recovery.

Nutraceuticals is a growing market in which nutrition and pharmaceutical are combined. Membranes are being used for the extraction, separation, concentrate and purifications of materials that fill this demand. Animal processing facilities generate significant volumes of blood that traditionally has been a costly waste stream. However, by concentrating the blood plasma, a valuable additive for biochemical processes or pet food can be produced, and a potential cost item becomes a revenue generating product.

Waste stream effluent reduction with membrane systems is wide spread. Pulp and paper mills utilize membrane systems to filter the effluent prior to discharge and minimize the actual amount of liquid that will be discharged from the facility. Production of paint and adhesives may use membranes and in the automotive and appliance industry that use water soluble paints, membranes are being used to recover the paint while improving batch conductivity by removing salts and process metals. Improvements in maintenance of the solids level in the process and reuse of the paint reduce the waste load from the plant and make the overall process economics more favorable. RO for the recycle of rinse water for pre-paint rinse system and recovery of paint solids from treatment waste streams has been used to improve painting economics. Fine chemicals and pharmaceutical production employ membranes for recovery and are used within the processes. Petroleum refining uses membranes for removal of particulates and tar products from the process streams. Biofuels are increasing in production and membranes are used in the process to remove by-products and raw materials from the final product.

There are some applications that demand very high purity or ultrapure water such as semiconductor chip rinsing and processing, high pressure boiler water make-up and assorted power plant needs. Membranes play an important part in producing this very low tds water. In these uses, the presence of a salt ion or impurity could be detrimental to the final product or the equipment in use and membrane technology coupled with other separation processes allow their success.

There is a technique for washing windows that employs highly purified water to accomplish the task rather than use detergents and membranes are used to produce this water in an environmentally friendly way that reduces the organic load in the wash water.

2.14.3 Other Applications

Nano filtration has been used in organic solvents to separate larger molecules from the organic solvent so that it can be reused. Non-thermal solvent recovery, decolorization of solvents, solvent exchange at room temperature, in-situ recovery of organic solvent, monomer removal are all uses that allow reuse and deliver product upgrades. Non-thermal recovery of

solvents and room temperature solvent extraction are accomplished with membranes. Some membranes can be operated in pure solvents or mixtures. They can be used for recovery of antibiotics and peptides, dissolved chemicals, polymeric binders and pigments, dissolved catalyzed and even recycling of hydrocarbons in cleaning processes. Some other applications include:

- Pigments and paints
- Latex suspensions
- Inks and dyes
- Emulsified oils
- Color removal for alcoholic beverages

Summary

Membrane processes have found a great variety of applications in which their use has improved products, recovered valuable components, added stability to the mixture, enhanced the aesthetics of the solutions and contributed to the economics of the processes. Microfiltration, ultrafiltration, reverse osmosis and nanofiltration each offer different separation options for industrial applications that will continue to grow in their use.

References

1. Coping with Water Scarcity: An Action Framework for Agriculture and Food Security; FAO: Rome, Italy, 2012.
2. Goh, P.S.; Ismail, A.F. A review on inorganic membranes for desalination and wastewater treatment. *Desalination* **2018**, 434, 60–80.
3. Mulder, M. *Basic Principles of Membrane Technology*, 2nd ed.; Kluwer Academic: Dordrecht, The Netherland; Boston, MA, USA, 1996.
4. Marchetti, P.; Solomon, M.F.J.; Szekely, G.; Livingston, A.G. Molecular separation with organic solvent nanofiltration: A critical review. *Chem. Rev.* **2014**, 114, 10735–10806.
5. Hofs, B.; Ogier, J.; Vries, D.; Beerendonk, E.F.; Cornelissen, E.R. Comparison of ceramic and polymeric membrane permeability and fouling using surface water. *Sep. Purif. Technol.* **2011**, 79, 365–374.
6. Li, W.; Dong, H.; Yu, H.; Wang, D.; Yu, H. Global characteristics and trends of research on ceramic membranes from 1998 to 2016: Based on bibliometric analysis combined with information visualization analysis. *Ceram. Int.* **2018**, 44, 6926–6934.

7. Wang, Y.H.; Tian, T.F.; Liu, X.Q.; Meng, G.Y. Titania membrane preparation with chemical stability for very harsh environments applications. *J. Membr. Sci.* **2006**, *280*, 261–269.
8. DeFriend, K.A.; Wiesner, M.R.; Barron, A.R. Alumina and aluminate ultrafiltration membranes derived from alumina nanoparticles. *J. Membr. Sci.* **2003**, *224*, 11–28.
9. Yoshino, Y.; Suzuki, T.; Nair, B.; Taguchi, H.; Itoh, N. Development of tubular substrates, silica based membranes and membrane modules for hydrogen separation at high temperature. *J. Membr. Sci.* **2005**, *267*, 8–17.
10. Nandi, B.K.; Uppaluri, R.; Purkait, M.K. Preparation and characterization of low cost ceramic membranes for micro-filtration applications. *Appl. Clay Sci.* **2008**, *42*, 102–110.
11. Vasanth, D.; Pugazhenthii, G.; Uppaluri, R. Fabrication and properties of low cost ceramic microfiltration membranes for separation of oil and bacteria from its solution. *J. Membr. Sci.* **2011**, *379*, 154–163.
12. Monash, P.; Pugazhenthii, G. Development of Ceramic Supports Derived from Low-Cost Raw Materials for Membrane Applications and its Optimization Based on Sintering Temperature. *Int. J. Appl. Ceram. Technol.* **2011**, *8*, 227–238.
13. Hubadillah, S.K.; Othman, M.H.D.; Matsuura, T.; Ismail, A.F.; Rahman, M.A.; Harun, Z.; Jaafar, J.; Nomura, M. Fabrications and applications of low cost ceramic membrane from kaolin: A comprehensive review. *Ceram. Int.* **2018**, *44*, 4538–4560.
14. Monash, P.; Pugazhenthii, G.; Saravanan, P. Various fabrication methods of porous ceramic supports for membrane applications. *Rev. Chem. Eng.* **2013**, *29*, 357–383.
15. Issaoui, M.; Limousy, L. Low-cost ceramic membranes: Synthesis, classifications, and applications. *C. R. Chim.* **2019**, *22*, 175–187.
16. Rhodes, D. *Clay and Glazes for the Potter*; Martino Publishing: Mansfield Centre, CT, USA, 2015.
17. Zhou, J.; Zhang, X.; Wang, Y.; Larbot, A.; Hu, X. Elaboration and characterization of tubular macroporous ceramic support for membranes from kaolin and dolomite. *J. Porous Mater.* **2010**, *17*, 1–9.
18. Harabi, A.; Zenikheri, F.; Boudaira, B.; Bouzerara, F.; Guechi, A.; Foughali, L. A new and economic approach to fabricate resistant porous membrane supports using kaolin and CaCO₃. *J. Eur. Ceram. Soc.* **2014**, *34*, 1329–1340.
19. Boudaira, B.; Harabi, A.; Bouzerara, F.; Zenikheri, F.; Foughali, L.; Guechi, A. Preparation and characterization of membrane supports for microfiltration and ultrafiltration using kaolin (DD2) and CaCO₃. *Desalin. Water Treat.* **2016**, *57*, 5258–5265.
20. Jana, S.; Purkait, M.K.; Mohanty, K. Preparation and characterization of low-cost ceramic microfiltration membranes for the removal of chromate from aqueous solutions. *Appl. Clay Sci.* **2010**, *47*, 317–324.

21. Hedfi, I.; Hamdi, N.; Srasra, E.; Rodríguez, M.A. The preparation of micro-porous membrane from a Tunisian kaolin. *Appl. Clay Sci.* **2014**, *101*, 574–578.
22. Mohtor, N.H.; Othman, M.H.D.; Ismail, A.F.; Rahman, M.A.; Jaafar, J.; Hashim, N.A. Investigation on the effect of sintering temperature on kaolin hollow fibre membrane for dye filtration. *Environ. Sci. Pollut. Res. Int.* **2017**, *24*, 15905–15917.
23. Ali, M.B.; Hamdi, N.; Rodriguez, M.A.; Mahmoudi, K.; Srasra, E. Preparation and characterization of new ceramic membranes for ultrafiltration. *Ceram. Int.* **2018**, *44*, 2328–2335.
24. Bellotto, M.; Gualtieri, A.; Artioli, G.; Clark, S.M. Kinetic study of the kaolinite-mullite reaction sequence. Part I: Kaolinite dihydroxylation. *Phys. Chem. Miner.* **1995**, *22*, 207–217.
25. Hubadillah, S.K.; Othman, M.H.D.; Harun, Z.; Ismail, A.F.; Rahman, M.A.; Jaafar, J.; Jamil, S.M.; Mohtor, N.H. Superhydrophilic, low cost kaolin-based hollow fibre membranes for efficient oily-wastewater separation. *Mater. Lett.* **2017**, *191*, 119–122.
26. Zhu, Z.; Wei, Z.; Sun, W.; Hou, J.; He, B.; Dong, Y. Cost-effective utilization of mineral-based raw materials for preparation of porous mullite ceramic membranes via in-situ reaction method. *Appl. Clay Sci.* **2016**, *120*, 135–141.
27. Chen, G.; Ge, X.; Wang, Y.; Xing, W.; Guo, Y. Design and preparation of high permeability porous mullite support for membranes by in-situ reaction. *Ceram. Int.* **2015**, *41*, 8282–8287.
28. Guechi, A.; Harabi, A.; Condoum, S.; Zenikheri, F.; Boudaira, B.; Bouzerara, F.; Foughali, L. Elaboration and characterization of tubular supports for membranes filtration. *Desalin. Water Treat.* **2016**, *57*, 5246–5252.
29. Almandoz, M. Preparation and characterization of non-supported microfiltration membranes from aluminosilicates. *J. Membr. Sci.* **2004**, *241*, 95–103.
30. Emani, S.; Uppaluri, R.; Purkait, M.K. Preparation and characterization of low cost ceramic membranes for mosambi juice clarification. *Desalination* **2013**, *317*, 32–40.
31. Emani, S.; Uppaluri, R.; Purkait, M.K. Cross flow microfiltration of oil–water emulsions using kaolin based low cost ceramic membranes. *Desalination* **2014**, *341*, 61–71.
32. Eom, J.-H.; Kim, Y.-W.; Yun, S.-H.; Song, I.-H. Low-cost clay-based membranes for oily wastewater treatment. *J. Ceram. Soc. Jpn.* **2014**, *122*, 788–794.
33. Hedfi, I.; Hamdi, N.; Rodriguez, M.A.; Srasra, E. Preparation of macroporous membrane using natural Kaolin and Tunisian lignite as a pore-forming agent. *Desalin. Water Treat.* **2016**, *57*, 13388–13393.
34. Rekik, S.B.; Bouaziz, J.; Deratani, A.; Beklouti, S. Study of Ceramic Membrane from Naturally Occurring-Kaolin Clays for Microfiltration Applications. *Period. Polytech. Chem. Eng.* **2017**, *61*, 206.
35. Hubadillah, S.K.; Othman, M.H.D.; Ismail, A.F.; Rahman, M.A.; Jaafar, J. A low cost hydrophobic kaolin hollow fiber membrane (h-KHFM) for arsenic removal from aqueous solution via direct contact membrane distillation. *Sep. Purif. Technol.* **2019**, *214*, 31–39.

36. Arzani, M.; Mahdavi, H.R.; Sheikhi, M.; Mohammadi, T.; Bakhtiari, O. Ceramic monolith as microfiltration membrane: Preparation, characterization and performance evaluation. *Appl. Clay Sci.* **2018**, *161*, 456–463.
37. Kumar, R.V.; Ghoshal, A.K.; Pugazhenthii, G. Elaboration of novel tubular ceramic membrane from inexpensive raw materials by extrusion method and its performance in microfiltration of synthetic oily wastewater treatment. *J. Membr. Sci.* **2015**, *490*, 92–102.
38. Harabi, A.; Guechi, A.; Condom, S. Production of Supports and Filtration Membranes from Algerian Kaolin and Limestone. *Proc. Eng.* **2012**, *33*, 220–224.
39. Das, B.; Chakrabarty, B.; Barkakati, P. Preparation and characterization of novel ceramic membranes for micro-filtration applications. *Ceram. Int.* **2016**, *42*, 14326–14333.
40. Kouras, N.; Harabi, A.; Bouzerara, F.; Foughali, L.; Policicchio, A.; Stelitano, S.; Galiano, F.; Figoli, A. Macro-porous ceramic supports for membranes prepared from quartz sand and calcite mixtures. *J. Eur. Ceram. Soc.* **2017**, *37*, 3159–3165.
41. Boudaira, B.; Harabia, A.; Bouzerara, F.; Condom, S. Preparation and characterization of microfiltration membranes and their supports using kaolin (DD2) and CaCO₃. *Desalin. Water Treat.* **2009**, *9*, 142–148.
42. Harabi, A.; Boudaira, B.; Bouzerara, F.; Foughali, L.; Zenikheri, F.; Guechi, A.; Ghouil, B.; Condom, S. Porous Ceramic Supports for Membranes Prepared from Kaolin (DD3) and Calcite Mixtures. *Acta Phys. Pol. A* **2015**, *127*, 1164–1166.
43. Bouzerara, F.; Harabi, A.; Condom, S. Porous ceramic membranes prepared from kaolin. *Desalin. Water Treat.* **2009**, *12*, 415–419.
44. Hubadillah, S.K.; Kumar, P.; Othman, M.H.D.; Ismail, A.F.; Rahman, M.A.; Jaafar, J. A low cost, superhydrophobic and superoleophilic hybrid kaolin-based hollow fibre membrane (KHFM) for efficient adsorption–separation of oil removal from water. *RSC Adv.* **2018**, *8*, 2986–2995.
45. Fritz, S.J. Ideality of Clay Membranes in Osmotic Processes: A Review. *Clays Clay Miner.* **1986**, *34*, 214–223.
46. Fan, B.; Wei, G.; Hao, H.; Guo, A.; Li, J. Preparation of a ceramic membrane from prevalent natural clay for the purification of phosphate wastewater. *Desalin. Water Treat.* **2016**, *57*, 17308–17321.
47. Zhou, J.-E.; Dong, Y.; Hampshire, S.; Meng, G. Utilization of sepiolite in the synthesis of porous cordierite ceramics. *Appl. Clay Sci.* **2011**, *52*, 328–332.
48. Almandoz, M.C.; Pagliero, C.L.; Ochoa, N.A.; Marchese, J. Composite ceramic membranes from natural aluminosilicates for microfiltration applications. *Ceram. Int.* **2015**, *41*, 5621–5633.
49. Henriques, J.D.D.; Pedrassani, M.W.; Klitzke, W.; Mariano, A.B.; Vargas, J.V.C.; Vieira, R.B. Thermal treatment of clay-based ceramic membranes for microfiltration of *Acutodesmus obliquus*. *Appl. Clay Sci.* **2017**, *150*, 217–224.

50. Zhu, Y.; Chen, D. Preparation and characterization of attapulgite-based nanofibrous membranes. *Mater. Design* **2017**, *113*, 60–67.
51. Zhu, Y.; Chen, D. Clay-based nanofibrous membranes reinforced by multi-walled carbon nanotubes. *Ceram. Int.* **2018**, *44*, 15873–15879.
52. Zhu, Y.; Chen, D. Novel clay-based nanofibrous membranes for effective oil/water emulsion separation. *Ceram. Int.* **2017**, *43*, 9465–9471.
53. Foorginezhad, S.; Zerafat, M.M. Microfiltration of cationic dyes using nano-clay membranes. *Ceram. Int.* **2017**, *43*, 15146–15159.
54. Ersoy, B.; Gunay, V. Preparation and Characterization of Sol-Gel Derived 4%La₂O₃-Al₂O₃ Ceramic Membrane on Clay-Based Supports. *Key Eng. Mater.* **2004**, 264–268, 403–406.
55. Saffaj, N.; Persin, M.; Younsi, S.A.; Albizane, A.; Cretin, M.; Larbot, A. Elaboration and characterization of microfiltration and ultrafiltration membranes deposited on raw support prepared from natural Moroccan clay: Application to filtration of solution containing dyes and salts. *Appl. Clay Sci.* **2006**, *31*, 110–119.
56. Saffaj, N.; Persin, M.; Younsi, S.A.; Albizane, A.; Bouhria, M.; Loukili, H.; Dach, H.; Larbot, A. Removal of salts and dyes by low ZnAl₂O₄-TiO₂ ultrafiltration membrane deposited on support made from raw clay. *Sep. Purif. Technol.* **2005**, *47*, 36–42.
57. Anbri, Y.; Tijani, N.; Coronas, J.; Mateo, E.; Menéndez, M.; Bentama, J. Clay plane membranes: Development and characterization. *Desalination* **2008**, *221*, 419–424.
58. Palacio, L.; Bouzerdi, Y.; Ouammou, M.; Albizane, A.; Bennazha, J.; Hernández, A.; Calvo, J.I. Ceramic membranes from Moroccan natural clay and phosphate for industrial water treatment. *Desalination* **2009**, *245*, 501–507.
59. Baraka, N.E.; Saffaj, N.; Mamouni, R.; Laknifli, A.; Younsi, S.A.; Albizane, A.; El Haddad, M. Elaboration of a new flat membrane support from Moroccan clay. *Desalin. Water Treat.* **2014**, *52*, 1357–1361.
60. Elomari, H.; Achiou, B.; Ouammou, M.; Albizane, A.; Bennazha, J.; Younsi, S.A.; Elamrani, I. Elaboration and characterization of flat membrane supports from Moroccan clays. Application for the treatment of wastewater. *Desalin. Water Treat.* **2016**, *57*, 20298–20306.
61. Bouazizi, A.; Saja, S.; Achiou, B.; Ouammou, M.; Calvo, J.I.; Aaddane, A.; Younsi, S.A. Elaboration and characterization of a new flat ceramic MF membrane made from natural Moroccan bentonite. Application to treatment of industrial wastewater. *Appl. Clay Sci.* **2016**, *132–133*, 33–40.
62. Bouazizi, A.; Breida, M.; Karim, A.; Achiou, B.; Ouammou, M.; Calvo, J.I.; Aaddane, A.; Khiat, K.; Younsi, S.A. Development of a new TiO₂ ultrafiltration membrane on flat ceramic support made from natural bentonite and micronized phosphate and applied for dye removal. *Ceram. Int.* **2017**, *43*, 1479–1487.

63. Mouiya, M.; Abourriche, A.; Bouazizi, A.; Benhammou, A.; el Hafiane, Y.; Abouliatim, Y.; Nibou, L.; Oumam, M.; Ouammou, M.; Smith, A.; et al. Flat ceramic microfiltration membrane based on natural clay and Moroccan phosphate for desalination and industrial wastewater treatment. *Desalination* **2018**, 427, 42–50.
64. Misrar, W.; Loutou, M.; Saadi, L.; Mansori, M.; Waqif, M.; Favotto, C. Cordierite containing ceramic membranes from smectetic clay using natural organic wastes as pore-forming agents. *J. Asian Ceram. Soc.* **2017**, 5, 199–208.
65. Eom, J.-H.; Yeom, H.-J.; Kim, Y.-W.; Song, I.-H. Ceramic Membranes Prepared from a Silicate and Clay-mineral Mixture for Treatment of Oily Wastewater. *Clays Clay Miner.* **2015**, 63, 222–234.
66. Abubakar, M.; Tamin, M.N.; Saleh, M.A.; Uday, M.B.; Ahmad, N. Preparation and characterization of a nigerian mesoporous clay-based membrane for uranium removal from underground water. *Ceram. Int.* **2016**, 42, 8212–8220.
67. Galán-Arboledas, R.J.; Cotes, T.; Martínez, C.; Bueno, S. Influence of waste addition on the porosity of clay-based ceramic membranes. *Desalin. Water Treat.* **2016**, 57, 2633–2639.
68. Lorente-Ayza, M.-M.; Mestre, S.; Menéndez, M.; Sánchez, E. Comparison of extruded and pressed low cost ceramic supports for microfiltration membranes. *J. Eur. Ceram. Soc.* **2015**, 35, 3681–3691.
69. Khemakhem, S.; Larbot, A.; Amar, R.B. Study of performances of ceramic microfiltration membrane from Tunisian clay applied to cuttlefish effluents treatment. *Desalination* **2006**, 200, 307–309.
70. Khemakhem, S.; Amar, R.B.; Larbot, A. Synthesis and characterization of a new inorganic ultrafiltration membrane composed entirely of Tunisian natural illite clay. *Desalination* **2007**, 206, 210–214.
71. Fakhfakh, S.; Baklouti, S.; Bouaziz, J. Elaboration and characterisation of low cost ceramic support membrane. *Adv. Appl. Ceram.* **2010**, 109, 31–38.
72. Haden, W.L.; Schwint, I.A. Attapulgit: Its Properties and Applications. *Ind. Eng. Chem.* **1967**, 59, 58–69.
73. Kallo, D. Applications of Natural Zeolites in Water and Wastewater Treatment. *Rev. Mineral. Geochem.* **2001**, 45, 519–550.
74. Hay, R.L. Geologic Occurrence of Zeolites and Some Associated Minerals. *Pure Appl. Chem.* **1986**, 58, 1339–1342.
75. Mumpton, F.A. La roca magica: Uses of natural zeolites in agriculture and industry. *Proc. Natl. Acad. Sci. USA* **1999**, 96, 3463–3470.
76. Earl, D.J.; Deem, M.W. Toward a Database of Hypothetical Zeolite Structures. *Ind. Eng. Chem. Res.* **2006**, 45, 5449–5454.

77. Wang, S.; Zhu, Z.H. Characterisation and environmental application of an Australian natural zeolite for basic dye removal from aqueous solution. *J. Hazard. Mater.* **2006**, 136, 946–952.
78. Wang, S.; Peng, Y. Natural zeolites as effective adsorbents in water and wastewater treatment. *Chem. Eng. J.* **2010**, 156, 11–24.
79. Strathmann H., Giorno L., Drioli E., *An introduction to Membrane Science and Technology*, Rome 2006
80. Prazeres D.M.F., Cabral J.M.S., *Enzyme and Microbial Technology* 1994,16, 738-754
81. Chang H. N. , Furusaki S., *Advances in Biochemical Engineering/Biotechnology*, Springer Berlin Heidelberg, 1991, 44, 27-64
82. Matson L., Quinn J.A., *Ann. NY Acad Sci* 1986, 469, 152-165.
83. Butterfield D.A., *Biofunctional membranes*, Plenum Press NY 1996, 117-129.
84. Butterfield D.A., D. Bhattacharyya, S. Daunert, L. Bachas, *Journal of Membrane Science*, 2001, 29-37
85. Amounas M., Innocent C., Cosnier S., Seta P.. *J. Memb. Sci.* 2000,176 169-
86. Amounas M., Magne V., Innocent C., Dejean E., Seta P.. *Enzyme and Microbial Technology* 2002, 31, 171-178.
87. Giorno L., Molinari R., Drioli E., Bianchi D., Cesti P., *J.Chem. Tech. Biotechnol.* 1995, 64, 345
88. Drioli E., Iorio G., Catalano G., *Handbook of industrial membrane technology*. New York: Noyes Publications 1989, 401-481
89. Goel M.K, www.rpi.edu/dept/chem-eng/Biotech-Environ/IMMOB/goel2nd.htm, 1994
90. Xie S., Svec F., J.M.J. Fréchet, *Biotech. Bioeng.* 1999, 62 , 30.
91. Bowen W.R., Hughes D.T., Properties of microfiltration membranes. Adsorption of bovine serum albumin at aluminium oxide membranes, *J. Membr. Sci* 51 (1990) 1898
92. Nystrom M. ; Lindstrom M. ; Matthiasson E., Streaming potential as a tool in the characterization of ultrafiltration membranes, *Colloids and surfaces*, 36 (1989) 297-312
93. Pontié, M.; Chasseray, X.; Lemordant, D.; Lainé, J.M., The streaming potential method for the characterization of ultrafiltration organic membranes and the control of cleaning treatments, *Journal of Membrane Science*, 129 (1997) 125-133
94. Keesom W.H., Zelenka r.L., Radke C.J., A zeta-potential model for surfactanat adsorbtion on an ionogenic hydrophobic surface, *J.Colloid Interace Sci* 125: 575 (1988)

CHAPTER 3

WASTEWATER SOURCES & RENEWABLE ENERGY DRIVEN MEMBRANE SEPARATION

3.0 Wastewater

Wastewater is the term for discarded or previously used water from a municipality or industry. The wastewater that is produced due to human activities in households is called domestic wastewater i.e. wastewater from the kitchen, bathroom, toilet and laundry. Such water usually contains dissolved as well as suspended matter and must be treated prior to its discharge into natural water. To examine the quality of wastewater to be discharged into aquatic Environment or to be treated and reused, the characteristics of wastewater in question must be defined precisely. Quantitative assessments of the quality of wastewater are made by considering many criteria, including temperature, dissolved oxygen level and concentration of organic as well as inorganic compounds. The most frequently used parameters are: Biochemical Oxygen Demand (BOD), Chemical Oxygen Demand (COD), Total Organic Carbon (TOC), Alkalinity, Chlorides, Nitrogen, Oil and Grease, Dissolved Oxygen, pH, Phosphorus, Gases, Sulphur, Solids, Temperature, Metals as well as Micro-organisms. In this lesson, these parameters are defined and methods for analysing them are discussed briefly. In addition sampling and determination techniques are discussed.

Wastewater is the water which is disposed from homes, offices and industry. It comes from toilets, sinks, showers, washing machines and industrial processes and was historically called sewage. At a global level, around 80% of wastewater produced is discharged into the environment untreated, causing widespread water pollution. Wastewater produced due to human activities in households is called domestic wastewater i.e. wastewater from the kitchen, shower, wash basin, toilet and laundry (see figure 3.1). The strength and composition of the domestic wastewater changes on hourly, daily and seasonal basis, with the average strength dependent on per capita water usage, habits, diet, living standard and life style. The main reason is variation in water usage in households. Households in developed countries use more water than those in developing countries.



Figure 3.1: Sources of domestic wastewater (Samwel 2005)

Wastewater components can be divided into different main groups as shown in Table 3.1. They can adversely affect the aquatic life if discharge them into environmental.

Component	Of special interest	Environmental effect
<u>Microorganisms</u>	Pathogenic bacteria, virus and worms eggs	Risk when bathing and eating shellfish
Biodegradable organic materials	Oxygen depletion in rivers and lakes	Fish death, odours
Other organic materials	Detergents, pesticides, fat, oil and grease, colouring, solvents, phenols, cyanide	Toxic effect, aesthetic inconveniences, bioaccumulation in the food chain
Nutrients	Nitrogen, phosphorus, ammonium	<u>Eutrophication</u> , oxygen depletion, toxic effect
Metals	Hg, Pb, Cd, Cr, Cu, Ni	Toxic effect, bioaccumulation
Other inorganic materials	Acids, for example hydrogen sulphide, bases	Corrosion, toxic effect
Thermal effects	Hot water	Changing living conditions for flora and fauna
Odour (and taste)	Hydrogen sulphide	Aesthetic inconveniences, toxic effect
Radioactivity		Toxic effect, accumulation

Table 3.1: Components present in domestic wastewater (Henze and Ledind; 2001)

Physically, domestic wastewater is usually characterised by a grey colour, musty odour and has a solids content of about 0.1%. The solid material is a mixture of faeces, food particles, toilet paper, grease, oil, soap, salts, metals, detergents, sand and grit. The solids can be suspended (about 30%) as well as dissolved (about

70%). Dissolved solids can be precipitated by chemical and biological processes. From a physical point of view, the suspended solids can lead to the development of sludge deposits and anaerobic conditions when discharged into the receiving Environment.

Chemically, wastewater is composed of organic (70%) and inorganic (30%) compounds as well as various gases. Organic compounds consist primarily of carbohydrates (25 %), proteins (65 %) and fats (10 %), which reflects the diet of the people. Inorganic components may consist of heavy metals, nitrogen, phosphorus, pH, sulphur, chlorides, alkalinity, toxic compounds, etc. However, since wastewater contains a higher portion of dissolved solids than suspended, about 85 to 90% of the total inorganic component is dissolved and about 55 to 60% of the total organic component is dissolved. Gases commonly dissolved in wastewater are hydrogen sulphide, methane, ammonia, oxygen, carbon dioxide and nitrogen. The first three gases result from the decomposition of organic matter present in the wastewater.

Biologically, wastewater contains various microorganisms but the ones that are of concern are those classified as protista, plants, and animals. The category of protista includes bacteria, fungi, protozoa, and algae. Plants include ferns, mosses, seed plants and liverworts. Invertebrates and vertebrates are included in the animal category. In terms of wastewater treatment, the most important category are the protista, especially the bacteria, algae, and protozoa. Also, wastewater contains many pathogenic organisms which generally originate from humans who are infected with disease or who are carriers of a particular disease. Typically, the concentration of faecal coliforms found in raw wastewater is about several hundred thousand to tens of million per 100 ml of sample.

Industrial wastewater is a by-product of industrial or commercial activities. Whether it's the food we eat, the beverages we drink, the clothes we wear, or the paper and chemical products we use, water is required for nearly every step of production across a multitude of different industries. The resulting wastewater must be carefully managed. Regardless of how wastewater is treated, the "end product" is called effluent. To comply with environmental protection laws, certain things must be removed from the wastewater. This includes organic matter, inorganics (sodium, potassium, calcium, magnesium, copper, lead, nickel, and zinc), pathogens, and nutrients (most notably nitrogen and phosphorus). The treated wastewater can then be safely discharged into water bodies, applied to land, or even reused in plant operations.

One option is to discharge untreated wastewater to the local municipal treatment plant, but with that comes considerable costs. The other—often more favourable—option is to treat wastewater at the manufacturing facility itself. This can be accomplished with the right wastewater treatment technology. On-site treatment can help your plant remain environmentally compliant and save money, while facilitating production increases and recovering valuable resources. Industrial wastewater is also one of the major sources of aquatic pollution which could significantly endanger surrounding environments and ecosystems. Industrial wastewater, especially from chemical and pharmaceutical production, often contains substances that need to be treated

before being discharged into a biological treatment plant and subsequent water bodies. Generally, this can be done close to the site of production itself, in selected wastewater streams before reaching a central treatment plant. Each of the approaches used has certain advantages and disadvantages. Furthermore, various wastewater treatment processes exist, but selection of the best technically and commercially viable solution is always a challenge. Industrialization has played a major role in this area and has been the driving force for many treatment methodologies that are being practiced today. There is a better understanding of the importance of protecting the environment and enhancing overall sustainability today. This chapter considers the past and present states of industrial wastewater treatment. It also outlines future challenges and likely developments in industrial wastewater treatment, recycling, and reuse. In the following table 3.2 we summarize the substances present in the industrial wastewater.

Substances	Present in Wastewaters from:
Acetic acid	Acetate rayon, beet root manufact
Acids	Chem. manufact, mines, textiles manufact
Alkalies	Cotton and straw kiering, wool scouring
Ammonia	Gas and coke and chem. manufacture
Arsenic	Sheep dipping
Cadmium	Plating
Chromium	Plating, chrome tanning, alum anodizing
Citric acid	Soft drinks and citrus fruit processing
Copper	Copper plating, copper pickling
Cyanides	Gas manufacture, plating, metal cleaning
Fats, oils, grease	Wool scouring, laundries, textile industry
Fluorides	Scrubbing of flue gases, glass etching
Formaldehyde	Synthetic resins and penicillin manufact
Free chlorine	Laundries, paper mills, textile bleaching
Hydrocarbons	Petrochemical and rubber factories
Free chlorine	Laundries, paper mills, textile bleaching
Mercaptans mills	Oil refining, pulp
Nickel	Plating
Nitro compounds	Explosives and chemical works
Organic acids	Distilleries and fermentation plants
Phenols	Gas and coke manufact., chem. plants
Starch	Food processing, textile industries
Sugars	Dairies, breweries, sweet industry
Sulfides	Textile industry, tanneries, gas manufact.
Sulfites	Pulp processing, viscose film manufact.
Tannic acid	Tanning, sawmills
Tartaric acid	Dyeing, wine, leather, chem. manufacture
Zinc	Galvanizing zinc plating, rubber process.

Table 3.2 Substances present in industrial effluents (Bond & Straub,1974)

3.1 Heavy metals and inorganic species

Several industries discharge heavy metals, it can be seen that of all of the heavy metals, chromium is the most widely used and discharged to the environment from different sources. Many of the pollutants entering aquatic ecosystems (e.g., mercury lead, pesticides, and herbicides) are very toxic to living organisms. They can lower reproductive success, prevent proper growth and development, and even cause death. However, chromium is not the metal that is most dangerous to living organisms. Such more toxic are cadmium, lead and mercury. These have a tremendous affinity for sulphur and disrupt enzyme function by forming bonds with sulphur groups in enzymes. Protein carboxylic acid (-CO₂H) and amino (-NH₂) groups are also chemically bound by heavy metals. Cadmium, copper, lead and mercury ions bind to cell membranes, hindering transport processes through the cell wall. Heavy metals may also precipitate phosphate bio-compounds or catalyze their decomposition. Heavy metals found in major industries shown in Table 3.3.

Industry	A	As	Cd	Cr	C	Hg	Pb	Ni	Zn
Pulp & paper mills				X	X	X	X	X	X
Organic chem.	X	X	X	X		X	X		X
Alkalis, Chlorine		X	X	X		X	X		X
Fertilizers	X	X	X	X	X	X	X	X	X
Petroleum refining	X	X	X	X	X		X	X	X
Steel works		X	X	X	X	X	X	X	X
Aircraft plating, finishing	X		X	X	X	X		X	
Flat glass, cement				X					
Textile mills				X					
Tanning				X					
Power plants				X					

Table 3.3: Heavy metals found in major industries (Bond & Straub, 1974)

The pollutant cadmium in water may arise from industrial discharges and mining wastes. Cadmium is widely used in metal plating. Chemically, cadmium is very similar to zinc, and these two metals frequently undergo geochemical processes together. Both metals are found in water in the +2 oxidation state. The effects of acute cadmium poisoning in humans are very serious. Among them are high blood pressure, kidney damage, destruction of testicular tissue, and destruction of red blood cells. Cadmium may replace zinc in some enzymes, thereby altering the stereo-structure of the enzyme and impairing its catalytic activity. Cadmium and zinc are common water and sediment pollutants in harbours surrounded by industrial facilities. Inorganic lead arising from a number of industrial and mining sources occurs in water in the +2 oxidation state. Lead from leaded gasoline used to be a major source of atmospheric and terrestrial lead, much of which eventually enters natural water systems. Acute lead poisoning in humans causes severe dysfunction in the kidneys, reproductive system, liver, and the brain and nervous system. Mercury is found as a trace component of many minerals, with continental rocks containing an average of around 80 ppb, or slightly less, of this element. Cinnabar, red

mercuric sulphide, is the chief commercial mercury ore. Metallic mercury is used as an electrode in the electrolytic generation of chlorine gas, in laboratory vacuum apparatuses and in other applications. Organic mercury compounds used to be widely applied as pesticides, particularly fungicides. Mercury enters the environment from a large number of miscellaneous sources related to human use of the element. These include discarded laboratory chemicals, batteries, broken thermometers, lawn fungicides, amalgam tooth fillings and pharmaceutical products. Sewage effluent sometimes contains up to 10 times the level of mercury found in typical natural waters. Among the toxicological effects of mercury were neurological damage, including irritability, paralysis, blindness, insanity, chromosome breakage and birth defects.

3.2 Parameters of wastewater significance in membrane

The quality of waste water is of particular importance in zones where extremes of temperature and low relative humidity result in high rates of evaporation, with consequent deposition of salt which tends to accumulate in the soil profile. The physical and mechanical properties of the soil, such as dispersion of particles, stability of aggregates, soil structure and permeability, are very sensitive to the type of exchangeable ions present in irrigation water. Thus, when effluent use is being planned, several factors related to soil properties must be taken into consideration.

Another aspect pollutants from agricultural sources concern is the effect of dissolved solids (TDS) in the irrigation water on the growth of plants. Dissolved salts increase the osmotic potential of soil water and an increase in osmotic pressure of the soil solution increases the amount of energy which plants must expend to take up water from the soil. As a result, respiration is increased and the growth and yield of most plants decline progressively as osmotic pressure increases. Although most plants respond to salinity as a function of the total osmotic potential of soil water, some plants are susceptible to specific ion toxicity.

Many of the ions which are harmless or even beneficial at relatively low concentrations may become toxic to plants at high concentration, either through direct interference with metabolic processes or through indirect effects on other nutrients, which might be rendered inaccessible. It has been previously reported that non-polluted soil, having around 0.4 and 0.5 ppm cadmium, may produce about 0.08 ppm Cd in brown rice, while only a little increase up to 0.82, 1.25 or 2.1 ppm of soil Cd has the potential to produce heavily polluted brown rice with 1.0 ppm Cd. Important agricultural water quality parameters include a number of specific properties of water that are relevant in relation to the yield and quality crops, maintenance of soil productivity and protection of the environment. These parameters mainly consist of certain physical and chemical characteristics of the waste water. Described in Table 3.4 presents a list of some of the important physical and chemical characteristics that are used in the evaluation of agricultural water quality. The primary wastewater quality parameters of importance from an agricultural viewpoint are:

Parameters	Symbol	Unit
Physical		
Total dissolved solids	TDS	mg/l
Electrical conductivity	E_{c_w}	dS/m ¹
Temperature	T	°C
Colour/Turbidity		NTU/JTU ²
Hardness		mg equiv. CaCO ₃ /l
Sediments		g/l
Chemical		
Acidity/Basicity	pH	
Type and concentration of anions and cations:		
Calcium	Ca ⁺⁺	me/l ³
Magnesium	Mg ⁺⁺	me/l
Sodium	Na ⁺	me/l
Carbonate	CO ₃ ⁻	me/l
Bicarbonate	HCO ₃ ⁻	me/l
Chloride	Cl _L	me/l
Sulphate	SO ₄ ⁻	me/l
Sodium adsorption ratio	SAR	
Boron	B	mg/l ⁴
Trace metals		mg/l
Heavy metals		mg/l
Nitrate-Nitrogen	NO ₃ -N	mg/l
Phosphate Phosphorus	PO ₄ -P	mg/l
Potassium	K	mg/l

Table 3.4 Parameters used in the evaluation of agricultural water quality

Total Salt Concentration

Total salt concentration (for all practical purposes, the total dissolved solids) is one of the most important waste water quality parameters. Total salt content is a measure of the presence of mainly sulfide salts with associated aluminium, magnesium, sodium, calcium and potassium cations or, more generally, any soluble anion or cation of the leaching solution. This is because the salinity of the soil water is related to, and often determined by, the salinity of the irrigation water. Total salt concentration is expressed in milligrams per litre (mg/l) or parts per million (ppm).

Electrical Conductivity

Electrical conductivity is widely used to indicate the total ionized constituents of water. It is directly related to the sum of the cations (or anions), as determined chemically and is closely correlated, in general, with the total salt concentration. Electrical conductivity is a rapid and reasonably precise determination and values are always expressed at a standard temperature of 25°C to enable comparison of readings taken under varying climatic conditions. It should be noted that the electrical conductivity of solutions increases approximately 2 percent per °C increase in temperature. The unit of electrical conductivity is deciSiemen per metre (dS/m).

Sodium Adsorption Ratio

Sodium is an unique cation because of its effect on wastewater. When present in the soil in exchangeable form, it causes adverse physico-chemical changes in the soil, particularly to soil structure. It has the ability to disperse soil, when present above a certain threshold value, relative to the concentration of total dissolved salts.

Toxic Ions

Irrigation water that contains certain ions at concentrations above threshold values can cause plant toxicity problems. Toxicity normally results in impaired growth, reduced yield, changes in the morphology of the plant and even its death. The degree of damage depends on the crop, its stage of growth, the concentration of the toxic ion, climate and soil conditions. The most common phytotoxic ions that may be present in municipal sewage and treated effluents in concentrations such as to cause toxicity are: boron (B), chloride (Cl) and sodium (Na). Hence, the concentration of these ions will have to be determined to assess the suitability of waste-water quality for use in agriculture.

Trace Elements and Heavy Metals

A number of elements are normally present in relatively low concentrations, usually less than a few mg/l, in conventional irrigation waters and are called trace elements. They are not normally included in routine analysis of regular irrigation water, but attention should be paid to them when using sewage effluents, particularly if contamination with industrial wastewater discharges is suspected. These include Aluminium (Al), Beryllium (Be), Cobalt (Co), Fluoride (F), Iron (Fe), Lithium (Li), Manganese (Mn), Molybdenum (Mo), Selenium (Se), Tin (Sn), Titanium (Ti), Tungsten (W) and Vanadium (V). Heavy metals are a special group of trace elements which have been shown to create

definite health hazards when taken up by plants. Under this group are included, Arsenic (As), Cadmium (Cd), Chromium (Cr), Copper (Cu), Lead (Pb), Mercury (Hg) and Zinc (Zn). These are called heavy metals because in their metallic form, their densities are greater than 4g/cc.

pH

pH is an indicator of the acidity or basicity of water but is seldom a problem by itself. The normal pH range for irrigation water is from 6.5 to 8.4; pH values outside this range are a good warning that the water is abnormal in quality. Normally, pH is a routine measurement in irrigation water quality assessment.

3.3 Conventional water treatment

The principal objective of wastewater treatment is generally to allow human and industrial effluents to be disposed of without danger to human health or unacceptable damage to the natural environment. Irrigation with wastewater is both disposal and utilization and indeed is an effective form of wastewater disposal (as in slow-rate land treatment). However, some degree of treatment must normally be provided to raw municipal wastewater before it can be used for agricultural or landscape irrigation or for aquaculture. The quality of treated effluent used in agriculture has a great influence on the operation and performance of the wastewater-soil-plant or aquaculture system. In the case of irrigation, the required quality of effluent will depend on the crop or crops to be irrigated, the soil conditions and the system of effluent distribution adopted. Through crop restriction and selection of irrigation systems which minimize health risk, the degree of pre-application wastewater treatment can be reduced. A similar approach is not feasible in aquaculture systems and more reliance will have to be placed on control through wastewater treatment.

The most appropriate wastewater treatment to be applied before effluent use in agriculture is that which will produce an effluent meeting the recommended microbiological and chemical quality guidelines both at low cost and with minimal operational and maintenance requirements. Adopting as low a level of treatment as possible is especially desirable in developing countries, not only from the point of view of cost but also in acknowledgement of the difficulty of operating complex systems reliably. In many locations it will be better to design the reuse system to accept a low-grade of effluent rather than to rely on advanced treatment processes producing a reclaimed effluent which continuously meets a stringent quality standard.

Conventional wastewater treatment consists of a combination of physical, chemical, and biological processes and operations to remove solids, organic matter and, sometimes, nutrients from wastewater. General terms used to describe different degrees of treatment, in order of increasing treatment level, are preliminary, primary, secondary, and tertiary and/or advanced wastewater treatment. In some countries, disinfection to remove pathogens sometimes follows the last treatment step. A generalized wastewater treatment diagram is shown in Figure 3.2

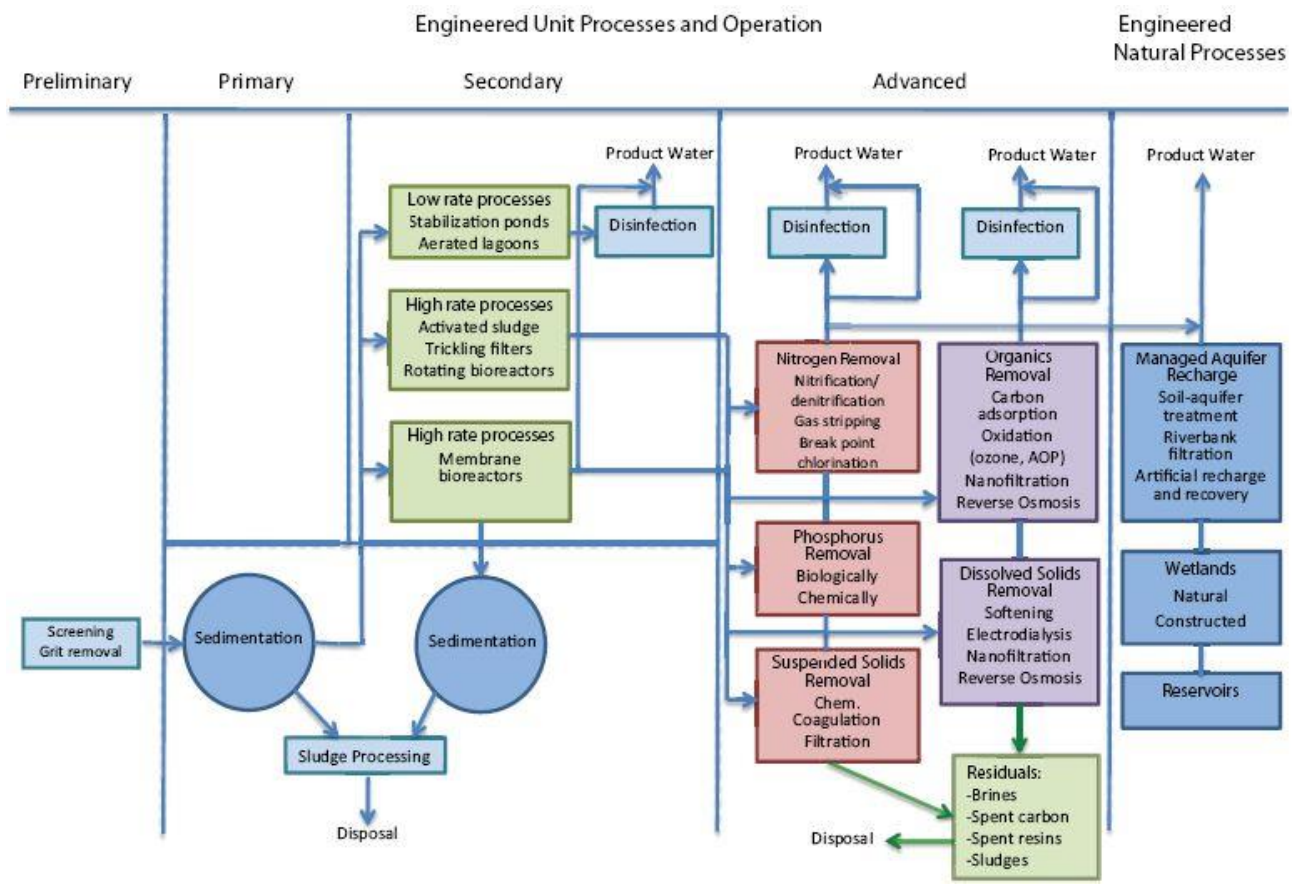


Fig 3.2 Generalized flow diagram for municipal wastewater treatment

Apart from that the most common wastewater treatment processes are given below.

- ✓ Preliminary treatment
- ✓ Primary treatment
- ✓ Secondary treatment
- ✓ Tertiary and/or advanced treatment
- ✓ Disinfection
- ✓ Effluent storage

But for a reliability of conventional and advanced wastewater treatment membrane based separation is emerging as a new technologies for removing most of the contaminants according to the size exclusion principal. The membrane separation technologies and processes is described below.

3.4 Membrane Based water treatment

In water treatment, membranes are barriers that allow water to pass through but stop unwanted substances from passing through with it. Working much like the cell walls in our bodies, technical membranes filter out salts, impurities, viruses, and other particles from water.

A membrane process is any method that relies on a membrane barrier to filter or remove particles from water. Fluid is passed through the membrane because of the pressure difference between one side of the membrane and the other. Contaminants remain on one side. Although many types of filtering media are used for water treatment — for instance, clay, silt, and sand — one of the properties that distinguishes membranes is their ability to separate smaller substances such as salts and ions from a liquid. Membranes were first applied to water treatment processes in the 1960s, but in the next decade, they became increasingly used for desalination.

3.5 Renewable energy driven water treatment

Sustainable energy is the key solution for addressing major concerns about the future such as climate change, environmental protection, and balanced growth of the economy and society. The past two decades have witnessed advancement in economic development in many nations. However, the rapid economic growth, industrial advancement, energy shortage, deterioration of the environment and increasing demands of growing populations pose a huge threat for future generations. For many years, economic development has been the key focus of many policy makers in sustainable development until the inception of the Kyoto protocol agreement in 1997, which includes environmental quality as a crucial variable for sustainable development. With global energy consumption and electricity demands expected to double in the next twenty-five years, major opportunities for innovation in how energy is produced, stored, transmitted and used have begun to open up. In particular, there is a huge interest in sustainable energy technologies capable of improving efficiency and reducing the global carbon footprint . The development of sustainable energy is, however, restricted by various factors, such as the availability of natural resources due to regional differences, sensitivity to the environmental impacts of fossil-fuel based energy, increasing water scarcity, and differing economic policies. Development of an approach to sustainable energy that addresses environmental concerns, greenhouse gas emission, cost, availability of resources, and social impact is a huge challenge. The key focus for attaining energy sustainability is to reduce and slowly replace power generation by fossil fuels with renewable energy sources. Though some aspects of this sustainable approach are being adopted, there are others yet to be translated at a commercial scale. For instance, major concerns about carbon dioxide (CO₂) emissions in traditional fossil fuel-based power generation has paved the way for several sustainable energy sources such as wind and solar, along with CO₂ capture and sequestration technologies. Apart from this, there is a growing recognition of technologies such as cogeneration plants, where a combination of techniques

contributes to reduced water demand while generating energy, resulting in effective water use to meet the demand. Water and energy are the two key aspects for sustainable development for the future. There is a significant amount of research and development work going on in the membrane sector, emphasizing the utilization of renewable energy in conjunction with membrane technology, although the efficiency of the process is still a high priority. Recently, membrane technologies have started to play a pivotal role in developing the infrastructure for sustainable energy, especially, in the water and energy sector. Some of the membrane-based approaches that are currently adapted at an industrial scale include desalination by reverse osmosis (RO), membrane-based bioreactors (MBR) for pure water generation, lithium-ion batteries, and membrane-based fuel cells and CO₂ capture.

Besides addressing the concerns related to energy demands and water scarcity, membrane technologies meet the criteria for sustainability in terms of feasibility, flexibility and adaptability. However, they still need to improve costs and affordability, which is achieved by advancement in membrane-based technologies.

3.6 Role of Membrane Technology in Sustainable Water Generation

Membrane-based approaches for the generation of potable water mainly rely on desalination and waste water treatment processes. The majority of the global reserves of water is saline and only 2.5% is available as fresh water. Moreover, only 0.007% of the total available stock is directly accessible for human use, as a major portion of the fresh water stock is either frozen in polar regions or difficult to access as remote aquifer. Of this meagre portion of the total available fresh water stock, some is polluted by industrial plants, mining, oil or gas exploration, use of fertilizers and pesticide residue from agriculture. Also, uneven distribution of the available water stocks pushes certain regions of the world to severe water scarcity. Hence, desalination and water reclamation is of utmost importance for securing localized water reserves for many arid regions and to meet the needs of our growing population.

With increasing demand for fresh water, various techniques have been developed in the past decades including vacuum distillation, multi-stage flash distillation (MSF), multiple-effect distillation (MED), and other membrane-based technologies, such as reverse osmosis (RO), membrane distillation (MD), etc., for sea water desalination. Among these technologies, membrane-based techniques such as RO, MD, and forward osmosis are seen as attractive alternatives due to their low energy consumption, lower capital requirements as well as less maintenance and lower operating costs.

The use of solar collectors is another attractive way to utilize the solar energy as a heat source in MD. The solar collectors can supply the energy in the form of heat (solar thermal) or electrical energy (solar photovoltaic). Solar collector devices are used to absorb solar energy and then transfer the energy into a collection media. Common solar collectors include the flat-plate collector (FPC), evacuated tube collector (ETC), compound parabolic collectors (CPC), parabolic trough (PTC), linear Fresnel (LFC), parabolic dish reflector (PDR), central receiver collector (CRC), and the solar pond, which can be categorized according to the temperature level that the collection medium can reach. Low temperature collectors (FPC or improved

FPC, ETC) operate below 80 C, which may not have application to conventional distillation systems, but are highly useful for MD applications.

The concentrated high solar energy is able to generate high temperature gradients and can be utilized either directly in thermal desalination process or applied to produce electricity using a steam turbine. By increasing the size of the high temperature collector and by implementing the sun tracking device, the efficiency can be enhanced sufficiently to supply the heat for large-scale thermal desalination processes. On the other hand, the low and medium temperature collectors may not be suitable for operating the conventional distillation process, but are highly appropriate for MD desalination that requires a relatively lower temperature gradient for water vapor generation. A schematic of a solar heating-assisted MD desalination system is presented in Figure 3.3.

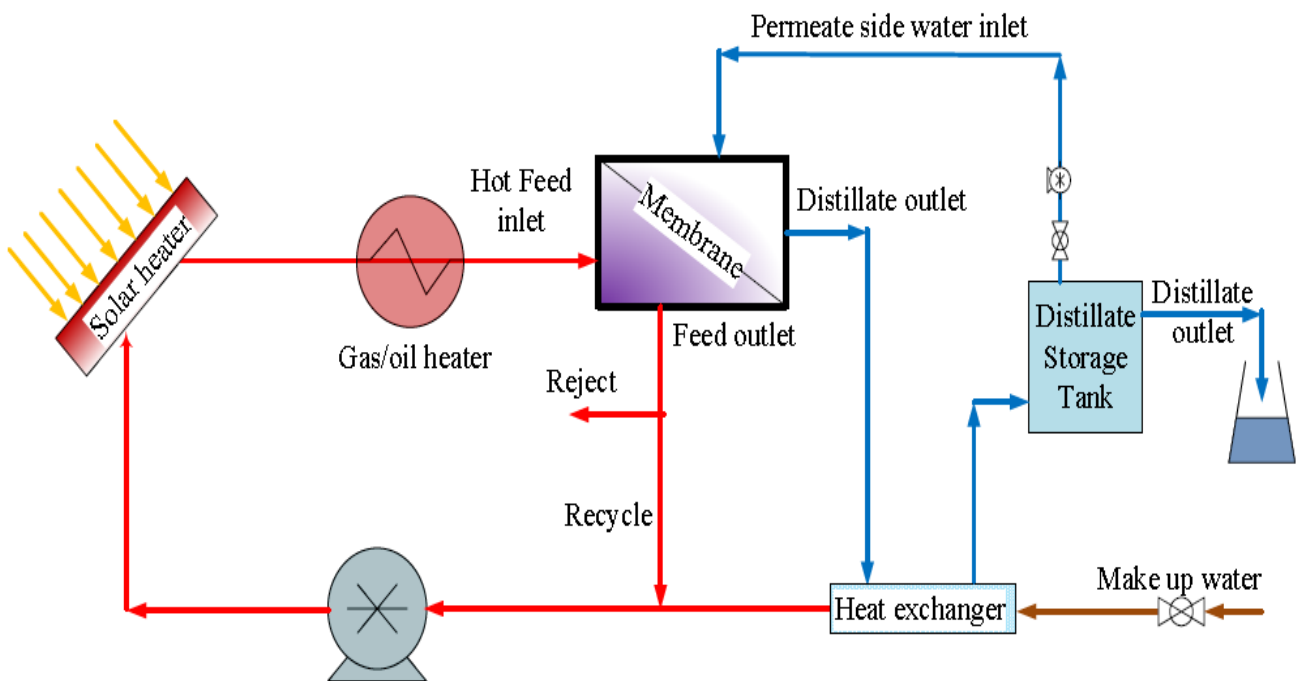


Fig 3.3 Schematic of solar heating assisted membrane distillation (MD) desalination

Another interesting way to convert solar energy is the use of photovoltaic (PVC) cells, which convert it into electrical energy by transferring the electrons. The PVC cell is the key component in PVC applications and is considered as a direct current power generator. The PVC cells can be categorized as first generation, which includes crystalline silicon (c-Si) technologies, second generation, which includes amorphous silicon thin-film (TF) technologies, and the nano-PVC technologies as third generation. The thin film PVC technology is growing very fast due to its high efficiency and lower cost. However, the lack of availability of the PVC materials and its initial investment costs hinder its implementation and further development in MD systems. Several solar power stations have been built throughout the world to supply sustainable heat energy to desalination industries and local regions for domestic usage.

Coupling solar energy collector with an MD system has shown great potential in recovering pure water and waste water concentration as MD can operate at low temperatures, as well as having the capability of bearing wide variation in operating parameters. Hogan et al. from the University of New South Wales, first published their work with a hollow fiber membrane MD system of 0.05 m³/day capacity using a 3 m² flat plate solar collector . The results revealed that the system required 55.6 kWh/m³ of total energy, and generated a water vapor flux of 17 L/day_m² of collector area, which is highly comparable to that reported for solar multi-stage flash distillation and multiple-effect distillation. Cabassud et al. proposed four different possible ways of coupling solar energy with MD systems: (1) feed solution was supplied by a salinity gradient solar pond (SGSP); (2) the MD module was immersed directly in the SGSP; (3) solar collectors were used to heat the feed solution; and (4) solar collectors were placed directly on the membrane to heat the feed. The schematic of the proposed configurations is shown in Figure 3.4. The results showed that the modules with solar collectors generated higher water flux compared to those with solar ponds.

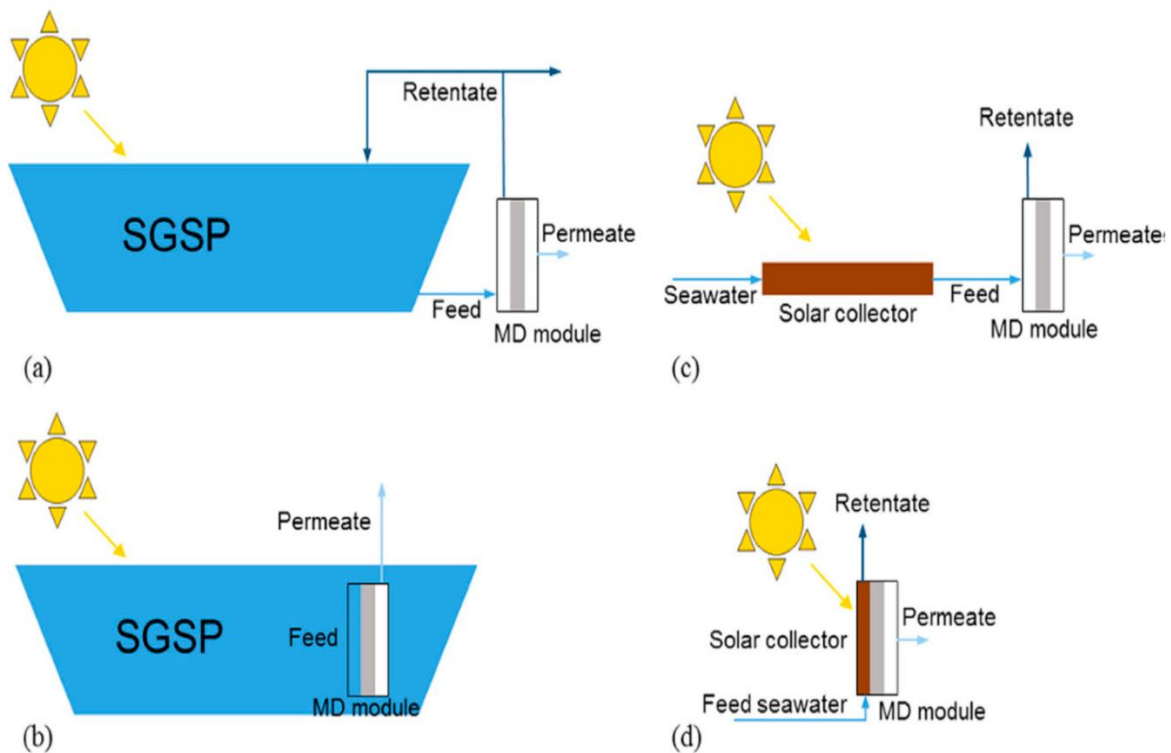


Figure 3.4 Four configurations coupling MD and solar energy: (a) feed water supplied by a SGSP; (b) module submerged directly in a SGSP; (c) feed water fed by solar collectors; (d) feed water heated directly on the membrane surface.

3.7 Other Membrane Processes

Nowadays, the membrane processes used in various desalination technologies are taking a leading role, especially RO which holds the majority of the world's market share (60–90%). Among other thermal evaporative processes, MED and MSF technology still lead the desalination process in Gulf countries.

However the limitations of the RO process and other thermal evaporative processes have paved the way for other emerging membrane-based processes for desalination such as pressure-retarded RO (PRO), forward osmosis (FO), membrane capacitive deionization (MCDI), electrodialysis (ED), nanofiltration (NF), pervaporation, etc. Recently, forward osmosis (FO) has received increased attention as an emerging purification technique and it has been investigated thoroughly for desalination in both the academic arena and industrial sectors decade. The technology was initially proposed to be a breakthrough in terms of lower power consumption and higher water recovery, however, challenges associated with membrane back salt diffusion, draw solution recovery, and membrane regeneration limit its energy efficiency and feasibility for desalination. Major disadvantages of the FO process are the per unit cost for production of freshwater for the amount of water treated, and the effect of concentration polarization on either side of FO membranes, which in turn affects transmembrane osmotic pressure, resulting in reduced flux and water recovery. These factors significantly impact the operating cost of FO processes. Alternatively, PRO is a method of producing renewable energy from a mixture of two streams with varying salinity, where surface water and seawater are separated by a semi-permeable membrane . Permeate from the diluted feed stream migrates to the concentrated draw stream under pressure via osmosis. A unique feature of the PRO process is that it facilitates the conversion of osmotic pressure difference between the separated solutions to hydraulic pressure, which is in turn utilized for generation of power driven by the hydro-turbines. This technique can be cost effective with optimized maintenance of osmotic pressure.

3.8 Hybrid Membranes Process

There is growing emphasis on combining two or more desalination processes to form an integrated approach, so that these processes complement each other by diluting the disadvantages of a single process by itself. These combined processes are win-win as the efficacy of these processes are higher than an individual stand-alone approach. This solution overcomes the barriers of the individual process and increases overall performance by integrating the processes. For instance, in a FO-RO hybrid mode, FO acts as a pretreatment process reducing the feed salt concentration, which upon introduction to the RO process requires lower hydraulic pressure and reduces fouling . The economic evaluation of the FO-RO hybrid system, carried out by Blandin et al. has shown the benefit of the hybrid process over a stand-alone RO system in terms of energy and operational costs. In the hybrid FO-RO process, the FO can effectively function as a pre-treatment for the RO process that reduces the membrane scaling and fouling in the RO process, and on the other hand, the RO can be efficiently utilized to recover the draw solution. Overall, the hybrid systems result in enhanced membrane performance, reduced energy requirements, and increased productivity in comparison to individual stand-alone processes . The hybrid FO-RO process still requires significant development before reaching its full commercial potential. This system not only offers enhanced water recovery, but also reduces the disposal issue of concentrated brine. Research data showed that the integration of vacuum-enhanced direct contact membrane distillation (VEDCMD) has achieved water recoveries up to 81% from the brines, however, it

suffers from scaling on membranes. Recently, Nano filtration (NF) has become highly important as an integrated process for commercial desalination industries. NF of aqueous and organic solutions has been used commercially for quite some time.

The combination of NF with other membrane separation processes was observed to be beneficial in terms of overall recovery and energy requirements. A recent study with nanofiltration (NF) membranes as a pre-treatment with MED was conducted by the SalineWater Desalination Research Institute (SWDRI) of SWCC and theWater Re-use Promotion Center (WRPC) of Japan together with Sasakura Engineering Co. Ltd. showed promising results in increasing the top brine temperature (TBT) from 65 C up to 125 C. The development of two stage NF-NF desalination systems was observed to be more effective than a conventional single stage RO system in removing mono and bivalent ions from seawater, as well as 20–30% lower energy costs.

Although the research has shown promising outcomes from the implementation of hybrid membrane systems in desalination and water treatment industries, the integrated systems need to be evaluated further to overcome their drawbacks. More studies are required to evaluate the overall energy consumption of the hybrid process as increase in energy consumption for a particular part may influence the energy consumption of the following process. The economic analysis of the mixed systems is one of the most important and crucial factors for determining the process viability, and very little information is available in this context.

It is concluded that benchmarking methods must be chosen depending on the purpose and extent of the analysis and reduction of energy cost of a complete system. Various benchmarking methods applied so far are mainly diagnostic tools that fail at prescribing any improvement strategy to make inefficient WWTPs efficient. Such strategies must be studied and implemented by managers through a better understanding of the plant operations. Membrane based treatment using solar energy has evolved as a solution to solve this problem and in the following chapter 4 it has been described in details.

References

1. Ang, W.L.; Mohammad, A.W.; Hilal, N.; Leo, C.P. A review on the applicability of integrated/hybrid membrane processes in water treatment and desalination plants. *Desalination* **2015**, *363*, 2–18.
2. Le, N.L.; Nunes, S.P. Materials and membrane technologies for water and energy sustainability. *Sustain. Mater. Technol.* **2016**, *7*, 1–28.
3. Bolin, B. *A History of the Science and Politics of Climate Change*; Cambridge University Press: Cambridge, UK, 2007.
4. Elimelech, M.; Phillip, W.A. The Future of Seawater Desalination: Energy, Technology, and the Environment. *Science* **2011**, *333*, 712–717.
5. Hondo, H. Life cycle GHG emission analysis of power generation systems: Japanese case. *Energy* **2005**, *30*, 2042–2056.
6. Böhringer, C.; Vogt, C. Economic and environmental impacts of the Kyoto Protocol. *Can. J. Econ. Rev. Can. D'économique* **2003**, *36*, 475–496.
7. Dincer, I. Environmental impacts of energy. *Energy Policy* **1999**, *27*, 845–854.
8. El-Kordy, M.N.; Badr, M.A.; Abed, K.A.; Ibrahim, S.M.A. Economical evaluation of electricity generation considering externalities. *Renew. Energy* **2002**, *25*, 317–328
9. Ali, A.; Tufa, R.A.; Macedonio, F.; Curcio, E.; Drioli, E. Membrane technology in renewable-energy-driven desalination. *Renew. Sustain. Energy Rev.* **2018**, *81*, 1–21.
10. Herzog, A.V.; Lipman, T.E.; Kammen, D.M. Renewable energy sources. In *Encyclopedia of Life Support Systems (EOLSS). Forerunner Volume—“Perspectives and Overview of Life Support Systems and Sustainable Development”*; University of California: Berkeley, CA, USA, 2001.
11. Johansson, T.B.; Burnham, L. *Renewable Energy: Sources for Fuels and Electricity*; Island Press: Washington, DC, USA, 1993.
12. Gibbins, J.; Chalmers, H. Carbon capture and storage. *Energy Policy* **2008**, *36*, 4317–4322.
13. Benson, S.; Bennaceur, K.; Cook, P.; Davison, J.; de Coninck, H.; Farhat, K.; Ramirez, C.; Simbeck, D.; Surles, T.; Verma, P. Carbon capture and storage. In *Global Energy Assessment—Toward a Sustainable Future*; Cambridge University Press: Cambridge, UK, 2012; p. 993.
14. Kajikawa, Y.; Yoshikawa, J.; Takeda, Y.; Matsushima, K. Tracking emerging technologies in energy research: Toward a roadmap for sustainable energy. *Technol. Forecast. Soc. Chang.* **2008**, *75*, 771–782. *Energies* **2018**, *11*, 2997–3021 of 32
15. Jacobsson, S.; Johnson, A. The diffusion of renewable energy technology: An analytical framework and key issues for research. *Energy Policy* **2000**, *28*, 625–640.
16. Chu, S.; Majumdar, A. Opportunities and challenges for a sustainable energy future. *Nature* **2012**, *488*, 294–303.

17. Sanders, D.F.; Smith, Z.P.; Guo, R.; Robeson, L.M.; McGrath, J.E.; Paul, D.R.; Freeman, B.D. Energy-efficient polymeric gas separation membranes for a sustainable future: A review. *Polymer* **2013**, *54*, 4729–4761.
18. Yip, N.Y.; Tiraferri, A.; Phillip, W.A.; Schiffman, J.D.; Hoover, L.A.; Kim, Y.C.; Elimelech, M. Thin-film composite pressure retarded osmosis membranes for sustainable power generation from salinity gradients. *Environ. Sci. Technol.* **2011**, *45*, 4360–4369.
19. Vörösmarty, C.J.; Green, P.; Salisbury, J.; Lammers, R.B. Global water resources: Vulnerability from climate change and population growth. *Science* **2000**, *289*, 284–288.
20. Arnell, N.W. Climate change and global water resources. *Glob. Environ. Chang.* **1999**, *9*, S31–S49.
21. Logan, B.E.; Elimelech, M. Membrane-based processes for sustainable power generation using water. *Nature*, **2012**, *488*, 313–319.
22. Côté, P.; Siverns, S.; Monti, S. Comparison of Membrane-based Solutions for Water Reclamation and Desalination. *Desalination* **2005**, *182*, 251–257.
23. Afgan, N.H. Sustainability Concept for Energy, Water and Environment Systems. In *Sustainable Energy Technologies: Options and Prospects*; Hanjalić, K., Van de Krol, R., Lekić, A., Eds.; Springer: Dordrecht, The Netherlands, 2008; pp. 25–49.
24. Evans, A.; Strezov, V.; Evans, T.J. Assessment of sustainability indicators for renewable energy technologies. *Renew. Sustain. Energy Rev.* **2009**, *13*, 1082–1088
25. Kurihara, M.; Takeuchi, H. SWRO-PRO System in “Mega-ton Water System” for Energy Reduction and Low Environmental Impact. *Water* **2018**, *10*, 48.
26. Ghaffour, N. The challenge of capacity-building strategies and perspectives for desalination for sustainable water use in MENA. *Desalin. Water Treat.* **2009**, *5*, 48–53.
27. El-Ghonemy, A.M.K. Future sustainable water desalination technologies for the Saudi Arabia: A review. *Renew. Sustain. Energy Rev.* **2012**, *16*, 6566–6597.
28. Ghaffour, N.; Missimer, T.M.; Amy, G.L. Technical review and evaluation of the economics of water desalination: Current and future challenges for better water supply sustainability. *Desalination* **2013**, *309*, 197–207.
29. Goh, P.S.; Ismail, A.F. Review: Is interplay between nanomaterial and membrane technology the way forward for desalination? *J. Chem. Technol. Biotechnol.* **2015**, *90*, 971–980.
30. Karagiannis, I.C.; Soldatos, P.G. Water desalination cost literature: Review and assessment. *Desalination* **2008**, *223*, 448–456.
31. Lee, K.P.; Arnot, T.C.; Mattia, D. A review of reverse osmosis membrane materials for desalination—Development to date and future potential. *J. Membr. Sci.* **2011**, *370*, 1–22.
32. Matsuura, T. Progress in membrane science and technology for seawater desalination—A review. *Desalination* **2001**, *134*, 47–54.
33. Nair, M.; Kumar, D. Water desalination and challenges: The Middle East perspective: A review. *Desalin. Water Treat.* **2013**, *51*, 2030–2040.

34. Service, R.F. Desalination freshens up. *Science* **2006**, 313, 1088.
35. Voutchkov, N. Energy use for membrane seawater desalination—Current status and trends. *Desalination* **2018**, 431, 2–14.
36. Council, N.R. *Desalination: A National Perspective*; National Academies Press: Washington, DC, USA, 2008.
37. Stillwell, A.S.; Webber, M.E. Predicting the specific energy consumption of reverse osmosis desalination. *Water* **2016**, 8, 601.
38. Greenlee, L.F.; Lawler, D.F.; Freeman, B.D.; Marrot, B.; Moulin, P. Reverse osmosis desalination: Water sources, technology, and today's challenges. *Water Res.* **2009**, 43, 2317–2348.
39. Van der Bruggen, B.; Vandecasteele, C. Distillation vs. membrane filtration: Overview of process evolutions in seawater desalination. *Desalination* **2002**, 143, 207–218.
40. Fritzmann, C.; Löwenberg, J.; Wintgens, T.; Melin, T. State-of-the-art of reverse osmosis desalination. *Desalination* **2007**, 216, 1–76.
41. Abad, E., Martínez, K., Planas, C., Palacios, O., Caixach, J., and Rivera, J. 2005. Priority organic pollutant assessment of sludges for agricultural purposes. *Chemosphere* 61:1358–1369.
42. Ak, N., and Dumrul, H. 2017. Wastewater treatment unit operations and processes. *Energy Educ. Sci. Tech-C* 9:1–12.
43. Aznar, M., San Anselmo, M., Manyà, J. J., and Murillo, M. B. 2009. Experimental study examining the evolution of nitrogen compounds during the gasification of dried sewage sludge. *Energy Fuels* 23:3236–3245.
44. Bharathiraja, B., Yogendran, D., Ranjith Kumar, R., Chakravarthy, M., and Palani, S. 2014. Biofuels from sewage sludge-A review. *Int. J. Chem. Tech. Res.* 6:4417–4427.
45. Barwal, A., and Chaudhary, R. 2014. To study the performance of biocarriers in moving bed biofilm reactor (MBBR) technology and kinetics of biofilm for retrofitting the existing aerobic treatment systems: a review. *Rev. Environ. Sci. Bio./Technol.* 13:285–299.
46. Berset, J. D., and Holzer, R. 1999. Quantitative determination of polycyclic aromatic hydrocarbons, polychlorinated biphenyls and organochlorine pesticides in sewage sludges using supercritical fluid extraction and mass spectrometric detection. *J. Chromatogr. A* 852:545–558.
47. Cai, Q.-Y., Mo, C.-H., Wu, Q.-T., Zeng, Q.-Y., and Katsoyiannis, A. 2007. Concentration and Speciation of heavy metals in six different sewage sludge-composts. *J. Hazard. Mater.* 147:1063–1072.
48. Demirbas, A. 2001. Recovery of boric and phosphoric acid residues from wastewater. *Int. J. Environ. Stud.* 58:805–811.
49. Demirbas, A. 2003. Fuels recovery from municipal solid and liquid wastes (MSLW). *Energy Sour.* 25:713–720.
50. Demirbas, A. 2006. Desulfurization of organic sulfur from lignite by electron transfer process. *Energy Sour. Part A* 28:1295–1301.

51. Demirbas, A. 2007. Adsorption of Co(II) and Hg(II) from water and wastewater onto modified lignin. *Energy Sour. Part A* 29:117–123.
52. Demirbas, A. 2008. Heavy metal adsorption onto agro based waste materials: A review. *J. Hazard. Mat.* 157:220–229.
53. Demirbas, A. 2016. Sulfur removal from crude oil using supercritical water. *Petrol. Sci. Technol.* 34:622–626.
54. Demirbas, A., Alidrisi, H., and Balubaid, M. A. 2015. API gravity, sulfur content and desulfurization of crude oil. *Petrol. Sci. Technol.* 33:93–101.
55. Demirbas, A., and Cakmak, I. 1996. Synthesis of epichlorhydrin-styrene block copolymers via cation-to-radical transformation process. *Macromolec. Rep. A* 33(Suppl10127–132).

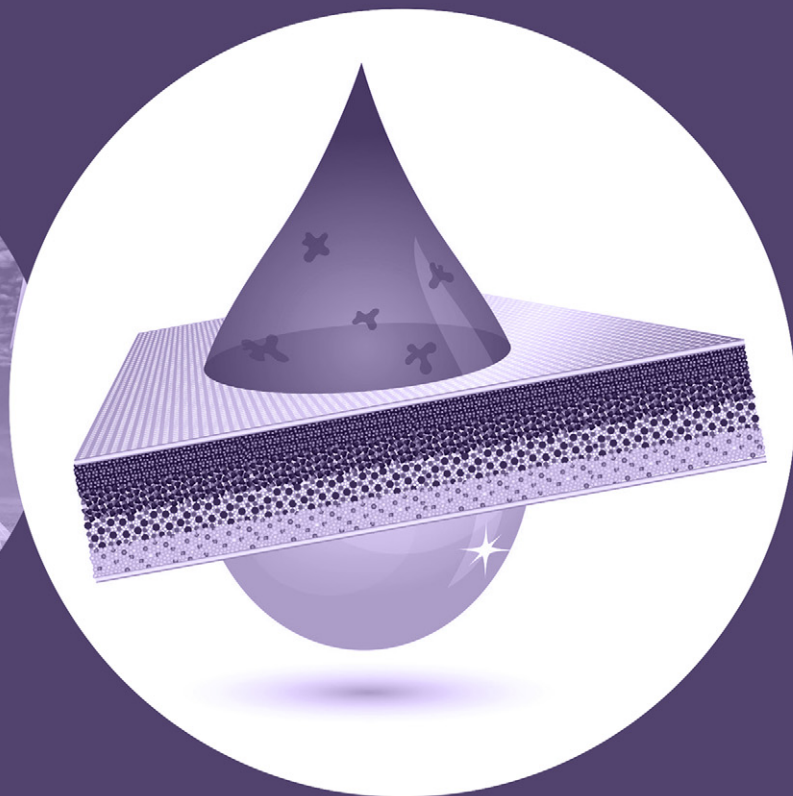
CHAPTER 4

Published Book Chapter



CURRENT TRENDS AND FUTURE DEVELOPMENTS ON (BIO-) MEMBRANES

RENEWABLE ENERGY INTEGRATED
WITH MEMBRANE OPERATIONS



EDITORS

ANGELO BASILE, ALFREDO CASSANO, ALBERTO FIGOLI

Renewable Energy-Powered Membrane Systems for Water Desalination

**A. Albloushi^{*}, A. Giwa^{*}, D. Mukherjee[†], V. Calabro[‡], A. Cassano[‡],
S. Chakraborty[†], S.W. Hasan^{*}**

^{}Department of Chemical Engineering, Khalifa University of Science and Technology, Abu Dhabi, United Arab Emirates, [†]Department of Informatics, Modeling, Electronics and Systems Engineering (DIMES), University of Calabria, Cosenza, Italy, [‡]ITM-CNR, Institute on Membrane Technology of the Italian National Research Council, Rende, Cosenza, Italy*

1 Introduction

Environmental disturbances arising from anthropogenic factors have necessitated calls for cleaner production of water and energy in recent times. Human activities have caused imbalances in carbon replenishment and emission of greenhouse gases, thereby leading to the deviations of nature from its state of carbon neutrality and stability (Walther et al., 2002). These imbalances are facilitated by humans' continued dependence on fossil fuels which invariably result in climate change (Whitmarsh et al., 2011; Wiedmann and Minx, 2008). Also, reserves of fossil fuels in geological formations are being depleted at an alarming rate and unconventional reservoirs are still being sourced worldwide. The unrestricted exploitation of crude oil and depletion of oil and gas resources pose significant threats to the environment and sustainability of mankind (Giwa et al., 2016a; Hughes and Rudolph, 2011). To address these threats, renewable and sustainable energy is needed to substitute fossil-based energy and reduce the release of hazardous emissions to the environment (Milano et al., 2016). Recently, thermal energy/electricity production from solar and wind-powered systems has been intensified in many places in the world. The global market share of solar and wind-based electricity has increased tremendously over the past few years and it is expected that the upward trend would be maintained (Pazheri et al., 2014; Kumar et al., 2016).

Energy is needed to produce fresh water; thus water-energy nexus is a crucial area of interest when considering the impact of fresh water production on sustainability (Giwa et al., 2017). A lot of fossil-based energy is consumed for water production worldwide, leading to considerable environmental impacts. As a result, schemes that can produce vast amounts of energy in a sustainable manner and ensure simultaneous production of fresh water are the most sought-after

systems (Manju and Sagar, 2017; Rakib et al., 2017). Such systems should be able to guarantee environmental and economic sustainability. Solar and wind energy are viable sources of sustainable energy because these sources are available everywhere in the world (Delucchi and Jacobson, 2011). Also, membrane desalination has been presented as a viable approach for fresh water production because of its numerous advantages over other methods, such as high quality of product water, lower energy consumption when compared to thermal approaches, and lower footprints (Koros, 2004; Alobaidani et al., 2008). The integration of solar and wind energy with membrane desalination would, therefore, play a significant role in the production of fresh water in the future.

Since 2004, within the frame of two European projects (SMADES and MEDIRAS), several compact solar-powered desalination units have been installed in different countries including Pozo Izquierdo and Tenerife (Gran Canaria), Alexandria (Egypt), Irbid (Jordan), Morocco, and Freiburg (Germany). Recently, compact systems have been installed in Tunisia and Tenerife and two more two loops systems have been installed in Gran Canaria and Pantelleria (Italy).

Five international water companies have been selected to construct and run pilot-scale membrane desalination plants integrated with renewable energy in in Abu Dhabi, United Arab Emirates (Todorova, 2014). The companies are: Spain's Abengoa, France's Degrémont (Suez), Veolia (Sidem) and Mascara, and the United States' Trevi Systems. The objective of the plants is to test the viability of the integrated systems to produce electricity for desalination in an environmentally friendly manner, and as precursors for the construction of large-scale desalination plants that would be run by renewable energy. Four of the five companies—Abengoa, Degrémont, Mascara, and Veolia—would test-run reverse osmosis (RO) pilot plants integrated with renewable energy while Trevi Systems would test-run a renewable energy-powered forward osmosis (FO) pilot plant. The pilot plants have a capacity of 1500 m³/day, enough to supply fresh water to 500 homes. Therefore, in this chapter, the recent advances in the integration of renewable energy with membrane desalination are presented. Solar and wind energy-powered desalination systems form the bulk of the systems developed recently; hence this chapter is focused mainly on these systems.

2 Solar Photovoltaic and Thermal Energy Integrated With Membrane Operations

Of all renewable energy sources, solar energy has been used mainly for membrane desalination. The integration of solar energy with membrane desalination has been predominantly studied in recent investigations and research articles (Ghaffour et al., 2014; Manju and Sagar, 2017; Gude, 2014). These research studies have focused mainly on membrane desalination techniques such as RO, FO, electrodialysis (ED) and membrane distillation (MD) for seawater and brackish water desalination. MD and RO technologies have been used primarily in recent solar

energy-powered seawater desalination. Small-scale solar powered MD systems are attractive for the production of fresh water in remote locations and rural areas where water and electricity infrastructures are unavailable. The integration of solar energy with MD is somehow a mature approach, as many studies have been carried out already in this area. However, the cost of water produced from small-scale solar powered MD system is comparatively higher than that produced from commercial RO systems because of the low productivity and high capital cost. Meanwhile, research on cheap and durable MD modules and solar collectors/photovoltaics (PV) panels will improve the economics of the solar power-assisted MD operations (Qtaishat and Banat, 2013).

2.1 Membrane Distillation Processes Driven by Thermal Solar Energy

Direct contact membrane distillation (DCMD) is a thermally driven membrane process in which the water vapor transfer is promoted by a vapor pressure difference between the two sides of a microporous hydrophobic membrane generated by a temperature difference: the feed is maintained at high temperature, while cold water is used as a stripping permeate. The mass transfer in DCMD can be described as a three-phase sequence: (1) formation of a vapor gap at the warm solution-interface; (2) transport of the vapor phase through membrane pores; (3) its condensation at the cold side membrane-solution interface (Lawson and Lloyd, 1997).

A promising system for renewable energy desalination is a low-temperature DCMD driven by thermal solar energy (Mathioulakis et al., 2007). This approach is well suited in arid regions characterized by high availability of solar energy, salt water surplus and fresh water shortage.

A compact solar thermal MD unit, operating with untreated seawater, was installed in the south of Jordan (Aqaba port) in 2006 (Banat et al., 2007). As illustrated in Fig. 1, the system had two loops, namely solar loop and desalination loop. The solar loop was constituted by flat-plate single-glassed collectors and a 3 m³ storage tank. The collectors were used to heat tap water pumped from the storage tank by a circulating pump. The desalination loop, separated by a heat exchanger from the solar loop, was constituted by spiral-wound polytetrafluoroethylene (PTFE) membrane module with 0.2 μm pore diameters, 35 μm thickness, and 80% porosity. The effective membrane area in each MD module was 10 m² (Fig. 1). Seawater with a conductivity of 55,000 μS/cm was successfully fed to the unit without any chemical pretreatment. The output from the unit was in the range of 2–11 L/day m² with specific energy consumption in the range of 200–300 kWh/m³. The distillate was water of low total dissolved solids (TDS) with a conductivity in the range of 20–250 μS/cm.

The estimated cost of potable water produced by the unit was 18 \$/m³ (Banat and Jwaied, 2008). The authors highlighted that membrane lifetime and plant lifetime are key factors in determining the water production cost. The cost decreases with increasing the membrane and/or plant lifetime.

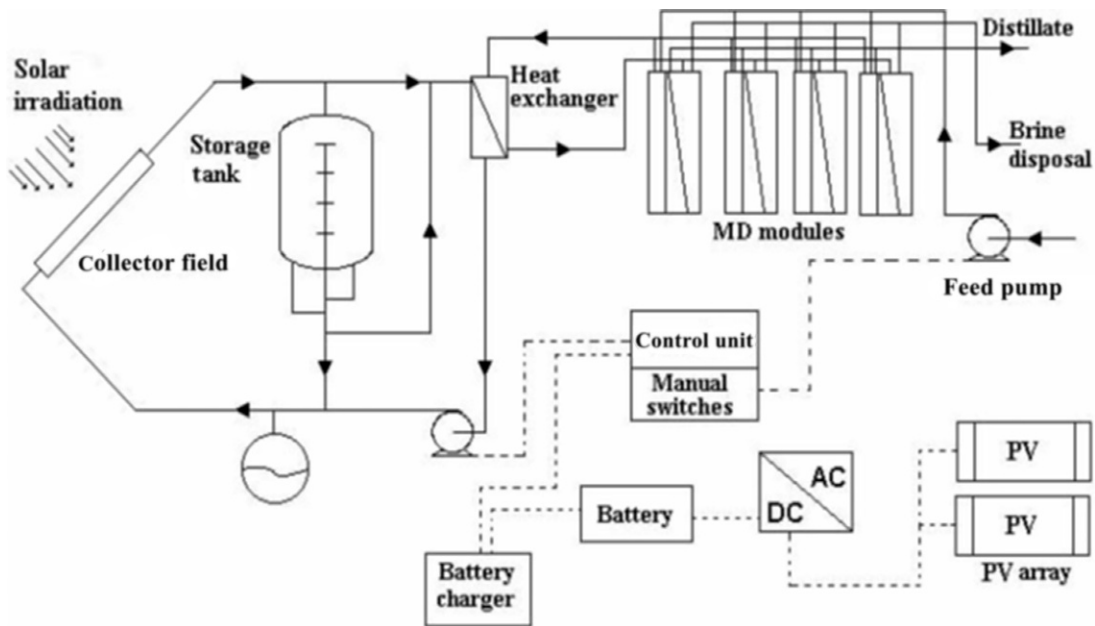


Fig. 1

Schematic diagram of the solar-powered membrane distillation unit installed in Aqaba, Jordan (Banat et al., 2007).

An ideal renewable heat source for MD systems is the salt-gradient solar pond (SGSP), a body of water that collects solar radiation and utilizes a salt gradient to store the collected solar radiation as thermal energy (Ruskowitz et al., 2014).

Common SGSPs consist of three distinct layers: (1) an upper convective zone (UCZ), consisting of the least saline water, located in the uppermost section of the solar pond; (2) a non-convective zone (NCZ), consisting of an increasing saline solution located below the UCZ; (3) a lower convective zone (LCZ), consisting of the most dense and saline solution, located below the NCZ. As the LCZ collects solar radiation and rises in temperature, the high salinity solution remains trapped below the NCZ due to its density. This salinity gradient allows the LCZ to collect and store solar energy for long time.

A schematic representation of a DCMD/SGSP system is illustrated in Fig. 2. In this approach seawater can be used as feed solution as well as a heat sink to maintain a low temperature in the permeate side of the membrane system (Suárez and Urtubia, 2016).

An experimental study of fresh water production in a coupled DCMD/SGSP system has been carried out recently to determine the fresh water production rates and the energetic requirements of the different components of the system (Suárez et al., 2015). It was found that the coupled DCMD/SGSP system treats approximately six times the water flow treated by a similar system that consisted of an air-gap membrane distillation unit driven by a SGSP.

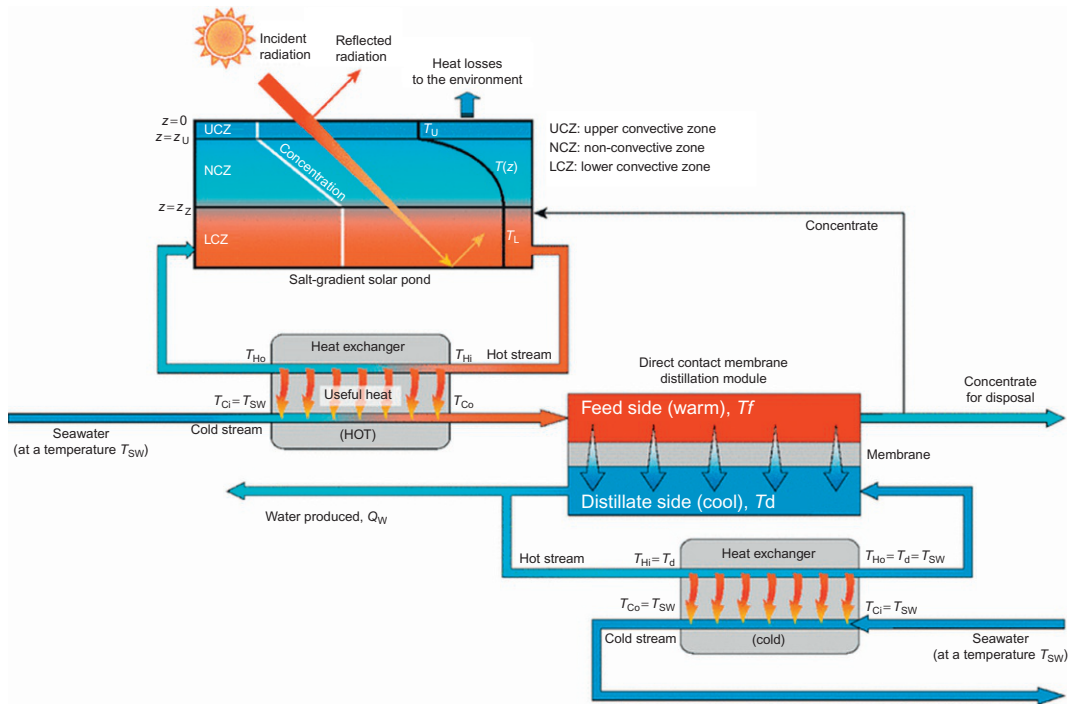


Fig. 2

Schematic representation of a membrane distillation system powered by a solar pond (Suárez and Urtubia, 2016).

In terms of the energetic requirements, approximately 70% of the heat extracted from the SGSP was utilized to drive thermal desalination and the rest was lost in different locations of the system. By reducing the heat losses throughout the system, higher water fluxes would be achieved. Therefore, further investigations on membrane properties, insulation of the system, or optimal design of the solar pond still need to be addressed in the future to address these heat losses.

Nakoa et al. (2015) investigated a DCMD/SGSP system by using a DCMD flat sheet membrane module (0.1 m^2) coupled to a 4.2-m-diameter, 1.85-m-deep solar pond located at the RMIT Bundoora east campus (Australia). Operating the DCMD module in a laminar regime ($\text{Re} \sim 500\text{--}2500$), the water production was of $1.2 \times 10^{-3} \text{ m}^3/\text{day}/\text{m}^2$ of solar pond when using a 1.3% of saline water as feed solution.

Tubular DCMD has also been integrated with solar power for fresh water production. Various geometric and operating frameworks on the system performance have been studied for this purpose (Elzahaby et al., 2016). The frameworks include the system temperature, water flow rate, salt absorption rate, cooling temperature, and the diameter of the system layer. The overall results indicated that productivity as well as the efficiency of the system can be increased by optimizing these operating conditions, indicating good opportunities for future prospects in the field.

Another solar energy-assisted DCMD system consisting of commercial PTFE membranes has been developed recently for seawater desalination. The energy consumption of the system was evaluated and an enhanced mathematical model was also employed to investigate the unsteady state predictions of permeate flux (Shim et al., 2015). For each membrane, the characterization of membrane properties, e.g., pore diameter, pore size distribution, the liquid entry pressure, and effective porosity was carried out. The theoretical and experimental investigations of long-term fouling phenomenon were also carried out. A two dimensional (2D) flat-plate dynamic model was developed from heat and mass transfer mechanisms and used for permeate flux predictions under different operating conditions. The numerical simulation agreed considerably with the experimental results. From the experimental investigation, the thermal power consumption was 896–1433 kWh/m³ and the gained output ratio (GOR) was 0.44–0.70. A continuous operation of the system run for more than 150 days showed that solar energy supplied about 77.3% of the thermal energy.

In another solar energy-assisted DCMD study, three commercially available hydrophobic microporous membranes (based on the pore size 0.2, 0.7 and 1.2 μm respectively) were used for seawater desalination (Palanisami et al., 2014). The dependence of permeation flux on operating conditions was investigated. By using a feed temperature of 65°C, permeate temperature of 25°C, flow rate of 2.5 L/min, and a short-term solar thermal power supply, i.e., for 1 day, desalination of real seawater was achieved without temperature control. Long-term seawater desalination (i.e., for 150 days) was also achieved by using both solar thermal and electric power. A very slight reduction of flux from 28.5 to 26.5 L/m² h was observed during the long-term investigation, indicating system feasibility.

An efficient integrated solar-driven desalination system based on the use of vacuum membrane distillation (VMD) has been developed by Chafidz et al. (2014, 2016). The system can be exploited in areas where electricity and potable water are not readily available. It consists of a solar-thermal system, a solar-PV system and a vacuum multi-effect membrane distillation (V-MEMD) module (Fig. 3).

The thermal collectors convert solar irradiation into thermal energy to drive the VMD process, whereas PV panel converts solar irradiation into electrical to power electrical equipment.

The system utilized solar energy without external energy from the grid. The distillate flux and the approximate conductivity of the distilled water produced by the system were of 1.5–2.6 L/m² h and 4.7 μS/cm, respectively.

Solar energy-assisted VMD has also been investigated recently by Zrelli et al. (2015). The effect of solar irradiation on the flow rate of the permeate produced by the VMD was evaluated. The membrane module was composed of two hollow fibers membrane wound in helically coiled shape. These fibers were placed in parabolic through concentrator absorber. The relatively hot solution (brine) in the absorber was used as the feed. A model was also developed

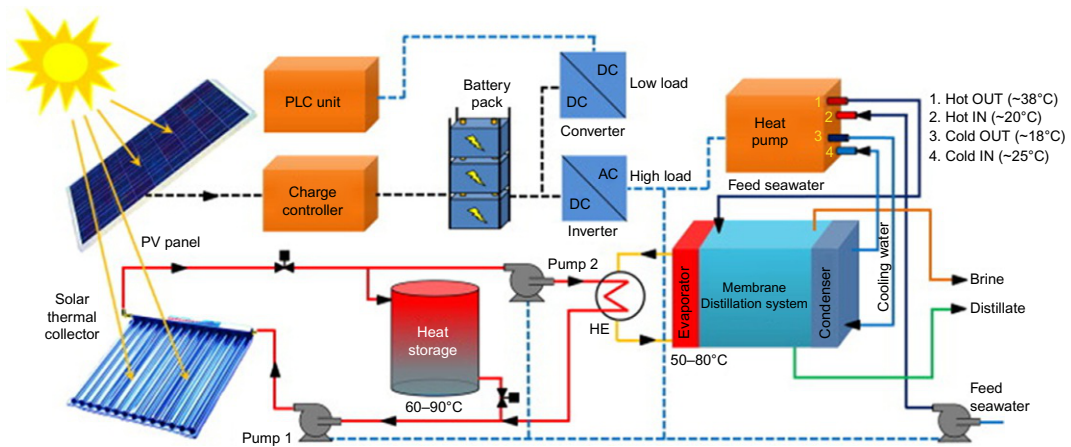


Fig. 3

Integrated solar-driven desalination system equipped with VMD membrane module (Chafidz et al., 2014).

by using the process governing equations and solved using the finite element method. The sensitivity of the permeate flow rate to the solar irradiation and feed salt concentration was obtained. When the solar irradiation increased from 200 to 800 W/m², the permeate flow rate rose from 0.14 to 0.36 kg/h. Meanwhile, a marginal effect of the feed salt concentration on the permeate flow rate was observed. An increase of the feed salt concentration from 10 to 300 g/L also resulted in a 12% drop of the permeate flux.

The Fraunhofer Institut of Solar Energy System (Freiburg, Germany) has developed a solar powered desalination system based on the use of spiral-wound air gap membrane distillation (AGMD) modules with internal heat recovery (Koschikowski et al., 2009). Koschikowski et al. (2003) indicate a distillate production ranging from 10 to 40 L/h for a module with a membrane surface area from 7 to 12 m², maximum feed flow rate of 500 L/h and specific thermal consumption in the range of 100–200 kWh/m³.

An original laboratory scale air gap membrane distillation (AGMD) unit for seawater desalination was designed and tested by Cipollina et al. (2012). Distillate flux varied from 2 to 12 L/m² h, with higher values achieved for higher feed flow rates and temperatures. On the basis of experimental data a conceptual design of a solar energy powered MD unit was carried out leading to a complete identification of design parameters and operating schemes.

2.2 RO Driven by Solar PV

PV-powered RO is considered one of the most-promising forms of renewable-energy-powered desalination. A schematic diagram of a PV-RO system is depicted in Fig. 4.

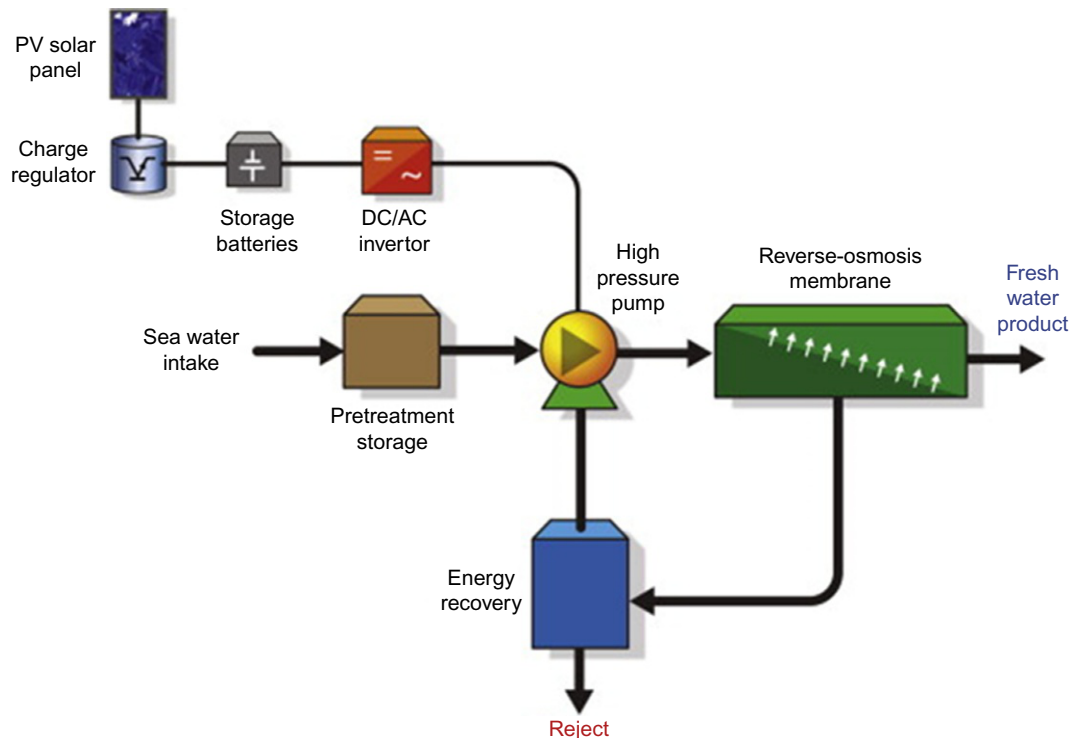


Fig. 4

Schematic diagram of a PV/RO system (Al-Karaghoul et al., 2010).

The osmotic pressure of seawater is much higher than that of brackish-water; therefore, its desalination requires much more energy and a larger PV array. In addition, plant components have to be mechanically resistant to the higher pressures found in seawater RO systems. Therefore, the total cost of water from seawater PV-RO systems is higher than that from brackish-water (Al-Karaghoul et al., 2010). Similarly, the capital and maintenance costs for a seawater treatment are higher when compared with those of a brackish water treatment due to the high costs of the membrane replacement. The energy requirement for brackish water desalination is in the range of 1–3 kWh/m³. It may exceed 15 kWh/m³ for seawater desalination.

In Saudi Arabia, frequent drought conditions and need for purified water are the main reasons for high water requirements. Solar PV are being tested in this country for the purpose of desalination because the cost of solar PV systems are becoming comparatively lower than those of fossil fuel-powered energy systems, which is gradually making PV-powered desalination systems to becoming a preferred choice nowadays. PV-RO plants have been constructed in Saudi Arabia. Two phases of these plants have been described in a recent study (Rand et al., 2016). The first phase includes the comparison between the technical equipment of dual-axis PV-RO plants using solar cells and other PV-RO plants using CdTe. The second phase includes

the cost analysis in which the condition of zero energy loss during storage is considered. From these investigations, it was observed that there is significant savings in diesel that is not used in the energy production process, which offset the cost of the PV panels. With the use of PV-RO plants, the financial cost and the harmful CO₂ emissions can be reduced extensively in Middle East region.

The use of PV as a power source to run a household RO unit was investigated by [Qiblawey et al. \(2009\)](#) by using water with a TDS concentration of 350 and 720 ppm and two different RO membranes (CSM and Filmtec). The performance of Filmtec membrane resulted better than the CSM membrane, with a production, on average, of 8 L/h of drinking water (about 16 ppm TDS) at specific energy consumption of 1.3 kWh/m³.

Small-scale PV powered seawater RO systems (up to 50 m³/day) have been developed by the Centre for Renewable Energy Systems Technology (CREST, UK) and by Instituto Tecnológico de Canarias (ITC) in Pozo Izquierdo, Gran Canaria Island. The first unit operated at variable flow without need of batteries at pressures between 38 and 51 bar. As feed water was used straight NaCl solution at around 32,800 ppm while the salinity of the permeate water varied between 470 and 800 ppm. The running costs were estimated at £2000 per year and the overall cost of water was around £2/m³ assuming a 20-year life of the system with pump replacement every 5 years and membrane replacement every year. The ITC system consisted of a 400 L/h seawater RO unit driven by a 4.8 kWp PV system and a 19 kW h battery backup system. The seawater salinity was of 35,000 ppm TDS, while the permeate salinity was <1000 ppm. The RO unit operated at 55 bar and a recovery ratio of 45%. The specific energy consumption was 5.5 kWh/m³. The estimated cost of the system was of 9 €/m³ ([Tzen et al., 2008](#)).

[Thomson and Infield \(2003, 2005\)](#) designed and tested a PV-powered seawater RO system without batteries ([Fig. 5](#)), since the rate of production of freshwater varied throughout the day according to the available solar power. The production of freshwater with the solar resource available in United Kingdom was of about 1.5 m³/day. A software model of the system predicted a production of over 3 m³/day nearer to the equator and with a PV array of only 2.4 kWp.

The desalination of brackish groundwater through a RO process driven by PV has been investigated to meet the water demands for irrigation and cooling of a greenhouse in north-west India ([Davies and Hossain, 2010](#)). Ventilation was produced by a fan which was tested and optimized with a PV module outdoors. For the RO system an optimal sizing of 0.12–1.3 m² of PV module per m² of membrane was estimated. The fan consumed <30 J of electrical energy per m³ of air moved which resulted less than that of standard fans. The energy consumption of the RO system (1–2.3 kWh/m³) was comparable to that reported in literature.

PV-powered RO is negatively affected by power fluctuations due to weather changes and clouds cover which may reduce the lifetime of membrane and quality of permeate. The use of batteries can improve the stability but it produces an increasing of both investment and

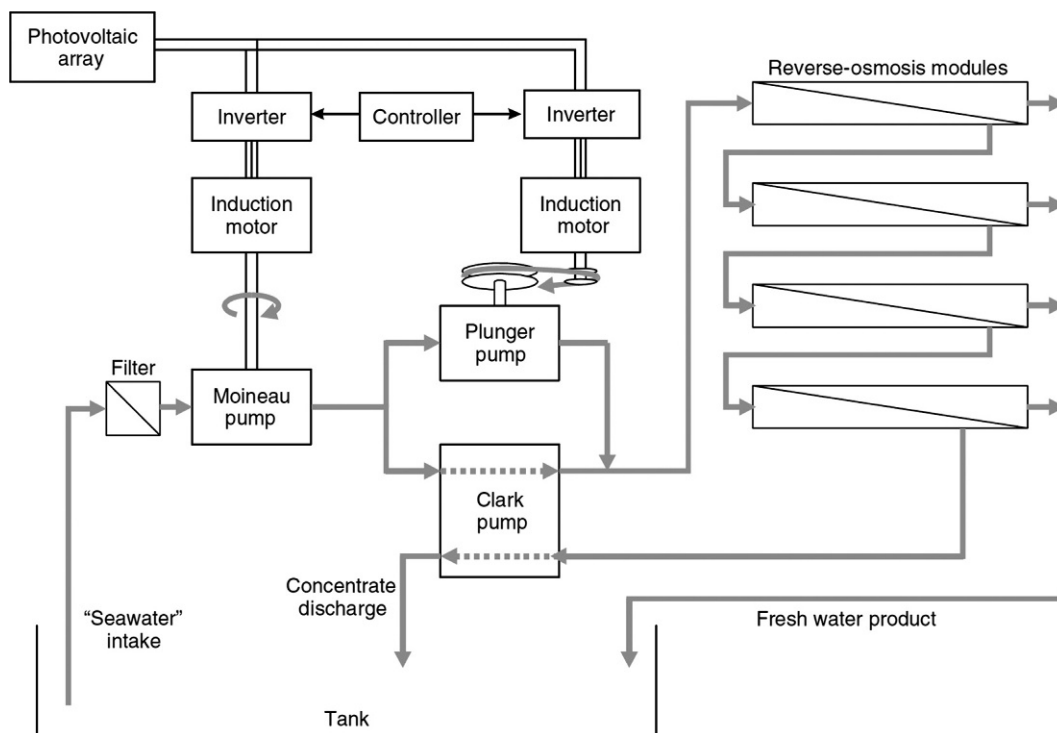


Fig. 5

PV-powered seawater RO system without batteries (Thomson and Infield, 2005).

maintenance costs. Another limitation is represented by biofouling of RO membranes especially for long-term operations (Ghermandi and Messalem, 2009).

2.3 ED Driven by PV

ED is based on the use of an electrical potential driving force and cationic- and anionic-exchange membranes installed in alternating series between two electrodes to separate charged components such as ions from a solution. The electrical current is carried through the solution, with the ions tending to migrate to the electrode with the opposite charge. The streams in alternating flow spacers are a sequence of diluted and concentrated water which flow in parallel to each other (Lee et al., 2002).

In a typical PV-ED system electrodes are connected to an outside PV source in a container of salt water. Salinity of the water is removed as water passes through ion-selective membranes positioned between the two electrodes (Fig. 6).

The integration of ED with solar PV is one of the very promising configurations that have been recently developed for brackish water desalination. For example, in a case study in the Canary

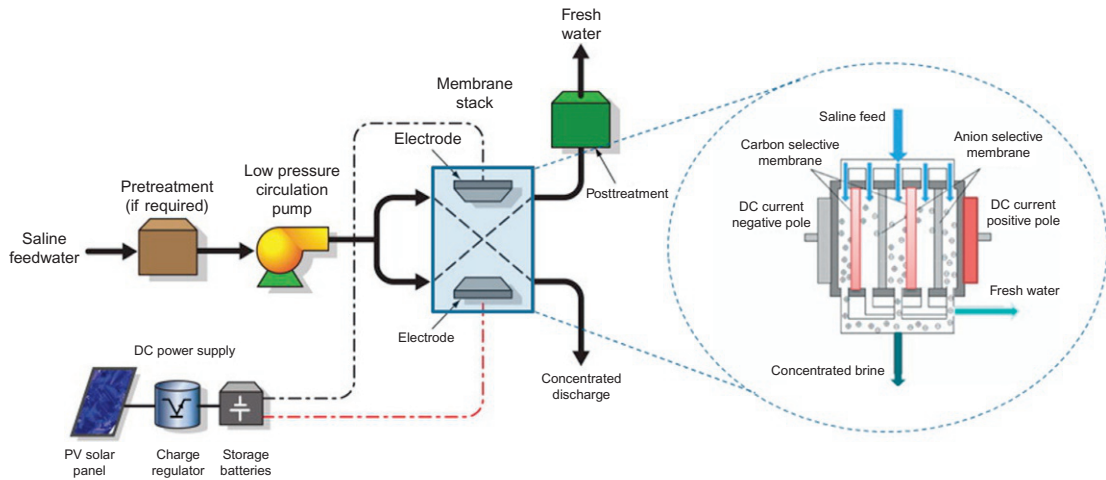


Fig. 6

Schematic diagram of a PV/ED system. Adapted from Al-Karaghoul, A., Renne, D., Kazmerski, L.L., 2010. *Technical and economic assessment of photovoltaic-driven desalination systems. Renew. Energy* 35, 323–328; Li, C., Goswami, Y., Stefanakos, E., 2013. *Solar assisted sea water desalination: a review. Renew. Sustain. Energy Rev.* 19, 136–163.

Islands, the sustainability of PV-ED integrated system for freshwater production through energy and environmental considerations was investigated (Fernandez-Gonzalez et al., 2015). PV-ED was compared with grid-connected system in the study. Energy consumption of 0.49–0.91 kWh/m³ was taken as the reference for the desalination of brackish water (2500–5000 mg/L) by PV-ED. From this energy consumption, the environmental impact of the PV-ED process in terms of CO₂ emission was 0.02–0.03 kgCO₂/m³ (only due to energy supply). This environmental impact is less than that contributed by the grid energy supply by one order of magnitude. Economic assessment also shows that PV-ED might be more cost-effective than conventional grid mix-supplied system, with a production costs of around 0.15–0.4 €/m³. Meanwhile, the major challenge associated with PV-ED is the inability to match intermittent output of the renewable energy with water demand in this location. This challenge hinders the capability of PV-ED to gain adequate market penetration. The efficiency of the solar panels is also a factor for consideration.

Solar PV-ED system has also been presented as an energy and cost-effective means of desalinating groundwater in rural India (Wright and Winter, 2014). The design requirements for a village-level scheme of PV-ED were provided. Saline groundwater, which underlies 60% of India, causes negative impact to human health. A quarter of India's population lives in villages of 2000–5000 people, many of whom do not have reliable access to electricity. Most village-scale, on-grid desalination plants use RO, which is economically infeasible in off-grid locations. Technical and ethnographic factors are used to develop an argument for PV-ED for rural locations, including: system capacity, biological and chemical contaminant removal;

water aesthetics; recovery ratio; energy source; economics of water provision; maintenance; and the energetic and cost considerations of available technologies. Within the salinity range of groundwater in India, ED requires less specific energy than RO (75% less at 1000 mg/L and 30% less at 3000 mg/L). At 2000 mg/L, this energetic scaling translates to a 50% lower PV power system cost for ED versus RO. PV-ED has the potential to greatly expand the reach of desalination units for rural India.

Another PV-ED integrated system has been employed to desalinate groundwater of medium salinity in Bahrain (AlMadani, 2003). Bahrain has sufficient solar irradiance. The country experiences about 13 h of sunshine per day during summer and 10 h of sunshine per day during winter. A small-scale ED stack consisting of 24 pairs of cells was employed. This stack was a commercial type and the cells were arranged in four hydraulic and two electrical stages. Two feed water sources were used, i.e., synthetic salt water prepared in the laboratory and groundwater of medium salinity at temperature of 10–40°C and product flow rates of 0.19–1.13 m³/day (50–300 gal/d). Experimental analysis showed that salt removal efficiency and product water concentration decreased when the flow rate was increased. However, higher temperatures resulted in improvements in the quality of the product water.

Ortiz et al. (2008) evaluated the feasibility of the desalination of brackish water from aquifers by a PV driven pilot scale ED system located in Alicante, Spain. The results indicated that the electric consumption to desalinate the water with a TDS ranging from 2329 until 5011 g/m³ to a potable quality (TDS < 400 g/m³) is in the range 0.92–1.69 kWh/m³. The cost of the desalinated water was estimated in the range of 0.14–0.23 €/m³ for irrigation uses and 0.17–0.32 €/m³ for drinking water uses.

Simple setup, compact design, robustness, and long lifetime of the energy supply system components are technical and techno-economic advantages of PV-ED integrated systems. On the other hand, the integration of ED with PV is limited by economical and technical barriers. Economical barriers, especially for seawater applications, are the large quantities of salt, the high cost of electrodes, the expensive ion exchange membranes and the relatively short life time of membranes when working in a high-density electric field (Li et al., 2013). A technical challenge is to establish suitable energy storage to smooth the output of renewable energy. For example, the use of batteries implies techno-economic problems such as premature battery failure and decrease in battery efficiency. In addition, ED can only remove salts and small amounts of charged organic compounds, while most of uncharged compounds remain in the treated water. Therefore integrated systems require specific unit operations for removing contaminants prior or after ED. In this view FO represents a new option as preliminary step to ED.

An integrated ED-FO system driven by solar energy, denoted as EDFORD (ED-FO Renewable energy Desalination), was investigated by Zhang et al. (2013) to produce potable water from secondary wastewater effluent or brackish water. In this approach, feedwater is drawn to the FO draw solution while organic and inorganic substances (ions, compounds, colloids, and

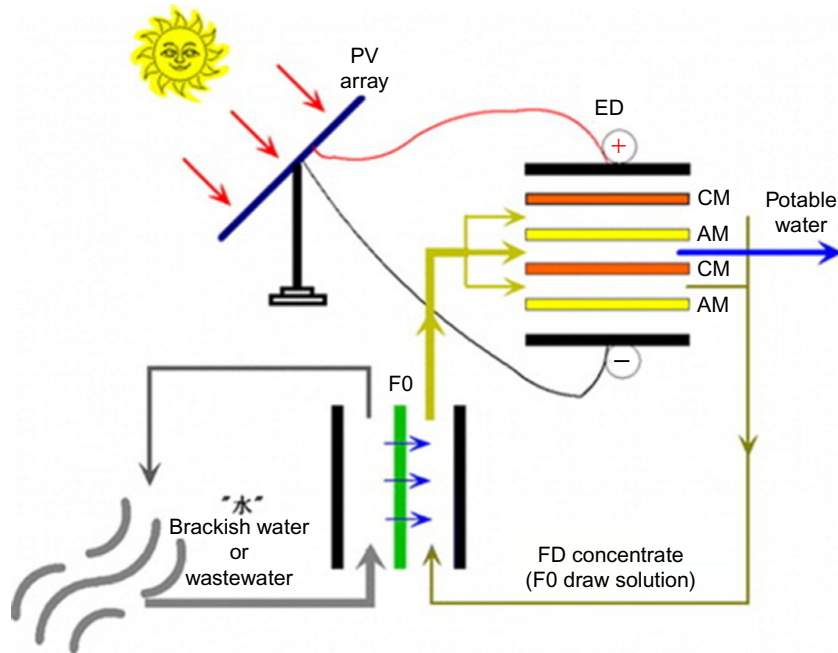


Fig. 7

Schematic diagram of a FO/ED integrated system driven by solar energy (Zhang et al., 2013).

particles) are rejected. The diluted draw solution is then pumped to the solar energy driven ED where the diluted draw solution is desalted producing high-quality water; the ED concentrate is recycled to the FO unit and reused as draw solution (Fig. 7). NaCl is used as draw solution to carry water from the brackish water to the ED unit where water is released by using solar energy; NaCl is recirculated in the system and no waste concentrate is discharged into the environment.

The water produced from the integrated system contained a low concentration of total organic carbon (TOC), low conductivity and parameters meeting potable water standards. The water production cost was estimated to be in the range 3.32–4.92 €/m³ for a small size potable water production system.

2.4 Electrodialysis Reversal—RO Driven by Solar Energy

To prevent scaling in ED the modern processes utilize inverters which reverse periodically (about every 20 min) the polarity of the electric field causing a reversal in the flow of ions and a cleaning of membrane surface. This process, called ED reversal, shows recoveries higher than other membrane technologies applied for brackish water desalination, such as RO, with average results higher than 90% (Valero and Arbós, 2010).

Pilot-scale experimental and modeling studies were performed by [Karimi et al. \(2015\)](#) to identify the energy consumptions of electrodialysis reversal (EDR) and RO when operated with different water salinities, flow rates, and temperatures. The pilot-scale experiments were conducted in at the Brackish Groundwater National Desalination Research Facility in Alamogordo, New Mexico. For the modeling, WATSYS software was used for EDR and Win Flows software was used for RO. From the experimental results, it was observed that product water flow rate and the salinity of feed water significantly affected the specific energy consumption (SEC) of EDR and RO. The SEC of EDR was more sensitive to feed water salinity variations, as compared to the SEC of RO. However, a slightly different response of the SEC of EDR and RO to product flow rate was observed. The SEC of EDR was not significantly influenced by temperature variations, while the SEC of RO was affected significantly by temperature variations. With the energy requirements for these systems identified under a range of operating conditions, HOMER software was used to identify optimal renewable energy systems for powering the desalination technologies under each combination of operating conditions. Lastly, the total net present cost of each renewable energy system was calculated, and the most economical systems were identified. It was proposed that solar energy can be used to power off-grid RO and ED/EDR systems at locations with similar environmental conditions as those of Alamogordo, New Mexico, by using the experimental/modeled energy consumption and production. For feed water with low salinity, solar-powered EDR was more efficient than solar-powered RO to a large extent, with a total net present cost difference of 48%–159%. However, for feed water with high salinity, solar-powered RO was more efficient.

Also, integrating renewable sources at lower scale units will not help in achieving the modular access for the RO units. However, small RO units might be applicable for use in the remote areas. A recent experimental study has examined the effects of weather change on the PV-powered brackish water RO desalination system in the inaccessible areas ([Alghoul et al., 2016](#)). It was observed that the power system was able to supply constant electricity without any external disturbance. The RO system cable units showed complete stability. The system was able to produce 5.1 m³ of fresh water when operating for 10 h daily. However, long exposure to the small cable units during the desalination system would create high temperature that is inadequate for the power units as well as for the battery room. The modeling of a solar PV-powered brackish water RO system has also been explored in Tunisia ([Laamari and Zghal, 2016](#)). The tourism sector, which is known as the huge market for pure water, was selected. So, the study aimed at providing autonomous gateways for RO systems powered by PV energy generator to produce fresh water in a hotel situated in Djerba Island, such that the system can be used to process the brackish water in the region to fresh water. The effectiveness of solar-powered PV desalination systems when solar irradiance is not stable is an important point to consider when operating these systems. Because of this reason, a recent study has explored the effect of solar irradiance variations on the performance of a brackish water RO system powered by solar energy ([Richards et al., 2015](#)). Unexpectedly, the water purification process was able to

run at solar radiant power lower than 400 W/m^2 (i.e., at the lowest energy levels). Thus, fluctuating energy source can also yield decent quantities of purified water with good quality. If a supercapacitor energy buffering is available, the system automatically becomes boosted in the shutdown period and yield good-quality desalinated water. At some instances, despite the system shutdown, good-quality water was produced and the system showed excellent performance in that duration.

2.5 FO Driven by Solar Energy

FO is an osmotic pressure-driven process for removing water across a selectively permeable membrane. The draw stream is a concentrated saline solution and the feed stream is generally low in salt concentration, facilitating the transport of water from the feed side to the draw solution, under the osmotic pressure gradient (Giwa et al., 2016b). FO has a high rejection of a wide range of contaminants and a lower fouling tendency if compared with pressure-driven membrane operations (Akther et al., 2015).

Solar energy has also been integrated with FO desalination technology for brackish water desalination. In one of the latest developments, bilayer polymer hydrogels were tested as the draw agent in the FO process (Razmjou et al., 2013). These hydrogels contained a water-absorptive layer consisting of particles of sodium acrylate and *N*-isopropylacrylamide copolymer, which provided the osmotic pressure. The hydrogels also contained a dewatering layer that contained particles of *N*-isopropylacrylamide, which allowed the steady release of the absorbed water during the regeneration step at 32°C . Concentrated solar energy was used as the thermal energy source during the regeneration step. The high temperature provided by the concentrated solar energy ensured that the lower critical solution temperature of the dewatering layer could be rapidly attained. When the solar concentrator increased the input energy from 0.5 to 2.0 kW/m^2 , the dewatering flux increased from 10 to $25 \text{ L/m}^2 \text{ h}$. The minimum energy required by this hydrogel-driven FO process was also obtained via thermodynamic analysis. Aside from the use of electricity produced from solar PV, there are few recent studies on the application of solar thermal energy for the desalination of brackish and low-salinity water (Mohan et al., 2016). Solar thermal energy is also applicable for decentralizing the water purification process in places with high solar irradiance. The gap between water scarcity and availability of solar energy in arid countries could help in migrating desalinated water to various water-deprived areas when desalination processes that utilize solar energy are deployed (Zaragoza et al., 2014).

2.6 Modeling of Renewable Energy-Powered Membrane Desalination Systems

Some modeling methods such as fresh water pinch analysis (FWPA), Energy PLAN analysis, and Aspen Custom Modeler (ACM) analysis have been used recently to show the viability of renewable energy-powered membrane desalination systems. The main aim of the FWPA

technique is to reduce the use of electricity consumption and improve groundwater recovery when a water storage tank is used during RO desalination (Janghorban Esfahani and Yoo, 2016). There are many types of equipment employed to check the use of electricity power, water storage capacity in tank and wasted electricity during the RO desalination. FWPA tools form an optimization algorithm that helps in understanding the annual cost of the system during the first year and normal operation year.

The Energy PLAN is an advanced energy tool through which analysis regarding the proper distribution of the renewable sources in a water desalination process can be carried out. Through Energy PLAN, a six-step structure has been designed for the development of renewable energy resources in Jordan, in such a way that renewable sources can be made to account for up to 76% of energy production (Novosel et al., 2015). Jordan is a water-deprived country but it also comprises of abundant renewable resources like solar and wind energy. Practically, renewable sources are not being utilized currently; instead imported fossil fuels are used for the water purification process leading to the emission of harmful CO₂ emissions that causes environmental pollution. From the analysis, it was observed that renewable sources like wind energy and PV units can be utilized to overcome these challenges when they are integrated with RO desalination process and brine- operated pump storage units. The brine pump used in the process will manage the fluctuation in weather conditions and reduce the use of fossil fuels.

Exergy analysis of renewable energy integrated with membrane operations is another recent modeling technique (Akhatov, 2016). Exergy analysis is used to investigate the condition whereby the system and surrounding reach an equilibrium point during the process of energy distribution for water desalination process. Exergy analysis is important to check the loss of energy during RO desalination process. Exergy analysis checks the exergy input and destruction, and shows the exergy flow rates at various RO system levels. Once the flow rates are available, the destroyed exergy components can be determined from the exergy balance process. Hence, exergy analysis is important from a thermodynamic point for proper utilization of solar energy during the RO desalination process.

The thermal efficiency reduction caused by temperature polarization is one of the main drawbacks in MD processes for water desalination coupled with solar thermal energy. In order to reduce temperature polarization phenomena, Cipollina et al. (2009) evaluated the effect of spacer and channel geometry through the use of computational fluid dynamics (CFD) techniques. A reference geometry was built to simulate flow and temperature fields of a portion of a spiral wound MD module channel. Results indicated that spacers can significantly affect temperature gradients within the channel modifying the effective driving force between both faces of the membrane.

A dynamic simulation model for a solar-driven MD desalination system has been developed on the ACM platform to optimize the system performance (Chang et al., 2010). This rigorous model was developed for a spiral-wound AGMD module. The model considered the heat and

mass transfer resistances associated with each composing layer. The effects of adopting different objective functions, solar radiation conditions, thermal storage tank configurations, as well as the flow rates to the MD module and the thermal storage tank on the optimized performance are reported. It was observed that a simple thermal storage tank and low flow rates are drivers of high water production rate. A control system using conventional PI (proportional/integral) controllers was proposed and the water production rate can reach about 87% of the optimal result during clear sky operation.

Recently, a computer model has been developed to simulate the performance of an integrated solar thermal driven DCMD system for seawater desalination using recorded weather data (Duong et al., 2017). Results indicated that the DCMD module exhibited a similar thermal efficiency under co-current and counter-current flow; however, the counter-current flow produced higher water fluxes, particularly at high feed temperatures. Indeed, at a high feed inlet temperature, a large ΔT value can be obtained and maintained along the membrane module, resulting in a higher water flux. In addition, simulation results indicated that an increase of cross flow velocities in feed and distillate sided increased ΔT under both co-current and counter-current configurations thus improving the process water flux and thermal efficiency.

By contrast, in the solar thermal DCMD process an increasing of water cross flow velocities reduced both water flux and thermal efficiency. This was attributed to the limited supply of solar thermal at any given time, with a consequent decrease of feed temperature when cross flow velocity is increased.

The simulated solar thermal driven DCMD system achieved a higher daily distillate production rate per m^2 of membrane. It was estimated that a system equipped with a 7.2 m^2 spiral-wound DCMD module and a 22.6 m^2 flat plate solar thermal collector can produce 19.7 kg of clean water per m^2 of membrane or 6.3 kg of clean water per m^2 of solar thermal collector.

A mathematical model to assess a DCMD/SGSP coupled system was developed by Suárez and Urtubia (2016). It was validated using experimental data available in literature. Results confirmed the suitability of the system in areas with high availability of water and salts and with enough solar radiation. Maximum freshwater flow rates and expected freshwater productions were of 3.0 L/day/m^2 of solar pond and 2.5 L/day/m^2 of solar pond, respectively. The coupled system had a thermal power consumption of $880 \pm 60 \text{ kWh/m}^3$ of distillate, similar to that of other MD systems. Authors estimated that the membrane area should be 1000 times smaller than the area of the solar pond to achieve continuous and sustainable operation.

Aside from developed software and mathematical applications, global mathematical models from conventional heat and mass balances have also been applied for renewable energy integrated with membrane desalination systems. Another model has been developed to test the performance and sensitivity of a MD unit integrated with a solar collector system to fluctuating internal and external conditions (Boukhriss et al., 2016). A global mathematical model was

used to investigate the operating methods and fluctuating parameters during the desalination process. Solar PV power has also been autonomously coupled with ED technology. Mathematical models, with particular emphasis on the ED process, were developed for process control to ensure that the product water quality is not influenced by fluctuations due to concentration, solar radiation and input flow to the ED cells (Troncoso et al., 2014). Simulation results for process monitoring based on the concept of sliding modes are presented. To reduce the cost and improve the reliability of PV-powered desalination systems, an ED system integrated with PV modules without battery storage or regulator has also been studied to solve the problem of drinking water shortage in South East of Spain (Ortiz et al., 2006). This location is an isolated area without electric grid connection but with access to contaminated brackish water wells. A mathematical model and experiments were used to investigate the feasibility of the integrated system under different environmental conditions. A good agreement between model simulation and experimental data was obtained. This model also provides an opportunity to design the PV unit in terms of the quantity and configuration of PV modules required to desalinate brackish water under different environmental conditions.

3 Wind Energy Integrated With Membrane Operations

Apart from solar energy, wind energy is another renewable energy source that has been considered for integration with membrane desalination in many recent studies. The implementation of wind energy for water desalination has become more advantageous because of its cost-effectiveness. Wind energy systems are more adaptable at higher levels to domestic, industrial, and agricultural production. The technological and economic aspects of fresh water production through a wind-powered desalination system for the small coastal areas and islands have been presented in a recent study (Gökçek and Gökçek, 2016). Unit costs and energy requirement tests were carried out to understand the benefits of using wind-powered desalination RO system. Upon estimation, the cost of water production through wind turbines was US\$2.9–6.5 per m³. It was also observed that CO₂ emissions reduced significantly when wind power was used for water purification, as compared to conventional energy sources. Overall, there was a reduction in the electricity costs as well, thereby indicating the benefits of using wind-powered RO plants in these areas. The Gulf Council Cooperation (GCC) has recently identified wind-powered RO desalination as a cost-effective process. An economic assessment of the Liwa ASR RO plant for water desalination through wind power has been carried out (Loutatidou et al., 2017). Since the RO plant was not established as the sole source of water in the region, the fluctuation in wind power was acceptable, making it economically viable on the days when the wind power was inadequate. The wind power system was found to be competitive economically in the GCC region as compared to the existing thermal systems for desalination.

Generalized design curves for process and operation variables of a wind-powered unit for RO desalination were derived by [Kiranoudis et al. \(1997\)](#). Authors reported that the unit cost of freshwater production by a conventional RO plant can be reduced up to 20% for regions with an average wind speed of 5 m/s or higher.

[Robinson et al. \(1992\)](#) evaluated the performance of a small-scale wind-powered RO system equipped with a small diesel or portable gasoline pump used in case of low available wind power. The system produced from 0.5 to 1 m³/day of fresh water which is the estimated volume needed by a typical remote community in Australia.

A prototype wind-powered RO system was also developed by [Liu et al. \(2002\)](#) for brackish water desalination. Data indicated that a feedwater flow of about 13 L/min could be maintained by this system at an average wind speed of 5 m/s. The average rejection rate and recovery ratio were 97% and 20%, respectively.

Wind energy-powered ED systems have also been studied in recent investigations. A wind-ED system with no energy storage was developed with the aim of investigating the impact of wind speed (2–10 m/s), turbulence intensities (0–0.6 TI), and periods of oscillation (0–180 s) on desalination performance and energy consumption ([Malek et al., 2016](#)). The system produced good-quality drinking water (600 mg/L NaCl) over the range of parameters tested. Water production and energy consumption increased with wind speed, until both factors leveled off at wind speeds above the rated value of the wind turbine (rated: 7.9–8.4 m/s). The impact of wind speed fluctuations on system performance was insignificant up to a TI of 0.4 (i.e., moderate fluctuations). The water production declined under high turbulence intensity fluctuations (TIs ≥ 0.5) and long periods of oscillation (N40 s). The main challenge in direct coupling of ED to wind energy was not the magnitude of fluctuations but the impact of power cycling off during long periods of oscillation and lengthy periods of no wind. Interestingly, the specific energy consumption of the process remained relatively unaffected by the fluctuations, suggesting the system to be an electrically robust and reliable off-grid desalination technique for remote water-stressed locations. Off-grid wind energy system has been used to run an ED brackish water desalination plant, as part of test studies carried out in Gran Canaria Island (Spain) ([Veza et al., 2004](#)). The off-grid system is a medium-scale wind farm. Meanwhile, adequate knowledge of the behavior of off-grid wind energy system is required before the system behavior can be analyzed; hence the operational modes and possible constraints were studied by running some test operations. The integrated system included power converters used as DC drivers and variable frequency drivers for the feed pump. The test studies were conducted to investigate the adaptability of the EDR unit to variations and intermittency of the wind power. The flow rate and conductivity of the product water were 3–8.5 m³/h and 200–500 μ S/cm, respectively. The power requirement was 4–19 kW. A control system that was slightly modified from a standard design was employed to ensure that the integrated system would be able to cope with sudden drops and rise of wind power. The EDR unit showed good flexibility with the wind power.

4 Hybrid Renewable Energy Systems Integrated With Membrane Operations

Hybrid solar and wind energy systems integrated with membrane desalination operations have been shown to be able to address daily and seasonal variabilities in these renewable energy sources. Excess wind energy, for example, can create serious problems and a wind farm might become difficult to operate under such an adverse condition. Hence a new system has been proposed in which renewable energy sources comprising of solar PV, diesel, and potential energy are combined with wind energy (Lai et al., 2016). Successful implementation and combination of these energy sources and the selection of the right operating conditions and energy storage can aid the design of a wind powered RO system. Multi-skid RO system has also been used to recover the energy loss due to fluctuations that occur during the transfer of renewable energy to the desalination process (Ntavou et al., 2016). Due to changing climate conditions, the use of solar and wind energy fluctuates the energy transmission process and hinders the water purification process. This system consists of three parallel skids that are used for the desalination process. A configuration of these three subsystems was introduced under the constant watch of axial position meter for the energy recovery process. The three subunits comprise of appropriate instruments, frequency inverters, and high-pressure pump frequency. After the process is tested under the three subunits using the local climate conditions, the power input from the PV resources was increased by about 10–20 kWp. Hence, a suitable condition for the RO desalination process using renewable energy sources was provided. Hybrid PV-wind-battery and power-to-gas (PtG) power plants have also been used to generate electricity for water desalination. It has been shown that plants using these resources can ensure competitive costs and lesser environmental pollution. The global costs for water in 2030 are estimated at 0.6–2.8 €/m³ but these can be marginally reduced with the use of these hybrid renewable sources (Caldera et al., 2016).

Recently, the dynamic performance characteristics of an RO plant integrated within hybrid energy systems configurations under flexible operation have been investigated (Kim et al., 2016).

Simulation results involving several case studies suggest that RO plants, when integrated with hybrid systems can provide operational flexibility to participate in energy management at the utility scale by dynamically optimizing the use of excess electrical energy.

5 Conclusions and Future Trends

Solar energy-assisted DCMD and VMD, solar PV-RO, salinity gradient-solar power-reverse electrodialysis (SGPRE), salt-gradient solar pond (SGSP), and solar PV-ED systems are some of the recent membrane desalination systems integrated with renewable energy for seawater and brackish water desalination. Modeling and simulation of solar energy requirements and fresh water production have also been carried out using WATSYS software, Win Flows

software, fresh water pinch analysis, Energy PLAN analysis, Aspen Custom Modeler and exergy analysis in recent studies. For wind energy, RO and ED are the main desalination processes that have been integrated with wind energy recently. To address the fluctuations in solar and wind energy, and optimize cost and productivity, hybrid systems such as solar PV-diesel-potential energy-wind energy, multi-skid RO system, PV-wind battery and PtG power plants have also been developed. These systems are contributing to the environmental, economic, and social sustainability of desalination processes.

List of Acronyms

ACM	Aspen Custom Modeler
AGMD	air gap membrane distillation
DCMD	direct contact membrane distillation
ED	electrodialysis
EDR	electrodialysis reversal
FO	forward osmosis
FWPA	fresh water pinch analysis
GOR	gained output ratio
LCZ	lower convective zone
MD	membrane distillation
NCZ	non-convective zone
PTFE	polytetrafluoroethylene
PV	photovoltaics
RO	reverse osmosis
SEC	specific energy consumption
SGSP	salt-gradient solar pond
TDS	total dissolved solids
TI	turbulence intensity
UCZ	upper convective zone
VMD	vacuum membrane distillation

References

- Akhatov, J.S., 2016. Energy and exergy analysis of solar PV powered reverse osmosis desalination. *Appl. Sol. Energy* 52, 265–270.
- Akther, N., Sodiq, A., Giwa, A., Daer, S., Arafat, H.A., Hasan, S.W., 2015. Recent advancements in forward osmosis desalination: a review. *Chem. Eng. J.* 281, 502–522.
- Alghoul, M.A., Poovanaesvaran, P., Mohammed, M.H., Fadhil, A.M., Muftah, A.F., Alkilani, M.M., et al., 2016. Design and experimental performance of brackish water reverse osmosis desalination unit powered by 2 kW photovoltaic system. *Renew. Energy* 93, 101–114.
- Al-Karaghoul, A., Renne, D., Kazmerski, L.L., 2010. Technical and economic assessment of photovoltaic-driven desalination systems. *Renew. Energy* 35, 323–328.
- AlMadani, H.M.N., 2003. Water desalination by solar powered electrodialysis process. *Renew. Energy* 28, 1915–1924.
- Alobaidani, S., Curcio, E., Macedonio, F., Di Profio, G., Alhinai, H., Drioli, E., 2008. Potential of membrane distillation in seawater desalination: thermal efficiency, sensitivity study and cost estimation. *J. Membr. Sci.* 323, 85–98.

- Banat, F., Jwaied, N., 2008. Economic evaluation of desalination by small-scale autonomous solar-powered membrane distillation units. *Desalination* 220, 566–573.
- Banat, F., Jwaied, N., Rommel, M., Koschikowski, J., Wiegand, M., 2007. Performance evaluation of the “large SMADES” autonomous desalination solar-driven membrane distillation plant in Aqaba, Jordan. *Desalination* 217, 17–28.
- Boukhriss, M., Zhani, K., Ben Bacha, H., 2016. Optimization of membrane distillation (MD) technology for specific application desalination. *Int. J. Adv. Manuf. Technol.* 88, 55–66.
- Caldera, U., Bogdanov, D., Breyer, C., 2016. Local cost of seawater RO desalination based on solar PV and wind energy: a global estimate. *Desalination* 385, 207–216.
- Chafidz, A., Al-Zahrani, S., Al-Otaibi, M.N., Hoong, C.F., Lai, T.F., Prabu, M., 2014. Portable and integrated solar-driven desalination system using membrane distillation for arid remote areas in Saudi Arabia. *Desalination* 345, 36–49.
- Chafidz, A., Kerme, E.D., Wazeer, I., Khalid, Y., Ajbar, A., Al-Zahrani, S., 2016. Design and fabrication of a portable and hybrid solar-powered membrane distillation system. *J. Clean Prod.* 133, 631–647.
- Chang, H., Wang, G.B., Chen, Y.H., Li, C.C., Chang, C.L., 2010. Modeling and optimization of a solar driven membrane distillation desalination system. *Renew. Energy* 35, 2714–2722.
- Cipollina, A., Di Miceli, A., Koschikowski, J., Micale, G., Rizzuti, L., 2009. CFD simulation of a membrane distillation module channel. *Desalin. Water. Treat.* 6, 177–183.
- Cipollina, A., Di Sparti, M.G., Tamburini, A., Micale, G., 2012. Development of a membrane distillation module for solar energy seawater desalination. *Chem. Eng. Res. Des.* 90, 2101–2121.
- Davies, P.A., Hossain, A.K., 2010. Development of an integrated reverse osmosis-greenhouse system driven by solar photovoltaic generators. *Desalin. Water. Treat.* 22, 161–173.
- Delucchi, M.A., Jacobson, M.Z., 2011. Providing all global energy with wind, water, and solar power, part II: reliability, system and transmission costs, and policies. *Energy Policy* 39, 1170–1190.
- Duong, H.C., Xia, L., Ma, Z., Cooper, P., Ela, W., Nghiem, L.D., 2017. Assessing the performance of solar thermal driven membrane distillation for seawater desalination by computer simulation. *J. Membr. Sci.* 542, 133–142.
- Elzahaby, A.M., Kabeel, A.E., Bassuoni, M.M., Elbar, A.R.A., 2016. Direct contact membrane water distillation assisted with solar energy. *Energy Convers. Manag.* 110, 397–406.
- Fernandez-Gonzalez, C., Dominguez-Ramos, A., Ibañez, R., Irabien, A., 2015. Sustainability assessment of electrodialysis powered by photovoltaic solar energy for freshwater production. *Renew. Sustain. Energy Rev.* 47, 604–615.
- Ghaffour, N., Bundschuh, J., Mahmoudi, H., Goosen, M.F.A., 2014. Renewable energy-driven desalination technologies: a comprehensive review on challenges and potential applications of integrated systems. *Desalination* 356, 94–114.
- Ghermandi, A., Messalem, R., 2009. Solar-driven desalination with reverse osmosis: the state of the art. *Desalin. Water. Treat.* 7, 285–296.
- Giwa, A., Akther, N., Housani, A., Haris, S., Hasan, S.W., 2016a. Recent advances in humidification dehumidification (HDH) desalination processes: improved designs and productivity. *Renew. Sustain. Energy Rev.* 57, 929–944.
- Giwa, A., Akther, N., Dufour, V., Hasan, S.W., 2016b. A critical review on recent polymeric and nano-enhanced membranes for reverse osmosis. *RSC Adv.* 6, 8134–8163.
- Giwa, A., Alabi, A., Yusuf, A., Olukan, T., 2017. A comprehensive review on biomass and solar energy for sustainable energy generation in Nigeria. *Renew. Sustain. Energy Rev.* 69, 620–641.
- Gökçek, M., Gökçek, Ö.B., 2016. Technical and economic evaluation of freshwater production from a wind-powered small-scale seawater reverse osmosis system (WP-SWRO). *Desalination* 381, 47–57.
- Gude, V.G., 2014. Energy storage for desalination processes powered by renewable energy and waste heat sources. *Appl. Energy* 137, 877–898.
- Hughes, L., Rudolph, J., 2011. Future world oil production: growth, plateau, or peak? *Curr. Opin. Environ. Sustain.* 3, 225–234.
- Janghorban Esfahani, I., Yoo, C., 2016. An optimization algorithm-based pinch analysis and GA for an off-grid batteryless photovoltaic-powered reverse osmosis desalination system. *Renew. Energy* 91, 233–248.

- Karimi, L., Abkar, L., Aghajani, M., Ghassemi, A., 2015. Technical feasibility comparison of off-grid PV-EDR and PV-RO desalination systems via their energy consumption. *Sep. Purif. Technol.* 151, 82–94.
- Kim, J.S., Chen, J., Garcia, H.E., 2016. Modeling, control, and dynamic performance analysis of a reverse osmosis desalination plant integrated within hybrid energy systems. *Energy* 112, 52–66.
- Kiranoudis, C.T., Voros, N.G., Maroulis, Z.B., 1997. Wind energy exploitation for reverse osmosis desalination plants. *Desalination* 109, 195–209.
- Koros, W.J., 2004. Evolving beyond the thermal age of separation processes: membranes can lead the way. *AIChE J.* 50, 2326–2334.
- Koschikowski, J., Wieghaus, M., Rommel, M., 2003. Solar thermal-driven desalination plants based on membrane distillation. *Desalination* 156, 295–304.
- Koschikowski, J., Wieghaus, M., Rommel, M., 2009. Membrane distillation for solar desalination. In: Cipollina, A., Micale, G., Rizzuti, L. (Eds.), *Seawater Desalination*. Springer-Verlag, Berlin, Heidelberg.
- Kumar, Y., Ringenberg, J., Depuru, S.S., Devabhaktuni, V.K., Lee, J.W., Nikolaidis, E., et al., 2016. Wind energy: trends and enabling technologies. *Renew. Sustain. Energy Rev.* 53, 209–224.
- Laamari, S., Zghal, W., 2016. Modeling of reverse osmosis system powered by photovoltaic energy. *Proc. of 7th International Renewable Energy Congress (IREC), Hammamet, Tunisia, March 22–24, 2016pp.* 1–6.
- Lai, W., Ma, Q., Lu, H., Weng, S., Fan, J., Fang, H., 2016. Effects of wind intermittence and fluctuation on reverse osmosis desalination process and solution strategies. *Desalination* 395, 17–27.
- Lawson, K.W., Lloyd, D.R., 1997. Membrane distillation. *J. Membr. Sci.* 124, 1–25.
- Lee, H.J., Sarfert, F., Strathmann, H., Moon, S.H., 2002. Designing of an electro dialysis desalination plant. *Desalination* 142, 267–286.
- Li, C., Goswami, Y., Stefanakos, E., 2013. Solar assisted sea water desalination: a review. *Renew. Sustain. Energy Rev.* 19, 136–163.
- Liu, C.C.K., Park, J.W., Migita, R., Qin, G., 2002. Experiments of a prototype wind-driven reverse osmosis desalination system with feedback control. *Desalination* 150, 277–287.
- Loutatidou, S., Liosis, N., Pohl, R., Ouada, T.B.M.J., Arafat, H.A., 2017. Wind-powered desalination for strategic water storage: techno-economic assessment of concept. *Desalination* 408, 36–51.
- Malek, P., Ortiz, J.M., Schulte-Herbrüggen, H.M.A., 2016. Decentralized desalination of brackish water using an electro dialysis system directly powered by wind energy. *Desalination* 377, 54–64.
- Manju, S., Sagar, N., 2017. Renewable energy integrated desalination: a sustainable solution to overcome future fresh-water scarcity in India. *Renew. Sustain. Energy Rev.* 73, 594–609.
- Mathioulakis, E., Belessiotis, V., Delyannis, E., 2007. Desalination by using alternative energy: review and state-of-the-art. *Desalination* 203, 346–365.
- Milano, J., Ong, H.C., Masjuki, H.H., Chong, W.T., Lam, M.K., Loh, P.K., et al., 2016. Microalgae biofuels as an alternative to fossil fuel for power generation. *Renew. Sustain. Energy Rev.* 58, 180–197.
- Mohan, G., Kumar, U., Pokhrel, M.K., Martin, A., 2016. A novel solar thermal polygeneration system for sustainable production of cooling, clean water and domestic hot water in United Arab Emirates: dynamic simulation and economic evaluation. *Appl. Energy* 167, 173–188.
- Nakoa, K., Rahaoui, K., Date, A., Akbarzadeh, A., 2015. An experimental review on coupling of solar pond with membrane distillation. *Sol. Energy* 119, 319–331.
- Novosel, T., Cosic, B., Puksec, T., Krajacic, G., Duic, N., Mathiesen, B.V., et al., 2015. Integration of renewables and reverse osmosis desalination—case study for the Jordanian energy system with a high share of wind and photovoltaics. *Energy* 92, 270–278.
- Ntavou, E., Kosmadakis, G., Manolakos, D., Papadakis, G., Papantonis, D., 2016. Experimental evaluation of a multi-skid reverse osmosis unit operating at fluctuating power input. *Desalination* 398, 77–86.
- Ortiz, J.M., Expósito, E., Gallud, F., García-García, V., Montiel, V., Aldaz, A., 2006. Photovoltaic electro dialysis system for brackish water desalination: modeling of global process. *J. Membr. Sci.* 274, 138–149.
- Ortiz, J.M., Expósito, E., Gallud, F., García-García, V., Montiel, V., Aldaz, A., 2008. Desalination of underground brackish waters using an electro dialysis system powered directly by photovoltaic energy. *Solar Energy Mater. Solar Cells* 92, 1677–1688.
- Palanisami, N., He, K., Moon, I.S., 2014. Utilization of solar energy for direct contact membrane distillation process: an experimental study for desalination of real seawater. *Korean J. Chem. Eng.* 31, 155–161.

- Pazheri, F.R., Othman, M.F., Malik, N.H., 2014. A review on global renewable electricity scenario. *Renew. Sustain. Energy Rev.* 31, 835–845.
- Qiblawey, H., Banat, F., Al-Nasser, Q., 2009. Laboratory setup for water purification using household PV-driven reverse osmosis unit. *Desalin. Water Treat.* 7, 53–59.
- Qtaishat, M.R., Banat, F., 2013. Desalination by solar powered membrane distillation systems. *Desalination* 308, 186–197.
- Rakib, M.I., Saidur, R., Mohamad, E.N., Afifi, A.M., 2017. Waste-heat utilization—the sustainable technologies to minimize energy consumption in Bangladesh textile sector. *J. Clean. Prod.* 142, 1867–1876.
- Rand, B.P., Genoe, J., Heremans, P., Poortmans, J., 2016. Solar cells utilizing small molecular weight organic semiconductors. *Prog. Photovolt. Res. Appl.* 15, 659–676.
- Razmjou, A., Liu, Q., Simon, G.P., Wang, H., 2013. Bifunctional polymer hydrogel layers as forward osmosis draw agents for continuous production of fresh water using solar energy. *Environ. Sci. Technol.* 47, 13160–13166.
- Richards, B.S., Capão, D.P.S., Früh, W.G., Schäfer, A.I., 2015. Renewable energy powered membrane technology: impact of solar irradiance fluctuations on performance of a brackish water reverse osmosis system. *Sep. Purif. Technol.* 156, 379–390.
- Robinson, R., Ho, G., Mathew, K., 1992. Development of a reliable low-cost reverse osmosis desalination unit for remote communities. *Desalination* 86, 9–26.
- Ruskowitz, J.A., Suárez, F., Tyler, S.W., Childress, A.E., 2014. Evaporation suppression and solar energy collection in a salt-gradient solar pond. *Sol. Energy* 99, 36–46.
- Shim, W.G., He, K., Gray, S., Moon, I.S., 2015. Solar energy assisted direct contact membrane distillation (DCMD) process for seawater desalination. *Sep. Purif. Technol.* 143, 94–104.
- Suárez, F., Urtubia, R., 2016. Tackling the water-energy nexus: an assessment of membrane distillation driven by salt-gradient solar ponds. *Clean Technol. Environ. Policy* 18, 1697–1712.
- Suárez, F., Ruskowitz, J.A., Tyler, S.W., Childress, A.E., 2015. Renewable water: direct contact membrane distillation coupled with solar ponds. *Appl. Energy* 158, 532–539.
- Thomson, M., Infield, D., 2003. A photovoltaic-powered seawater reverse-osmosis system without batteries. *Desalination* 153, 1–8.
- Thomson, M., Infield, D., 2005. Laboratory demonstration of a photovoltaic-powered seawater reverse-osmosis system without batteries. *Desalination* 183, 105–111.
- Todorova, V., 2014. Four companies chosen for Abu Dhabi desalination pilot scheme. *The National*. Available from: <http://www.thenational.ae/uae/environment/four-companies-chosen-for-desalination-pilot-schemes-in-abu-dhabi>. Accessed 21 June 2017.
- Troncoso, P., Mantz, R., Battaiotto, P., 2014. Electrodialysis processes assisted by photovoltaic panels. Concentration control. *IEEE Lat. Am. Trans.* 12, 864–870.
- Tzen, E., Theofiloyianakos, D., Kologios, Z., 2008. Autonomous reverse osmosis units driven by RE sources experiences and lessons learned. *Desalination* 221, 29–36.
- Valero, F., Arbós, R., 2010. Desalination of brackish river water using electrodialysis reversal (EDR). Control of the THMs formation in the Barcelona (NE Spain) area. *Desalination* 253, 170–174.
- Veza, J.M., Penate, B., Castellano, F., 2004. Electrodialysis desalination designed for off-grid wind energy. *Desalination* 160, 211–221.
- Walther, G.R., Post, E., Convey, P., Menzel, A., Parmesan, C., Beebee, T.J.C., et al., 2002. Ecological responses to recent climate change. *Nature* 416, 389–395.
- Whitmarsh, L., Seyfang, G., O'Neill, S., 2011. Public engagement with carbon and climate change: to what extent is the public “carbon capable”? *Glob. Environ. Chang.* 21, 56–65.
- Wiedmann, T., Minx, J., 2008. A definition of ‘carbon footprint’. In: Pertsova, C.C. (Ed.), *Ecological Economics Research Trends*. Nova Science Publishers, Hauppauge, NY, pp. 1–11. Chapter 1.
- Wright, N.C., Winter, A.G., 2014. Justification for community-scale photovoltaic-powered electrodialysis desalination systems for inland rural villages in India. *Desalination* 352, 82–91.

- Zaragoza, G., Ruiz-Aguirre, A., Guillén-Burrieza, E., 2014. Efficiency in the use of solar thermal energy of small membrane desalination systems for decentralized water production. *Appl. Energy* 130, 491–499.
- Zhang, Y., Pinoy, L., Meesschaert, B., Van der Bruggen, B., 2013. A natural driven membrane process for brackish and wastewater treatment: photovoltaic powered ED and FO hybrid system. *Environ. Sci. Technol.* 47, 10548–10555.
- Zrelli, A., Chaouchi, B., Gabsi, S., 2015. Use of solar energy for desalination by membrane distillation installation equipped with helically coiled fibers. *Proceedings of 6th International Renewable Energy Congress (IREC)*, Sousse, Tunisia, March 24–26, 2015.

CHAPTER 5

Published Book Chapter

eBook Information

Organic Pollutants in Wastewater I

Methods of Analysis, Removal and Treatment

Eds. Inamuddin, Abdullah M. Asiri, Ali Mohammad

eBook PDF / eBook PDF

Wastewater represents an alternative to freshwater if it can be treated successfully for re-use applications. Promising techniques involve photocatalysis, adsorption, nanocomposites, and membranes. The book focusses on several topics related to the removal of organic pollutants from wastewater.

Keyword: Wastewater Treatment, Organic Pollutants, Organic Dyes, Photocatalysis, Nanocomposite Photocatalysts, Photocatalytic Degradation, Adsorption, Membrane Filtration, Fenton Processes, Biosorbents, Phenolic Compounds, Carbon Quantum Dots, Methylene Blue Degradation, ZnO Composites, TiO₂ Based Nanocomposites

ISBN 13: 978-1-945291-63-0, **Publication Date:** 2018 (4/1/2018)

Direct URL: <http://www.mrforum.com/product/organic-pollutants-wastewater-1>
362 pages, eBook PDF, USD 135.00

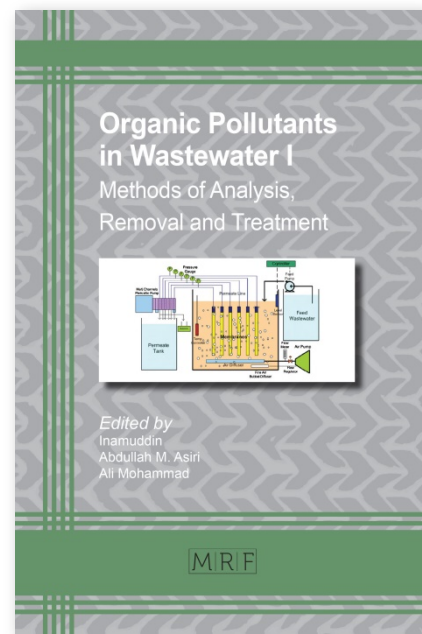
Materials Research Foundations Vol. 29 / **BISAC:** TEC021000 / **BIC/Thema:** TGM

Imprint: Materials Research Forum LLC, *Publisher's sales rights are Worldwide*

Summary:

Wastewater represents an alternative to freshwater if it can be treated successfully for re-use applications. Promising techniques involve photocatalysis, adsorption, nanocomposites, and membranes. The book focusses on the following topics:

Effluent detoxification and degradation kinetics of organic dyes using Fenton and photo-Fenton processes. Degradation of methylene blue using nanocomposites as a potential photocatalyst. Agricultural and agro-industries based wastes as low-cost biosorbents. Use of carbon quantum dots (CQDs) for photocatalytic degradation of organic pollutants. Detection, determination and removal of phenolic compounds from wastewater. Decomposition of organic dyes via photocatalysis. Oxide-semiconductor nanomaterials for photocatalytic wastewater purification. Photocatalytic efficiency of various ZnO composites for degradation of organic pollutants. TiO₂ based nanocomposites. Membrane filtration processes for the removal of organics from industrial wastewater.



CHAPTER 5

Industrial Water Pollution and Treatment - Can Membranes be a Solution?

Catia Giovanna Lopresto, Debolina Mukherjee, Karen Alejandra Bueno Zabala, Vincenza Calabro, Stefano Curcio, Sudip Chakraborty*

Department of DIMES, University of Calabria, Via P. Bucci, Cubo 42/a, 87036 Rende (CS) – Italy

sudip.chakraborty@unical.it*

Abstract

Industry is one of the main sources of water pollution since a long time and currently increasing day by day. Industries produces pollutants that are not only extremely harmful to people but also to the aquatic environment. Many industrial facilities use freshwater to carry away waste from the industrial plants into rivers, lakes and oceans. During the last century a huge amount of industrial wastewater was discharged into rivers, lakes and coastal areas. This resulted in serious pollution problems in the water bodies and caused negative effects to the eco-system and human's life. There are many types of industrial wastewater pollutants based on different industries and each sector produces its own particular combination of pollutants from the processes. The technology for the treatment of industrial wastewater must be designed more specifically for the particular type of pollutants produced. Membrane has made important contributions to the welfare of people with positive quality of life more than the majority of all other disciplines. In this chapter most of the industrial pollutants and their membrane based treatment mechanisms are described.

Keywords

Membrane, Bioreactor, Industrial Wastewater, Water Pollution, Environmental Impact, Membrane Materials

Contents

1. Introduction.....	296
2. Industrial pollutants and their impact on water	297

3.	Treatment technologies	300
4.	Agro industrial wastewater.....	302
4.1	Olive mill wastewater	302
3.2	Palm oil mill wastewater	312
3.3	Dairy industry	317
3.4	Tomato-processing wastewater	323
3.5	Fish-processing wastewater	323
3.6	Distillery wastewater	325
3.7	Molasses spent wash.....	325
3.8	Winery wastewater	328
	Conclusions	335
	References	335

1. Introduction

Wastewaters from agro-industries are characterized by high levels of chemical oxygen demand (COD), together with the presence of nitrogen and phosphorus.

The classic technologies used for the treatment of industrial wastewater are insufficient to meet current demand. Advanced technologies in wastewater treatment include membrane processes, ion-exchange processes, adsorption processes, ozonation, UV/ozone/H₂O₂ combinations, Fenton's process, and nitrogen and phosphorus removal technologies. Membrane separation processes associated with a number of advantages, including appreciable energy savings, clean and easy operation, higher effectiveness, and greater flexibility in system design have been preferred. Membrane processes have recently become a great topic of research due to their applicability in wastewater treatment. Decreasing costs of installation and operation of membranes favored the use of membrane processes. Of the membrane processes, microfiltration and ultrafiltration are used mainly for primary treatment purposes while nanofiltration and reverse osmosis are used for final treatment. Specifically, reverse osmosis membranes offer such a high treatment efficiencies that they are used in a wide range of applications including recovery of materials from industrial wastewaters and treatment of sea water for drinking purposes.

The present chapter focuses on the various kinds of pollution present in food and agro alimentary industries. The remediation of the pollutants by application of membrane is

also discussed in this chapter. An overview about the different pollutants and treatment technologies including membrane is presented. The use of different membranes in the remediation of agro food pollutants is described with more attention to downstream purification. A large volume of wastewater in the form of either oil-in-water (o/w) or water-in-oil (w/o) emulsions is generated from various process industries such as metallurgical, transportation, food processing and petrochemical as well as petroleum refineries. In the following sections, we will focus on oil-in-water emulsions derived from vegetable oil processing.

2. Industrial pollutants and their impact on water

Agro-industries are major contributors to worldwide industrial pollution. Effluents from many agro-food industries are hazardous to the environment and require appropriate and a comprehensive management approach [1]. The quantity, composition and concentration of different agro-food wastewaters depend on the final products, production processes, equipment used, and composition variations [2].

Table 1 Characteristics of typical agro-food industrial wastewater.

Industry	COD mg/L	BOD mg/L	pH	TS mg/L	TN mg/L	TP mg/L	Temperature °C	Reference
Distillery	85,000 - 1,000,000	42,000 - 51,000	3.1 - 4.7	70,000- 95,000	800- 1,200	180-- 350	85-95	[3]
Sugar factories	8,339- 9,033	1,010- 5,103	4.4 - 9.5	1,344	44-53	1 – 5	29.1	[2,4]
Dairies	346	50	7.3	250 – 2,750	42	3.3	--	[1,5]
Winery	1,800 – 21,000	--	--	150- 200	310- 410	40-60	--	[1]
Food procesing ^a	1,000- 8,000	600- 4,000	--	--	50	3	--	[1]
Olive mil	130,100	--	4.9	9,090	270	110	--	[1,6]

Notes: ^a contains flour, soybean, tomato, pepper, and salt.

TS: Total solids; TN: Total nitrogen; TP: Total phosphorus; BOD: Biochemical oxygen demand; COD: Chemical oxygen demand.

Table 1 summarizes the physicochemical characteristics of agro-food industrial wastewater reported by various authors.

As evident from the data presented in Table 1, there is significant variation in COD (346 – 1,000,000 mg/L) and BOD (50–51,000 mg/L). The pH and total solids (TS) concentration varies in the range of 3,1 – 9,5 and 6,150 – 95,000 mg/L, respectively; and significant amount of nutrients, 42 – 1,200 mg/L of total nitrogen (TN) and 1 – 350 mg/L of total phosphorous are also found in agro-food industry wastewater. The wastewaters impact colour and unpleasant odor in water bodies but some of wastewaters exhibit good biodegradability [7].

One of the main characteristics of agro-food wastewater is the amount of water consumption. The high amount of effluent produced, raises specific problems for the treatment process. These relate to the volume and composition of the wastewater produced and consequently treatment plants must be versatile in relation to the loading regime and at the same time be able to cope with a succession of start-ups and closedowns, including periods of inactivity [8].

The untreated wastewater issued by agro-food industries can cause water and soil pollution and therefore permanent risk of environmental pollution (Fig. 1) [5,9]. Due to high organic loading, the oxygen depleting potential of agro-food wastewater is 100 times that of domestic sewage [10]. The conductivity of the agro-food wastewater exceeds 1,500 $\mu\text{S}/\text{cm}$, which proves excessive mineralization of the wastewater. For turbidity, the value is greater than 50 NTU, proving that the analyzed water is cloudy [5] and its dark color obstructs photosynthesis and causes adverse effect on aquatic life [3].

Wastewaters also alter the physico-chemical characteristics of the receiving aquatic bodies and affect aquatic flora and fauna. When discharged into the environment, wastewaters create serious health hazards to the rural and semi-urban populations. Agro-food effluent has an obnoxious odour and unpleasant colour when released into the environment without proper treatment. Contaminants, such as chloride, sulphate, phosphate, magnesium and nitrate, are discharged with the effluent of various industries, which create a nuisance due to physical appearance, odour and taste. Such harmful water is injurious to plants, animals and human beings [2,4].



Figure 1 Effects of agro-food wastewater on the environment.

The major chemical pollutants in agro-food wastewater are nitrogen and phosphorus. The presence of nitrogen in discharged wastewater is undesirable because its ecological impacts and adverse effect on public health. A major problem in some plants is a low pH (pH = 6) which arises due to extensive nitrification and low wastewater alkalinity. Nitrogen in the form of ammonia is toxic to fish and exerts an oxygen demand on receiving water by nitrifiers [11].

Surface waters may also contain phosphorus in various compounds, which is an essential constituent of living organisms. In natural conditions, phosphorus concentration in waters is balanced; however, when phosphorus input to waters is higher than that can be assimilated by a population of living organisms, the problem of excess phosphorus content occurs. Since phosphate is the limiting component for growth in most ecosystems and the emission of phosphate in surface waters lead to eutrophication and algae bloom, thus having negative impacts on nature conservation, recreation, and drinking water production [11]. Algal blooms are esthetically undesirable and they alter the native composition and species diversity of aquatic communities, in addition to impair recreational values of surface waters, impede commercial fishing, and pose problems for water treatment. When deprived of oxygen, fishes and other aquatic organisms die, emitting foul odors [12].

Agro-food effluents contain carbohydrate organics, dissolved and suspended solids. The immediate oxygen demands by these effluents cause rapid depletion of dissolved oxygen in receiving streams and produce anaerobic conditions. High solids level would have an

adverse impact on aquatic life, render the receiving water unfit for drinking and domestic purposes, reduce crop yields if used for irrigation, and exacerbate corrosion in water systems and pipes [13].

Agro-food wastewaters also affect the soil. The bacteria and fungi which maintain the soil fertility are affected by the release of highly toxic chemicals, causing concerns about the sustainability of continued reuse of treated wastewater in agriculture. The risks posed for human health represent another question at the heart of any discussion on wastewater reuse. These risks cannot be accurately estimated at the moment, but cannot be ignored. The evidences reported in the literature, as well as the critical analyses on the limitations of some experimental approaches highlight the importance of the accumulation and propagation of biological contaminants in soils due to wastewater irrigation. Human and animal pathogens, phytopathogens and antibiotic resistant bacteria and their genes are important biological contaminants that can be transported by wastewater and/or be enriched in soil. Also, numerous other chemical contaminants, such as xenobiotics, pharmaceuticals and metals, can threaten the environmental and human health. The mixture of these contaminants may have unpredictable consequences on both environment and human health [14].

3. Treatment technologies

The summary of opportunities and limitations of anaerobic, aerobic, physico-chemical and membrane treatment methods for agro-food wastewater is presented in Table 2.

Table 2 Opportunities and limitations of anaerobic, aerobic, physicochemical and membrane treatment methods for agro-food wastewater.

Treatment method	Opportunities	Limitations
Anaerobic	<ul style="list-style-type: none"> *Energy production is possible due to the generation of methane during degradation of organic matters. *Less sludge production. *Effluent quality in terms of COD is good but nitrogen removal is low. 	<ul style="list-style-type: none"> *Oil and grease are not easily degraded. *Post-treatment of effluent is often required.
Aerobic	<ul style="list-style-type: none"> *Excellent effluent quality in terms of COD, BOD and nutrient removal. *Aerobic-SBOR has been reported to give high percentage of organics removal. 	<ul style="list-style-type: none"> *Excess sludge produced is high. *Require larger area. *Complete removal of organics is not possible.

	*In the case of aerobic SBR, smaller area is needed as compared to other aerobic activated sludge processes.	*Aerobic SBR treatment systems offer better controlling.
Physico-chemical	*Coagulation/flocculation, adsorption and electrochemical methods are the various physicochemical methods.*Electro-oxidation was better treatment option in comparison to electro-coagulation. *No generation of secondary pollutants take place in electro-oxidation method.	*Chemical coagulation/flocculation process generates secondary pollutants. *In the case of electrocoagulation, treated effluent may be contaminated with electrode material.
Membranes	*Membrane assisted treatments methods such as RO, MF, NF, UF are most suitable to produce high-quality effluents to reuse directly. * Membrane separation can be used in dilute streams. *Effective in removal of recalcitrant contaminants. *Product recovery is possible. *Smaller footprint. *Improve nitrification and denitrification processes.	*Volumes pumped are very high comparing to other food industry branches, the solutions exhibit high viscosity and high osmotic pressure. * Membrane fouling might be severe at the later stage of treatment.

Notes: Reverse osmosis (RO), microfiltration (MF), nanofiltration (NF), ultrafiltration (UF). Adapted from [2,15,16]

Depending on the characteristics of the wastewater and the preferred final disposal routes, wastewater treatment methods can involve a simple single operation or a series of separate operations, involving multiple units. Anaerobic treatment method for concentrated wastewater, in terms of pollutants is a widely used method in the industries. It has several advantages over aerobic processes, which include lesser energy requirement; methane (a source of energy) production due to the degradation of organic; and lesser sludge production, which indirectly reduces the sludge disposal cost [2,17].

In case of aerobic treatment process (Table 2), aerated lagoons, aerated submerged fixed-film culture, and mixed culture activated sludge process have been used for the treatment of agro-food wastewater. However, future studies are hoped to focus on aerobic

sequential batch reactor (SBR) treatment, a mixed culture activated sludge process. In the case of aerobic SBR, smaller area is needed as compared to other aerobic activated sludge processes. Both technologies, anaerobic and aerobic are complementary to one another in respect of removing organics and nitrogen completely from agro-food industry wastewater [17].

As agro-food wastewaters have high loading of dissolved solids and suspended solids, physicochemical methods like adsorption and coagulation are well suited for their treatment. Khan *et al* [18] reported coagulation with lime and subsequent adsorption with activated charcoal. BOD and COD removal efficiencies were reported to be 96 and 95%, respectively.

Membrane assisted treatment methods are very capable to produce high-quality effluent to reuse directly. Future research in MBR is likely to focus on reduction in energy demand and membrane fouling during the operation. Therefore, in view of producing good quality treated wastewater for reuse, hybrid system comprising of membranes with aerobic/anaerobic treatment methods and/or physicochemical methods may be promising [2].

4. Agro industrial wastewater

4.1 Olive mill wastewater

Olive oil production is an important agricultural and economic activity in Mediterranean countries. Olive oil processing (traditional press method or the most used three phase continuous process) produces large amounts of olive oil mill wastewaters (OOMW). OOMW are composed of olive pulpwater containing vegetable components and minerals, plus water components used for the olive washing, plant cleaning, olive paste dilution in the continuous process, and the residual olive pulp oil. The organic fraction contains sugars, tannins, polyphenols, polyalcohols, pectins, lipids, proteins and organic acids such as acetic, malic, fumaric, lactic, malonic, citric, tartaric, ossalic and succinic [19]. The composition of OOMW is not constant and exhibits great variability because it depends on a lot of parameters such as kind of olive and ripeness, oil extraction technology, and duration of aging.

OOMW from olive mills represent one of the greatest environmental problems in the Mediterranean area, where olives cultivation is widespread and large volumes of effluents are produced in a concentrated period of a few months. The polluting load depends on the high COD values and the presence of phyto-toxic and antibacterial polyphenolic components. Indeed, in these effluents, the presence of phytotoxic recalcitrant pollutants

makes them resistant to biological degradation and thus inhibits the efficiency of biological and conventional processes [20].

OOMW are often illegally discharged or widespread in agricultural fields, with adverse consequences on the field fertility. Straight discharge of OOMW has been reported by several authors to cause strong odor nuisance, soil contamination, plants growth inhibition, underground leaks, water body pollution and hindrance of self-purification processes, as well as severe impacts on the aquatic fauna and ecological status, due to the presence of bio-refractory contaminants, including a wide variety of phenolic compounds, tannins, fatty acids and organohalogenated pollutants. Inorganic compounds including chloride, sulfate and phosphoric salts of potassium, calcium, iron, magnesium, sodium, copper and traces of other elements are also common traits of OOMW [20].

Flexible and efficient treatment plants should assure not only a significant reduction of BOD and COD values but also the possibility of selectively recovering some valuable compounds that could be used in the same production cycle or as raw materials for other processes.

Scientific studies on OOMW treatment principally concentrated on the removal of the polluting load [21]. Physical and physico-chemical processes include thermal processes (evaporation, gasification, combustion) [22], thermochemical processes [23], electro-coagulation [7,24], flocculation/clarification, adsorption, extraction [25], and ozonation [26]. Nevertheless, these conventional treatments are not capable to abate the high concentration of dissolved monovalent and divalent ions present in OOMW, which present hazardous salinity levels according to the guidelines established by the Food and Agricultural Organization (F.A.O.) for irrigation uses [20]. Generally, physico-chemical processes need an integrative biological treatment for the complete degradation of the organic substances [27]. Biological treatments can be divided into aerobic and anaerobic. Anaerobic processes have greater efficiency in the pull down of the pollutant load and produce biogas reusable as energetic resource [28]. Anyway, both in the aerobic and in the anaerobic processes, microorganism growth is particularly difficult for the antibacterial action of polyphenols. Although the efficiency of the coupled physico-chemical and biological treatment of OOMW is better, from an environmental point of view, the discharge of the great amount of sludge produced, with volumes comparable to that of the OOMW treated, is a great problem [29].

Recently, researches have began to consider the recovering of polyphenols, as high value compounds with biological activities [30], the antioxidant, anti-inflammatory activities and radicalic elimination [31], and the antimicrobial activity [32], transforming OOMW from effluents to raw material with high potential economic value [33,34].

In this case, technologies offer high efficiency and moderate investment and maintenance expenses [21,35], even if final treatment of OOMW by membrane processes has not been widely accepted, yet, and limited research papers have been published up to date. Recently, Pulido [20] discussed the state of the art of the different pretreatment methods and integral membrane processes proposed up to 2016 for the reclamation and disposal of the effluents generated in olive mills operating with batch-press and two-phase as well as three-phase processes, comprising microfiltration (MF), ultrafiltration (UF), nanofiltration (NF) and reverse osmosis (RO), along with membrane bioreactors (MBRs) [36], with an insight into the problem of fouling. MF and UF have been used mainly for primary treatment purposes, while NF and RO have been used for final treatment [37,38].

Several novel treatment approaches (Table 3) based on tangential flow membrane filtrations for the selective separation and total recovery of hydroxytyrosol, water and organic substances have been patented by ENEA and Verdiana Company [39]. MF and UF of OOMW without preliminary centrifugation step, operating with pilot plants with fixed process parameters were investigated by [38]. MF/UF permeates can be concentrated in RO. MF and UF permeates or RO concentrate can be used as functional integrators or in pharmacologic compositions. RO permeate can be used as base for the beverage industry. MF and UF concentrates can be used as fertilizers or in the production of biogas.

Membrane distillation (MD) is a non-isothermal process that has attracted the interest of academic and scientific communities during the last few years. It can be used successfully for OOMW with the objective to obtain pure water – which can be useful for irrigation or industrial uses – and a concentrate containing high amounts of polyphenols, which can be extracted later. Compared to other separation processes, MD has many advantages. It exhibits a complete rejection of dissolved, non-volatile species, lower operating pressure than the pressure-driven membrane processes, reduced vapor space, etc. The obtained concentrate of OOMW may represent a source of high added value compounds like sugar and polyphenols and the residue can be utilized in agriculture as a fertilizing agent through its high load of organic compounds [40].

One common problem of membrane filtration of OOMW is the membrane fouling that drastically reduces the efficiency of permeate and also changes its selectivity. Therefore, a pretreatment step is necessary to decrease membrane fouling and to increase filtration efficiency. The centrifuging process was found to be a promising pretreatment method [37]. Several MD processes have been identified (Figs. 2-4).

Hybrid processes, combining biological treatments, chemical processes and membrane technology, were developed too [41,42] in order to reach high removal efficiencies of

COD and mono-phenolic compounds. The important treatments processes based on membrane filtration are listed in Table 3.

Table 3 Several novel treatment approaches based on membrane filtration.

	Filtration System	Membranes (manufacturer)	Material	Cut-off	Feed	Ref.
MF	Tangential flow	Ceramic Tami	Zirconium oxide	0.8 μm 0.45 μm	Acidified OOMW	[38]
	Tangential flow	Ceramic Tami isoflux	Zirconium oxide	0.45 μm	Acidified OOMW	[38]
	Tangential flow	Polymeric Nadir	Spiral-wound PES	500 Kd	Acidified OOMW	[38]
	/	(Inopor GmbH)	Al_2O_3	/	Pre-filtered OOMW	[43]
	/	Osmonics JX	/	/	Pre-treated OOMW	[44]
	MBR	Carbosep (Novasep Orelis)	Carbon with ZrO_2 - TiO_2	0.14 μm	Diluted OOMW	[36]
UF	Tangential flow	Polymeric Osmonics	Spiral-wound PS	80 Kd 20 Kd 6 Kd	MF permeates	[38]
	Tangential flow	Ceramic Tami	Zirconium oxide	1 Kd	MF permeates	[38]
	Cross-flow	JW Osmonics	PVDF	30 kDa	Pre-treated OOMW	[45]
	Cross-flow	MW Osmonics	Ultrafilic	100 kDa	Pre-treated OOMW	[45]
	Cross-flow	Membralox-Ceraver	Ultrafine porous ZrO_2 / coarse porous alumina	0.05 μm	Olive mill solid wastewater	[42]
	Cross-flow	UF-PES-004H (Macrodyn-Nadir)	Permanently hydrophilic PES	4 kDa	Pre-filtered OOMW	[19]
	Cross-flow	C005F (Macrodyn-Nadir)	Regenerated cellulose	5 kDa	Pre-filtered	[19]

					OOMW	
	Cross-flow	C010F (Macrodyn-Nadir)	Regenerated cellulose	10 kDa	Pre-filtered OOMW	[19]
	Cross-flow	P010F (Macrodyn-Nadir)	Permanently hydrophilic PES	10 kDa	Pre-filtered OOMW	[19]
	Cross-flow	Etna 01PP (Alfa Laval)	Composite fluoropolymer	1 kDa	UF permeates	[46]
	Cross-flow	/	Ceramic (zirconia)	/	Pre-filtered OOMW	[47]
	/	HFS (Toray)	PVDF	/	Pre-filtered OOMW	[46]
	/	UC010 (Macrodyn® Nadir)	Cellulose	10 kDa	Centrifuge d OOMW	[37]
	/	Osmonics GM	/	/	MF permeates	[44]
	/	Desal-5 GM4040F (Osmonics)	Composite	/	Pre-treated OOMW	[48]
	/	PCI France	/	2-25-100 kDa	Pre-treated OOMW	[41]
	Micellar enhanced	/	PVDF	/	OOMW	[49]
NF	/	NF90 (DOW-Filmtec)	Thin-film	/	UF permeates	[46]
	/	NP010 (Macrodyn® Nadir)	PES	/	UF permeates	[37]
	/	NP030 (Macrodyn® Nadir)	Permanently PES	/	UF permeates	[37]
	/	NF270 (DOW Filmtec™)	PA	200-300 kDa	UF permeates	[37]

	/	DK2540F Osmonics	/	0.5 nm	Pre-treated OOMW	[50]
	/	/	Polymeric	200	UF permeates	[47]
	/	Osmonics DK	/	/	MF permeates	[44]
	/	Desal-5 DK4040F (Osmonics)	Composite	/	UF permeates	[48]
RO	Tangentia 1 flow	Polymeric hydronautics	Composite PA	/	UF permeates	[38]
	/	XLE (DOW Filmtec™) BW30 (DOW Filmtec™)	PA	/	UF permeates	[37]
	/	/	Polymeric	100	UF permeates	[47]
	/	Osmonics SC	/	/	NF permeates	[44]
MD	Direct contact MD	GVHP (Millipore)	PVDF	/	OOMW	[40]
	Direct contact MD	TF200 (Gelman)	PTFE	/	OOMW	[40]
	Direct contact MD	TF200 (Gelman)	PTFE	/	Pre-treated OOMW	[51]
	Direct contact MD	TF200 (Gelman) TF450 (Gelman) TF1000 (Gelman)	PTFE/ PP	/	Micro- filtered OOMW	[52]
	Osmotic distillatio n	TF200 (Gelman) TF450 (Gelman) TF1000 (Gelman)	PTFE/ PP	/	OOMW	[53]
	Osmotic distillatio n	/	PP	/	NF permeates	[43]

Vacuum MD	TF200 (Gelman) TF450 (Gelman) TF1000 (Gelman)	PTFE/PP	/	OOMW	[53]
Vacuum MD	/	PP or PVDF	/	NF permeates	[43]

Note: PA: polyamide; PES: polyethersulfone; PP: polypropylene; PS: polysulfone; PTFE: polytetrafluoroethylene; PVDF: polyvinylidene difluoride.

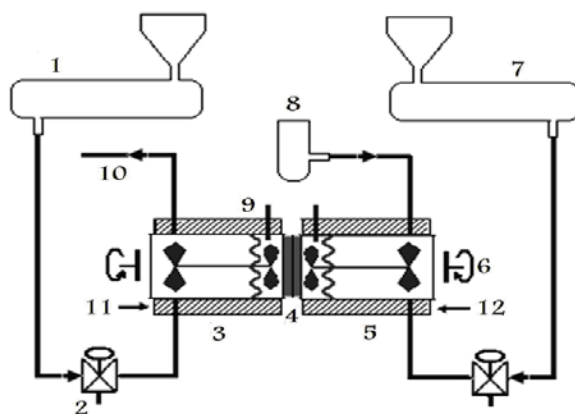


Figure 2 Direct contact membrane distillation system: (1) distilled water reservoir , (2) three-way valve, (3) cold unit, (4) flat sheet membrane module, (5) warm unit, (6) magnetic stirrer (7) feed reservoir, (8) feed tank to keep the feed volume constant (9) temperature sensor, (10) permeate outlet, (11) jacket connected to cold thermostat and (12) jacket connected to hot thermostat [40].

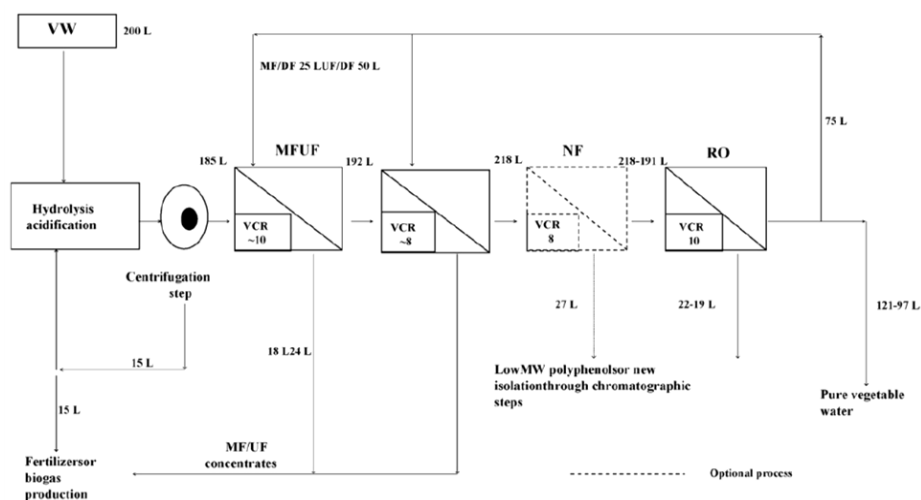


Figure 3 Hypothetical vegetation waters (VW) industrial treatment process [38].

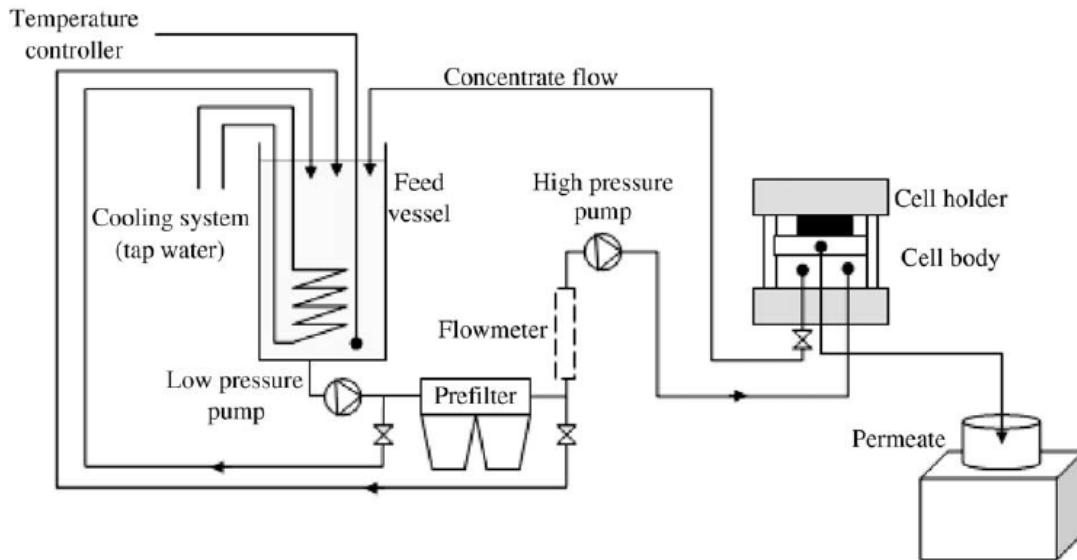


Figure 4 Schematic flow diagram of the experimental set-up [45].

Several integrated membrane processes (a sequence of two UF processes followed by a final NF step or one step of UF followed by NF and RO, or MF followed by NF and osmotic distillation or vacuum membrane distillation) have been also proposed to achieve high levels of purification of OOMWs and a water fraction which can be discharged in aquatic systems or to be reused in the olive oil extraction process [43,46,47,54]. Experimental results confirm that the future direction of the processes for the recovery of antioxidants from OOMW will be toward the utilization of membranes in a sequential design.

Micellar enhanced ultrafiltration (MEUF) treatment method for removal and concentration of polyphenols was developed, using an anionic surfactant (sodium dodecyl sulfate salt) and a hydrophobic poly(vinylidene fluoride) (PVDF) membrane [49]. Some of the schemes of the single or hybrid membrane processes are illustrated below in the form of Figs. 5-8.

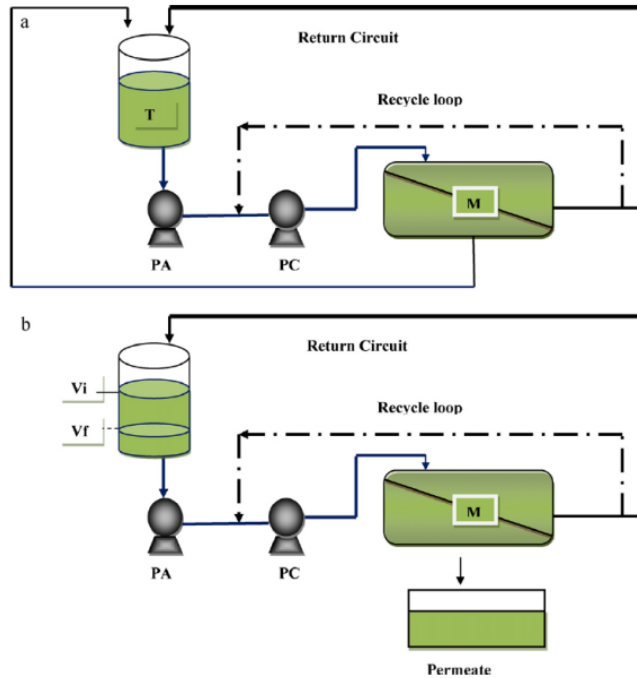


Figure5 Ultrafiltration process T: feed tank, PC: Recycling pump, PA: Feed Pump, M: Ultrafiltration module adapted from reference [42].

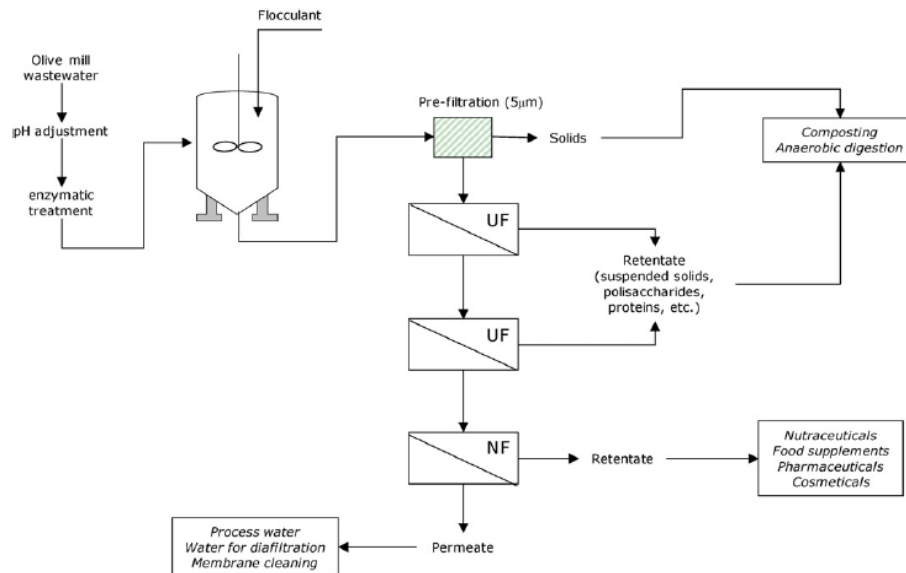


Figure 6 Proposed process scheme for the recovery of water and phenolic compounds from OOMWs [46].

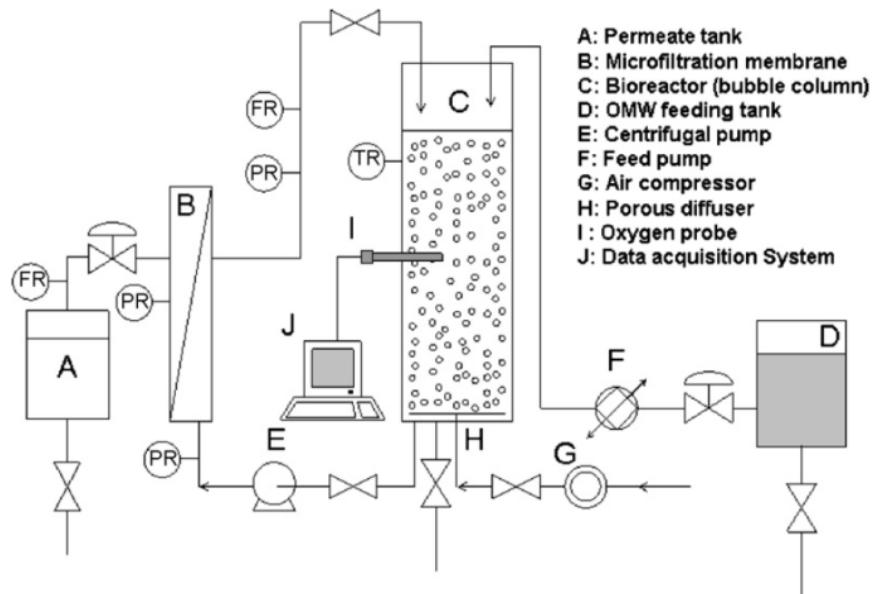


Figure 7 Schematic representation of membrane bioreactor used for OOMW treatment [36].

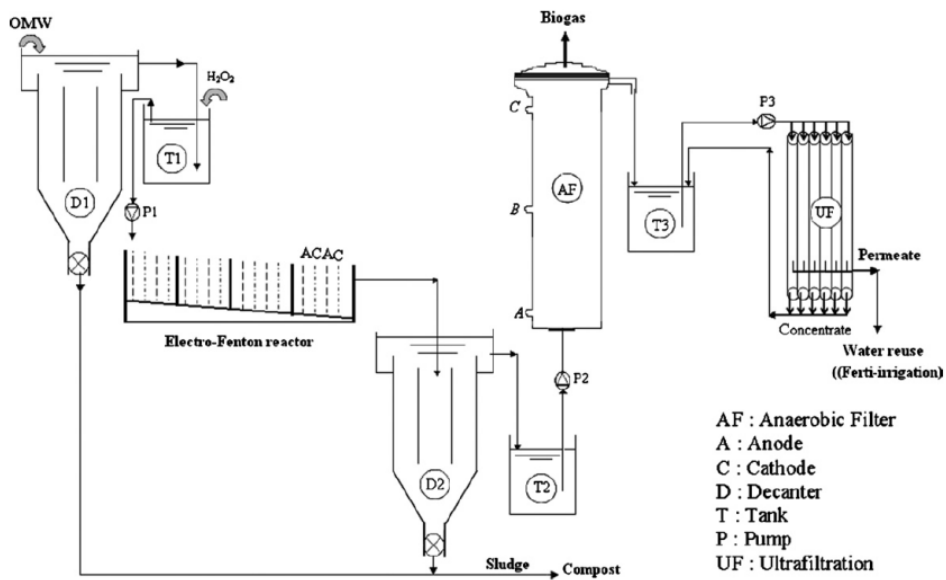


Figure 8 Schematic flow diagram of pilot plant for OOMW treatment [41].

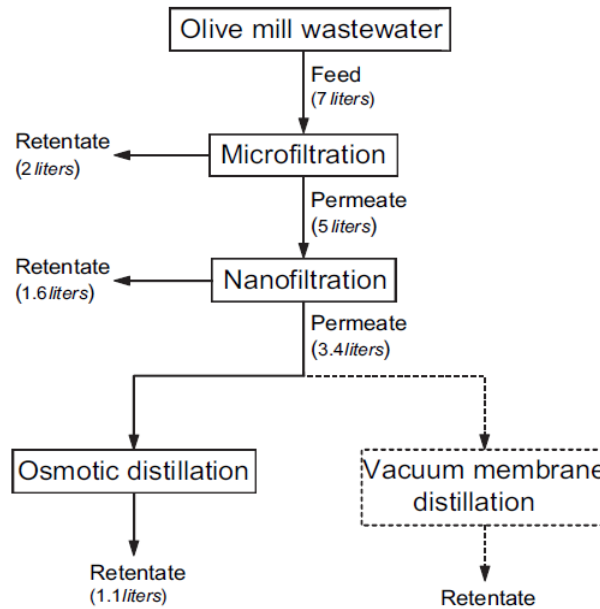


Figure 9 Flowchart of OOMW treatment processes.

In the above flowchart (Fig. 9), the activities carried out for the recovery, purification and concentration of polyphenols from olive mill wastewater are illustrated [43].

3.2 Palm oil mill wastewater

Palm oil is one of the world's most rapidly expanding equatorial crops. Indonesia and Malaysia are the two largest oil palm producing countries, but its by-product—palm oil mill effluent (POME), posed a great threat to the water environment. Palm oil processing, similar to other agricultural and industrial activities, raised environmental issues particularly water pollution, which adversely affects aquatic life and domestic water supply [55]. About half of the water used in the extraction process from the fresh fruit bunch results in highly polluting palm oil mill wastewater (POMW) as evident from Fig. 10. POMW is a colloidal suspension of water (95-96%), oil (0.6-0.7%) and total solids (4-5%). It is non-toxic as no chemicals are added during oil extraction but has an unpleasant odor. It is highly polluting and characterized by low pH (average pH: 3.5–4.2), enhanced biological and chemical oxygen demands ($BOD_{3d, 30^{\circ}C}$: 10–44 g/L, COD_{cr} : 16–100 g/L), increased salt content, and high suspended solids (SS: 5–54 g/L) [56]. The typical POMW characteristics are reported in the following Table 4 [57].

Table 4 Characteristics of palm oil mill effluent [57].

Parameter	Concentration (mg/L)
Ammonical Nitrogen	35
BOD	25000
Boron	7.6
Calcium	439
COD	50000
Copper	0.89
Elements	
Iron	46.5
Magnesium	615
Magnesium	2
Oil & Grease	4000
pH	4.7
Phosphate	180
Potassium	2270
SS	18000
TDS	40500
Total Nitrogen	750
Total volatile solids	34000
Zinc	2.3

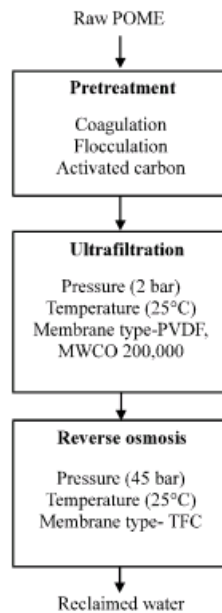


Figure 10 Flowchart of POME treatment using membrane technology [57].

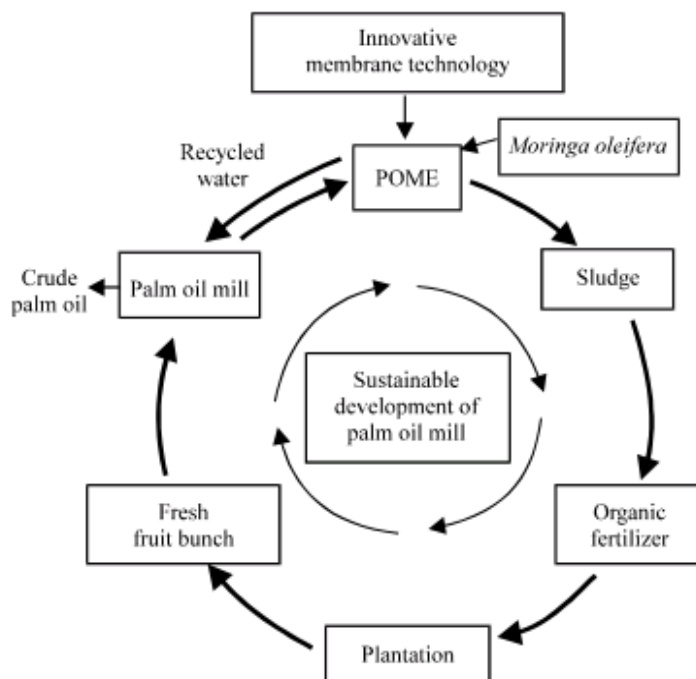


Figure 11 Sustainable development of palm oil mill with zero discharge using membrane technology [57].

The high content of suspended solids and organic matter in the effluent discharge can cause severe pollution of waterways due to oxygen-depletion and other related effects. POMW contains high concentrations of protein, carbohydrate, nitrogenous compounds, lipids and minerals that may be converted into useful materials using microbial processes [58].

There is an urgent need to find a compromising way that will enable the balance between environmental protection and sustainable reuse of the nutrient sources found in the POMW (Fig. 11).

Currently, POMWs are treated by conventional biological processes of anaerobic [59] or aerobic digestion [60]. Several researchers have proposed other biological treatment systems which include aerated lagoon system, conventional anaerobic digester, anaerobic contact process, up-flow anaerobic sludge blanket (UASB) reactor, close tank digester, trickling filter, aerobic lagoon system, aerobic rotating biological contactor and evaporation processes [55,61–63]. However, the proposed biological treatment systems are only confined to lab scale analysis. Moreover, the nutrient sources available in the

POMW cannot be effectively reused as a substrate in fermentation after the conventional treatment process has been adopted.

Membrane separation technology is recognized as an efficient, economical, sustainable and reliable technology that exhibits high potential to be applied in POMW treatment. In the last decade, very few membrane processes were investigated. Ultrafiltration (UF) has been successfully developed from a useful laboratory tool to an industrial process. The main bottleneck of membrane separation is membrane fouling. Therefore, effective techniques of membrane cleaning need to be studied to mitigate membrane fouling.

A two-stage pilot-scale plant was investigated for POMW treatment. Biodegradation constituted the first biological stage, while ultrafiltration (UF) and reverse osmosis (RO) membrane units were combined as the second membrane separation stage [56,61].

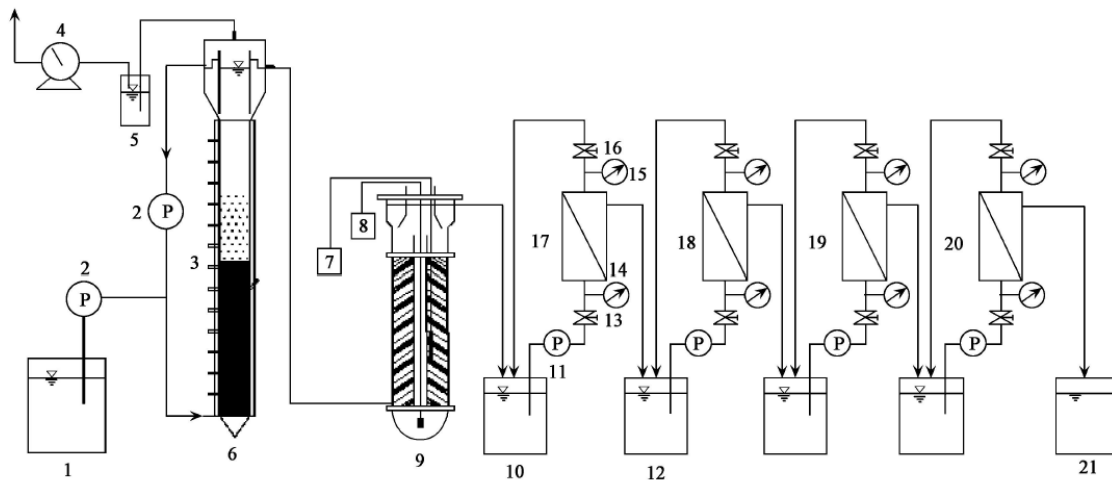


Figure 12 Schematic diagram of a pilot plant for palm oil mill effluent treatment [56].

The investigation on the feasibility and suitability of the membrane separation technology in POME treatment was carried out extensively in a pilot plant (Fig. 12) with the capacity of 450 L/h [64,65]. Three designs of industrial scale membrane based POMW treatment plant were investigated and optimized for evaluation of performance and cost, in order to develop and design an industrial scale membrane plant suitable for a typical palm oil mill in Malaysia [61] (Fig. 13).

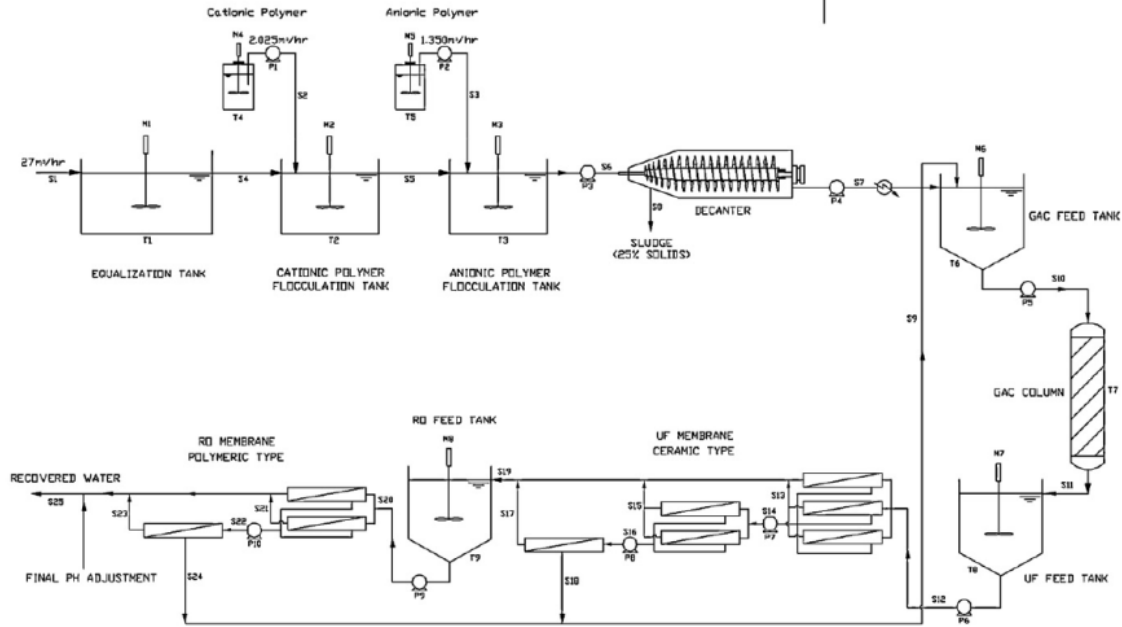


Figure 1 Process flow diagram of membrane based POME treatment system for design A [61].

Recently membrane bioreactors (MBRs) have been developed. However, high loading of MBR system was affected due to biofouling on the membrane surface. A treatment process is necessary to remove the high content of organics in POMW that would otherwise severely resulted in fouling of the membrane and to a shorter membrane life-span (Table 5). Powdered activated carbon, zeolite, and *Moringa oleifera* were used as biofouling reducers (BFRs) and added into aerobic MBR [66].

A membrane anaerobic system (MAS) as depicted in Fig. 14 was investigated in order to treat POMW [67].

Table 5 Membrane filtration systems used for pretreatment of POMW.

	Filtration System	Membranes (manufacturer)	Material	Cut-off	Feed	Ref.
UF	Dead-end	DSS-GR61PP (Alfa Laval)	PS	20000 g/mol	Pre-treated POMW	[58]
	Dead-end	DSS-GR70PP (Alfa Laval)	PS	20000 g/mol	Pre-treated POMW	[68]
	Dead-end	DSS- GR81PP (Alfa Laval)	PES	10000 g/mol	Pre-treated POMW	[68]
	Dead-end	DSS- GR95PP (Alfa Laval)	PES	2000 g/mol	Pre-treated POMW	[68]
	Cross-flow	(PCI-Memtech)	Ceramic Polymeric	/	Pre-treated POMW	[61]
	Cross-flow	/	/	200000 g/mol	/	[67]
	/	/	/	100000 g/mol	Pre-treated POMW	[56]
	/	/	PVDF	200000 g/mol	Pre-treated POMW	[57]
R O	Cross-flow	(PCI-Memtech)	Polymeric	/	UF permeates	[61]
	Cross-flow	(PCI-Memtech)	PVDF		Pre-treated POMW	[69]
	/	ESPA-2 (Hydranautics)	/	/	UF permeates	[56]
	/	/	TFC	/	UF permeates	[57]

Note: PES: polyethersulfone; PS: polysulfone; PVDF: polyvinylidene difluoride; TFC: thin-film composite.

3.3 Dairy industry

The dairy industry involves processing raw milk into products such as milk, butter, cheese, yogurt, condensed milk, dried milk (milk powder), and ice cream, using methods such as chilling, pasteurization, and homogenization. Water is used in all of the activities of the dairy industry, including cleaning, sanitization, heating, cooling, and floor washing. Consequently, nowadays, the dairy industry is considered the major source of

food processing wastewater in regard to its large water consumption [70]. The effluent is characterized by variable volumes, flow rates and organic matter content. Dairy wastewater (DW) is distinguished by the higher BOD and COD values along with high levels of dissolved or suspended organic components (whey proteins, lactose, fats, oils, grease and minerals), nutrients (ammonia or minerals and phosphates), and cleaning chemicals (acids, alkalis and detergents) [71,72]. DWs, therefore, require specialized treatments to meet effluent discharge standards and to reduce the risk of environmental problems such as eutrophication in rivers, lakes and coastal waters.

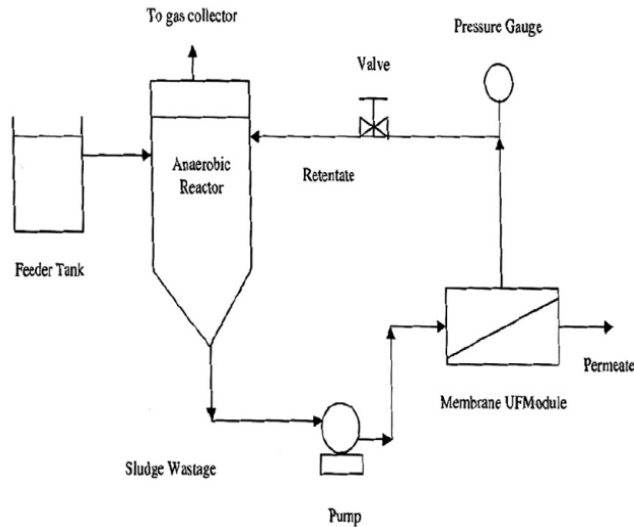


Figure 14 Membrane anaerobic system [67].

The highly variable nature of dairy wastewaters in terms of volume and flow rates as well as in terms of the pH and suspended solids content makes it difficult to choose an effective wastewater treatment regime. Conventional dairy wastewater treatment plants mainly based on activated sludge processes that involve the aerobic microbial metabolism of fats, lactose and proteins [73], anaerobic treatments [74–77], coagulation [78,79], and ecological treatment system [80]. Recently, there is an emerging interest focused on the energy recovery from wastes; in this field, microbial fuel cells (MFC) are gaining promising interest and a bio-electrochemical treatment system along with bioelectricity generation was used with real field dairy based wastewater as substrate [81].

Membrane technologies applied in the dairy industry since the early 1970s have been considered promising to treat DWs in order to produce reusable water [82]. Ultrafiltration (UF) of dairy wastewater yields a high permeate flux at low transmembrane pressure, but

its permeate water is not reusable as it contains too much lactose [83]. Instead, nanofiltration (NF) and reverse osmosis (RO) permit the recovery of lactose and milk proteins for non-human consumption. In fact, the concentrate retentate could be precipitated by coagulation and reutilized as feed supplement for animals, or could be treated by anaerobic digestion to collect renewable energy sources (H_2 and CH_4). Thus, it is regarded as an economical and environment-friendly process for treatment of dairy wastewater. Permeate water obtained from NF/RO treatment of dairy wastewater can be discharged into river or reused, but with the increase of organic solutes and inorganic salts in retentate during a concentration process; concentration polarization and osmotic pressure increase rapidly, leading to a large flux decline. Consequently, the advantages of membrane filtration in wastewater treatment are adversely affected by concentration polarization and subsequent membrane fouling as these factors cause flux decline and permeate quality deterioration. One of the principal limitations on the optimal performance of membrane processes is membrane fouling, which leads to a decrease in membrane flux with time.

Milk proteins, lactose and mineral salts present in DW are the possible ingredients of fouling layer on/in NF membranes [84]. In particular, available data on the electrophoretic mobility of α -lactalbumin and β -lactoglobulin allowed to suggest that serum proteins would also participate in the flux variations with a possible specific impact of α -lactalbumin as an internal foulant in UF [85].

Membrane selection and operating conditions have been important issues in minimizing membrane fouling. To control the fouling and to improve the productivity and life of membranes, use of coagulant and adsorbent before membrane application were done in primary and secondary effluent treatments [72]. Frappart et al. [86] confirmed the high potential of high shear dynamic filtration in reverse osmosis due to a minimization of concentration polarization, resulting in higher permeate fluxes and better solute rejection than with cross-flow filtration modules equipped with the same membrane.

Another problem related to NF/RO treatment of dairy wastewater is the difficulty of nutrient recovery. That is, because cleaning chemicals contained in dairy wastewater, are all retained by NF/RO membranes, contaminate the nutrients (lipids, proteins and lactose), and lipids have a negative impact on anaerobic digestion because these are difficult to degrade and thus plug the sludge bed [87]. A two-stage UF/NF process was proposed for utilization of whey protein and lactose, as proteins were retained by UF membrane and lactose in UF permeate was concentrated by NF [88]. For dairy wastewater treatment, a similar approach was also applied [89,90]. This approach could simultaneously eliminate pollution, produce reusable water, and recycle waste.

In the dairy industry, the use of acid, alkaline cleaners and sanitizers affects wastewater characteristics and typically results in a highly variable pH, which will bring an impact on the wastewater on-line treatment (Fig. 15). The effect of pH on the treatment of dairy wastewater by nanofiltration was investigated by Luo & Ding [91] using a rotating disk membrane module. The role of calcium and inorganic phosphate over the wide pH range was discussed by taking calculated salt equilibrium of milk as a function of acidic pH [85].

There is a growing interest in combining membranes with biological wastewater treatment. The membrane bioreactors (MBR) offer distinct advantages over traditional biological processes: higher biodegradation efficiency, smaller footprint, better quality of treated water, the absolute control of solids and hydraulic retention time, retention of all microorganisms and viruses, and easy control of operating conditions [92]. In Table 6, the membrane treatments used for dairy wastewater are summarized.

Table 6 Membrane treatment used for dairy wastewater.

	Filtration System	Membrane (manufacturer)	Material	Cut-off	Feed	Ref.
MF	Cross-flow	(Orelis)	Ceramic	0.45 μm	Pre-treated DW	[72]
UF	Dead-end	(Millipore Corporation)	Cellulose acetate	1 kDa 10 kDa	Pre-treated DW	[72]
	Dead-end	UP005P (Microdyn-Nadir)	PES	5 kDa	Model DW	[89]
	Dead-end	UH030P (Microdyn-Nadir)	PES	30 kDa	Model DW	[89]
	Dead-end	Ultracel PLGC (Millipore)	Regenerated cellulose	10 kDa	Model DW	[89]
	Cross-flow	HFK-131 (Koch)	PES	150-300 $\text{g}\cdot\text{mol}^{-1}$	Skim milk	[85]
	Cross-flow (integrated into a Jet Loop MBR)	(Jiuwu Hitech, Chinese)	Ceramic ($\text{Al}_2\text{O}_3/\text{ZrO}_2$)	50 nm	DW	[92]
	Rotating disk membrane	UP005P (Microdyn-Nadir)	PES	5 kDa	Model DW	[93]

	Rotating disk membrane	P010F (Microdyn-Nadir)	PES	10 kDa	Model DW	[93]
	Rotating disk membrane	P020F (Microdyn-Nadir)	PES	20 kDa	Model DW	[93]
	Rotating disk membrane	UH030P (Microdyn-Nadir)	Permanently hydrophilic PES	30 kDa	Model DW	[93]
	Rotating disk membrane	UH050P (Microdyn-Nadir)	Permanently hydrophilic PES	50 kDa	Model DW	[93]
	Rotating disk membrane	PES50 (Microdyn-Nadir)	PES	50 kDa	Model DW	[93]
	Rotating disk membrane	US100P (Microdyn-Nadir)	Permanently hydrophilic PS	100 kDa	Model DW	[93]
NF	Dead-end	(Permionics Pvt.)	PA/PE	300 Da	Pre-treated DW	[72]
	Dead-end	NF 270 (DOW-Filmtec)	PA	150 Da	UF permeates	[89]
	Dead-end	NF 90 (DOW-Filmtec)	PA	90 Da	UF permeates	[89]
	Dead-end	Nanomax 50 (Millipore)	PA	400 Da	UF permeates	[89]
	Dead-end	Desal-5 DL (GE Osmonics)	PA	327 Da	UF permeates	[89]
	Dead-end	Desal-5 DK (GE Osmonics)	PA	225 Da	UF permeates	[89]
	Cross-flow	Desal-5 DL (Osmonics)	PA	5-10 kg·mol ⁻¹	Skim milk	[85]
	Cross-flow	TFC-SR3 (Koch)	PA	200 Da	Skim milk UF permeates	[94]
	Cross-flow	NF 90 (DOW-Filmtec)	PA	100 Da	Biologically pre-treated DW	[95]
	Cross-flow	Desal-5 DL (GE Osmonics)	PA	150-300 Da	Biologically pre-treated	[95]

					DW	
	Cross-flow	FM NP010 (Mycrodin-Nadir GmbH)	PES	1000 Da	Biologically pre-treated DW	[95]
	Cross-flow	NF 270 (DOW-Filmtec)	Semiaromatic piperazine-based PA	200-300 Da	Biologically pre-treated DW	[95]
	Rotating disk membrane	NF270 (DOW-Filmtec)	PA/PS	~ 270 Da	Model DW	[84,91,96,97]
RO	/	Duratherm HF (GE Water & Process Technologies)	Composite	/	Pre-filtered low-pollutant DW	[98]
	Dead-end	(Permionics PVt.)	PA/PE	/	Pre-treated DW	[72]
	Dead-end	(Osmonics)	Spiral-wound cellulose acetate	/	MF permeates	[72]
	Cross-flow	TFC HR SW 2540	Spiral-wound composite (TFC)/PA	/	DW	[99]
	Cross-flow	TFC HR (Koch)	Spiral-wound composite (TFC)/PA	/	Skim milk	[85]
	Cross-flow	TFC (GE Osmonics)	Aromatic PA-urea	/	NF permeates	[95]
	Shear-enhanced	Desal AG (Osmonics)	PA/PS	/	Model DW	[86]

Note: PA: polyamide; PE: polyester; PES: polyethersulfone; PS: polysulfone; TFC: thin-film composite.

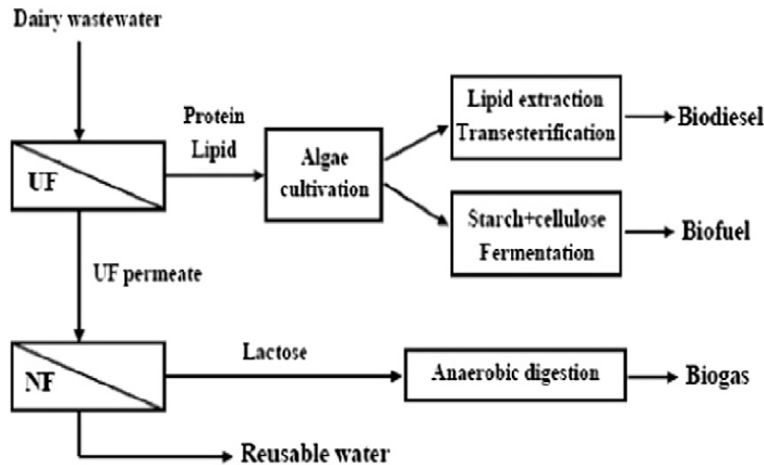


Figure 15 Schematic diagram of a two-step UF/NF process for dairy wastewater treatment and utilization for biorefinery processes [89].

3.4 Tomato-processing wastewater

The tomato industry produces huge amounts of wastewater effluents during tomato manufacturing. Tomato-processing wastewaters generally contain high organic content along with sufficient particulate and colloidal fractions that are not only slowly biodegradable but also exhibit very poor settling characteristics [100]. The wastewater stream produced during tomato manufacturing is characterized by dark color, bad smell, and high content of organics, as well as suspended solids particles. The concentration of pollutants in the effluent can vary considerably with time and space due to the changes in the harvested fruit composition and season. A discharge in the municipal sewage system of these streams is not directly possible because of the high organic contents exceeding the legally tolerated limits [101].

Recently, a process consisting of a biological pretreatment step and a batch nanofiltration process step was developed [101]. The spiral-wound module used for the separation step was a thin-film composite Desal-5 membrane (model DK2540) produced and supplied by Osmonics. Results showed that membrane processes can be successfully used to purify wastewater streams when operated at pressures far away from fouling conditions.

3.5 Fish-processing wastewater

Fish processing requires large amounts of water, primarily for washing and cleaning purposes, but also as media for storage and refrigeration of fish products before and

during processing. In addition, water is an important lubricant and transport medium in the various handling and processing steps of bulk fish processing. Consequently, fish processing operations produce wastewater, which contains organic contaminants in soluble, colloidal and particulate forms. Depending on the particular operation, the degree of contamination may be small (e.g., washing operations), mild (e.g., fish filleting), or heavy (e.g., bloodwater drained from fish storage tanks). In fishery wastewater the contaminants present are undefined mixtures of mostly organic substances. Moreover, it is difficult to generalize the extent of the problem created by this wastewater as it depends on the effluent strength, wastewater discharge rate and the absorbing capacity of the receiving water body [102]. Generally fish-processing and seafood-processing units release food waste with high content of organic nitrogen which is easily biodegradable [103].

Fish processing wastewaters have been treated using physical-chemical methods and biological treatments where microorganisms are involved in degradation of organic matter or a combination of both biological and chemical techniques [102,104–107].

A limiting factor for reuse of treated fish canning wastewater in industrial plants and other purposes is the high salt content, which persists even after conventional treatment. So, for the reuse of fish canning industrial wastewater, it was treated by combining conventional treatments, such as sedimentation, chemical coagulation-flocculation and aerobic biological degradation (activated sludge process) followed by a polishing step by reverse osmosis (RO) and ultraviolet (UV) disinfection. The final clarified effluent was found to have the quality requirements to be recycled or reused in the industrial plant, allowing the reduction of the effluent to be discharged, the water use and the costs of tap water for industrial use [104].

It is clear that the modern trend is to remove the polluting species from processing waters by various pressure-driven membrane techniques either integrated or not with other processes. Cross-flow MF is used in pre-treatment step for removal of suspended matter and during UF step, the proteins are concentrated. However, for complete recovery of proteins, NF step is required [108,109].

Also, the MBR technology is an attractive option for the treatment of such industrial wastewaters [110,111]. The experimental results have strongly confirmed the efficiency of the MBR, with good removal efficiencies in terms of BOD₅ and COD [103]. A new pilot-scale hybrid biofilm-suspended biomass membrane bioreactor was used to treat two wastewater streams generated in a fish canning factory [111].

3.6 Distillery wastewater

Distillery spent wash is the unwanted residual liquid waste generated during alcohol production in distilleries and the pollution caused by it is one of the most critical environmental issue. There are a number of large-scale distilleries integrated with sugar mills. The waste products from sugar mill comprise bagasse (residue from the sugarcane crushing), pressmud (mud and dirt residue from juice clarification) and molasses (final residue from sugar crystallization section). Bagasse is used in paper manufacturing and as fuel in boilers; molasses as raw material in distillery for alcohol production while pressmud has no direct industrial application. The major sugar producing countries are listed in Table 7.

Table 7 Major sugar producing countries.

Period	Production (MT)	Export in (MT)	Population (millions)	Per capita consumption
Brazil	34	21.95	190	58
Australia	6.83	4.750	20	47
China	16.79	-	1 314	11
EU	21.567	2.400	490	34
India	30.8	3.298	1 117	20
Mexico	5.978	1	107	52
Pakistan	4.891	-	165	25
SADC	5.834	2.8	157	22
Thailand	8.033	6.25	65	36
United States	8.701	-	301	29

Note: MT: metric tonn; SADC: Southern African Development Community

3.7 Molasses spent wash

The effluents from molasses based distilleries contain large amounts of molasses spent wash (MSW) leading to extensive soil and water pollution. MSW is one of the most difficult waste products to dispose of because of low pH, elevated temperature, high concentrations of organic and inorganic substances, colorants (melanoidin, phenolics,

caramel and melanin), polymers with relatively low biodegradability [112], and high ash content. The BOD and COD values typically ranged between 35000–50000 and 100000–150000 mg/L, respectively [113]. The production and characteristics of spentwash are highly variable and dependent on feedstocks and various aspects of the ethanol production process. Together with its pollution and toxic profile, MSW has been widely reviewed [113–115]. The MSW is a potential water pollutant in two ways. First, the highly coloured nature of MSW can block out sunlight from rivers and streams, thus reducing oxygenation of the water by photosynthesis and hence becomes detrimental to aquatic life. Secondly, it has a high pollution load which would result in eutrophication of contaminated water bodies. Moreover, undiluted effluent has shown toxic effect on fishes and other aquatic organisms. MSW also leads to significant levels of soil pollution and acidification in the cases of inappropriate land discharge.

Elimination of pollutants and color from distillery effluent is becoming increasingly important from environmental and aesthetic point of view. Stillage, fermenter and condenser cooling water and fermenter wastewater are the primary polluting streams of a typical distillery. Due to the large volumes of effluent and presence of certain recalcitrant compounds, the treatment of this stream is rather challenging by conventional methods. Therefore, to supplement the existing treatments, a number of studies encompassing physicochemical and biological advanced treatment processes have been conducted [113–116].

Membrane processes can result in significant color removal thereby permitting reuse of the treated effluent [117,118]. MSW can be pre-treated with ceramic membranes prior to anaerobic digestion to reduce COD and improve the efficiency of the anaerobic process possibly due to the removal of inhibiting substances (Fig. 16). Reverse osmosis (RO) has also been employed for distillery wastewater treatment. Since spent wash is a complex, multicomponent stream that is known to cause considerable fouling, an understanding of the components those are primarily responsible for this phenomenon would assist in appropriate feed pre-treatment, for the efficient operation of the membrane system. For this reason, some of the membrane processes developed in last decade are summarized in Table 8.

Table 8 Membrane processes used in hard drinks industries.

	Filtration System	Membranes (manufacturer)	Material	Cut-off	Feed	Ref.
UF	/	TFC-PA (Permionics)	/	/	Distillery effluent	[119]
NF	/	/	Composite polyamide	/	Pre-treated distillery effluent	[120]
RO	/	(Permionics)	/	/	UF permeates	[119]
	/	ESPA2 (Hydranautics) LFC3 (Hydranautics) CPA2 (Hydranautics) BW30 (Filmtec) BW30LE (Filmtec) SG (Osmonics) SE (Osmonics) CE (Osmonics)	/	/	Pre-treated distillery effluent	[121]
	MBR	/	Polymeric	/	Synthetic wastewater	[112]
	MBR equipped with filters prepared from waste fly ash	/	/	/	Pre-treated distillery effluent	[122]
	MBR equipped with a mesh filter	/	/	/	Distillery effluent	[123]

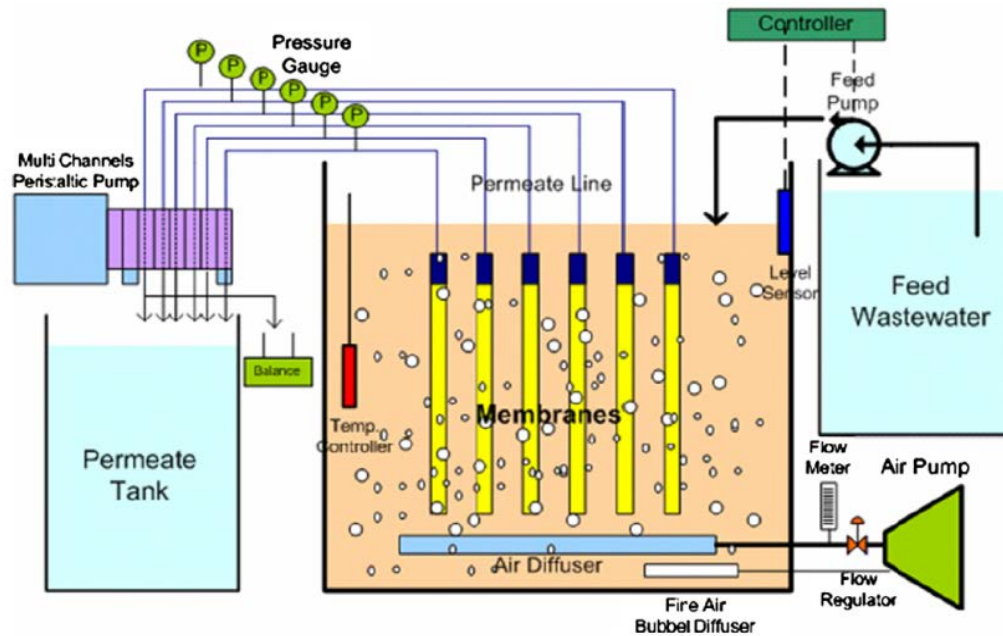


Figure 16 Schematic diagram of the HT-MBR system [112].

3.8 Winery wastewater

Wineries and other grape-processing industries are important distillery industries. These industries generate large volumes of wastewater annually [124]. Wine distillery wastewater, or vinasse, is produced by the distillation of wine, wine lees, or fermented grape juice to extract ethanol or flavor compounds. The winery wastewaters mainly originate from various washing operations during the crushing and pressing of grapes, as well as rinsing of fermentation tanks, barrels, and other equipment as illustrated in Fig. 17 [125]. Winery wastewater contains various pollutants such as sugars, ethanol, esters, glycerol, organic acids, polyphenolic compounds, and numerous population of bacteria and yeasts [126]. The chemical analysis of winery wastewater has indicated that sugars constituted large portion of the COD, whereas organic acids played a more prominent role in the acidity of the wastewater. Due to the acidity, color, and high COD, this wastewater is treated prior to discharge, in order to avoid eutrophication of the receiving environment. Cleaning agents (NaOH, KOH) could be present in winery wastewaters. Numerous phenolic compounds are present in wines as a result of their extraction from the skin, flesh, and seeds of grapes. Phenolic compounds, though form a relatively small portion of the wastewater, offer great negative effects upon treatment systems as well as environmental damage if released untreated. The inhibitory effects of wine distillery

wastewater on plant growth can be attributed to the high percentage of organic compounds and salts, and thus high electrical conductivity of winery wastewater makes water uptake by seeds difficult and causes retardation of germination. Consequently, winery effluents are environmentally undesirable and require appropriate treatment. On the other hand, such effluents are valuable source for the recovery of polyphenols. As a result, numerous methods have been reported to treat or dispose of the phenolic-rich wastes that originate from wineries and distilleries. Among treatment methods, physical and chemical processes (such as filtration, oxidation by ozone, chlorine dioxide, hydrogen peroxide, and radiation as well as adsorption) and biological treatment techniques (including aerobic or anaerobic digestion) have been most popular [8,124–129].

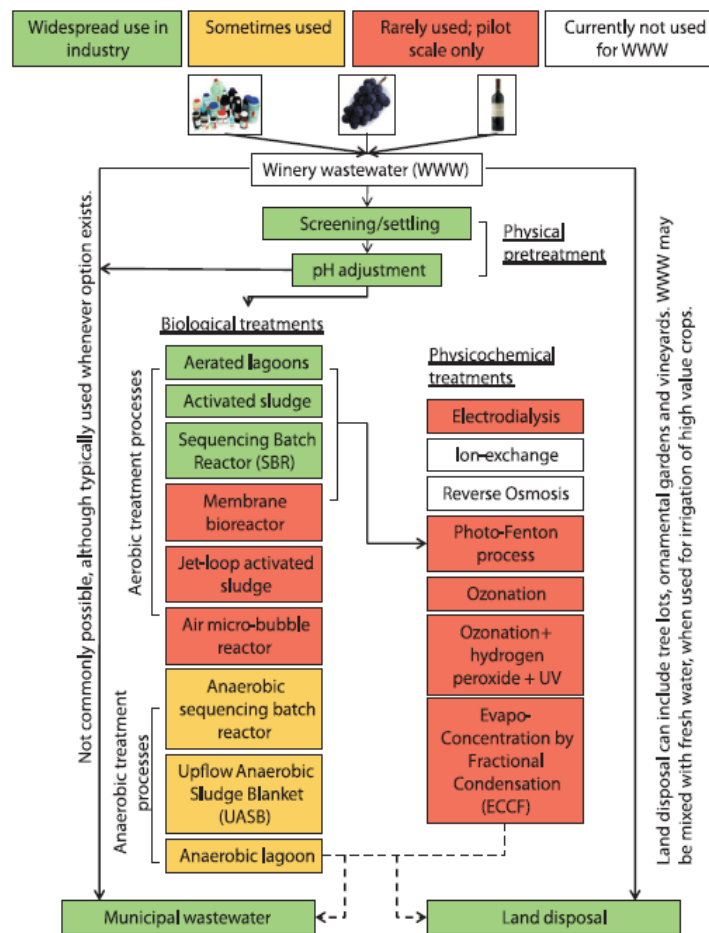


Figure 17 Schematic of process used in winery wastewater treatment [125].

Table 9 Membrane processes applied in winery wastewater treatment.

	Filtration System	Membranes (manufacturer)	Material	Cut-off	Feed	Ref.
MF	Total recirculation mode	V0.2 (Synder Filtration)	PVDF	/	Winery effluents from second racking	[132]
	Total recirculation mode	MFP5 (Alfa Laval)	Fluoro polymer	/	Winery effluents from second racking	[132]
	Concentration mode	(PAM Membranas Seletivas)	PI	/	Winery effluents from second racking	[132]
UF	Total recirculation mode	GR95PP (Alfa Laval)	/	7600 Da	Winery effluents from second racking	[133]
NF	Total recirculation mode	CA 400-22, CA 400-26, CA 400-28 (Laboratory made)	Cellulose acetate	/	UF permeates	[134]
	Total recirculation mode	NF270 (Filmtec Corp.)	/	/	UF permeates	[134]
	Total recirculation mode	ETNA01PP (Alpha Laval)	/	/	UF permeates	[134]
RO	/	AG2521TF (Desal)	PA	/	Pre-treated winery wastewater	[130]

Note: PA: polyamide; PI: polyimide; PVDF: polyvinylidene difluoride.

Biological treatment is particularly well suited to the treatment of winery wastewater, because the majority of the organic components present in the waste stream are readily biodegradable. Nevertheless, pollutants in winery wastewater like various recalcitrant high molecular weight compounds (e.g. polyphenols, tannins and lignins) are not mineralized by the biological treatment [130].

Consequently, other technologies for more exhaustive winery wastewater treatment must be applied to reach effluent quality standards for discharge in the environment. Membrane separation processes are becoming quite popular in wastewater treatment and reclamation since these combine process stability and excellent effluent quality.

Since winery effluents are rich in phenolic compounds, membrane treatments were applied with the aim of both reducing polluting compounds and recovering high-added values phenols. Beyond the application of UF for the fractionation of phenolic compounds and their separation from other co-extracted components in winery sludge [131], membrane processes as shown in Table 9 have been applied to winery wastewaters. Among these, reverse osmosis (Fig. 18) followed by solar photo-Fenton oxidation of the RO concentrate proved to be most successful combined process for the integrated treatment of winery effluents [130].

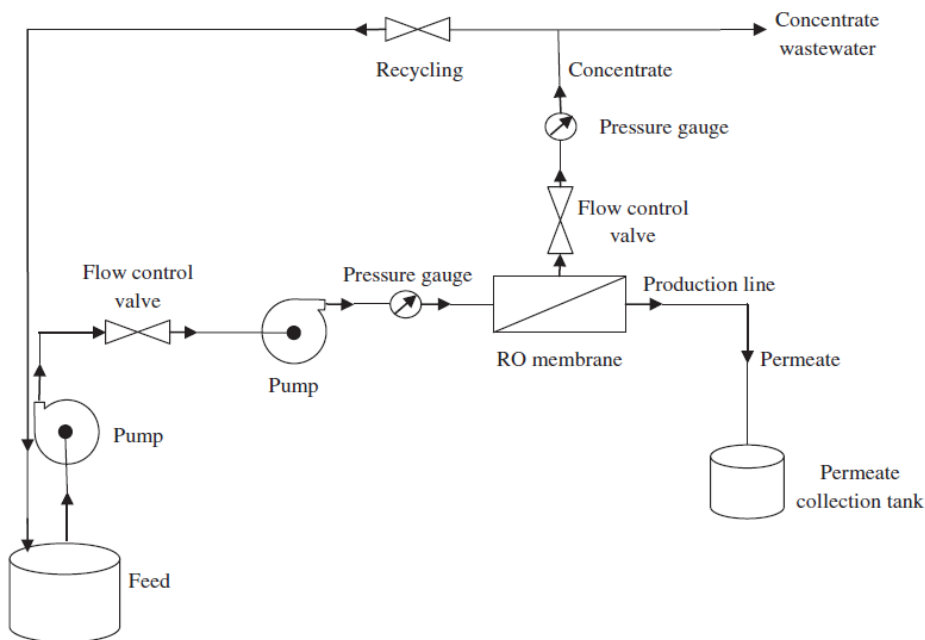
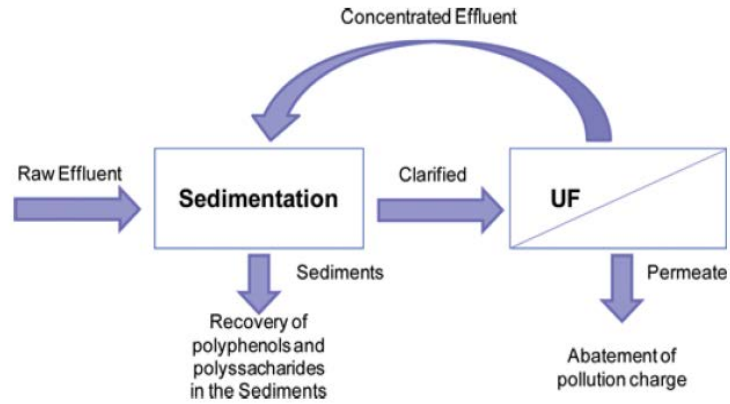
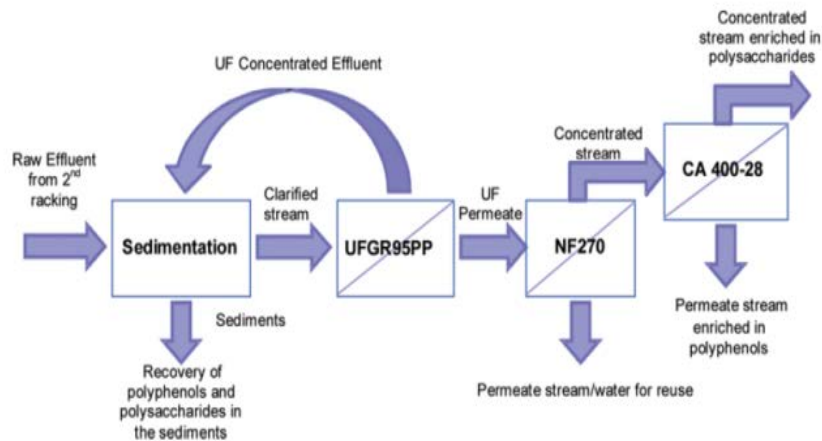


Figure 18. Flow diagram of RO unit [130].



(a)



(b)

Figure 19 (a,b) Development of a process to treat winery effluent and recover polyphenols and polysaccharides [133,134].

Another important enzymatic activity in wine making and especially in wine clarification process is pectinases. Free enzyme membrane reactor (FEMR) is the main membrane bioreactor configuration used in wine clarification. The soluble enzyme is confined to the retentate side of the membranes where it is in contact with the substrate. In the following Table 10 some examples and membrane materials applied for the hydrolysis using

pectinases are reported. These applications are referred both to the wine and fruit juice treatments as described in Fig. 19(a,b).

Table 10 List of biocatalysts and membrane materials used in wine production.

Biocatalyst	Membrane	Bioreactor configuration	Application	Reference
pectin lyase from <i>Penicillium italicum</i>		STR with an ultrafiltration unit	--	[144]
polygalacturonase from <i>A. niger</i>	30 kDa flat regenerated cellulose membrane	STR with an ultrafiltration unit	--	[145]
Polygalacturonase and pectin lyase from <i>A. niger</i>	Spiral wound polysulfone membrane (10 kDa)	STR with an ultrafiltration unit	--	[146]
Endo-polygalacturonase from <i>Aspergillus pulverulentus</i>	Amicon 10 kDa	STR with an ultrafiltration unit	Production of pectic oligosaccharides	[147]
Polygalacturonase from <i>A. niger</i>	Titania microfiltration	Biocatalytic membrane reactor	Pre-treatment of fruit juice	[(148]
Amylase and pectinase	Polysulfone single-hollow fiber	Biocatalytic membrane reactor	Fruit juice processing	[149]
Commerical pectinase	Hollow fiber ultrafiltration	Biocatalytic membrane reactor	Fruit juice processing	[150]
Endopeptidase from <i>A. niger</i>	10 kDa Spiral wound polysulfone	STR with an ultrafiltration unit	Apple pectin hydrolysis	[146]

Membrane treatment methods have been investigated to remove heavy metals. Indeed, in most cases of winery effluent, the heavy metals, especially zinc and copper, did not meet

the limits for the discharge as imposed by the most restrictive regulations at international level [135].

Winery wastewaters have different compositions and hence are difficult to treat by means of the conventional activated sludge processes because of the high organic loading associated with their production. To face this situation, membrane bioreactors (MBR) have been widely applied to treat winery wastewaters since 2007 [129,136–143]. MBR offers several benefits, such as rapid start-up, good effluent quality, low footprint area, and absence of voluminous secondary settler. Additionally, its operation is not affected by the settling properties of the sludge.

Cell immobilization is rapidly expanding research area. The main purpose to use this technique is to improve wine production. Many supports (inorganic, organic and natural materials) have been used for cell immobilization in this field. Some of the supports and their main applications have been listed in Table 11.

Table 11 Porous supports used in wine production processes.

Support		Immobilized cell	Application	System configuration	Reference
Inorganic support	Mineral kassis	<i>Saccaromices</i>	Aroma improvement	Batch and continuous wine-making	[151]
	γ -aluminium	<i>Saccaromices</i>		Continuous wine-making	[152]
Organic support	Cellulose covered with Ca-alginate	<i>Saccaromices and Candida</i>	Enhance glycerol formation in wine		[153]
	Ca-alginate beds	<i>Saccaromices</i>	Must fermentation	Immobilized cell-recycle batch process	[154]
Natural support	Delignified cellulose	<i>Saccaromices</i>	Fermentation	-	[155,156]
	Gluten pellets		Production of wine with less alcohol content		[153,157]

Compared with organic supports, inorganic supports have been more advantageous, because of providing improved fermentation productivity and in most cases better wine aroma [158]

Conclusions

Membrane applications for the treatment of agro-industrial wastewater focus on separating water from contaminants, using semi-permeable membranes under applied driving forces. Pressure is applied to reverse the natural equilibrium between the clean water and wastewater. The basic principle of natural equilibrium is that the clean water tends to migrate to the wastewater side to equalize the concentrations across the membrane. Mechanical pressure is used to force water molecules from the wastewater side to the clean water side and, thus, a "high-tech" filtration of the wastewater occurs. In this way, the pollutants can be separated in terms of process intensification strategies. In the past, the energy needed to apply the pressure and the fragility of the membrane surface made use of these alternatives economically unjustifiable. But due to stringent regulation before waste discharge forcing the industry to opt for the advanced treatment mechanism. Various industries have opted as discussed but still there are gaps between fundamental research and application in real life of membrane application in pollution remediation. Also problems with membrane applications include fouling and fragility of the membrane surface. Toxic synthetic compounds can oxidize the surface of the membrane and thus are injurious to membranes. Innovations in membrane technology have advanced the "cleanability" and research on reuse of membranes. The suitability of stainless steel and ceramic materials for membranes has greatly improved the use of these materials in developing advanced wastewater treatment techniques.

References

- [1] R. Rajagopal, N.M.C. Saady, M. Torrijos, J.V. Thanikal, Y.-T. Hung, Sustainable Agro-Food Industrial Wastewater Treatment Using High Rate Anaerobic Process, *Water*. 5 (2013) 292–311. <https://doi.org/10.3390/w5010292>
- [2] J.P. Kushwaha, A review on sugar industry wastewater: sources, treatment technologies, and reuse, *Desalin. Water Treat.* 53 (2017) 309–318. <https://doi.org/10.1080/19443994.2013.838526>
- [3] A. Chaudhary, A. Sharma, B. Singh, Study of physio-chemical characteristics and biological treatment of molasses-based distillery effluent, *Int. J. Bioassays*. 2 (2013) 612–615.

- [4] P.M. Ayyasamy, R. Yasodha, S. Rajakumar, P. Lakshmanaperumalsamy, P.K.S.M. Rahman, S. Lee, Impact of Sugar Factory Effluent on the Growth and Biochemical Characteristics of Terrestrial and Aquatic Plants, *Bull. Environ. Contam. Toxicol.* 81 (2008) 449–454. <https://doi.org/10.1007/s00128-008-9523-5>
- [5] C.F. Bennani, B. Ousji, D.J. Ennigrou, Desalination and Water Treatment Reclamation of dairy wastewater using ultrafiltration process, *Desalin. Water Treat. Publ.* 55 (2014) 37–41.
- [6] F. Battista, D. Fino, F. Erriquens, G. Mancini, B. Ruggeri, Scaled-up experimental biogas production from two agro-food waste mixtures having high inhibitory compound concentrations, *Renew. Energy.* 81 (2015)
- [7] N. Adhoum, L. Monser, Decolourization and removal of phenolic compounds from olive mill wastewater by electrocoagulation, *Chem. Eng. Process. Process Intensif.* 43 (2004) 1281–1287. <https://doi.org/10.1016/j.cep.2003.12.001>
- [8] R. Ganesh, R. Rajinikanth, J.V. Thanikal, R.A. Ramanujam, M. Torrijos, Anaerobic treatment of winery wastewater in fixed bed reactors, *Bioprocess Biosyst. Eng.* 33 (2010) 619–628. <https://doi.org/10.1007/s00449-009-0387-9>
- [9] C. Wei, T. Zhang, C. Feng, H. Wu, Z. Deng, C. Wu, B. Lu, Treatment of food processing wastewater in a full-scale jet biogas internal loop anaerobic fluidized bed reactor, *Biodegradation.* 22 (2011) 347–357. <https://doi.org/10.1007/s10532-010-9405-5>
- [10] R.P. Singh, M.H. Ibrahim, N. Esa, M.S. Iliyana, Composting of waste from palm oil mill: a sustainable waste management practice, *Rev. Environ. Sci. Bio/Technology.* 9 (2010) 331–344. <https://doi.org/10.1007/s11157-010-9199-2>
- [11] Y. Jiang, H. Wang, Y. Shang, K. Yang, Simultaneous removal of aniline, nitrogen and phosphorus in aniline-containing wastewater treatment by using sequencing batch reactor, *Bioresour. Technol.* 207 (2016) 422–429. <https://doi.org/10.1016/j.biortech.2016.02.014>
- [12] A. Solovchenko, A.M. Verschoor, N.D. Jablonowski, L. Nedbal, Phosphorus from wastewater to crops: An alternative path involving microalgae, *Biotechnol. Adv.* 34 (2016) 550–564. <https://doi.org/10.1016/j.biotechadv.2016.01.002>
- [13] P.O. Sahu, P.K. Chaudhari, The Characteristics , Effects , and Treatment of Wastewater in Sugarcane Industry, *Water Qual. Expo. Heal.* 7 (2015) 435–444. <https://doi.org/10.1007/s12403-015-0158-6>

- [14] C. Becerra-Castro, A.R. López, I. Vaz-Moreira, E.F. Silva, C.M. Manaia, O.C. Nunes, Wastewater reuse in irrigation: a microbiological perspective on implications in soil fertility and human and environmental health, *Environ. Int.* 75 (2015) 117–135. <https://doi.org/10.1016/j.envint.2014.11.001>
- [15] A. Hinkova, Z. Bubník, P. Kadlec, J. Pridal, Potentials of separation membranes in the sugar industry, *Sep. Purif. Technol.* 26 (2002) 101–110. [https://doi.org/10.1016/S1383-5866\(01\)00121-6](https://doi.org/10.1016/S1383-5866(01)00121-6)
- [16] C.H. Neoh, Z.Z. Noor, N.S.A. Mutamim, K.C. Lim, Green technology in wastewater treatment technologies: Integration of membrane bioreactor with various wastewater treatment systems, *Chem. Eng. J.* 283 (2016) 582–594. <https://doi.org/10.1016/j.cej.2015.07.060>
- [17] J. Akunna, J. Bartie, Wastewater Treatment Infrastructure and Design, in: Colin A. Booth and Susanne M. Charlesworth (Ed.), *Water Resour. Built Environ. Manag. Issues Solut.*, First Edit, John Wiley & Sons, Ltd., 2014: pp. 350–370. <https://doi.org/10.1002/9781118809167.ch26>
- [18] M. Khan, U. Kalsoom, T. Mahmood, M. Riaz, R. Khan, Characterization and treatment of industrial effluents from sugar industry, *J. Chem. Soc. Pak.* 25 (2003).
- [19] A. Cassano, C. Conidi, E. Drioli, Comparison of the performance of UF membranes in olive mill wastewaters treatment, *Water Res.* 45 (2011) 3197–3204. <https://doi.org/10.1016/j.watres.2011.03.041>
- [20] J.M.O. Pulido, A review on the use of membrane technology and fouling control for olive mill wastewater treatment, *Sci. Total Environ.* 563–564 (2016) 664–675. <https://doi.org/10.1016/j.scitotenv.2015.09.151>
- [21] A.Y. Gebreyohannes, R. Mazzei, L. Giorno, Trends and current practices of olive mill wastewater treatment: Application of integrated membrane process and its future perspective, *Sep. Purif. Technol.* 162 (2016) 45–60. <https://doi.org/10.1016/j.seppur.2016.02.001>
- [22] A.C. Caputo, F. Scacchia, P.M. Pelagagge, Disposal of by-products in olive oil industry: waste-to-energy solutions, *Appl. Therm. Eng.* 23.2 (2003) 197–214. [https://doi.org/10.1016/S1359-4311\(02\)00173-4](https://doi.org/10.1016/S1359-4311(02)00173-4)
- [23] G. Taralas, M.G. Kontominas, Thermochemical treatment of solid and wastewater effluents originating from the olive oil food industry, *Energy and Fuels.* 19 (2005) 1179–1185. <https://doi.org/10.1021/ef040078r>

- [24] N. Adhoum, M. Lotfi, Decolourization and removal of phenolic compounds from olive mill wastewater by electrocoagulation, *Chem. Eng. Process. Process Intensif.* 43.10 (2004) 1281–1287. <https://doi.org/10.1016/j.cep.2003.12.001>
- [25] L. Bertin, F. Ferri, A. Scoma, L. Marchetti, F. Fava, Recovery of high added value natural polyphenols from actual olive mill wastewater through solid phase extraction, *Chem. Eng. J.* 171 (2011) 1287–1293. <https://doi.org/10.1016/j.cej.2011.05.056>
- [26] J. Beltran de Heredia, J. Garcia, Process integration: Continuous Anaerobic digestion–ozonation treatment of olive mill wastewater, *Ind. Eng. Chem. Res.* 44 (2005) 8750–8755. <https://doi.org/10.1021/ie040232x>
- [27] A. Fiorentino, A. Gentili, M. Isidori, M. Lavorgna, A. Parrella, F. Temussi, Olive oil mill wastewater treatment using a chemical and biological approach, *J. Agric. Food Chem.* 52 (2004) 5151–5154. <https://doi.org/10.1021/jf049799e>
- [28] I.P. Marques, Anaerobic digestion treatment of olive mill wastewater for effluent re-use in irrigation, *Desalination* 137 (2001) 233–239. [https://doi.org/10.1016/S0011-9164\(01\)00224-7](https://doi.org/10.1016/S0011-9164(01)00224-7)
- [29] A. Rozzi, F. Malpei, Treatment and disposal of olive mill effluents, *Int. Biodeterior. Biodegradation.* 38 (1996) 135–144. [https://doi.org/10.1016/S0964-8305\(96\)00042-X](https://doi.org/10.1016/S0964-8305(96)00042-X)
- [30] A. Ranalli, L. Lucera, S. Contento, antioxidizing potency of phenol compounds in olive oil mill wastewater, *J. Agric. Food Chem.* 51 (2003) 7636–7641. <https://doi.org/10.1021/jf034879o>
- [31] F. Visioli, A. Romani, N. Mulinacci, S. Zarini, D. Conte, F.F. Vincieri, C. Galli, Antioxidant and other biological activities of olive mill waste waters, *J. Agric. Food Chem.* 47 (1999) 3397–3401. <https://doi.org/10.1021/jf9900534>
- [32] G. Bisignano, A. Tomaino, R. Lo Cascio, G. Crisafi, N. Uccella, A. Saija, On the in-vitro antimicrobial activity of oleuropein and hydroxytyrosol, *J. Pharm. Pharmacol.* 51 (1999) 971–974. <https://doi.org/10.1211/0022357991773258>
- [33] S. Takaç, A. Karakaya, Recovery of Phenolic Antioxidants from Olive Mill Wastewater, *Recent Patents Chem. Eng.* 2 (2009) 230–237. <https://doi.org/10.2174/2211334710902030230>
- [34] F. Federici, F. Fava, N. Kalogerakis, D. Mantzavinos, Valorisation of agro-industrial by-products, effluents and waste: Concept, opportunities and the case of

- olive mill waste waters, *J. Chem. Technol. Biotechnol.* 84 (2009) 895–900.
<https://doi.org/10.1002/jctb.2165>
- [35] O.A. Mudimu, M. Peters, F. Brauner, G. Braun, Overview of membrane processes for the recovery of polyphenols from olive mill wastewater olive mill wastewater, *Am. J. Environ. Sci.* 8 (2012) 195–201.
<https://doi.org/10.3844/ajessp.2012.195.201>
- [36] H. Dhaouadi, B. Marrot, Olive mill wastewater treatment in a membrane bioreactor: Process feasibility and performances, *Chem. Eng. J.* 145 (2008) 225–231. <https://doi.org/10.1016/j.cej.2008.04.017>
- [37] T. Coskun, E. Debik, N.M. Demir, Treatment of olive mill wastewaters by nanofiltration and reverse osmosis membranes, *Desalination.* 259 (2010) 65–70.
<https://doi.org/10.1016/j.desal.2010.04.034>
- [38] C. Russo, A new membrane process for the selective fractionation and total recovery of polyphenols, water and organic substances from vegetation waters (VW), *J. Memb. Sci.* 288 (2007) 239–246.
<https://doi.org/10.1016/j.memsci.2006.11.020>
- [39] M. Pizzichini, C. Russo, Process for recovering the components of olive mill wastewater with membrane technologies, WO2005/123603, 2005.
- [40] A. El-Abbassi, A. Hafidi, M.C. García-Payo, M. Khayet, Concentration of olive mill wastewater by membrane distillation for polyphenols recovery, *Desalination.* 245 (2009) 670–674. <https://doi.org/10.1016/j.desal.2009.02.035>
- [41] S. Khoufi, F. Aloui, S. Sayadi, Pilot scale hybrid process for olive mill wastewater treatment and reuse, *Chem. Eng. Process. Process Intensif.* 48 (2009) 643–650.
<https://doi.org/10.1016/j.cep.2008.07.007>
- [42] O. Yahiaoui, H. Lounici, N. Abdi, N. Drouiche, N. Ghaffour, A. Pauss, N. Mameri, Treatment of olive mill wastewater by the combination of ultrafiltration and bipolar electrochemical reactor processes, *Chem. Eng. Process. Process Intensif.* 50 (2011) 37–41. <https://doi.org/10.1016/j.cep.2010.11.003>
- [43] E. Garcia-Castello, A. Cassano, A. Criscuoli, C. Conidi, E. Drioli, Recovery and concentration of polyphenols from olive mill wastewaters by integrated membrane system, *Water Res.* 44 (2010) 3883–3892.
<https://doi.org/10.1016/j.watres.2010.05.005>

- [44] M. Stoller, M. Bravi, Critical flux analyses on differently pretreated olive vegetation waste water streams: Some case studies, *Desalination*. 250 (2010) 578–582. <https://doi.org/10.1016/j.desal.2009.09.027>
- [45] E.O. Akdemir, A. Ozer, Investigation of two ultrafiltration membranes for treatment of olive oil mill wastewater, *Desalination*. 249 (2009) 660–666. <https://doi.org/10.1016/j.desal.2008.06.035>
- [46] A. Cassano, C. Conidi, L. Giorno, E. Drioli, Fractionation of olive mill wastewaters by membrane separation techniques, *J. Hazard. Mater.* 248–249 (2013) 185–193. <https://doi.org/10.1016/j.jhazmat.2013.01.006>
- [47] C.A. Paraskeva, V.G. Papadakis, E. Tsarouchi, D.G. Kanellopoulou, P.G. Koutsoukos, Membrane processing for olive mill wastewater fractionation, *Desalination*. 213 (2007) 218–229. <https://doi.org/10.1016/j.desal.2006.04.087>
- [48] M. Stoller, Technical optimization of a dual ultrafiltration and nanofiltration pilot plant in batch operation by means of the critical flux theory: A case study, *Chem. Eng. Process. Process Intensif.* 47 (2008) 1165–1170. <https://doi.org/10.1016/j.cep.2007.07.012>
- [49] A. El-Abbassi, M. Khayet, A. Hafidi, Micellar enhanced ultrafiltration process for the treatment of olive mill wastewater, *Water Res.* 45 (2011) 4522–4530. <https://doi.org/10.1016/j.watres.2011.05.044>
- [50] M. Stoller, Effective fouling inhibition by critical flux based optimization methods on a NF membrane module for olive mill wastewater treatment, *Chem. Eng. J.* 168 (2011) 1140–1148. <https://doi.org/10.1016/j.cej.2011.01.098>
- [51] A. El-Abbassi, A. Hafidi, M. Khayet, M.C. García-Payo, Integrated direct contact membrane distillation for olive mill wastewater treatment, *Desalination*. 323 (2013) 31–38. <https://doi.org/10.1016/j.desal.2012.06.014>
- [52] A. El-Abbassi, H. Kiai, A. Hafidi, M.C. García-Payo, M. Khayet, Treatment of olive mill wastewater by membrane distillation using polytetrafluoroethylene membranes, *Sep. Purif. Technol.* 98 (2012) 55–61. <https://doi.org/10.1016/j.seppur.2012.06.026>
- [53] A. El-Abbassi, M. Khayet, H. Kiai, A. Hafidi, M.C. García-Payo, Treatment of crude olive mill wastewaters by osmotic distillation and osmotic membrane distillation, *Sep. Purif. Technol.* 104 (2013) 327–332. <https://doi.org/10.1016/j.seppur.2012.12.006>

- [54] C.A. Paraskeva, V.G. Papadakis, D.G. Kanellopoulou, P.G. Koutsoukos, K.C. Angelopoulos, Membrane filtration of olive mill wastewater and exploitation of its fractions, *Water Environ. Res.* 79 (2007).
<https://doi.org/10.2175/106143006X115345>
- [55] T.Y. Wu, A.W. Mohammad, J.M. Jahim, N. Anuar, Pollution control technologies for the treatment of palm oil mill effluent (POME) through end-of-pipe processes, *J. Environ. Manage.* 91 (2010) 1467–1490.
<https://doi.org/10.1016/j.jenvman.2010.02.008>
- [56] Y. Zhang, L. Yan, X. Qiao, L. Chi, X. Niu, Z. Mei, Z. Zhang, Integration of biological method and membrane technology in treating palm oil mill effluent, *J. Environ. Sci.* 20 (2008) 558–564. [https://doi.org/10.1016/S1001-0742\(08\)62094-X](https://doi.org/10.1016/S1001-0742(08)62094-X)
- [57] A.L. Ahmad, C.Y. Chan, Sustainability of palm oil industries: an innovative treatment via membrane technology, *J. Appl. Sci.* 9 (2009) 3074–3079.
<https://doi.org/10.3923/jas.2009.3074.3079>
- [58] T.Y. Wu, A.W. Mohammad, J.M. Jahim, N. Anuar, Palm oil mill effluent (POME) treatment and bioresources recovery using ultrafiltration membrane: Effect of pressure on membrane fouling, *Biochem. Eng. J.* 35 (2007) 309–317.
<https://doi.org/10.1016/j.bej.2007.01.029>
- [59] P.E. Poh, M.F. Chong, Development of anaerobic digestion methods for palm oil mill effluent (POME) treatment, *Bioresour. Technol.* 100 (2009) 1–9.
<https://doi.org/10.1016/j.biortech.2008.06.022>
- [60] K. Vijayaraghavan, D. Ahmad, M. Ezani Bin Abdul Aziz, Aerobic treatment of palm oil mill effluent, *J. Environ. Manage.* 82 (2007) 24–31.
<https://doi.org/10.1016/j.jenvman.2005.11.016>
- [61] A.L. Ahmad, M.F. Chong, S. Bhatia, A comparative study on the membrane based palm oil mill effluent (POME) treatment plant, *J. Hazard. Mater.* 171 (2009) 166–174. <https://doi.org/10.1016/j.jhazmat.2009.05.114>
- [62] P.F. Rupani, P.S. Rajeev, M.H. Ibrahim, N. Esa, Review of current palm oil mill effluent (POME) Treatment methods: Vermicomposting as a sustainable practice, *World Appl. Sci. J.* 11 (2010) 70–81.
- [63] J.C. Igwe, C.C. Onyegbado, A review of palm oil mill effluent (Pome) water treatment, *Glob. J. Environ. Res.* 1 (2007) 54–62.

- [64] A.L. Ahmad, S. Ismail, S. Bhatia, Water recycling from palm oil mill effluent (POME) using membrane technology, *Desalination*. 157 (2003) 87–95. [https://doi.org/10.1016/S0011-9164\(03\)00387-4](https://doi.org/10.1016/S0011-9164(03)00387-4)
- [65] A.L. Ahmad, M.F. Chong, S. Bhatia, S. Ismail, Drinking water reclamation from palm oil mill effluent (POME) using membrane technology, *Desalination*. 191 (2006) 35–44. <https://doi.org/10.1016/j.desal.2005.06.033>
- [66] A. Damayanti, Z. Ujang, M.R. Salim, The influenced of PAC, zeolite, and *Moringa oleifera* as biofouling reducer (BFR) on hybrid membrane bioreactor of palm oil mill effluent (POME), *Bioresour. Technol.* 102 (2011) 4341–4346. <https://doi.org/10.1016/j.biortech.2010.12.061>
- [67] T.Y. Wu, A.W. Mohammad, J.M. Jahim, N. Anuar, A holistic approach to managing palm oil mill effluent (POME): Biotechnological advances in the sustainable reuse of POME, *Biotechnol. Adv.* 27 (2009) 40–52. <https://doi.org/10.1016/j.biotechadv.2008.08.005>
- [68] A.W. Mohammad, P.T. Yap, T.Y. Wu, Performance of hydrophobic ultrafiltration membranes in the treatment and protein recovery from palm oil mill effluent (POME), *Desalin. Water Treat.* 10 (2009) 332–338. <https://doi.org/10.5004/dwt.2009.932>
- [69] A.L. Ahmad, M.F. Chong, S. Bhatia, Mathematical modeling of multiple solutes system for reverse osmosis process in palm oil mill effluent (POME) treatment, *Chem. Eng. J.* 132 (2007) 183–193. <https://doi.org/10.1016/j.cej.2006.12.022>
- [70] F.X. Milani, D. Nutter, G. Thoma, Environmental impacts of dairy processing and products: A review, *J. Dairy Sci.* 94 (2011) 4243–4254. <https://doi.org/10.3168/jds.2010-3955>
- [71] T.J. Britz, C. van Schalkwyk, Y.-T. Hung, Treatment of dairy processing wastewater, in: *Waste Treat. Food Process. Ind.*, CRC Press, Boca Raton, FL, 2006: pp. 1–28.
- [72] B. Sarkar, P.P. Chakrabarti, A. Vijaykumar, V. Kale, Wastewater treatment in dairy industries - possibility of reuse, *Desalination*. 195 (2006) 141–152. <https://doi.org/10.1016/j.desal.2005.11.015>
- [73] C. Tocchi, E. Federici, L. Fidati, R. Manzi, V. Vincigurerra, M. Petruccioli, Aerobic treatment of dairy wastewater in an industrial three-reactor plant: Effect of aeration regime on performances and on protozoan and bacterial communities, *Water Res.* 46 (2012) 3334–3344. <https://doi.org/10.1016/j.watres.2012.03.032>

- [74] M. Jedrzejewska-Cicinska, K. Kozak, M. Krzemieniewski, A comparison of the technological effectiveness of dairy wastewater treatment in anaerobic UASB reactor and anaerobic reactor with an innovative design, *Environ. Technol.* 28 (2007) 1127–1133. <https://doi.org/10.1080/09593332808618868>
- [75] S. Venkata Mohan, V. Lalit Babu, P.N. Sarma, Anaerobic biohydrogen production from dairy wastewater treatment in sequencing batch reactor (AnSBR): Effect of organic loading rate, *Enzyme Microb. Technol.* 41 (2007) 506–515. <https://doi.org/10.1016/j.enzmictec.2007.04.007>
- [76] B. Demirel, O. Yenigun, T.T. Onay, Anaerobic treatment of dairy wastewaters: A review, *Process Biochem.* 40 (2005) 2583–2595. <https://doi.org/10.1016/j.procbio.2004.12.015>
- [77] M. Passeggi, I. López, L. Borzacconi, Modified UASB reactor for dairy industry wastewater: Performance indicators and comparison with the traditional approach, *J. Clean. Prod.* 26 (2012) 90–94. <https://doi.org/10.1016/j.jclepro.2011.12.022>
- [78] P. Seesuriyachan, A. Kuntiya, K. Sasaki, C. Techapun, Biocoagulation of dairy wastewater by *Lactobacillus casei* TISTR 1500 for protein recovery using micro-aerobic sequencing batch reactor (micro-aerobic SBR), *Process Biochem.* 44 (2009) 406–411. <https://doi.org/10.1016/j.procbio.2008.12.006>
- [79] S. Tchamango, C.P. Nansu-Njiki, E. Ngameni, D. Hadjiev, A. Darchen, Treatment of dairy effluents by electrocoagulation using aluminium electrodes, *Sci. Total Environ.* 408 (2010) 947–952. <https://doi.org/10.1016/j.scitotenv.2009.10.026>
- [80] S.L. Lansing, J.F. Martin, Use of an ecological treatment system (ETS) for removal of nutrients from dairy wastewater, *Ecol. Eng.* 28 (2006) 235–245. <https://doi.org/10.1016/j.ecoleng.2006.04.006>
- [81] S. Venkata Mohan, G. Mohanakrishna, G. Velvizhi, V.L. Babu, P.N. Sarma, Biocatalyzed electrochemical treatment of real field dairy wastewater with simultaneous power generation, *Biochem. Eng. J.* 51 (2010) 32–39. <https://doi.org/10.1016/j.bej.2010.04.012>
- [82] Y. Pouliot, Membrane processes in dairy technology-From a simple idea to worldwide panacea, *Int. Dairy J.* 18 (2008) 735–740. <https://doi.org/10.1016/j.idairyj.2008.03.005>

- [83] A. Chollangi, M.M. Hossain, Separation of proteins and lactose from dairy wastewater, *Chem. Eng. Process. Process Intensif.* 46 (2007) 398–404. <https://doi.org/10.1016/j.cep.2006.05.022>
- [84] J. Luo, L. Ding, Y. Wan, P. Paullier, M.Y. Jaffrin, Fouling behavior of dairy wastewater treatment by nanofiltration under shear-enhanced extreme hydraulic conditions, *Sep. Purif. Technol.* 88 (2012) 79–86. <https://doi.org/10.1016/j.seppur.2011.12.008>
- [85] M. Rabiller-Baudry, H. Bouzid, B. Chaufer, L. Paugam, D. Delaunay, O. Mekmene, S. Ahmad, F. Gaucheron, On the origin of flux dependence in pH-modified skim milk filtration, *Dairy Sci. Technol.* 89 (2009) 363–385. <https://doi.org/10.1051/dst/2009018>
- [86] M. Frappart, M. Jaffrin, L.H. Ding, Reverse osmosis of diluted skim milk: Comparison of results obtained from vibratory and rotating disk modules, *Sep. Purif. Technol.* 60 (2008) 321–329. <https://doi.org/10.1016/j.seppur.2007.09.007>
- [87] M. Passeggi, I. López, L. Borzacconi, Integrated anaerobic treatment of dairy industrial wastewater and sludge, *Water Sci. Technol.* 59 (2009) 501–506. <https://doi.org/10.2166/wst.2009.010>
- [88] M.S. Yorgun, I. Akmehmet Balcioglu, O. Saygin, Performance comparison of ultrafiltration, nanofiltration and reverse osmosis on whey treatment, *Desalination.* 229 (2008) 204–216. <https://doi.org/10.1016/j.desal.2007.09.008>
- [89] J. Luo, L. Ding, B. Qi, M.Y. Jaffrin, Y. Wan, A two-stage ultrafiltration and nanofiltration process for recycling dairy wastewater, *Bioresour. Technol.* 102 (2011) 7437–7442. <https://doi.org/10.1016/j.biortech.2011.05.012>
- [90] Y.-W. Gong, H.-X. Zhang, X.-N. Cheng, Treatment of dairy wastewater by two-stage membrane operation with ultrafiltration and nanofiltration, *Water Sci. Technol.* 65 (2012) 915–919. <https://doi.org/10.2166/wst.2012.937>
- [91] J. Luo, L. Ding, Influence of pH on treatment of dairy wastewater by nanofiltration using shear-enhanced filtration system, *Desalination.* 278 (2011) 150–156. <https://doi.org/10.1016/j.desal.2011.05.025>
- [92] B. Farizoglu, S. Uzuner, The investigation of dairy industry wastewater treatment in a biological high performance membrane system, *Biochem. Eng. J.* 57 (2011) 46–54. <https://doi.org/10.1016/j.bej.2011.08.007>

- [93] J. Luo, W. Cao, L. Ding, Z. Zhu, Y. Wan, M.Y. Jaffrin, Treatment of dairy effluent by shear-enhanced membrane filtration: The role of foulants, *Sep. Purif. Technol.* 96 (2012) 194–203. <https://doi.org/10.1016/j.seppur.2012.06.009>
- [94] G. Rice, A. Barber, A. O'Connor, G. Stevens, S. Kentish, Fouling of NF membranes by dairy ultrafiltration permeates, *J. Memb. Sci.* 330 (2009) 117–126. <https://doi.org/10.1016/j.memsci.2008.12.048>
- [95] R. Hepsen, Y. Kaya, Optimization of membrane fouling using experimental design: An example from dairy wastewater treatment, *Ind. Eng. Chem. Res.* 51 (2012) 16074–16084. <https://doi.org/10.1021/ie302450s>
- [96] J. Luo, L. Ding, Y. Wan, M.Y. Jaffrin, Threshold flux for shear-enhanced nanofiltration: Experimental observation in dairy wastewater treatment, *J. Memb. Sci.* 409–410 (2012) 276–284. <https://doi.org/10.1016/j.memsci.2012.03.065>
- [97] J. Luo, L. Ding, Y. Wan, P. Paullier, M.Y. Jaffrin, Application of NF-RDM (nanofiltration rotating disk membrane) module under extreme hydraulic conditions for the treatment of dairy wastewater, *Chem. Eng. J.* 163 (2010) 307–316. <https://doi.org/10.1016/j.cej.2010.08.007>
- [98] A. Suárez, T. Fidalgo, F.A. Riera, Recovery of dairy industry wastewaters by reverse osmosis. Production of boiler water, *Sep. Purif. Technol.* 133 (2014) 204–211. <https://doi.org/10.1016/j.seppur.2014.06.041>
- [99] M. Vourch, B. Balannec, B. Chaufer, G. Dorange, Treatment of dairy industry wastewater by reverse osmosis for water reuse, *Desalination* 219 (2008) 190–202. <https://doi.org/10.1016/j.desal.2007.05.013>
- [100] Z. Xu, G. Nakhla, J. Patel, Characterization and modeling of nutrient-deficient tomato-processing wastewater treatment using an anaerobic/aerobic system, *Chemosphere* 65 (2006) 1171–1181. <https://doi.org/10.1016/j.chemosphere.2006.03.063>
- [101] M. Iaquinta, M. Stoller, C. Merli, Optimization of a nanofiltration membrane process for tomato industry wastewater effluent treatment, *Desalination*. 245 (2009) 314–320. <https://doi.org/10.1016/j.desal.2008.05.028>
- [102] P. Chowdhury, T. Viraraghavan, A. Srinivasan, Biological treatment processes for fish processing wastewater - A review, *Bioresour. Technol.* 101 (2010) 439–449. <https://doi.org/10.1016/j.biortech.2009.08.065>

- [103] P.C. Sridang, J. Kaiman, A. Pottier, C. Wisniewski, Benefits of MBR in seafood wastewater treatment and water reuse: study case in Southern part of Thailand, *Desalination*. 200 (2006) 712–714. <https://doi.org/10.1016/j.desal.2006.03.509>
- [104] R.O. Cristóvão, C.M. Botelho, R.J.E. Martins, J.M. Loureiro, R.A.R. Boaventura, Fish canning industry wastewater treatment for water reuse – a case study, *J. Clean. Prod.* 87 (2015) 603–612. <https://doi.org/10.1016/j.jclepro.2014.10.076>
- [105] R. Cristóvão, C. Botelho, R. Martins, R. Boaventura, Chemical and Biological Treatment of Fish Canning Wastewaters, *Int. J. Biosci. Biochem. Bioinforma.* 2 (2012) 7763. <https://doi.org/10.7763/IJBBB.2012.V2.108>
- [106] R.O. Cristóvão, C. Gonçalves, C.M. Botelho, R.J.E. Martins, J.M. Loureiro, R.A.R. Boaventura, Fish canning wastewater treatment by activated sludge: Application of factorial design optimization. Biological treatment by activated sludge of fish canning wastewater., *Water Resour. Ind.* 10 (2015) 29–38. <https://doi.org/10.1016/j.wri.2015.03.001>
- [107] M.D. Afonso, R. Borquez, Review of the treatment of seafood processing wastewaters and recovery of proteins therein by membrane separation processes - Prospects of the ultrafiltration of wastewaters from the fish meal industry, *Desalination* 142 (2002) 29–45. <https://doi.org/10.1016/j.desal.2008.01.068>
- [108] M. Kuca, D. Szaniawska, Application of microfiltration and ceramic membranes for treatment of salted aqueous effluents from fish processing, *Desalination* 241 (2009) 227–235.
- [109] R. Pérez-Gálvez, E.M. Guadix, J.P. Bergé, A. Guadix, Operation and cleaning of ceramic membranes for the filtration of fish press liquor, *J. Memb. Sci.* 384 (2011) 142–148. <https://doi.org/10.1016/j.memsci.2011.09.019>
- [110] P.C. Sridang, A. Pottier, C. Wisniewski, A. Grasmick, Performance and microbial surveying in submerged membrane bioreactor for seafood processing wastewater treatment, *J. Memb. Sci.* 317 (2008) 43–49. <https://doi.org/10.1016/j.memsci.2007.11.011>
- [111] P. Artiga, G. García-Toriello, R. Méndez, J.M. Garrido, Use of a hybrid membrane bioreactor for the treatment of saline wastewater from a fish canning factory, *Desalination*. 221 (2008) 518–525. <https://doi.org/10.1016/j.desal.2007.01.112>
- [112] M.R. Bilad, P. Declerck, A. Piasecka, L. Vanysacker, X. Yan, I.F.J. Vankelecom, Treatment of molasses wastewater in a membrane bioreactor: Influence of membrane pore size, *Sep. Purif. Technol.* 78 (2011) 105–112.

- [113] D. Pant, A. Adholeya, Biological approaches for treatment of distillery wastewater: A review, *Bioresour. Technol.* 98 (2007) 2321–2334. <https://doi.org/10.1016/j.biortech.2006.09.027>
- [114] Y. Satyawali, M. Balakrishnan, Wastewater treatment in molasses-based alcohol distilleries for COD and color removal: A review, *J. Environ. Manage.* 86 (2008) 481–497. <https://doi.org/10.1016/j.jenvman.2006.12.024>
- [115] S. Mohana, B.K. Acharya, D. Madamwar, Distillery spent wash: Treatment technologies and potential applications, *J. Hazard. Mater.* 163 (2009) 12–25. <https://doi.org/10.1016/j.jhazmat.2008.06.079>
- [116] L.A. Ioannou, G.L. Puma, D. Fatta-Kassinos, Treatment of winery wastewater by physicochemical, biological and advanced processes: A review, *J. Hazard. Mater.* 286 (2015) 343–368. <https://doi.org/10.1016/j.jhazmat.2014.12.043>
- [117] S.K. Nataraj, K.M. Hosamani, T.M. Aminabhavi, Distillery wastewater treatment by the membrane-based nanofiltration and reverse osmosis processes, *Water Res.* 40 (2006) 2349–2356. <https://doi.org/10.1016/j.watres.2006.04.022>
- [118] P.A. Shivajirao, Treatment of distillery wastewater using membrane technologies, *Int. J. Adv. Eng. Res. Stud. I* (2012) 275–283.
- [119] Z.V.P. Murthy, L.B. Chaudhari, Treatment of Distillery Spent Wash By Combined UF and RO Processes, *Glob. NEST J.* 11 (2009) 235–240.
- [120] U.K. Rai, M. Muthukrishnan, B.K. Guha, Tertiary treatment of distillery wastewater by nanofiltration, *Desalination.* 230 (2008) 70–78. <https://doi.org/10.1016/j.desal.2007.11.017>
- [121] C. Sagne, C. Fargues, R. Lewandowski, M.-L. Lameloise, M. Decloux, Screening of reverse osmosis membranes for the treatment and reuse of distillery condensates into alcoholic fermentation, *Desalination.* 219 (2008) 335–347. <https://doi.org/10.1016/j.desal.2007.05.020>
- [122] R. Gupta, Y. Satyawali, V.S. Batra, M. Balakrishnan, Submerged membrane bioreactor using fly ash filters: trials with distillery wastewater, *Water Sci. Technol.* 58 (2008) 1281–1284. <https://doi.org/10.2166/wst.2008.352>
- [123] Y. Satyawali, M. Balakrishnan, Treatment of distillery effluent in a membrane bioreactor (MBR) equipped with mesh filter, *Sep. Purif. Technol.* 63 (2008) 278–286. <https://doi.org/10.1016/j.seppur.2008.05.008>

- [124] X.L. Melamane, P.J. Strong, J.E. Burgess, Treatment of wine distillery wastewater: a review with emphasis on anaerobic membrane reactors, *S. Afr. J. Enol. Vitic.* 28 (2007) 25–36.
- [125] K.P.M. Mosse, A.F. Patti, E.W. Christen, T.R. Cavagnaro, Review: Winery wastewater quality and treatment options in Australia, *Aust. J. Grape Wine Res.* 17 (2011) 111–122. <https://doi.org/10.1111/j.1755-0238.2011.00132.x>
- [126] G. Lofrano, S. Meric, A comprehensive approach to winery wastewater treatment: a review of the state-of-the-art, *Desalin. Water Treat.* 57 (2016) 3011–3028. <https://doi.org/10.1080/19443994.2014.982196>
- [127] P.J. Strong, J.E. Burgess, Treatment Methods for Wine-Related and Distillery Wastewaters: A Review, *Bioremediat. J.* 12 (2008) 70–8770. <https://doi.org/10.1080/10889860802060063>
- [128] G. Andreottola, P. Foladori, G. Ziglio, Biological treatment of winery wastewater: An overview, *Water Sci. Technol.* 60 (2009) 1117–1125. <https://doi.org/10.2166/wst.2009.551>
- [129] N. Basset, S. López-Palau, J. Dosta, J. Mata-Álvarez, Comparison of aerobic granulation and anaerobic membrane bioreactor technologies for winery wastewater treatment, *Water Sci. Technol.* 69 (2014) 320–327. <https://doi.org/10.2166/wst.2013.713>
- [130] L.A. Ioannou, C. Michael, N. Vakondios, K. Drosou, N.P. Xekoukoulotakis, E. Diamadopoulou, D. Fatta-Kassinos, Winery wastewater purification by reverse osmosis and oxidation of the concentrate by solar photo-Fenton, *Sep. Purif. Technol.* 118 (2013) 659–669. <https://doi.org/10.1016/j.seppur.2013.07.049>
- [131] C.M. Galanakis, E. Markouli, V. Gekas, Recovery and fractionation of different phenolic classes from winery sludge using ultrafiltration, *Sep. Purif. Technol.* 107 (2013) 245–251. <https://doi.org/10.1016/j.seppur.2013.01.034>
- [132] A. Giacobbo, J.M. Do Prado, A. Meneguzzi, A.M. Bernardes, M.N. De Pinho, Microfiltration for the recovery of polyphenols from winery effluents, *Sep. Purif. Technol.* 143 (2015) 12–18. <https://doi.org/10.1016/j.seppur.2015.01.019>
- [133] A. Giacobbo, M. Oliveira, E.C.N.F. Duarte, H.M.C. Mira, A.M. Bernardes, M.N. De Pinho, Ultrafiltration based process for the recovery of polysaccharides and polyphenols from winery effluents, *Sep. Sci. Technol.* 48 (2013) 438–444. <https://doi.org/10.1080/01496395.2012.725793>

- [134] A. Giacobbo, A.M. Bernardes, M.N. de Pinho, Nanofiltration for the Recovery of Low Molecular Weight Polysaccharides and Polyphenols from Winery Effluents, *Sep. Sci. Technol.* 48 (2013) 2524–2530.
<https://doi.org/10.1080/01496395.2013.809762>
- [135] G. Andreottola, M. Cadonna, P. Foladori, G. Gatti, F. Lorenzi, P. Nardelli, Heavy metal removal from winery wastewater in the case of restrictive discharge regulation, *Water Sci. Technol.* 56 (2007) 111–120.
<https://doi.org/10.2166/wst.2007.479>
- [136] P. Artiga, M. Carballa, J.M. Garrido, R. Méndez, Treatment of winery wastewaters in a membrane submerged bioreactor, *Water Sci. Technol.* 56 (2007) 63–69.
<https://doi.org/10.2166/wst.2007.473>
- [137] A. Shah, J. Bulleri, R. Ross, J. Carter, M. Long, Successful plant scale winery wastewater treatment using membrane bioreactor in Northern California, in: *Proc. Water Environ. Fed.* (2008) 3408–3425.
<https://doi.org/10.2175/193864708788733107>
- [138] V. Ferre, A. Trepin, T. Giménez, S. Lluch, Design and performance of full-scale iMBR plants treating winery wastewater effluents in Italy and Spain, in: *5th Int. Spec. Conf. Sustain. Vitic. Winer. Waste Ecol. Impacts Manag.*, Trento, Italy, 2009: pp.
- [139] G. Guglielmi, G. Andreottola, P. Foladori, G. Ziglio, Membrane bioreactors for winery wastewater treatment: Case-studies at full scale, *Water Sci. Technol.* 60 (2009) 1201–1207. <https://doi.org/10.2166/wst.2009.560>
- [140] D. Bolzonella, F. Fatone, P. Pavan, F. Cecchi, Application of a membrane bioreactor for winery wastewater treatment, *Water Sci. Technol.* 62 (2010) 2754–2759. <https://doi.org/10.2166/wst.2010.645>
- [141] N. Basset, C. Vidal, A. Coll, I. Fernández, J. Dosta, AnMBR technologies (CSTR and UASB type) for winery wastewater treatment at low temperatures, (2012).
- [142] C. Valderrama, G. Ribera, N. Bah, M. Rovira, T. Giménez, R. Nomen, S. Lluch, M. Yuste, X. Martinez-Lladó, Winery wastewater treatment for water reuse purpose: Conventional activated sludge versus membrane bioreactor (MBR). A comparative case study, *Desalination* 306 (2012) 1–7.
<https://doi.org/10.1016/j.desal.2012.08.016>

- [143] N. Basset, E. Santos, J. Dosta, J. Mata-Álvarez, Start-up and operation of an AnMBR for winery wastewater treatment, *Ecol. Eng.* 86 (2016) 279–289. <https://doi.org/10.1016/j.ecoleng.2015.11.003>
- [144] I. Alkorta , C. Garbisu, M.J. Llama, J.L. Serra, β -Transeliminación of citrus pectin catalyzed by penicillium italicum pectin lyase in a membrane reactor, *Applied Biochemistry and Biotechnology* 55 (1995) 249- 259. <https://doi.org/10.1007/BF02786864>
- [145] K. Bélafi-Bakò, M. Eszterle, K. Kiss, N. Nemestóthy, L. Gubicza, Hydrolysis of pectin by *Aspergillus niger* polygalacturonase in a membrane bioreactor, *J. Food Eng.* 78 (2007) 438-442. <https://doi.org/10.1016/j.jfoodeng.2005.10.012>
- [146] J.M Rodriguez-Nogales, N. Ortega , M. Perez-Mateos, M. Busto, Pectin hydrolysis in a free enzyme membrane reactor: An approach to the wine and juice clarification, *Food Chem.* 107 (2008) 112-119. <https://doi.org/10.1016/j.foodchem.2007.07.057>
- [147] E. Olano-Martin, K.C. Mountzouris , G.R.Gibson, R.A. Rastall, Continuous production of pectic oligosaccharides in an enzyme membrane reactor, *J. Food Sci.* 66 (2001) 966-971. <https://doi.org/10.1111/j.1365-2621.2001.tb08220.x>
- [148] A.R. Szaniawski, H.G. Spencer, Effects of pectin concentration and crossflow velocity on permeability in the microfiltration of dilute pectin solutions by macroporous titania membranes containing immobilized pectinase, *Biotechnol. Prog.* 12 (1996) 403-405. <https://doi.org/10.1021/bp9500829>
- [149] M.E. Carrín., L.N. Ceci, J.E.Lozano, Ultrafiltration fibers like bioreactors, *Latin American Applied Research* 31 (2001) 241-245.
- [150] M.E Carrín, L.N Ceci, J.E. Lozano, Effects of pectinase immobilization during hollow fiber ultrafiltration of apple juice, *J. Food Proc. Eng.* 23 (2000) 281-298. <https://doi.org/10.1111/j.1745-4530.2000.tb00516.x>
- [151] V. Bakoyianis, A.A Koutinas, A catalytic multistage fixed-bed tower bioreactor in an industrial-scale pilot plant for alcohol production, *Biotechnol. Bioeng.* 49 (1996) 197–203. [https://doi.org/10.1002/\(SICI\)1097-0290\(19960120\)49:2<197::AID-BIT8>3.0.CO;2-L](https://doi.org/10.1002/(SICI)1097-0290(19960120)49:2<197::AID-BIT8>3.0.CO;2-L)
- [152] P. Loukatos, M. Kiaris, I. Ligas, G .Bourgos, M. Kanellaki, M. Komaitis, A.A. Koutinas, Continuous wine making by γ -alumina-supported biocatalyst, *Appl. Biochem. Biotechnol.* 89 (2000) 1–13. <https://doi.org/10.1385/ABAB:89:1:1>

- [153] M. Ciani, L. Ferraro, Enhanced glycerol content in wines made with immobilized *Candida stellata* Cells, *Appl. Env. Microbiol.* 62 (1996) 128–132.
- [154] G. Suzzi, P. Romano, L. Vannini, L. Turbanti, P. Domizio, Cell-recycle batch fermentation using immobilized cells of flocculent *Saccharomyces cerevisiae* wine strains, *World J. Microbiol. Biotechnol.* 12 (1996) 25–27.
<https://doi.org/10.1007/BF00327794>
- [155] E.P. Bardi, A.A. Koutinas, Immobilization of yeast on delignified cellulosic material for room temperature and low-temperature wine making, *J. Agric. Food Chem.* 42 (1994) 221–226. <https://doi.org/10.1007/BF00327794>
- [156] E.P. Bardi, A.A. Koutinas, M. Kanellaki, Room and low temperature brewing with yeast immobilized on gluten pellets, *Process Biochem.* 32 (1997) 691–696.
[https://doi.org/10.1016/S0032-9592\(97\)00030-7](https://doi.org/10.1016/S0032-9592(97)00030-7)
- [157] E.P. Bardi, A.A. Koutinas, M. Soupioni, M. Kanellaki, Immobilization of yeast on delignified cellulosic material for low temperature brewing, *J. Agric. Food Chem.* 44 (1996), 463–467. <https://doi.org/10.1021/jf9501406>
- [158] Y. Kourkoutas, A. Ekatorou, I.M. Banat, R. Marchant, A.A. Koutinas, Immobilization technologies and support materials suitable in alcohol beverages production: a review, *Food Microb.* 21 (2004) 377-397.
<https://doi.org/10.1016/j.fm.2003.10.005>

CHAPTER 6

Published Book Chapter

Photocatalytic Membrane Reactor for Sustainable Environmental Remediation

Sudip Chakraborty, Jaya Sikder, Debolina Mukherjee, Stefano Curcio,
and Vincenza Calabro

Keywords

Photocatalysis • TiO₂ • Membrane reactor • Environmental remediation • Pharmaceuticle waste • Nanocatalyst

1 Introduction

The photo mineralization of organics by semiconductor photocatalysts is an area of intensive research, ideally the end products of these processes should be carbon dioxide, water, and inorganic mineral salts, which have a minimum environmental impact. Waste discharge from pharmaceutical industries is a major source of water pollution and is increasing day by day (Giraldo et al. 2010). Due to stringent environmental regulations it is necessary to remove the active component from the waste discharge before throwing it into the environment. In addition and to avoid the contamination of natural water bodies by residual pharmaceutical waste compounds, pretreatment to degrade these compounds in municipal and industrial effluents is needed before their release into the environment described by chen and chu (2012) and also Elmolla and Chaudhuri (2010). In this work, the degradation of aqueous solution of chlorhexidine digluconate (CHD), an antibiotic drug, by heterogeneous photocatalysis was studied using supported TiO₂ nanoparticle. The major concern of this study is to bring down the limitations of suspension mode heterogeneous photocatalysis by the implementation of immobilized TiO₂ with the help of porous membrane which was briefly mentioned by Dasgupta et al. (2015), Sarkar et al. (2015).

The degradation by heterogeneous photocatalysis using TiO₂ nanoparticles immobilized on membranes surface was thoroughly studied previously by Dasgupta et al. (2015), Laera et al. (2011) as well as by Zhang et al. (2010). Polymeric hollow fiber membranes were functionalized and modified at room temperature with the aim of degrading pharmaceutical model contaminant CHD under UV irradiation mentioned by Achilleos et al. (2010), Das (2014). The progress of the reaction was monitored by absorbing and measuring the reduction in COD and TOC throughout the experiment. The adsorption study has shown good confirmation with Langmuir isotherm and during the reaction at initial stage, it followed pseudo-first-order reaction. In this study, the photocatalytic treatment of the pharmaceutical CHD was carried out at a higher concentration level ($\sim 1500 \text{ mg}\cdot\text{L}^{-1}$) using the photocatalyst TiO₂ in the presence of UV irradiation. Finally, the present study confirmed that there is a significant effect of adsorption on photocatalytic degradation. The membranes used degraded significant amount of Chlorhexidine digluconate, showcasing the potential of membranes for purification of pharmaceutical wastewater.

2 Materials and Methods

Two catalyst systems of titanium dioxide photocatalyst nanopowder (pure anatase, 637254) of particle size $<25 \text{ nm}$ and specific surface area $45\text{--}55 \text{ m}^2\cdot\text{g}^{-1}$ (Cat₁) and AeroxideP25 (mixture of rutile and anatase, 718467) of particle size 21 nm with surface area (BET) $35\text{--}65 \text{ m}^2\cdot\text{g}^{-1}$ (Cat₂) from Sigma-Aldrich, were used. Chlorhexidine digluconate solution (20% w/v, from Sigma-Aldrich) was used to prepare the simulated solutions to standardize the analytical process. A batch

S. Chakraborty (✉) · D. Mukherjee · S. Curcio · V. Calabro
Laboratory of Transport Phenomena and Biotechnology,
University of Calabria, Via- P. Bucci, Cubo 42/A, 87036 Rende,
CS, Italy
e-mail: sudip.chakraborty@unical.it; zsudip.c@gmail.com

J. Sikder
Department of Chemical Engineering, National Institute of
Technology Durgapur, Durgapur, West Bengal 713209, India

photoreactor was used for the treatment of synthetic wastewater. The reactor comprises a chamber (17 cm × 17 cm × 17 cm) with UVA lamp (10 W) from the top of the reactor and a magnetic stirrer to ascertain the proper mixing of the reaction solution and even distribution of UV irradiation to the catalyst system. The distance of sample solution (upper surface) to the radiation source maintained during the photodegradation process was 7 cm, and the reaction solution thickness was 3 cm. The UV light intensity was controlled with an external controller, and the inside intensity was measured using a solar UVA meter (TM 208, Tenmars, Taiwan).

3 Results and Discussion

3.1 Adsorption Behavior of CHD on to the Catalyst System

The extent of the adsorption for substrate molecules on to the catalyst surface controls the rate of the photo degradation process. Adsorption behavior changes with the nature of the catalyst system, respective surface properties, and availability of the substrate on to catalyst surface. Results show about 6.8% more adsorption of CHD for AeroxideP25 (Cat₂) as compared to pure anatase (Cat₁). This is probably due to the contribution of higher negative charges of the rutile phase compared to pure anatase in AeroxideP25. In the mentioned range of experimental process conditions for photo-degradation, maximum adsorption of CHD was observed, about 29.8% for AeroxideP25(Cat₂) and 27.8% for pure anatase (Cat₁) at pH 10.5. Figure 1 illustrates the effect of the substrate to catalyst ratio (S/C value) on the degradation behavior of the CHD for the Cat₁ system. The figure shows the removal percent of CHD at different medium pH under UV irradiation of 50 $\mu\text{W}\cdot\text{cm}^{-2}$. A decreasing trend of the removal efficiency with increasing S/C value could be observed from the figure. A regression analysis was done to correlate the percent removal of CHD with the substrate to catalyst ratio (S/C value) which helps theoretically to predict the percent removal of CHD under an optimized set of reaction parameters for a chosen S/C value. In the pH range under investigation, the removal percent of CHD followed a second-order fitting with R² values ranging from 0.95 to 0.98.

3.2 Effect of UV Intensity

At a given wavelength, UV intensity determines the extent of radiation absorbed by the semiconductor catalyst. The rate of initiation of photocatalysis, the electron hole formation in the photochemical reaction is strongly dependent on the UV intensity. The light intensity distribution within the reactor

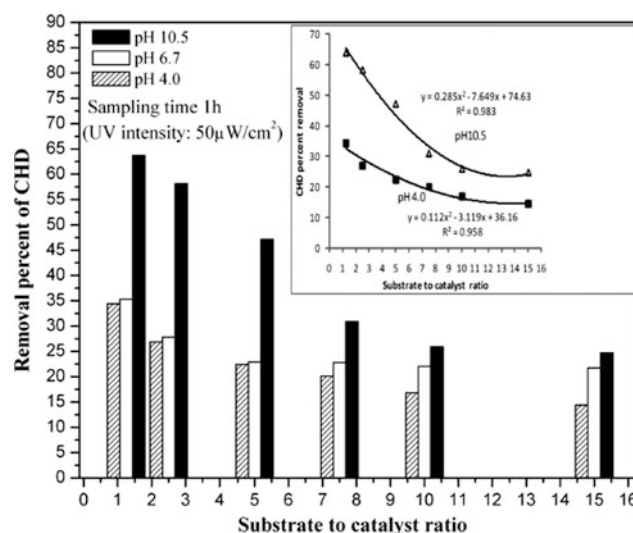


Fig. 1 Effect of contaminating substrate to catalyst ratio (S/C) and solution pH on percent removal of CHD

also was reported to invariably determine the overall substrate conversion and degradation efficiency. The effect of UV intensity on the CHD removal percentage has been highlighted in Fig. 2 under constant S/C value and medium pH. In this study, CHD removal efficiency was found to increase with increasing intensity from 50 to 80 $\mu\text{W}\cdot\text{cm}^{-2}$ which is likely because of enhanced formation of an electron hole, facilitating the photocatalytic degradation. Under such a condition, electron hole recombination is insignificant. Thus, the initial increase in degradation probably results from the generation of more electron hole pairs, which ultimately produce the reactive species. The decreasing value of the CHD removal at 125 $\mu\text{W}\cdot\text{cm}^{-2}$ could probably

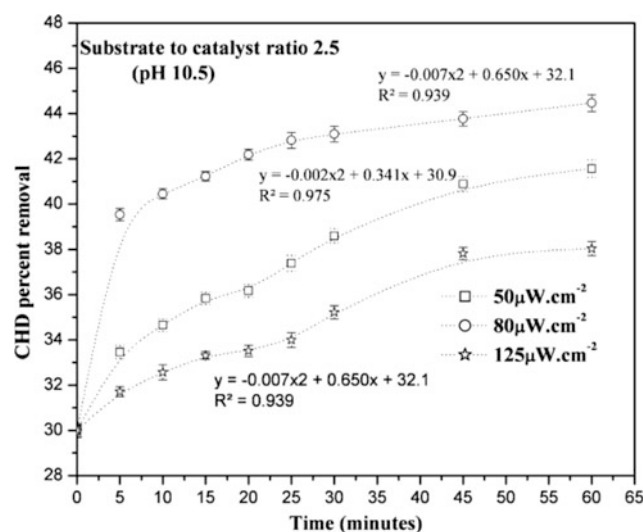


Fig. 2 Effect of UV intensity on the removal efficiency of CHD at fixed pH and S/C value

be explained on the basis of an increased rate of hole electron recombination rate under high UV-radiant flux.

4 Conclusion

This study highlights the feasible application of a TiO₂ photocatalyst-based process for the treatment of a pharmaceutical compound CHD, in pharmaceutical wastewater in a batch slurry photoreactor. The monitoring of the degradation profiles for CHD concentrations revealed that the proposed system is capable of treating CHD and can reduce the toxicity level of the treated wastewater being disposed. Under optimum reaction conditions, about 68.2% removal of CHD was achieved after 1 h reaction time. The antimicrobial susceptibility test was also performed to assess the final toxicity level of the reaction products, which gave negative a response suggesting a safe eco friendly discharge to the atmosphere. The outcomes from this study indicated that the TiO₂ based system has a high potential to be utilized as a sustainable treatment system for pharmaceutical wastewater containing CHD.

References

- Achilleos A, Hapeshi E, Xekoukoulotakis NP, Mantzavinos D, Fatta-Kassinos D. Factors affecting diclofenac decomposition in water by UV-A/TiO₂ photocatalysis. *Chem Eng J.* 2010;161:53.
- Chen M, Chu W. Degradation of antibiotic norfloxacin in aqueous solution by visible-light-mediated C-TiO₂ photocatalysis. *J Hazard Mater.* 2012;183:219–220.
- Das R, Sarkar S, Chakraborty S, Choi H, Bhattacharjee C. Remediation of antiseptic components in wastewater by photocatalysis using TiO₂ nanoparticles. *Ind Eng Chem Res.* 2014;26:3012–20.
- Dasgupta J, Singh M, Sikder J, Padarthy V, Chakraborty S, Curcio S. Response surface-optimized removal of Reactive Red 120 dye from its aqueous solutions using polyethyleneimine enhanced ultrafiltration. *Ecotox Environ Safe.* 2015;121:271–278.
- Elmolla ES, Chaudhuri M. Photocatalytic degradation of amoxicillin, ampicillin, and cloxacillin antibiotics in aqueous solution using UV/TiO₂ and UV/H₂O₂/TiO₂ photocatalysis. *Desalination.* 2010;252:46.
- Giraldo AL, Penuela GA, Torres-Palma RA, Pino NJ, Palominos RA, Mansilla HD. Degradation of the antibiotic oxolinic acid by photocatalysis with TiO₂ in suspension. *Water Res.* 2010;44:5158.
- Laera G, Chong MN, Jin B, Lopez A. An integrated MBR—TiO₂ photocatalysis process for the removal of Carbamazepine from simulated pharmaceutical industrial effluent. *Bioresour Technol.* 2011;102:7012.
- Sarkar S, Chakraborty S, Bhattacharjee C. Photocatalytic degradation of pharmaceutical wastes by alginate supported TiO₂ nanoparticles in packed bed photo reactor (PBPR). *Ecotox Environ Safe.* 2015;263–270:121.
- Zhang J, Fu D, Xu Y, Cuiyun Liu C. Optimization of parameters on photocatalytic degradation of chloramphenicol using TiO₂ as photocatalyst by response surface methodology. *J Environ Sci.* 2010;22(8):1281.

CHAPTER 7

MEMBRANE FABRICATION AND EXPERIMENTAL SET UP

The challenge in the fabrication of low-cost membranes relates to the obtainment of structures that exhibit the appropriate micro-scale pore structures to effectuate pollutant separation while maintaining sufficient mass transport and mechanical robustness. Numerous materials and processing approaches have been examined to achieve this aim using low-cost feedstock, including unprocessed minerals, clays, and ash. The main difference between the low cost materials are their composition which has already been described in different section of this chapter. The microstructures, durability, and filtration performance of membranes fabricated from impure raw materials sourced directly from mineral deposits or waste streams can be significantly altered through the use of pore formers, binders, fluxes, and other additives. The design of appropriate processing techniques, including thermal treatment, further governs the efficacy of the obtained membranes and influence overall system. To date, the challenges facing the development of ceramic filtration membranes in low-cost processes have not been comprehensively reviewed. Some issues relating to the design and fabrication of diverse kaolin-based membranes were presented in, while the preparation and application of low-cost support membranes have been discussed elsewhere. In this chapter, we present the fabrication of different ceramic membrane during different phase of my Ph.D. as well as the way we implemented the membrane for the wastewater treatment from different industry.

7.0 Membrane fabrication plan

In the first part we will present the work done in India for the fabrication of Kaolin clay membrane. Their Characterization and application for removal of acetic acid solution will also be discussed. Due to the conflict of interest and confidentiality it is not possible to present all the study as the project was a part of funded by defence research in India.

In the second part, Membrane with natural geopolymer was fabricated and characterized. Active carbon(AC) will be introduced with the ceramic matrix to increase the mechanical strength and also performance efficiency. The elaboration of microfiltration and ultrafiltration membranes supported by geopolymer and mixed with AC was applied for the treatment of textile dye. Artificial solar simulator will be used to reproduce the technology of photocatalytic reactor in line of renewable energy utilization for water treatment.

In the third phase in Tunisia the low cost support membrane made of a natural clay Turkish zeolite powder. The clay support and their main properties will be discussed and performance will be analysed by industrial wastewater treatment. In all the above cases filtration tests were performed by means of these membranes.

7.1 Materials

Phase I (India)

For fabrication of ceramic membranes, α -alumina powder with a purity of 99.6% was supplied by Indian Alumina Company. Kaolin clay was purchased from the Zenooz mine, Tabriz, Iran. Natural zeolite powder was provided from Semnan mines, Iran. The results of chemical analysis of kaolin clay, natural zeolite and α -alumina powder are presented in Table 7.1. Tritton X-100 was supplied by Merck Company, Germany. Also, distilled water with a conductivity of less than $5 \mu\text{s}\cdot\text{cm}^{-1}$ was used. The mean particle sizes of the kaolin, α -alumina and natural zeolite were 25, 75 and $50 \mu\text{m}$, respectively, according to the supplier's catalogs.

Reagent grade glacial acetic acid produced by Sigma Aldrich (India) was used as received. Then 2 wt-% aqueous solutions of acetic acid in first-distilled water, simulating the products from biofermentation, were prepared. Chloroform (Aldrich), methyl isobutyl ketone (MIBK, Yakuri Co., Osaka, Japan), and 2-octanol (Junsei Co., Tokyo, Japan) utilized as organic phases were used as received. They were immiscible with aqueous solution. To evaluate the efficiency of acid-extraction as a function of partition coefficient, the extractants such as di-ethylamine (DEA), tri-ethylamine (TEA), and tri-n-octylamine (TOA) produced by Aldrich were added in organic phase.

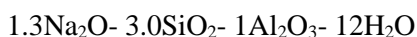
Component	Percent (%)			Phases	Percent (%)
	Kaolin	α -alumina	Natural zeolite	kaolin	kaolin
SiO ₂	61.62	0.013	68.5	Kaolinite	64
TiO ₂	0.4	0.011	-		
Al ₂ O ₃	24–25	99	11	Illite	2.4
Fe ₂ O ₃	0.45–0.65	0.014	0.2–0.9		
K ₂ O	0.4	0.011	4.4	Quartz	27
Na ₂ O	0.5	0.46	3.8		
L.O.I	9.5–10	0.5	10–12	Feldespare	6.6
Total	100	100	100		100

Table 7.1 : Chemical analysis of kaolin clay and natural zeolite powder for preparation of ceramic membranes.

Phase II (Italy)

Geopolymer-zeolites one-pot nanocomposites were prepared using metakaolin as alumina-silicate powder source. It was provided by Personal Factory S.r.l and X-ray fluorescence spectroscopy was used to determine

its composition in terms of oxides. SiO₂ (42.02%wt), Al₂O₃ (53.9%wt) Fe₂O₃ (1.52%wt) and TiO₂ (1.90%wt) were found to be its mainly components. Its average particles size of 1.59 nm was calculated on a volume distribution base. Sodium silicate solution (supplied by Condea Augusta S.P.A) was composed by SiO₂ (29.6%wt) Na₂O (13.6%wt) and water. Sodium Hydroxide (AR grade) has been purchased by Sigma Aldrich. Self-bonded 13X zeolite (Figure 7.1), with hierarchical porosity, was obtained through a hydrothermal treatment using metakaolin, sodium hydroxide and sodium silicate as raw materials and the following final molar composition:



De-oiled olive pomace or sansa esausta (SE), obtained from an olive mill RI.AM Srl located in Rossano, Cosenza, Italy, was used as raw material for the production of olive-based activated biochar (OAB). All chemicals used in this work were of analytical grade and used without further purification. Methylene blue (M.wt of 319.86; molecular formula of C₁₈H₁₈N₃SCl₃H₂O; λ_{max} of 663–667 nm; cationic) was obtained from Chemjet (India) and was used for the preparation of the modelled wastewater. The pH of the wastewater was adjusted prior to each experiment using solutions of NaOH (Gateway; 97%) and H₂SO₄ (SDFCL; 98%). Distilled water was used in all the experiments.

Mechanical Solar simulator were used (model 21117 from Newport USA. Power: 1500 W), to generate the artificial photo source during the degradation test.

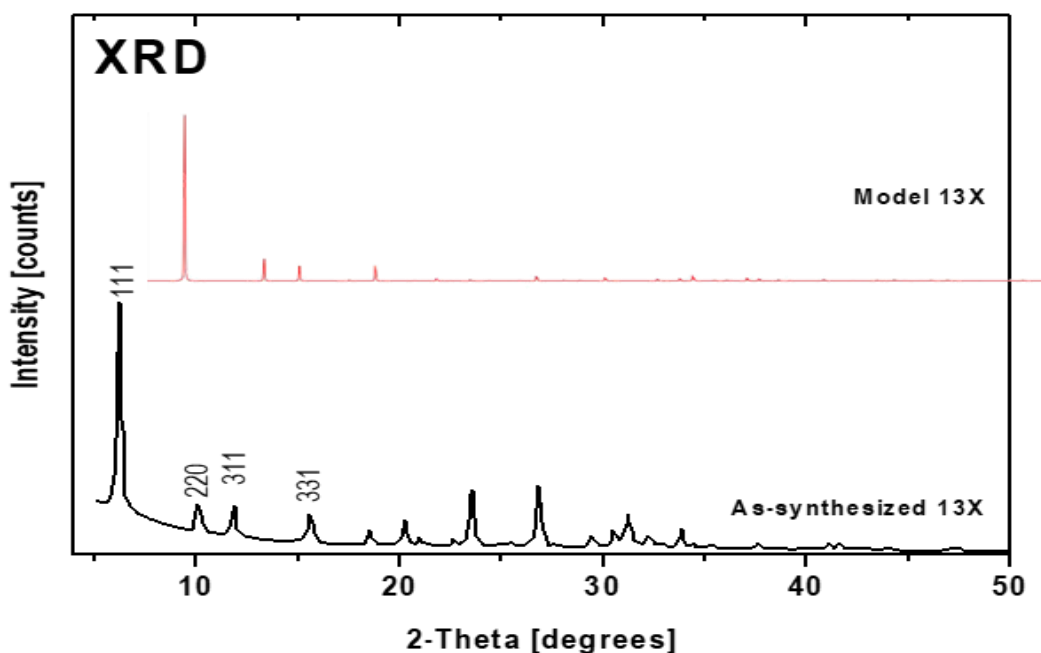


Figure 7.1 XRD pattern of Self bonded 13 X zeolite

Phase III (Tunisia)

The natural zeolite NZ used in this work has been sourced from Bigadiç deposit located near Balıkesir in Western Anatolia (Turkey). From XRD analysis of the raw zeolite powder (Figure 7.2), it can be seen that the

main crystalline phases are clinoptilolite and calcite. The energy dispersion X-ray (EDX) spectrum is depicted in Figure 7.3 and the chemical composition of natural zeolite is shown in Table 7.2. It can be showed that clinoptilolite contained exchangeable ions of sodium, potassium, calcium and magnesium. This zeolite has Si/Al ratio of 4.8 (mol/mol) and the corresponding ratio of (Na + K)/Ca of 0.717 [41]. The cationic reagent, hexadecyltrimethylammonium bromide (CTAB) $[(CH_3)_3 N (CH_2)_{15} CH_3 Br]$ has been purchased from Sigma.

SiO ₂	Al ₂ O ₃	CaO	K ₂ O	Sr O	Ba O	MgO	Fe ₂ O ₂	Na ₂ O
76.66	13.77	3.2	1.67	1.34	0.91	0.88	0.37	0.17

Table 7.2 : Composition of natural zeolite powder (%W).

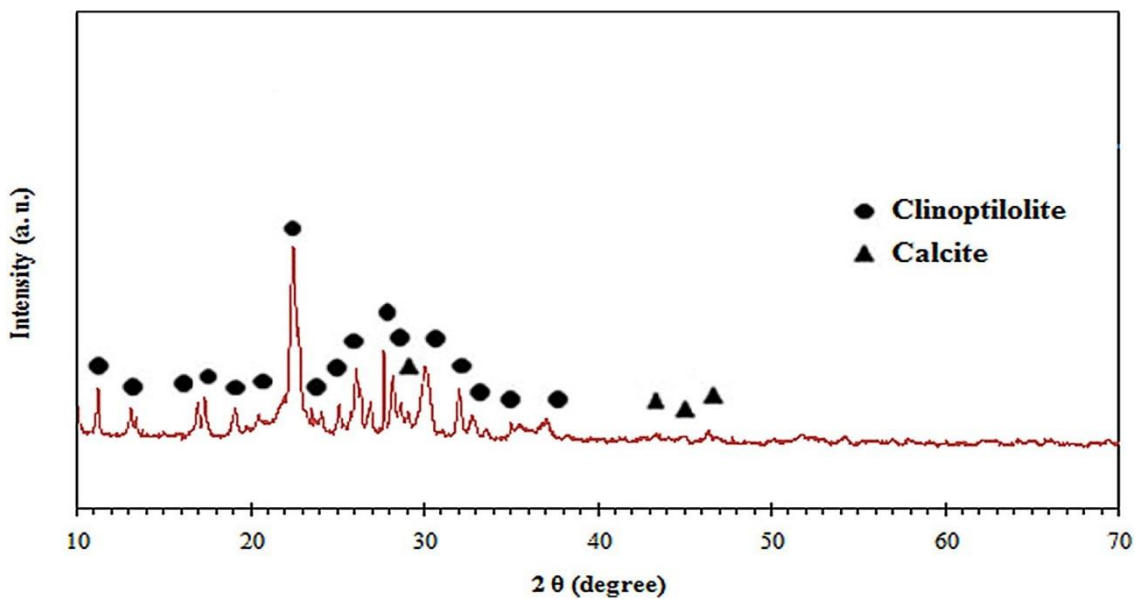


Figure 7.2. XRD patterns of natural zeolite

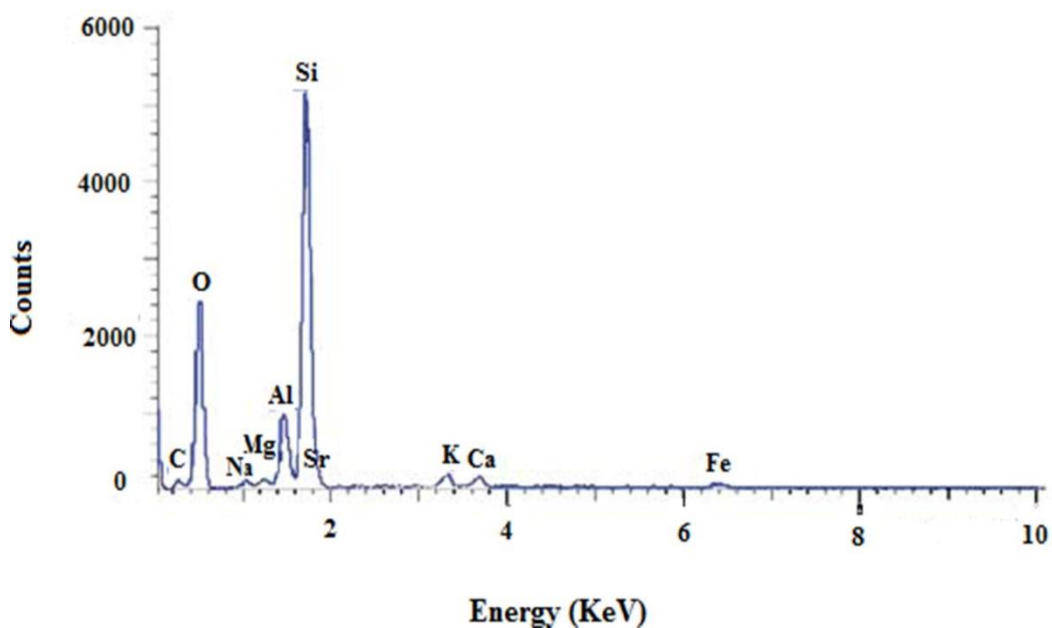


Figure 7.3. EDX spectrum of natural zeolite.

7.2 Membrane Fabrication:

7.2.1 Ceramic membranes fabrication (Phase I)

Before mixing, massive kaolin samples were triturated by employing a crushing machine to obtain fine powders with a 200 mesh sieve size. For mullite membrane preparation, 62–68% kaolin clay was mixed with 32–38% distilled water using a high-powered mechanical mixer for 1 h. The mixture was then extruded to form tubular membranes. All the fabricated membranes had a 10 mm inner diameter, 14 mm outer diameter, and 10 cm length. The in-house fabricated membranes were then dried for 24 h at room temperature, followed by sintering in a programmed electric furnace (1200C MINI LAB ELECTRIC, T-Long, China). The temperature gradient used from room temperature to 550°C was 5°C/min. Then, the temperature was kept constant at 550°C for an hour. From 550°C to 975°C, the temperature was increased at a rate of 5°C/min. Finally, after 1 h, the temperature was fixed at 975°C, and then raised from 975°C to 1250°C at a rate of 3°C/min. In order to avoid breaking the sintered membranes due to sudden changes in temperature, the membranes were taken out after 8 h cooling in the furnace. The suitable calcination temperatures and periods are those at which the clay is converted to mullite and free silica. Good results have been achieved by calcining at temperatures of about 1250°C. The cost of membrane production has yet not been identified since it is out of scope of this work. Also LCA has yet to be done.

Free silica can be washed in a strong alkali solution (20 wt% NaOH) for 5 h at 80°C in an oven (WN 30, Lenton, UK) in order to increase the porosity of the fabricated membranes. Finally, the remaining NaOH was removed by washing the membranes with distilled water in an oven for 10 h at 80°C.

Mullite membrane was prepared without mixing alumina whereas Mullite alumina (MA) membranes were prepared by adding 10–50 wt% α -alumina powder to a kaolin and distilled water mixture. The geometrical dimensions and preparation procedures were similar to those of mullite membrane preparation, but the final calcination temperature was 1300°C. α -Al₂O₃ is transformed completely to the corundum phase at temperatures from 1100°C to 1300°C, and 1300°C was therefore chosen as the final calcination temperature. The different other parameters apart from temperature are % of different composition, porosity, pore diameter, pH of the sample. The flow diagram of the membrane fabrication is described in Figure 7.4. Table 7.3 presents the composition, porosity and mean pore size of all the fabricated membranes.

Test number	Membrane	Kaolin (%)	Alumina (%)	Zeolite (%)	Porosity (%)	Mean pore diameter size (µm)
1	Mullite	100	0	0	32.6	0.451
2	MA (10%)	90	10	0	32.8	0.462
3	MA (20%)	80	20	0	33.2	0.468
4	MA (30%)	70	30	0	36.4	0.485
5	MA (40%)	60	40	0	38.2	0.498
6	MA (50%)	50	50	0	40.4	0.507

Table 7.3. Compositions, porosity and mean pore size of synthesized membranes.

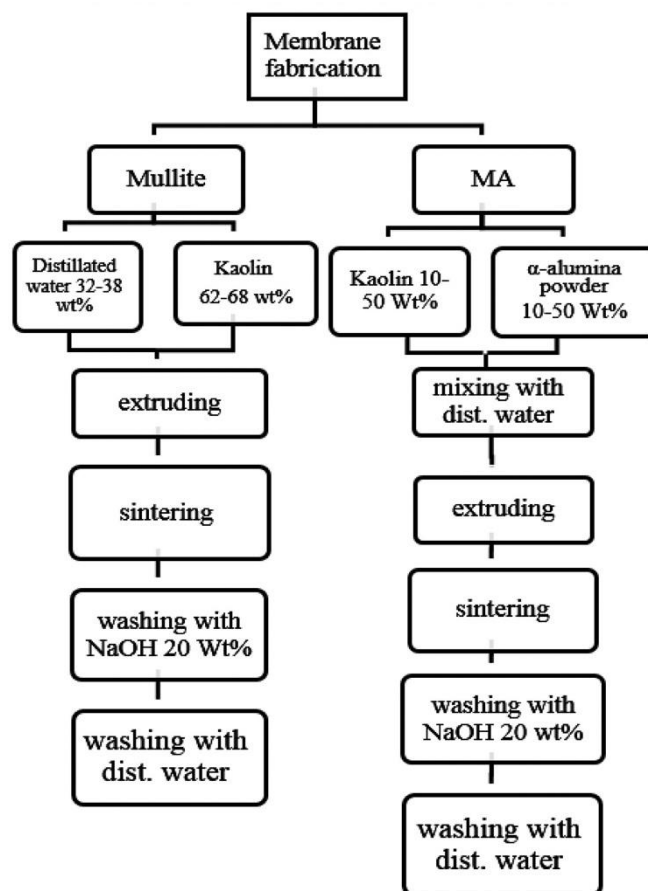


Fig 7.4: Schematic representation of procedures for membrane fabrication.

7.2.2 Ceramic membranes fabrication (Phase II)

Geopolymeric membrane and modification with Active carbon/biochar

Geopolymers are alkali activated semi-crystalline aluminosilicate material that has good combination of physical and chemical properties, and excellent mechanical, thermal and chemical stability. Active carbon are being prepared by pyrolysis method and final grinding. There is no chemical treatment necessary to get this nano particle. Apart from Olive there are numerous plant based adsorbent (such as skins from banana, nuts, ananas , bamboo etc) which can be use to prepare the biochar and finally nanomaterials. The size of the particle is arpunf 50-80 nanometer. Further improvement of geopolymer properties is an active field of research and has been demonstrated by previous studies. One particular improvement parameter is porosity. Aging and reorientation of geopolymers during inorganic polymerization reaction often lead to the crystallization of zeolite—a well-structured porous material with great industrial importance in catalysis, separation process, sensing, medicine and electronics. Geopolymer monolith is a composite material containing amorphous aluminosilicates, unreacted components and zeolites. Improvement of zeolite growth within the geopolymer matrix would also mean improving the porosity of the material as well as extending its application similar to specialty materials. Further improvement of the material's porosity can be made by adding more porous

material to its structure or apply foaming techniques to introduce macropores. If intended use of the will be on separation processes like adsorption, improvement should consider surface properties.

On this basis, the main objective for this phase is to fabricate geopolymeric as well as geopolymer-zeolite composites, membrane for the removal of pollutants.

Geopolymer synthesis

Geopolymers are synthesized by combining two main components: aluminosilicate precursor and alkali activator. The most commonly used aluminosilicate precursor is metakaolin due to its availability, abundance and low cost. Metakaolin are dehydroxylated kaolinite (550–950°C); the heat treatment improves the thermal stability of kaolinite and make it more easy to be modified for intercalation, chemical activation, etc . Secondary products like coal fly ash , red mud from bauxite tailings, slags, and biomass ash are also used as precursors for geopolymer synthesis. Alkali activators such as alkaline hydroxides, silicates, aluminates, carbonates, sulphates, or their combinations are used for deprotonation and subsequent dissolution of aluminosilicate precursor. Geopolymerization is an exothermic reaction that involves several steps: destruction, coagulation, condensation and crystallization (Fig. 7.5). The final monolith formed have regions of varying crystallinity (highly crystalline to fully amorphous) depending on the condition that will allow zeolite to form; often it is considered zeolite-like, zeolite precursor and metastable amorphous zeolite.

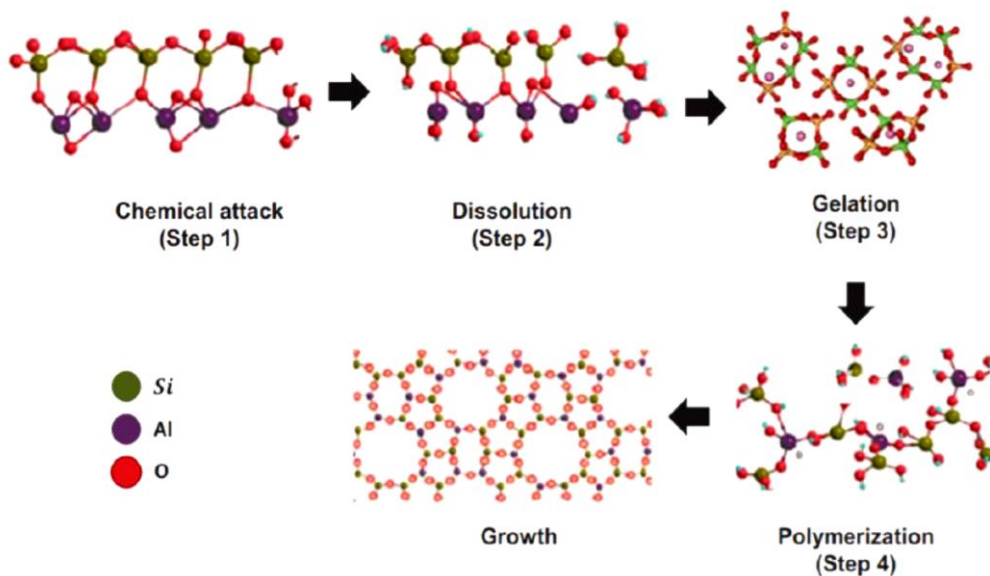


Figure 7.5 Scheme of Geopolymerization.

Zeolites are crystalline aluminosilicates with specific framework structure, and channels that are filled with ions and water. Fig. 7.6 shows the common structures of zeolites. Zeolites can be crystallized from geopolymers; improvement of zeolite formation within the geopolymer matrix provide a more sustainable approach of zeolite synthesis since the conventional method is energy- and time-intensive. Geopolymer and zeolite formation can proceed in parallel during geopolymerization but since they differ in liquid/solid ratios and alkalinities (zeolite: $H_2O/SiO_2=10-100$; geopolymer: $OH-/SiO_2=2-20$), zeolite formation will occur on

specific regions where nuclei are formed; the resulting material will be a combination of amorphous and crystalline phases.

Geopolymer-zeolite composites have merge properties of zeolite and geopolymer; while geopolymeric gel serves as a strong and durable support for zeolites, zeolites provide higher surface area, porosity and cation exchange capacity. If the application involves organic or nonpolar species, use of zeolite /geopolymer-zeolite composites may not be effective. Adding material of the same porous nature but with high binding affinity to organics may be used to improve zeolite composites properties.

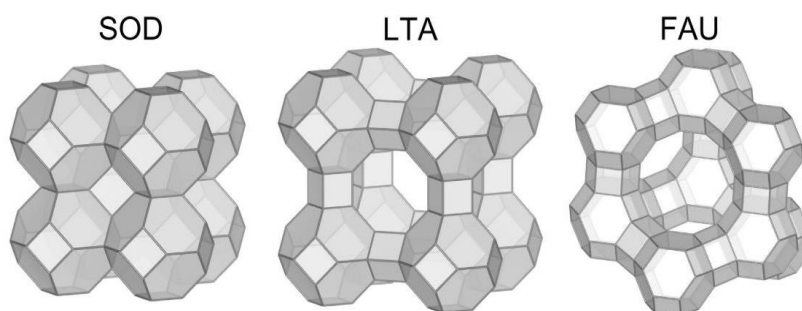


Figure 7.6 Structures of zeolite.

Activated biochar (AB) are porous carbon material with high affinity to slightly polar to non-polar substances. It is a product of an activation process of carbonaceous materials from diverse sources and has over 60 % of carbon content. It is composed of interconnected domains of benzene rings and graphite plate organized with some localized order on a molecular level. It also has displaced extended interparticulate surface area and high degree of porosity. The properties of the raw materials both in terms of physical and chemical compositions, as well as the process condition and method employed for activation, determined the adsorption properties of AB and its pore size distribution of activated biochar.

Properties of activated biochar is sometimes enhanced by oxidation, sulfuration, nitrogenation, coordinated ligand functionalization treatments or coupled with another material for combined properties. Modification is normally centered on enhancing sorption properties for specific sorbates. Like activated biochar, zeolite undergoes modification to enhance surface properties. Combination of these two porous material has demonstrated superior properties than their lone form. Table 7.4 listed some studies dedicated to enhance zeolite and AB properties by combining them together into composite material.

AB source	Zeolite (Z)	Z Precursor	Application	Relevant properties
Cypress sawdust AC	Sodalite	Kaolin	MB and NH ₄ ⁺ adsorption	754.75 mgMB/g; 9.0 mg NH ₄ ⁺ /g S _{BET} = 378 cm ² /g
Unburnt coal	NaX, NaA	Fly ash	-	S _{BET} = 6 m ² /g
Unburnt oil pam C	NS	Oil palm ash + kaolin	MB adsorption	285.71 mg MB/g S _{BET} =615 cm ² /g

Elutrilithe	X	Elutrilithe + SiO ₂	CH ₄ /N ₂ adsorption	17.3 cm ³ CH ₄ /g; 5.10 cm ³ N ₂ /g S _{BET} =802 cm ² /g
-------------	---	--------------------------------	--	---

Table 7.4 Summary of known zeolite-AC composites

Olive activated biochar production and optimization

Fig. 7.7 shows the process flow of producing olive activated biochar. Deoiled olive pomace (SE) of 3 mm mean particle size was placed in sealed ceramic containers and heated at 300-400 oC for 40 mins in a muffle furnace (Fisarc, QRTC) to promote carbonization of the biomass. Carbonized SE (CSE) was then ground to ~1.19 mm and mixed with KOH (0.2-1.2 KOH/CSE) prior to activation. The mixture was heated at 700oC for 40-80 min promote activation. Activated sample was washed with distilled water up to stable pH and

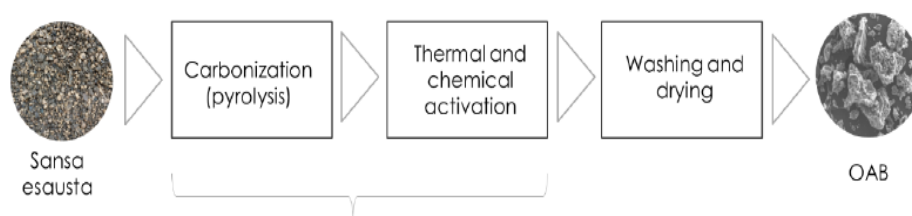


Figure 7.7 Olive activated biochar production.

Geopolymer-13X-OAB synthesis and chemical treatment

Geopolymer composite synthesis involves two main components (alkali activator and aluminosilicate source) and one additive. The alkali activator is prepared by mixing sodium silicate solution, NaOH and distilled water at specific mass ratios. Metakaolin with and without OAB additive is mixed with the alkali activator and mixed for 15 min prior to casting. Casted slurry is allowed to set in a convection oven for one (1) hour at 50oC. Set geopolymer was hydrothermally treated in an autoclave for 24 h at 90°C. Hydrothermally treated geopolymer with grown 13X zeolite is washed, dried and stored in sealed containers. Summary of the synthesis is shown in Fig. 7.8.

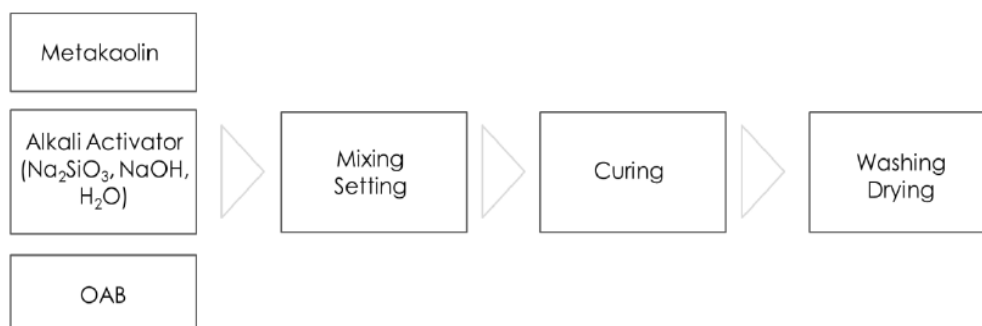


Figure 7.8 Geopolymer-13X and 13X-OAB production.

Metakaolin served as alumino-silicate source for geopolymer-13X synthesis. The metakaolin is provided by Personal Factory S.r.l with composition in terms of oxides: SiO₂ (42.02%wt), Al₂O₃ (53.9%wt) Fe₂O₃ (1.52%wt) and TiO₂ (1.90%wt) as main components of metakaolin. The powder has mean size of metakaolin

is 1.59 microns. Sodium silicate solution (supplied by Condea Augusta S.P.A) acted as alkali activator for the synthesis and is composed of SiO₂ (29.6% wt) Na₂O (13.6% wt) and water.

A mixture of 20.7 g of sodium silicate solution, 9.2 g NaOH and water was stirred until a clear solution at room temperature is obtained. 30 g of metakaolin powder is weighed and mixed with the wet solution and stirred for 14 minutes prior to casting; this sample is referred to as bare geopolymer-13X sample (13X). Another set of dry mixture is prepared by combining metakaolin with 6 g of OAB; the dry mixture is carefully mixed for 20 minutes followed by 10-min mixing with wet solution; this sample is referred to as geopolymer-13X-olive activated biochar composite (13X-OAB). Both slurries were casted in PE molds and allowed to set for one (1) hour at 50°C followed by 24-hour curing in an autoclave at 90°C. Cured monoliths are washed with distilled water and air-dried for 20 hours. Dried monoliths are ground and sieved to 0.149mm, and stored in sealed container.

Water amount, with a value greater than those used in the geopolymer production, was used with the dual purpose to favour the zeolites synthesis and to increase the final porosity of the monoliths. Membranes were synthesized by activating metakaolin with activator solutions. Firstly, the sodium hydroxide solution was obtained by dissolution of NaOH pellets in ultrapure water, with container kept sealed wherever possible to minimize contamination by atmospheric carbonation and prevent water evaporation. The solution was stirred until the NaOH pellets had dissolved and the solution became clear. Once cooled down it was poured into sodium silicate solution. The so obtained alkali activator solution was sealed, stirred and allowed to cool back down to room temperature (RT = ~25 °C). Finally, the activator solution was added to metakaolin powder and the slurry was mechanically vigorously mixed for 10 minutes (In figure 7.9 a). The slurries were, afterwards, rapidly casted into open and dismantable Teflon moulds (Figure 7.9 b) in order to disk shaped membrane of dimensions 5cm diameter 3 mm of height. The moulds were then sealed from the atmosphere to prevent the moisture loss and cured for 1 h at 60 °C. After this step, the hardened membranes were unmolded and subjected to the hydrothermal treatment at 90 °C in autoclave for 24h to develop the crystalline phase. The obtained selfbonded zeolitic membranes were then washed with distilled water to remove Sodium excess.



Figure 7.9 a). Slurry made from metakaolin, alkali activator and OAB

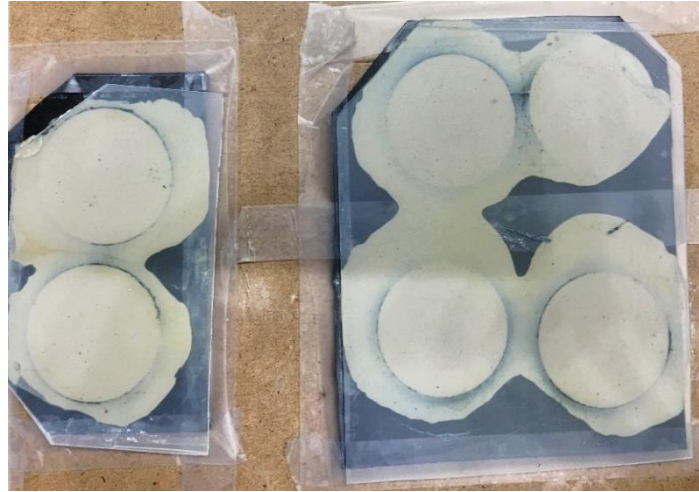


Figure 7.9 b. Casted geopolymer after setting at 50°C

7.2.3 Ceramic membranes fabrication (Phase III)

Natural Turkish zeolite powder (Biga, Çanakkale Province) has been used to make both the filtration layer and the tubular microporous supports. The zeolite supports were prepared in our laboratory via the extrusion process. Three filtration layers were prepared from the same zeolite powder namely:

- (i) Decanted zeolite "DZ", which was obtained by ball-milling the raw zeolite powder for 4 h at 400 rpm using a ball-mill device (Retsch PM 100) and decanting for 4 min in aqueous suspension (4 wt%). The suspension was collected and allowed to settle down for 24 h and then dried to obtain fine decanted zeolite "DZ";
- (ii) Modified zeolite "MZ", which was prepared by modifying the anionic surface of the natural zeolite of average particle size 63 μm using a cationic quaternary ammonium surfactant CTAB (Hexadecyltrimethyl ammonium bromide $\text{C}_{19}\text{H}_{42}\text{BrN}$);
- (iii) Zeolite of average particle size ($\Phi < 42 \mu\text{m}$) and designated by "Z42" was obtained by ball milling the raw zeolite powder for 2 h at 400 rpm using a ball mill (Retsch PM 100). The modified (MZ) and unmodified (DZ and Z42) powders were examined using a zeta potential meter (Zetasizer Nano-ZS) to determine the surface charges.

Then, three ultrafiltration membranes (DZ/Z, MZ/Z and Z42/Z) were synthesized via the slip-casting method by depositing/coating on the tubular microporous zeolite support (Z), having average pore size and porosity of 0.55 μm and 43.7% , respectively, the filtration layers (DZ, MZ and Z42). The optimal composition (wt %) of

the deflocculated slip was: 2 wt% of zeolite powder, 30 w% of polyvinyl alcohol (12% w/w aqueous solution), and 68 w% of water. In order to obtain efficient membranes with adequate thickness in the ultrafiltration range, the optimal coating time for the three layers was fixed at 7 min. After drying at room temperature for 24 h, the different ultrafiltration membranes were sintered at 880°C for 3 h at heating rate of about 2°C/ min. Morphology of the prepared membranes was checked by using scanning electron microscopy (SEM, JEOL-JSM-5410, Japan) and pore size distribution of the top layers were obtained from nitrogen adsorption / desorption isotherm using a Micrometrics ASAP 2020. Pore diameter was estimated via the BJH (Barret-Joyner-Halenda) model.

7.3 Characterization

7.3.1 Membrane Phase 1

All the synthesized membranes have been characterized using SEM, XRD, a mean pore size calculation and the mechanical strength. Scanning electron microscopy (SEM) using a TESCAN Vega 3 microscope (Czech Republic) with an accelerating voltage of 20 kV was utilized to study the properties of the membranes' structure. To identify the phases formed in the sintered membranes, powder X-ray diffraction (XRD) was conducted using a PW1800 X-ray diffractometer (Philips, Netherlands) with Cu K α radiation at a tension of 40 kV and current of 20 mA.

The membranes' porosity was measured simply by calculating the water mass trapped in a membrane immersed in a water bath. The soaked membrane, which had a mass of W_1 when dry, adsorbed a water mass of $(W_2 - W_1)$ after 24 h immersion in pure water at ambient temperature. W_2 was the mass of the membrane after immersion. The volume of uptake water was then calculated as $(W_2 - W_1)/\rho_m$. Eventually, the membrane porosity was calculated as follows

$$porosity = \left(\frac{W_1 - W_2}{\rho_M V_M} \right) \times 100$$

where W_2 , W_1 , and V_M are the dry and wet masses and volume of the membrane, respectively, and ρ_m is the water density at the experimental temperature.

The 3-point bend test with ASTM C1505-01 was selected to measure the membranes' mechanical strength using a SANTAM, STM-150 universal testing machine, with a 150 KN capacity, total grip distance of 690 mm, dimensions (width \times depth \times height) of 1070 \times 700 \times 2430 and 200 V 50–60 Hz power. SANTAM universal testing machines are used in industrial quality-control laboratories and research centers. The

machines are able to test the mechanical properties of a wide range of materials such as metals and ceramics. The membrane average pore radius (r_m) was measured by the Guerout-Elford-Ferry equation:

$$r_m = \sqrt{\frac{(2.9 - 1.75\varepsilon)8\mu l J}{\varepsilon \text{TMP}}}$$

where ε is the membrane porosity (%), μ is the water viscosity (8.9×10^{-4} Pa.s) at the operating temperature, l is the membrane thickness (m), and J is the pure water flux under the specific applied TMP.

The pure water flux for each trans-membrane pressure (TMP) in the range of (0.25–4 bar) was measured for pure Mullite and MA membranes. r_m was then obtained from the slope (S) of the linear line from TMP versus pure J applying the least square method as follows:

$$J = \frac{r_m^2 \varepsilon \text{TMP}}{(2.9 - 1.75\varepsilon)8\mu l}$$

Thermogravimetric (TG) analysis was applied with the aid of a TGA METTLER instrument (METTLER TOLEDO, model TGA DSC 1, Switzerland) on a mullite membrane sample, heated from 25°C to an endpoint of 800°C at a heating rate of 10°C min⁻¹ in an air environment.

7.3.2 Membrane Phase II

The prepared membrane including active carbon shows the micrographs of geopolymer-13X and geopolymer-13X-OAB composite. SEM, EDAX, FTIR has been performed to analyze the samples. Mesoporosity of the material is validated by the appearance of mesoporous peak between 2θ of 1.00 to 1.75 degrees of 13X and 13X-OAB composites. Wide-angle scan has also been performed. Then the initial feed and final permeate concentration of the sample are being measured for the measurement of the adsorption efficiency. SEM has been performed to understand the structure of the membrane and EDAX and FTIR for the functional group and presence of the active carbon. The concentration of the dye use in the adsorption test is given below in Table 7.5

C ₀ [mol/l]	ABS
0	0
6.25*10 ⁻⁶	0.5216
9.38*10 ⁻⁶	0.714
1.25*10 ⁻⁵	0.8936
1.88*10 ⁻⁵	1.3353
2.50*10 ⁻⁵	1.6372
3.13*10 ⁻⁵	2.064

Table 7.5 Concentration of dye wastewater

Concentration of dye before and after the test has been measured by UV Spectrophotometer and it was monitored continuously for the permeate quality.

7.3.3 Membrane Phase III

Permeability test and membrane regeneration

Permeability tests were performed on the membranes at ambient temperature and transmembrane pressure (TMP) ranged between 3 and 7 bar using a custom-made pilot plant described elsewhere. Regeneration of the membrane was carried out via a back-flushing procedure for 15 min, followed by acidic (nitric acid 2% at 60 °C) or basic (NaOH 2% at 80 °C) treatment for 20 min. After which the treated membranes were, rinsed with distilled water until neutral pH. The efficiency of the cleaning protocol was verified by measuring water flux after the cleaning cycle.

Effluent characterization

The prepared zeolite ultrafiltration membranes were used to treat wastewater obtained from the cuttlefish conditioning industry and the electroplating industry. Physico-chemical parameters of both raw and treated effluents were estimated according to the standard methods suggested by American Public Health Association. The conductivity and pH of the effluent were measured with the use of a conductivity-meter (ISTEK EC-400L, USA) and a pH-meter (ISTEK pH-220L, Japan), respectively. Turbidity was obtained by using a turbidity-meter (Hach RATIO 2100A, USA) in accordance with standard method 2130B. Chemical Oxygen Demand (COD) of the wastewater was estimated by colorimetric method (Fisher Bioblock Scientific reactor COD 10119, Japan. Equilibrium concentration of Fe³⁺ was determined by using an Atomic Absorption Spectrophotometer (AAS) (Perkin Elmer Analyst 200). Chloride amount was calculated after a simple dosage with AgNO₃.

The synthesized and characterized membranes were employed in the treatment of two wastewater sources namely: Synthetic dye wastewater.(EF1) and Cuttlefish effluent (Sfax, Tunisia) (EF2) and. Results of the characterization of EF2 and EF1 are presented in Table 1 and Table 7.6.

Table 7.6 . Characterization of wastewater from effluent

Sample	pH	Conductivity (mS/cm)	Turbidity (NTU)	COD (mg/L)	Fe ³⁺ (mg/L)	Cl ⁻ (mg/L)
EF1	7.05	1.15	188	1350	-	-
EF2	2.90	3.34	-	1048	6.23	828

Different membrane has been used to treat the industrial effluent (turbidity and COD) Membrane was also been characterized by XRD, EDAX, SEM.

7.4 Operating Procedure and set up

Phase 1 : Membrane Contactor: Apparatus and Procedure

The aqueous phase of feed side was pumped through the lumen of the fibers to circulate from the respective reservoir and back into the reservoir. The organic phase of extraction side circulates cocurrently in the shell side of the module.

Mechanically driven gear pump (FMI, RP-D-2 pump) was used. To measure both aqueous and organic flow rates during the experiments, flowmeters were used. The pressure of the aqueous phase was maintained higher than the pressure of the organic phase in order to stabilize the interface within the membrane, as the hydrophobic fibres are preferentially wetted by the organic phase. The pressure was adjusted using the four valves at the inlet and outlet of the modules, preventing the emulsion formation.

Jacketed reservoirs were used to maintain a constant temperature (25°C). The solution was magnetically stirred to prepare the homogeneous solutions. The instrument was designed to measure the acid concentration in the feed reservoir as a function of time. The experimental setup is schematically shown in Fig. 7.10. The experiments were carried out with cocurrent flow of aqueous and organic solution at a feed flow rate of 8.2 cm³/sec.

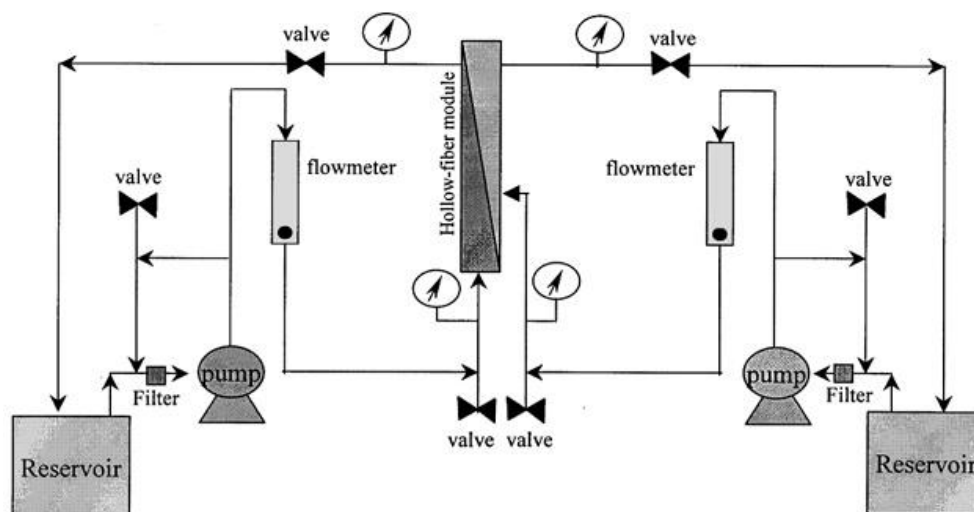


Figure 7.10. Experimental setup for membrane extraction. The hollow fiber module was shown in the center of the figure. It is attached to the two liquid reservoirs whose concentrations are measured as a function of time.

Analytical Method

To determine the concentration of acid transferred in the liquid–liquid extraction equilibrium and membrane contactor experiments, the concentration of the acid in aqueous phase was determined by conductivity measurement. The conductivity meter (Orion Instrument, model 162) used was calibrated with standard solutions. The conductivity of pure water (first-distilled water, pK_a : 15.7) was about $0 \mu\text{S}/\text{cm}$, whereas that of the 2 wt-% acetic acid and propionic acid in aqueous phase indicated $2.77 \times 10^3 \mu\text{S}/\text{cm}$ and $2.34 \times 10^3 \mu\text{S}/\text{cm}$, respectively. This result was in accordance with their respective trend of pK_a values. The pK_a value of acetic acid and propionic acid is 2.75 and 2.89, respectively. Therefore, as pK_a value increases, the conductivity decreases. The acid concentration of organic phase was determined by two-phase titration (1 cm^3 of the organic solvent mixed with 7 cm^3 of ethanol and 3 cm^3 of distilled water) with NaOH solution, using phenolphthalein as an indicator.

Liquid–Liquid Extraction and Partition Coefficient (H)

Liquid–liquid extraction at equilibrium state was determined by contacting the known volume and concentration of both organic and aqueous solutions, the latter being 2 wt-% acetic acid. The total volume of the sample, adding up to 50 cm^3 , was placed in a capped flask and magnetically mixed and thermostated in a water bath at 25°C . Once the two phases have settled, the concentration of acetic acid was determined in aqueous phase.

The partition coefficient (H) of the solute (acid) between the organic and aqueous phase assuming to be constant during the extraction process is usually described by the equilibrium conditions at the interface and defined as in following Equation.

$$H = \frac{M_{org}}{M_{aq}} \text{ (at equilibrium state)}$$

where M_{org} and M_{aq} is the molar concentration of acid in the organic phase and in the aqueous phase, respectively. The partition coefficient is the efficiency of the transition of solute in aqueous solution into organic solution. Therefore, the high partition coefficient implied a good extraction property.

Phase II : Membrane based dye adsorption set up:

The experimental set up is describe below in the figure 7.11. As you can see that the reservoir has two chamber.in the upper chamber we fill it with feed solution whereas the lower chamber is to collect the permeate. In between two we place the prepared membrane. During the measurement of the permeability we

collect the permeate in respect to time and calculate the flux and permeability in a certain pressure. On the other side during the adsorption test we completely fill the upper chamber by dye solution and we collect the permeate and measure the flux. A gas cylinder is connected with the upper chamber to regulate the applied pressure. 13X and 13X-OAB ceramic membranes were carefully placed O-rings in the Teflon membrane separation module (Fig. 7.11). The module is first filled with distilled water and permeation is measured at different operating pressure (1, 1.5, 2, 2.5 and 3 bar air pressure). The module is emptied and filled with 100 mg L⁻¹ MB. MB separation is performed at 2 bar pressure and permeate is collected at predetermined time interval. Initial data on MB separation were measured as well as the final concentration..

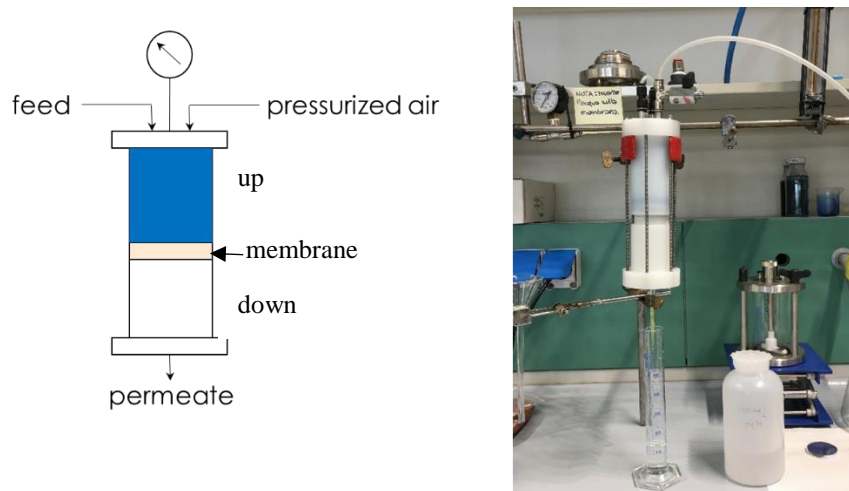


Figure 7.11: experimental set up for the dye adsorption and degradation.

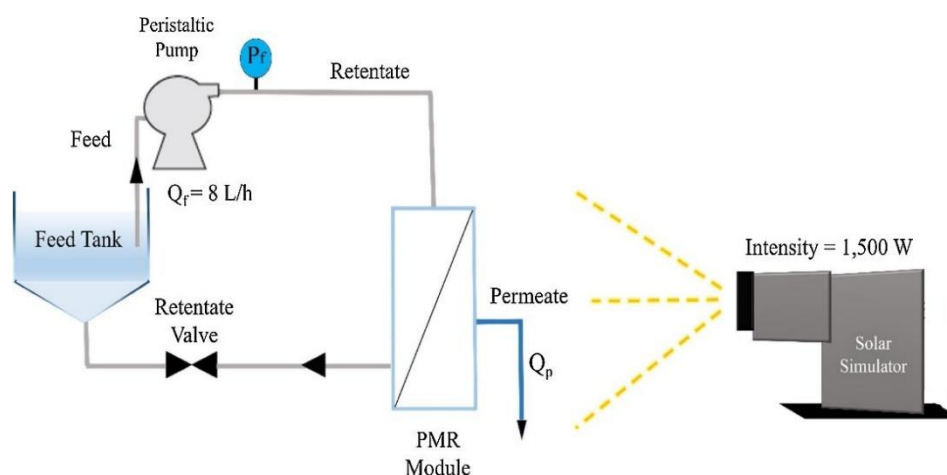
A new taflon module (Fig 7.12) has been developed in our laboratory for the permeation and adsorption test. The casted membrane is being placed in the module within two soft support to avoid the membrane break as described in above figure.



Figure 7.12. Taflon module for the dye adsorption test

Photo-degradation studies of dye using renewable energy

A same set up was used to test the effect of Active carbon prepared from olive waste on the decomposition of contaminants under simulated solar radiation. The membrane module used was 22 cm long with a diameter of 4.5 cm made in-house. The fabricated flat membranes were fixed tightly into the modules. The module had two inlets and one outlets. The available effective membrane surface area was 34.22 cm². Photodegradation studies were conducted for both only geopolymeric membrane and also using the membrane with active carbon made from olive waste. Aqueous feed solutions containing MB was used in known concentration. A simplified schematic of the set-up employed in the degradation studies is depicted in Fig. 7.13 . The main components were a solar simulator (model 21117 from Newport USA. Power: 1500 W), a peristaltic pump from Masterflex and the PMR modules. The feed was supplied on the shell side at a constant axial velocity of $0.20 \pm 0.01 \text{ ms}^{-1}$, whereas the permeate was collected on the lumen side. The initial feed volume in the feed tank which is used for dye adsorption is 200 mL. The retentate stream from the PMR module was recycled back to the feed tank, while the permeate stream was continuously removed from the system. Replenishment feed amounts were added to feed tank, equal to the amounts of permeate, to maintain a fixed feed volume and concentration. The rationale behind this arrangement is that the retentate had the same composition as the feed since the membrane didn't have size-selectivity of the feed components as they were too small to be blocked by the membrane pores. The permeate, on the other hand, had a different composition than the feed due to the photo-degradation of MB as they passed through the membrane. A valve was used to control the flow rate of the retentate stream, indirectly controlling the TMP. Throughout the test, at fixed time intervals, samples were collected from the permeate line and analyzed.



In our tests, it was important to ensure that any possible adsorption of the studied pollutant on the membrane surface is completed before the beginning of the photocatalytic runs, in order to isolate the adsorption and catalytic degradation phenomena. For that, the feed solution containing either MB was circulated in the dark (i.e., in the absence of any solar light) and the concentration of MB in the permeate was measured until a

steady state was reached, at which the concentration became stable. This initial phase, which is referred to as the “dark phase” and lasted for 12 h, ensured the full loading of the pollutant on the catalyst in the absence of simulated solar radiation. After the end of the dark phase, the “light phase” was initiated by switching on the solar simulator in order to trigger the photocatalytic reaction on the coated membrane surface.

To ensure reproducibility, all other parameters such as feed flow rate, TMP and light radiation intensity were measured and maintained constant. The radiation intensities reaching the reactor were kept at the values of 678 and 362 W/m² in the 450–950 nm and 315–400 nm range, respectively, thanks to the fixed position of the PMR module with respect to the radiation source. Although the surface of the membrane facing the solar simulator is theoretically more exposed to the light source, the diffused radiation is equally distributed throughout the membrane surface due to the design of the membrane modules. It has thus been observed that the radiation intensity at the side facing the light and that behind the membrane had a variation less than 0.5%, which can be neglected in this context.

In each experimental run, pollutant degradation was monitored in terms of the residual pollutant concentration over time. The photocatalytic activity of the membrane was presented by the percent removal of the contaminant contained in the feed (R, %), which was calculated based on the following equation (Eq. (3)):

$$R (\%) = (C_0 - C_t) / C_t$$

Where C_0 : initial concentration of the pollutant in the feed (ppm) and C_t : permeate concentration of the pollutant at time t (ppm).

Phase III

The filtration tests on the prepared zeolite membranes, DZ/Z, MZ/Z and Z42/Z, were conducted at room temperature and at transmembrane pressure ranged from 3 to 5 bar. The permeate flux as a function of time for the membranes was measured time to time. A cross flow membrane system was used to study the permeate flux as well as the treatment of industrial wastewater. The results reveal that the permeate flux decreased slightly with time to obtain a stable value after 30 min of filtration. The decrease of permeate flux with time is a typical behaviour of an ultrafiltration membrane, indicating presence of concentration polarization and fouling due to the interaction between membrane material and the feed solution.

Table 7.7 gives the composition of the treated effluents for the membranes at 3 bar. It is noteworthy to mention that no significant variation in pH and conductivity between the feed and permeate was observed during the tests. The surface charge of the material is a significant parameter incorporating the separation effectiveness of the membrane and it is dependent on the pH of the solution, especially when removing ionic species. When a charged membrane is in contact with the salt solution, the concentration of co-ions (ions with the same charge as the membrane) close to the membrane surface will be less than that in the solution. But the concentration of counter ions (ions with the opposite charge as the membrane) in the membrane will be higher than that in the solution. As a consequence, a potential difference, known as the Donnan potential, is generated between the membrane and the solution to maintain the electrochemical equilibrium. Thus, the co-ions are repelled by the membrane.

Effluents	Permeate sample	pH	Conductivity (mS/cm)	Turbidity (NTU)	COD (mg/L)	Fe ³⁺ (mg/L)	Cl ⁻ (mg/L)
EF1	DZ/Z	6.90	1.12	0.73	162.5	-	-
	MZ/Z	6.87	1.07	0.78	177.5	-	-
	Z42/Z	6.89	1.04	0.30	122.5	-	-
EF2	DZ/Z	4.80	2.52	-	152.0	2.60	530
	MZ/Z	4.16	2.65	-	165.0	0.63	355
	Z42/Z	5.05	2.40	-	140.0	2.05	473

Table 7.7 Main composition of the treated effluents with the different zeolite ultrafiltration membranes at 3 bar.

Zeta potential of modified (MZ) and unmodified (DZ and Z42) zeolite membranes was measured at pH range from 2 to 10 in order to explain the interaction with the textile effluent. At the end these obtained results finally help to do the experimental work from industrial effluents.

7.5 Permeate product characterization

MB concentration in the feed and permeate was determined using UV–vis spectrophotometry at 693 nm, following proper calibration. To validate the accuracy of the measurements, quantitative determination of the compounds present in the solution was also performed by means of a Thermo Scientific HPLC (Dionex UltiMate 3000 Photodiode Array Detector), equipped with an Acclaim-120 C18 Reversed-phase LC column working at 25 °C. The injection volume was 10 µL and the eluent flow rate was 0.2 mL min⁻¹. The mobile phases used for the measurement of MB concentrations were 60% methanol/40% water and 33% water/33% acetonitrile/34% methanol, respectively. Product concentrations were measured from the peak areas as obtained in the HPLC chromatogram.

References

- [1] M. Barjasteh-Moghaddam, A. Habibi-Yangjeh; Effect of operational parameters on photodegradation of methylene blue on ZnS nanoparticles prepared in presence of an ionic liquid as a highly efficient photocatalyst, *J. Iran. Chem. Soc.*, 8 (2012), pp. S169-S175
- [2] S.B. Gajbhiye ; Photocatalytic degradation study of methylene blue solutions and its application to dye industry effluent; *IJMER*, 2 (2012), pp. 1204-1208
- [3] A. Houas, H. Lachheb, M. Ksibi, E. Elaloui, C. Guillard, J.-M. Herrmann; Photocatalytic degradation pathway of methylene blue in water; *Appl. Catal. B Environ.*, 31 (2001), pp. 145-157
- [4] U.G. Akpan, B.H. Hameed; Parameters affecting the photocatalytic degradation of dyes using TiO₂-based photocatalysts: a review; *J. Hazard. Mater.*, 170 (2009), pp. 520-529
- [5] M. Salehi, H. Hashemipour, M. Mirzaee; Experimental study of influencing factors and kinetics in catalytic removal of methylene blue with TiO₂ nanopowder, *Am. J. Environ. Eng.*, 2 (2012), pp. 1-7
- [6] R.V. Kandisa, N.S. Kv, K.B. Shaik, R. Gopinath; Dye removal by adsorption: a review; *J. Bioremediation Biodegrad.*, 7 (2016), pp. 1-4
- [7] N. Al-Bastaki; Removal of methyl orange dye and Na₂SO₄ salt from synthetic waste water using reverse osmosis; *Chem. Eng. Process. Process Intensif.*, 43 (2004), pp. 1561-1567
- [8] E. Alventosa-deLara, S. Barredo-Damas, M.I. Alcaina-Miranda, M.I. Iborra-Clar; Ultrafiltration technology with a ceramic membrane for reactive dye removal: optimization of membrane performance; *J. Hazard. Mater.*, 209–210 (2012), pp. 492-500
- [9] M. Wawrzekiewicz, Z. Hubicki; Anion exchange resins as effective sorbents for removal of acid, reactive, and direct dyes from textile; *Wastewaters* (2015)
- [10] M. Brik, B. Chamam, P. Schöberl, R. Braun, W. Fuchs; Effect of ozone, chlorine and hydrogen peroxide on the elimination of colour in treated textile wastewater by MBR; *Water Sci. Technol. J. Int. Assoc. Water Pollut. Res.*, 49 (2004), pp. 299-303
- [11] S. Bai Gajbhiye; Photocatalytic degradation study of methylene blue solutions and its application to dye industry effluent; *Int. J. Mod. Eng. Res.*, 2 (2012), pp. 1204-1208
- [12] S. Chakrabarti, B.K. Dutta; Photocatalytic degradation of model textile dyes in wastewater using ZnO as semiconductor catalyst; *J. Hazard. Mater.*, 112 (2004), pp. 269-278
- [13] M. Sleiman, D. Vildoza, C. Ferronato, J.-M. Chovelon; Photocatalytic degradation of azo dye Metanil Yellow: optimization and kinetic modeling using a chemometric approach; *Appl. Catal. B Environ.*, 77 (2007), pp. 1-11
- [14] M.R. Hoffmann, S.T. Martin, W. Choi, D.W. Bahnemann; Environmental Applications of Semiconductor Photocatalysis; *Chem. Rev.*, 95 (1995), pp. 69-96
- [15] P. Borker, A.V. Salker; Photocatalytic degradation of textile azo dye over Ce_{1-x}Sn_xO₂ series *Mater. Sci. Eng. B*, 133 (2006), pp. 55-60

[16]J.-M. Herrmann;Heterogeneous photocatalysis: fundamentals and applications to the removal of various types of aqueous pollutants;Catal. Today, 53 (1999), pp. 115-129

[17]A.O. Ibadon, P. Fitzpatrick;Heterogeneous photocatalysis: recent advances and applications; Catalysts, 3 (2013), pp. 189-218

CHAPTER 8

RESULTS AND DISCUSSIONS

The challenge in the fabrication of low-cost membranes relates to the obtainment of structures that exhibit the appropriate micro-scale pore structures to effectuate pollutant separation while maintaining sufficient mass transport and mechanical robustness. Numerous materials and processing approaches have been examined to achieve this aim using low-cost feedstock, including unprocessed minerals, clays, and ash. The microstructures, durability, and filtration performance of membranes fabricated from impure raw materials sourced directly from mineral deposits or waste streams can be significantly altered through the use of pore formers, binders, fluxes, and other additives. In this chapter the results from all 3 different stages of my PhD will be summarized.

8.1 Membranes characterizations

Phase I

8.1.1 SEM analysis

SEM micrographs of the fabricated membranes are shown in Figure 8.1 (a, b). As these images show, the surface morphology of the mullite and MA membranes resemble each other less closely. This is due to the fact that kaolin clay and natural zeolite powder are the main constituents of mullite and in MA membranes α -alumina powders are fully embedded in the MA. It is clearly apparent that the pore size and pore structure change with the alumina and natural zeolite content of the membranes. SEM observation shows that all membranes are porous and have a rough surface morphology. MA membranes are more porous than others due to the fact that increasing the sintering temperature from 1100°C to 1400°C causes the particles to agglomerate creating denser ceramic bodies. As a result, the porosity of the membranes increases slightly and the bulk density decreases accordingly. Also, SEM observation shows that the membrane surfaces have no defects in their structures.

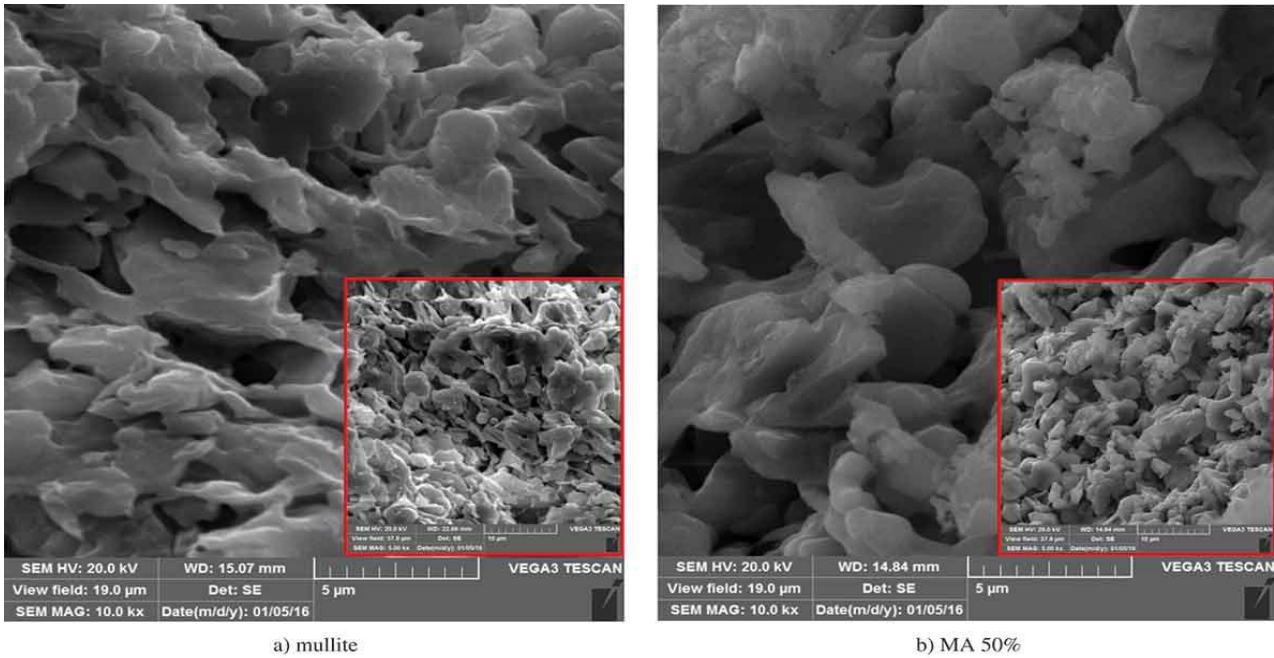
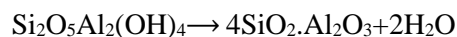


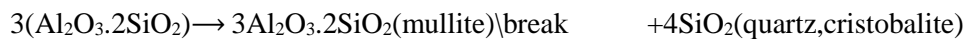
Figure 8.1 Micrograph of membranes (5000 X): (a) mullite, (b) MA 50%

8.1.2. XRD analysis

The XRD patterns for two types of membranes are shown in Figure 8.2(a,b). As the XRD patterns show, major phases in mullite and MA membranes are quartz (ref. code: 00-046-1045) and corundum (ref. code: 00.010.0173), and quartz. For these membranes, the minor phases are mullite and corundum. The quartz and corundum phases can be washed with a strong alkali solution (20 wt% NaOH) in order to increase in the porosity of the membranes. It is reported that elimination of the kaolinite phase occurs in the temperature range of 450–600°C. During water evacuation, kaolinite is converted to metakaolin in which the Si–O bonds remain constant and the Al–O bonds change their position, as illustrated below.

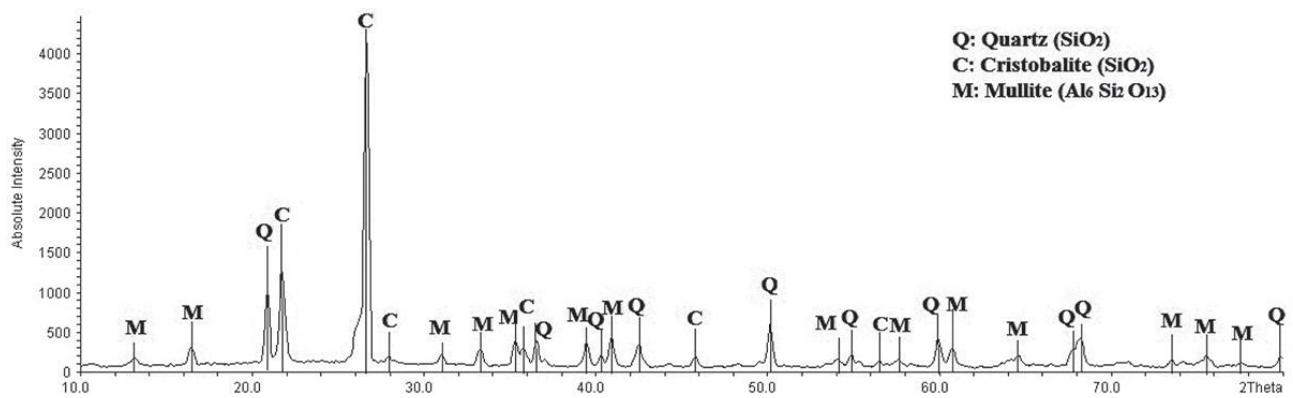


Raising in the sintering temperature above 900 °C results in decomposition of the metakaolinite into mullite and cristobalite.

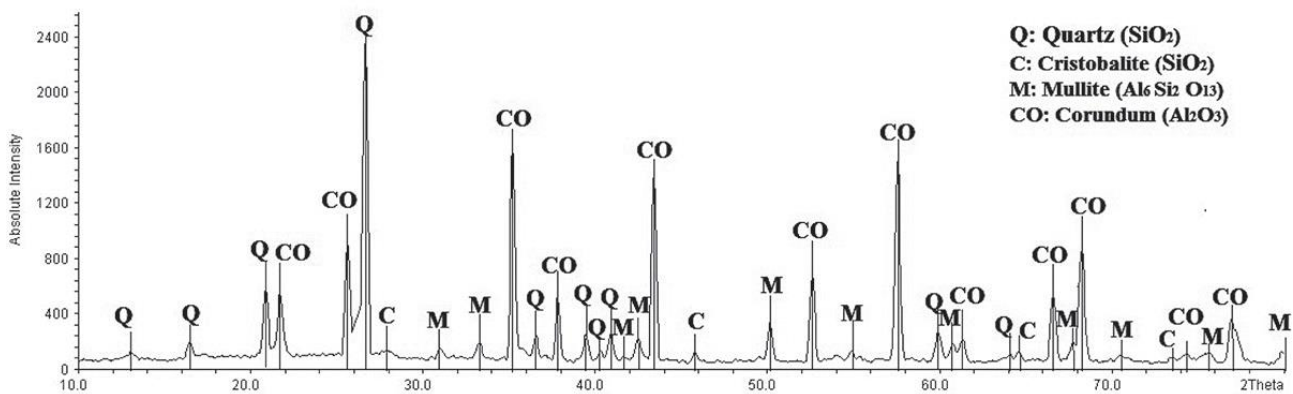


Corundum is the most stable Al_2O_3 phase at all temperatures under ambient pressure. Other metastable Al_2O_3 polymorphs are often formed before reaching the most stable $\alpha\text{-Al}_2\text{O}_3$ phase under circumstances such as decomposition of aluminium hydroxide and aluminium oxy-hydroxide, high-temperature oxidation of alumina-forming alloys, and recrystallization of amorphous alumina.

In MA and mullite membranes, α -alumina powder is transformed to the corundum crystalline phase at under 1300°C.



a) Mullite



b) MA 50 %

Figure 8.2. XRD pattern of (a) mullite, (b) MA 50%

As shown in Figure 6(a,b), the absolute intensity and formation of the corundum phase in the structure of MA membranes are greater than in mullite membranes because more α -alumina powder is present in the MA membrane structure. This X-ray diffraction (XRD) microstructure can be understood as the submicrostructure, taking into account that mineral grains are formed by a mosaic of crystallites. In the field of ceramic materials, the application of XRD microstructure analysis is not habitual for different reasons. One of them is the line overlapping, typical for ceramic materials, making an accurate treatment of line profiles corresponding to phases of interest difficult. Another problem is caused by the narrowness of some line profiles, since in these cases the extraction of microstructural information sometimes is not possible. On the other hand, the results obtained via the XRD microstructure analysis are referred to such parameters as the crystallite size (or X-ray coherence lengths) which have a physical meaning different to the grain size, frequently used for ceramic researchers. Nevertheless, in our opinion the XRD microstructure analysis offers some advantages with regard to the classic analytical methods; the sample do not need a special treatment and requires only an adequate choice of the conditions for recording the XRD powder pattern. Thus, the mineralogical analysis (qualitative and quantitative) and the microstructure analysis could be performed on the same data collected. Furthermore, the results of the XRD microstructure analysis set up statistical characteristics of the sample.

8.1.3. Mean pore size analysis

The mean pore diameter of prepared membranes is shown in Table 8.1. As this table shows, mullite membranes have the smallest mean pore diameter of 0.451 μm among all the fabricated membranes. The mean pore size was measured by porometer instrument by applying pressure and on other side measuring the permeate in respect to time. An ascending trend in the mean pore diameter of MA membranes by 10–50 wt% α -alumina powder content can be observed. For MA membranes with 10–50 wt% α -alumina powder content, the mean pore diameter increases from 0.462 μm to 0.507 μm . The mean pore size and porosity of MA membranes are enhanced by the addition of α -alumina powder because of the positioning of α -alumina particles between kaolin particles in the membrane structure.

Test number	Membrane	Kaolin (%)	Alumina (%)	Zeolite (%)	Porosity (%)	Mean pore diameter size (μm)
1	Mullite	100	0	0	32.6	0.451
2	MA (10%)	90	10	0	32.8	0.462
3	MA (20%)	80	20	0	33.2	0.468
4	MA (30%)	70	30	0	36.4	0.485
5	MA (40%)	60	40	0	38.2	0.498
6	MA (50%)	50	50	0	40.4	0.507

Table 8.1. Compositions, porosity and mean pore size of synthesized membranes.

The porosity of all the prepared membranes is also shown in Table 8.1. As can be seen, the porosity of the mullite membrane was 32.6%, the lowest value among all the membranes, with the overall mean pore diameter values. The porosity of MA membranes with α -alumina content of 10–50 wt% added grew steadily from 32.8% to 40.4%. As mentioned above, the addition of α -alumina powder increased the mean pore diameter and porosity of MA membranes.

8.1.4. Mechanical strength

The mechanical strengths of mullite, MA 50%, are 18.3, 24.6 MPa, respectively. As mentioned in section 8.1.2 above concerning XRD analysis, α -alumina powder in the MA membrane structure is transformed into the corundum crystalline phase at a temperature of 1300°C. It is well known that the main characteristics of the corundum crystalline phase are hardness, high mechanical strength and anti-abrasion

properties. The mechanical strength of MA membranes was, therefore, higher than that of other membranes due to greater formation of the corundum phase.

8.1.5. TGA

Figure 8.3 shows a TGA graph of a mullite membrane sample which is heated from room temperature to 800°C at a heating rate of 10°C min⁻¹. Regarding the diagram, two major weight loss steps can be found. The first which occurred at temperatures ranging from almost 25°C to 150°C (approximately 1.5% loss), is an endothermic reaction related to the removal of adsorbed water. The second, a roughly 6% weight loss reported at temperatures of 475–750°C, can be attributed to an endothermic reaction in which hydroxyl groups are separated from the kaolin (kaolin dehydroxylation) structure to form metakaolinite. Further heating leads to the formation of primary mullite. This analysis also confirms that the membrane sample was highly stable at high temperatures. These findings are in good agreement with other published results.

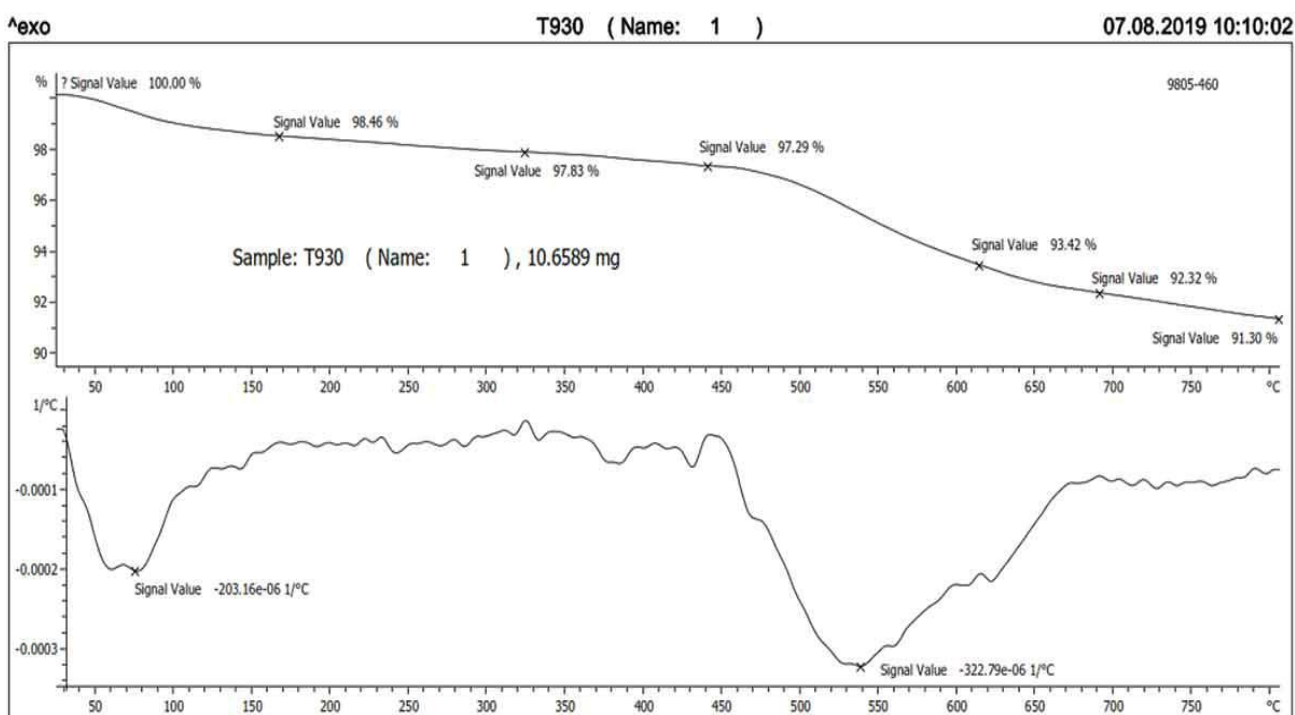


Figure 8.3. TG analysis of mullite membrane sample at 10°C min⁻¹.

8.2 Effect of Organic Solvent on Partition Coefficient

The organic solvent having a high partition coefficient must be selected to increase the efficiency of extraction of low-molecular-weight acid in aqueous phase. Experiments were carried out using three solvents such as methyl isobutyl ketone (MIBK), chloroform, and 2-octanol. These solvents are immiscible with an aqueous phase. We choose acetic acid as a model pollutant from ballistic industry.

Then 50 g of 2 wt-% aqueous acetic acid solutions were prepared by adding 16.6 mmol acetic acid to 367 mmol first-distilled water. Each 50 g of organic phases, extractant phase, containing various tri-octylamine (TOA) content of 0, 10, 20, 30, and 40 wt-%, respectively, were contacted with aqueous acid solution prepared above. The mixed solutions, which were observed at the interface between aqueous and organic phases formed in the middle of the mixed solution without emulsion, were kept to reach an equilibrium state within 30 min. Then, the concentration of acid both in aqueous and in organic phases were simultaneously measured. Partition coefficient presented in Fig.8.4. It could be seen from this figure that the partition coefficients of methyl isobutyl ketone (MIBK) and chloroform increased with TOA content to attain a maximum at 40 wt-% TOA. Thereafter it did not increase despite of further increase of TOA content. However, when 2-octanol was used as an organic phase, partition coefficient reached a maximum at 20 wt-% TOA and then slightly decreased thereafter. Figure 8.4 also showed that MIBK has excellent acid-extraction properties compared with other two solvents.

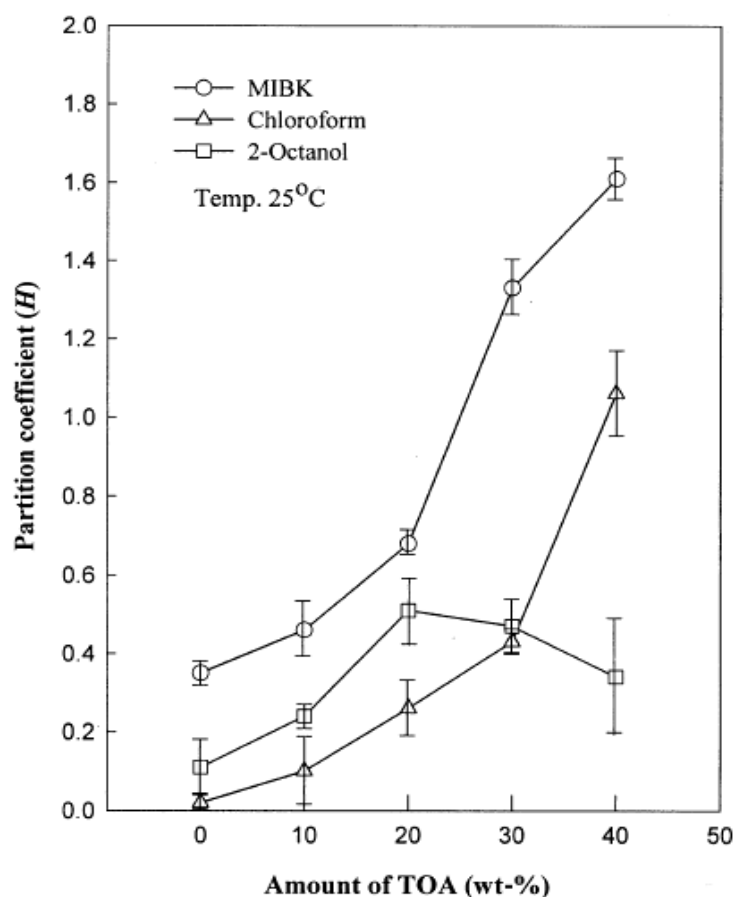


Figure 8.4. The effects of various organic phases on the partition coefficient; solid line denotes a regression.

8.3 Effect of Amine Extractant on the Removal of Acetic Acid

The selection of extractant is very important at the reactive extraction process. It has been investigated that the addition of amine extractant to organic phase could increase the extraction performance due to

the increase of the partition coefficient. In general, tertiary amine and quaternary ammonium salt were extensively utilized. In this study, organic phase (MIBK) containing various tertiary amines such as DEA, TEA, and TOA was used to investigate the effect of the degree of alkylation of amine and that of alkyl group on extraction performance. The experimental results for the acetic acid concentration removed in aqueous phase vs. the amount of tertiary amine is presented in Fig.8.5. As can be noticed, amine exhibits a better extraction performance than secondary amine. Also, as the number of carbon in alkyl group of tertiary amine increases, the extraction performance of acetic acid in aqueous phase is enhanced. Because hydrocarbon acts as an electron donor, it has generally been well known that the increase of the number of either carbon in alkyl group or alkyl group itself makes a strong nonpair electron charge density of nitrogen atom in amine. Therefore, at the interface of an aqueous phase/organic phase, the complex between tertiary amine and acetic acid was easily formed, compared with that of other amines, to transfer toward organic phase.

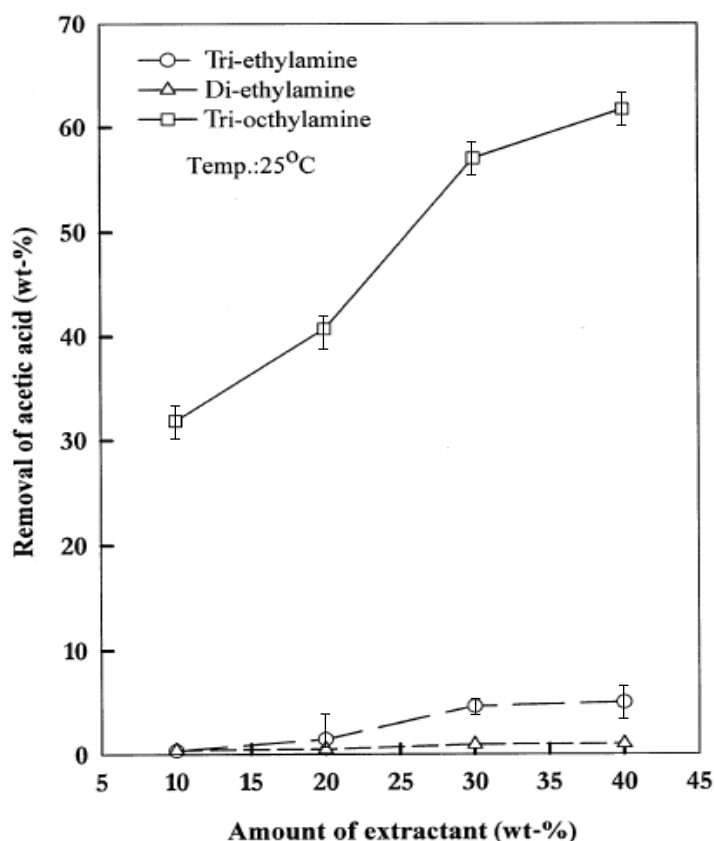


Figure 8.5. Removal of acetic acid with various amines.

A schematic of extraction mechanism was presented in Fig.8.6. Under the steady-state condition, the mass transfer for a facilitation factor with reaction in the interface between the two phases was derived by the reaction rate expression for one-dimensional, steady-state diffusion with reaction in a homogeneous medium. $K_e (= k_1/k_2)$, is the rate constant for the formation of the acid-base complex $[N(R_3)H^+][ACOO^-]$.

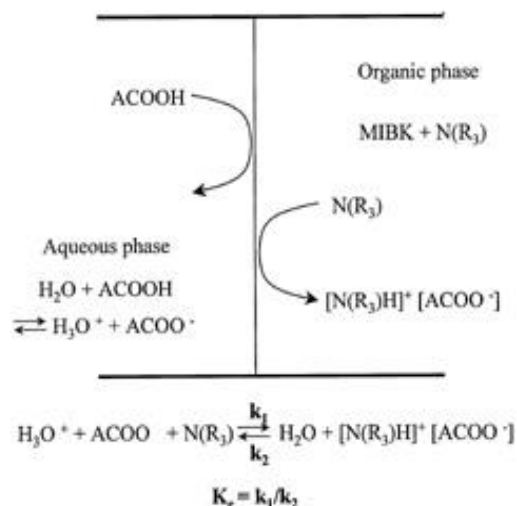


Figure 8.6. The schematics of reactive extraction at interface between aqueous and organic phase. K_e is the equilibrium constant of the interfacial reaction.

8.4 Removal of Acetic Acid with Temperature

The effect of temperature with tri-n-octylamine content of 0–40 wt-% on the removal efficiency of acetic acid is shown in Figs. 8.7. Examining these figures, the removal efficiency of acetic acid in aqueous phase generally increased with temperature and the content of TOA. TOA in organic phase plays a role as a carrier, causing acetic acid to facilitate transfer to organic phase. Therefore, the removal of acetic acid increased with the content of amine. However, the maximum value of extraction performance was different according to the experimental conditions such as organic solvent, temperature, and TOA content. In the case of MIBK/TOA system and chloroform/TOA used as organic phases, a maximum value for the removal of acetic acid was 64 wt-% and 53 wt-%, respectively, under the condition of 40 wt-% TOA content at 25°C. However, when 2-octanol/TOA system was used as an organic phase (see Fig. 8.8), the extraction performance had a convex trend with TOA content in the temperature range of 25–60°C. Also a maximum point moved into 20 to 30 wt-% TOA content. Notice that the maximum removal efficiency of acetic acid is 67 wt-% under condition of 30 wt-% TOA at 50°C. Based on the energy efficiency, it may be deduced that the optimum condition of organic phase for the extraction of acetic acid in aqueous phase was 40 wt-% TOA/MIBK at 25°C. This condition will be later used to calculate the mass-transfer rate.

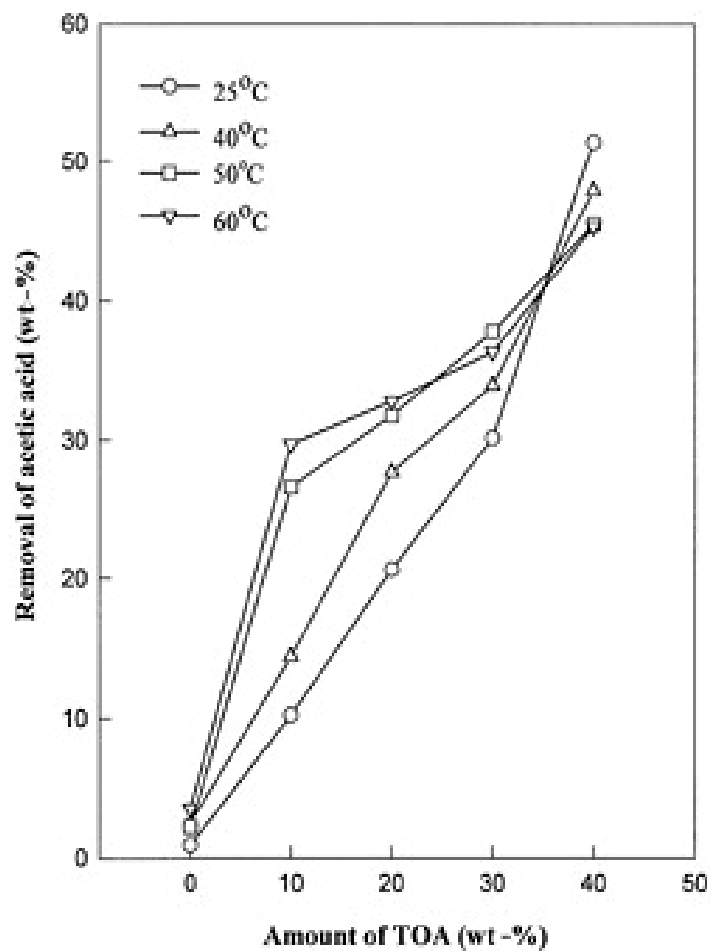


Figure 8.7. The effects of temperature on removal of acetic acid in aqueous phase using MIBK/TOA as organic extraction phase.

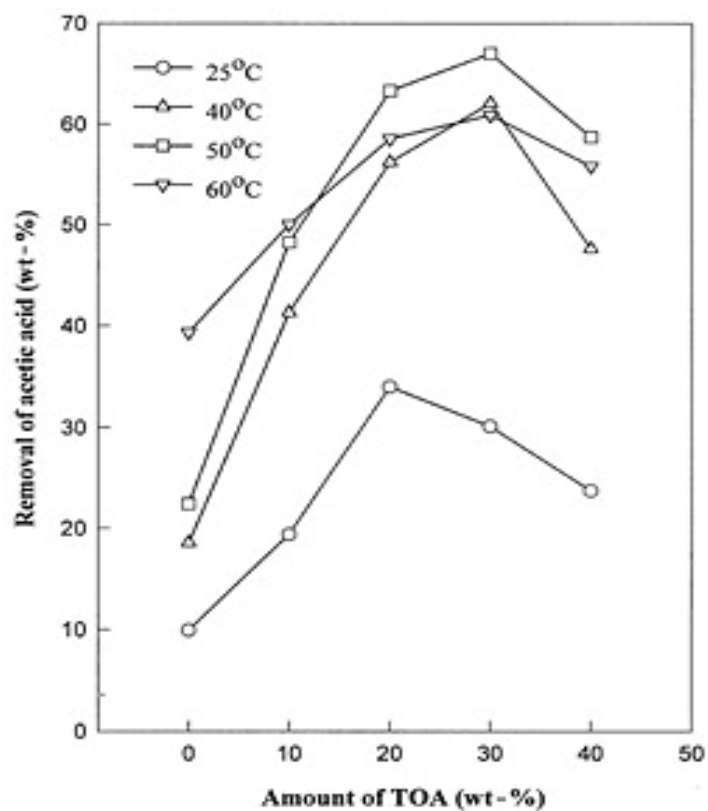


Figure 8.8. The effects of temperature on removal of acetic acid in aqueous phase using 2-octanol/TOA as organic extraction phase.

8.5 Calculation of the Overall Mass-Transfer Coefficient

Considering the resistance in series model, the reciprocal of the overall mass-transfer coefficient is the total resistance (R_a) to mass transfer and can be described as the sum of the mass-transfer resistance inside fiber (aqueous feed side, R_{aq}), across the fiber wall (membrane resistance, R_m), and outside the fibers (organic extractant side, R_{org}).

$$R_a = R_{aq} + R_m + R_{org}$$

Following Equation can be converted into the form of

$$\frac{1}{K_a} = \frac{1}{k_{aq}} + \frac{d_i}{H \cdot k_m \cdot d_{lm}} + \frac{d_i}{H \cdot k_{org} \cdot d_e}$$

where K_a represents the overall mass-transfer coefficient, k_{aq} , k_m , k_{org} are the local mass-transfer coefficients on the fiber inside, membrane, and fiber shell side, respectively. H is the solute partition coefficient between the two contacting phases, and d_i , d_e , d_{lm} are the internal, external, and logarithmic length of fiber, respectively.

Using the membrane extraction process with a hollow-fiber membrane contactor, the overall mass-transfer coefficient was calculated by Wilson-plot method under the assumption of constant partition coefficient. In the case of nonconstant H , another approach for mass balance should be considered over the extraction process. The concentration of the acid in the aqueous solution was measured as a function of time to determine the overall mass-transfer coefficient (K_a) defined by

$$J_{sol} = Q_{sol}/A_m (C_{(a)} - C_{(a)}^*) = K_a (C_{(a)} - C_{(a)}^*)$$

where J_{sol} was the solute flux, A_m was effective membrane area, $C_{(a)}$ was the concentration in aqueous solution at time (t), and $C_{(a)}^*$ was the equilibrium acid concentration in the aqueous phase. An exponential dependency of the concentration of the solute in aqueous phase with time can be established. According to the following equation, the concentration of the acid in the aqueous phase varies with time in the form of an exponential equation.

$$C_{(a)} = \alpha + \beta \exp(-\gamma t)$$

where α and β depend only on known parameters, and their values can be determined in advance. By fitting the experimental data to this exponential equation, optimal values for γ are obtained. The experimental results obtained for acetic acid concentration in feed phase ($C_{(a)}$) vs. time for one of the

experiments is presented in Fig. 8.9. K_a is determined by substituting the value of the other parameters in below equation.

$$K_a = \frac{-Q_{(a)}}{(1 + Q_{(a)}) \cdot A_m} \ln \left(1 - \gamma \left(\frac{V_a}{Q_a} \right) \left(\frac{1 + Q}{1 + V} \right) \right)$$

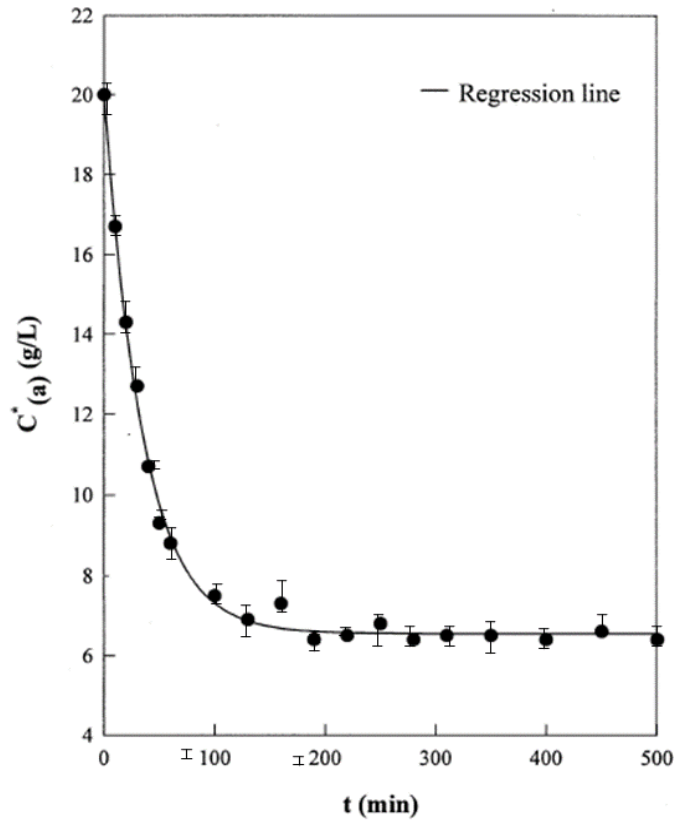


Figure 8.9. Acetic acid concentration as a function of time. This experiment was carried out under condition of constant aqueous velocity of $8.2 \text{ cm}^3/\text{sec}$ at 25°C .

Table 8.2 shows the overall mass-transfer coefficients calculated for the extraction process. These values indicate a significant increase in the mass-transfer coefficient with increasing TOA content. Coelho et al. reported that increasing extractant concentration (Aliquat 336) improved the mass-transfer process because the use of a higher amine concentration had an effect on increasing partition coefficient, whereas the diffusion coefficient of solute decreased with increasing amine concentration due to the increase of the viscosity in organic phase.

TOA Content (wt-%)	H	K_a ($10^{-6}\text{m}/\text{sec}$)
0	0.35	15.1
10	0.46	18.5
20	0.68	21.3
30	1.33	24.7

40	1.61	26.4
----	------	------

Table 8.2 shows the overall mass-transfer coefficients calculated for the extraction process

Consequently, the overall mass-transfer rate decreased with increasing amine extractant, which was regarded as a combined effect of the partition coefficient and diffusion coefficient of solute. Therefore, the membrane resistance is identical to the limiting step on the mass-transfer process. Assuming that the limiting step is the membrane resistance, the overall mass-transfer coefficient may be expressed as

$$K_a = \text{const. } H \cdot D_{org}$$

It indicates that the overall mass-transfer coefficient is proportional to the product of the partition coefficient and the diffusion coefficient of solute. In the TOA/MIBK organic system, the use of higher TOA content in organic phase made a contribution toward increasing partition coefficient and diffusion coefficient of solute at the same time. This means that viscosity does not considerably increase despite of increasing TOA content. Therefore, it was concluded that the high extraction performance of the present system was caused by a significant increase in diffusion coefficient of a solute.

Phase II

8.6 Characterization of Active Carbon

Observation of the surface morphology of raw deoiled olive pomace and activated biochar is shown in Fig. 8.10. Raw deoiled olive pomace has dense structure with almost no pores in it but the OAB produced at optimized setting is highly porous with micropores, transitional pores, and meso- and macropores of varying shapes. Apparent size of the pores range between micro- to mesopores and are not well-structured but evident of open porosity.

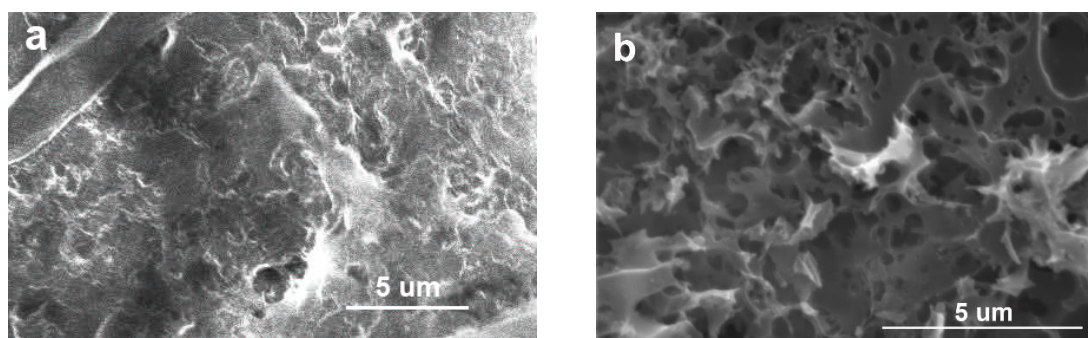


Figure 8.10. SEM micrographs of (a) raw deoiled olive pomace and (b) olive-based activated biochar produced at numerically optimized setting

Mesoporosity of the material is further validated by the appearance of mesoporous peak between 2θ of 1.00 to 1.75 degrees of OAB diffractogram (Fig. 8.11a). The peak is broad in a sense that the OAB is

not well-structured and pores are distributed to a certain range of values. Wide angle scan of OAB showed typical diffractogram of activated carbon.

Fig. 8.11 b shows the FTIR spectra of raw deoiled olive pomace (SE) and OAB. OAB spectrum shows shoulder peaks around 1005, 1523 and 423 cm^{-1} due to C=C, C-O and M-O functional groups, respectively. SE spectrum shows peaks 3350, 2926, 2849 and 1158 cm^{-1} for O-H stretching; 1688 cm^{-1} for C=C; 1612 cm^{-1} shoulder peak for C-O; and 1045 cm^{-1} for C-H.

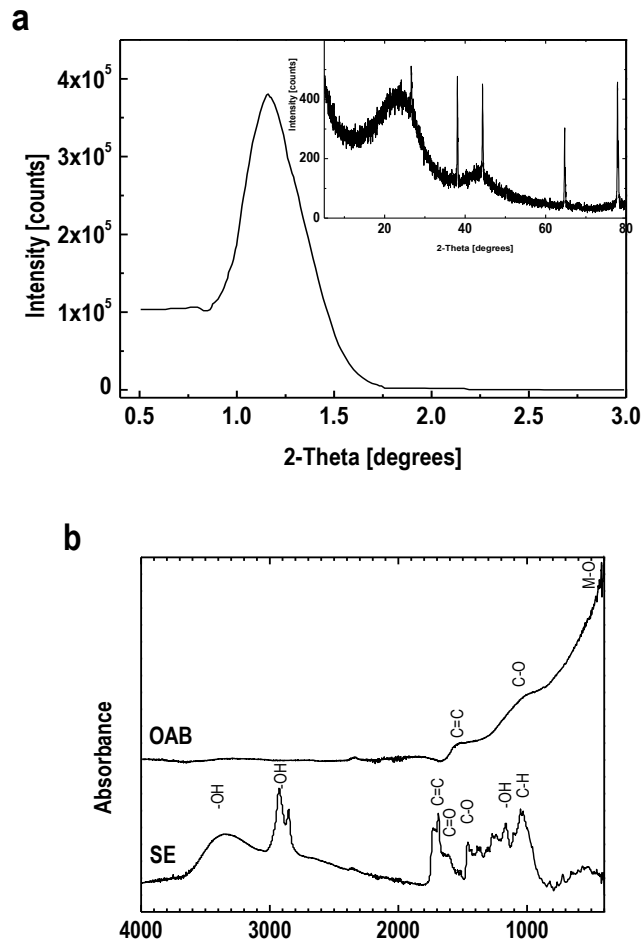


Figure 8.11 . Diffractogram and FTIR spectra of olive-based activated biochar produced at numerically optimized setting.

The interpolated curve of zeta potential of suspended OAB is plotted as function of pH in Fig. 8.12 The zero point charge pH_{zpc} of OAB is 6.63. This means that the OAB surface is positively charged if the pH is lower than pH_{zpc} and negatively charged if the pH is higher than pH_{zpc} .

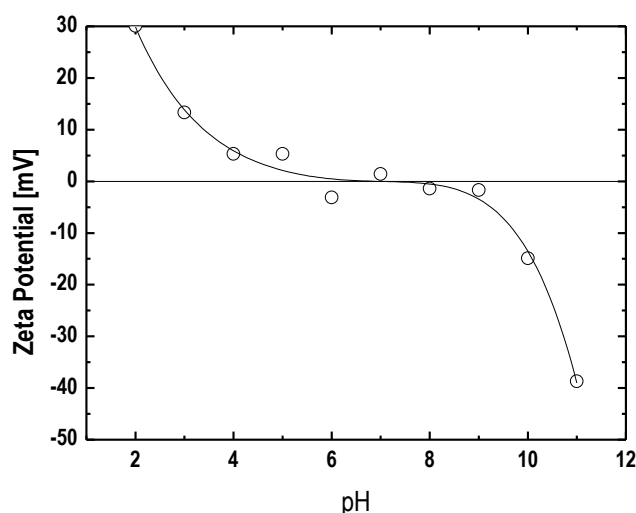


Figure Error! No text of specified style in document.-1. Zeta potential of OAB as function of solution pH.

FTIR

Fourier transform infrared spectrometer (FTIR-ATR, Nicolet 6700, Thermo Scientific) was used for determining functional groups present, scanning electron microscopy (SEM, S-3400N, Hitachi) for crystal morphology, thermogravimetric analyzer (TGA, DTG-60H, Shimadzu) for non-isothermal degradation, X-ray diffraction (XRD, XRD-600, Shimadzu) for crystal structure, lattice parameters and presence of mesoporous peak. N₂ adsorption/desorption were performed in ASAP 2020 physisorption instrument. The surface area and pore size distribution of the material was approximated using Brunauer–Emmet–Teller (BET) and Barret–Joyner– Halenda (BJH) method, respectively.

The zero point charge of the activated biochar was determined by measuring zeta potential of suspension in water containing OAB at different pH values. Polynomial interpolation of was performed to determine the pH at which the value of zeta potential is zero.

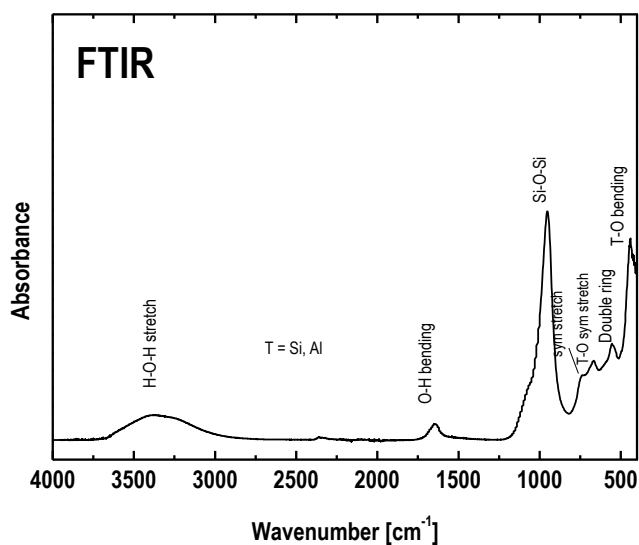


Figure 8.13 FRIT curve of the active carbon

Thermal analysis

Figure 8.14 shows the TG and DTA curves obtained from the thermo gravimetric experiment at the heating rate of $10\text{ }^{\circ}\text{C min}^{-1}$. The thermal decomposition of SE is a three-stage process involving (1) dehydration of adsorbed moisture at $0\text{-}180^{\circ}\text{C}$, (2) degradation of biodegradable component like hydrocarbons at $200\text{-}350^{\circ}\text{C}$, and (3) degradation of protein, sugars and aliphatic compounds at $380\text{-}500^{\circ}\text{C}$ with the last two processes as main degradation steps for the decomposition of lignocellulosic SE. Range 1 ($200\text{-}350^{\circ}\text{C}$) has an activation temperature of 228°C while Range 2 ($380\text{-}500^{\circ}\text{C}$) has an activation temperature of 414°C . DTA for both range of temperatures showed endothermic peaks with maximum endothermic peak at $380\text{-}500^{\circ}\text{C}$.

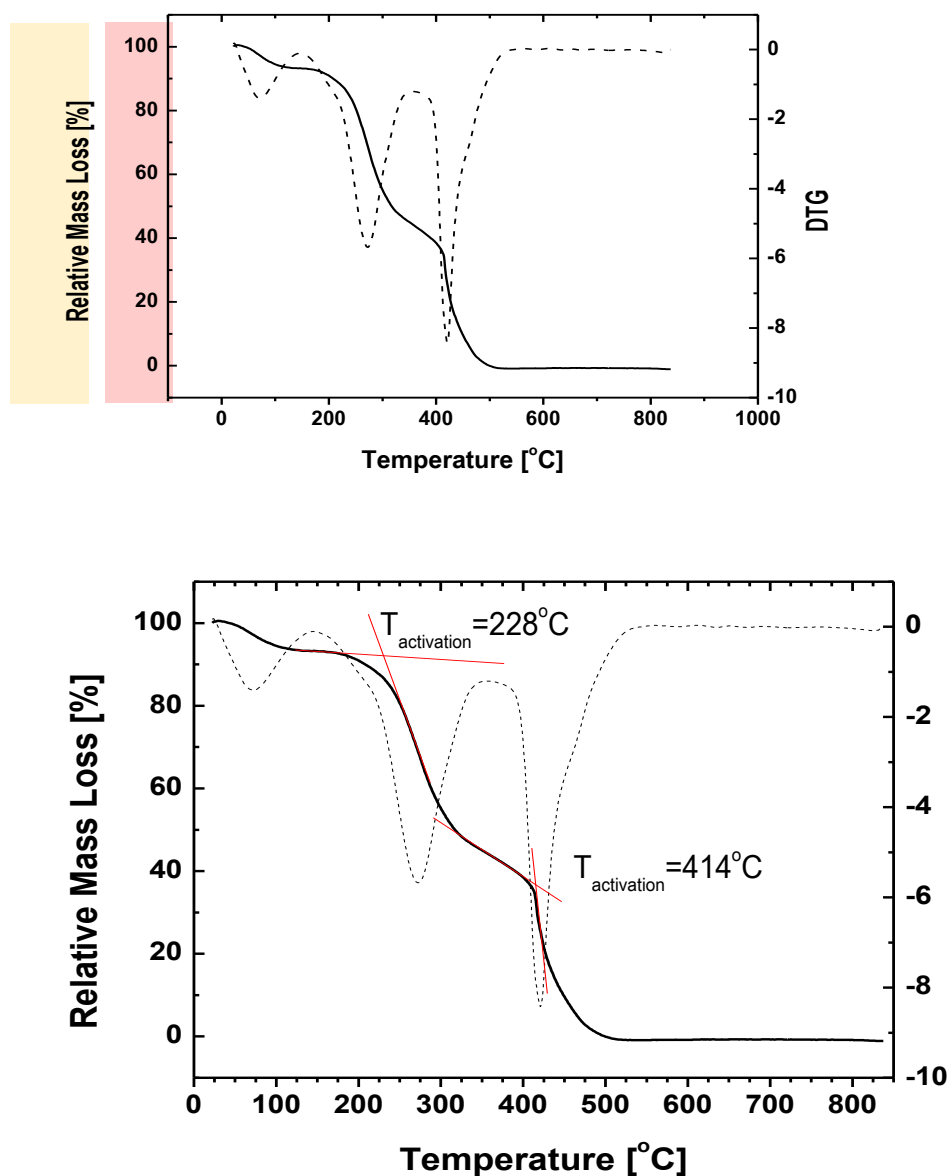


Figure 8.14 TG and DTA of deoiled olive pomace.

Table 8.3 shows different models for $g(\alpha)$ and their corresponding R^2 during linear fitting. The activation energy of every process (dehydration and deamination) leads to the values of the kinetic and thermodynamic parameters (Table 8.3). Based on the calculated thermodynamic parameters, both range of temperatures tend to be thermodynamically unstable due to positive values of ΔG^\ddagger , and non-spontaneous for Range 1 and spontaneous for Range 2 due to the negative and positive ΔS^\ddagger , respectively. The positive values of ΔH^\ddagger for both range of temperatures only mean that the degradation highly endothermic due to a drastic loss of weight of SE.

Table 8.3 Listed fitting values of deoiled olive pomace at different kinetic models.

Code	Function name	$g(\alpha)$	Range	
			200-350 °C	380-500 °C
Rxn Order Models				
R1	Mampel	$-\ln(1-\alpha)$	0.98282	0.97927
R1.5	Chemical reaction order 1.5	$2[(1-\alpha)^{-3/2}-1]$	0.99275	0.99501
R2	Chemical reaction order 2	$(1-\alpha)^{-1}-1$	0.99036	0.99493
Nucleation Models				
A2	Avrami-Erofeev 2	$[-\ln(1-\alpha)]^{1/2}$	0.84982	0.91462
A3	Avrami-Erofeev 3	$[-\ln(1-\alpha)]^{1/3}$	0.94187	0.95193
A4	Avrami-Erofeev 4	$[-\ln(1-\alpha)]^{1/4}$	0.97066	0.96962
P4	Power law 1/4	$\alpha^{1/4}$	0.41341	0.76711
P3	Power law 1/3	$\alpha^{1/3}$	0.84971	0.18626
P2	Power law 1/2	$\alpha^{1/2}$	0.9408	0.42227
P1	Power law 1	α	0.96987	0.83627
Diffusion models				
D1	One dimensional diffusion	α^2	0.97722	0.8985
D2	Two dimensional diffusion	$\alpha+(1-\alpha)\ln(1-\alpha)$	0.98058	0.93501
D3	Jander	$[1-(1-\alpha)^{1/3}]^2$	0.98375	0.96721
D4	Ginstling and Brounshtein	$1-(2/3)\alpha-(1-\alpha)^{2/3}$	0.98172	0.94895
Geometrical contraction				
C1	Contracting cylinder	$1-(1-\alpha)^{1/2}$	0.97718	0.94167
C2	Contracting sphere /cube	$1-(1-\alpha)^{1/3}$	0.97923	0.95862

Range	Activation energy (Ea) (kJ mol ⁻¹)	Frequency Factor (A) (min ⁻¹)	ΔS^\ddagger (J mol ⁻¹ K ⁻¹)	ΔH^\ddagger (J mol ⁻¹)	ΔG^\ddagger (J mol ⁻¹)
200-350 °C	56.80	1.08×10^5	-186.98	48462.12	1.42×10^5
380-500 °C	218.51	2.18×10^{17}	48.68	207082.50	1.74×10^5

Table 8.4 Kinetic and thermodynamic parameters for the thermal decomposition of deoiled olive pomace.

8.7 Geopolymers Characterization

SEM:

Given the unique three-dimensional network structure, geopolymer-based inorganic membranes can intercept, capture and fix heavy metal ions. SEM analysis diagram of the geopolymer-based inorganic membrane is shown in Fig. 8.15. The geopolymer-based inorganic membrane surface was smooth and the inner was an obvious porous structure, which provided good passages for water permeation [3]. These gels were converted into three-dimensional network structures (whilst forming a porous structure)

after dehydration. As the molar ratio of H₂O/Na₂O increased, both the dense degree of the inorganic membrane surface and intergranular gelation degree were reduced, but the particles of the edges and corners cleared gradually and the aperture increased, as shown in Fig. 8.15 (A-D)

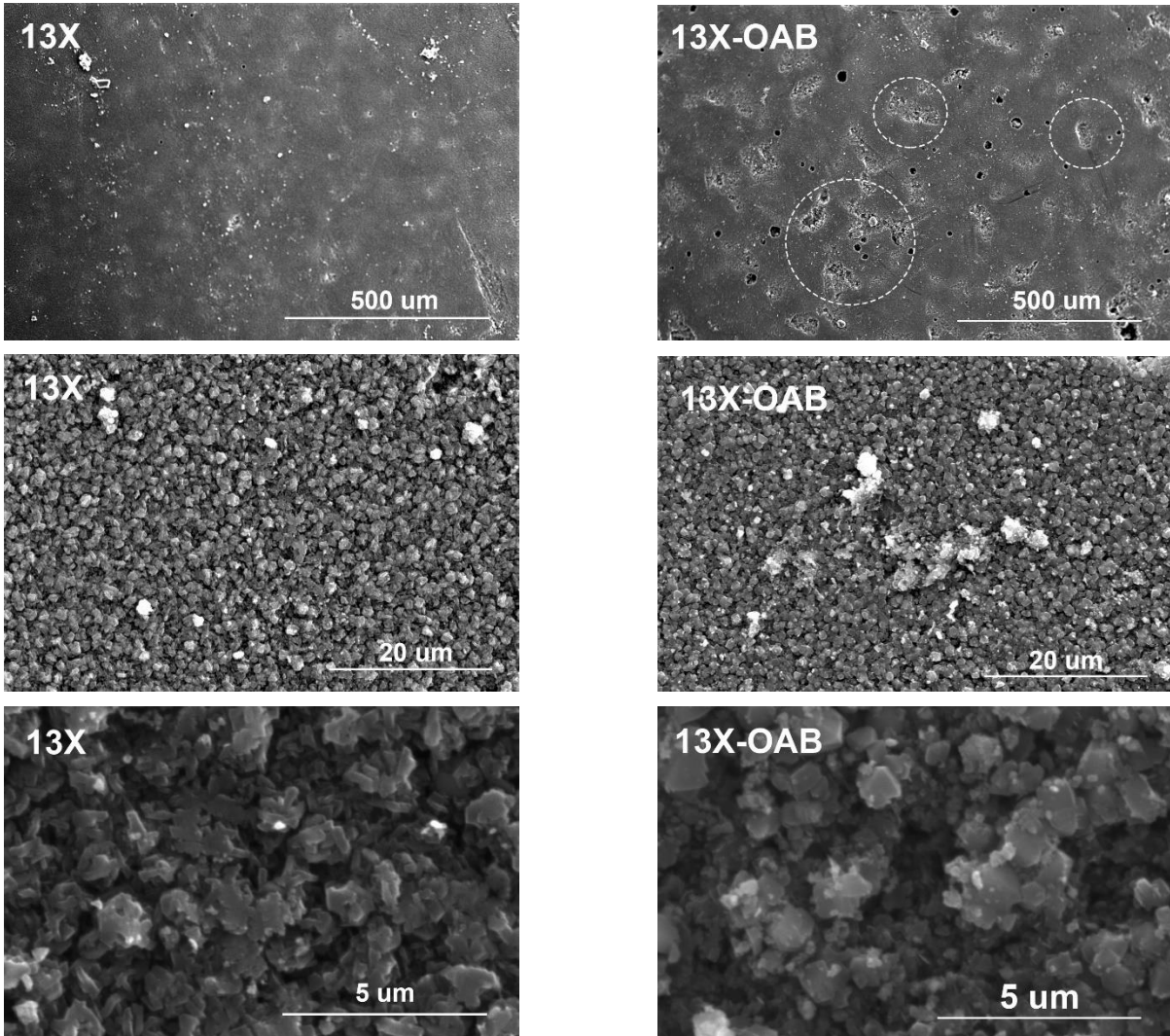
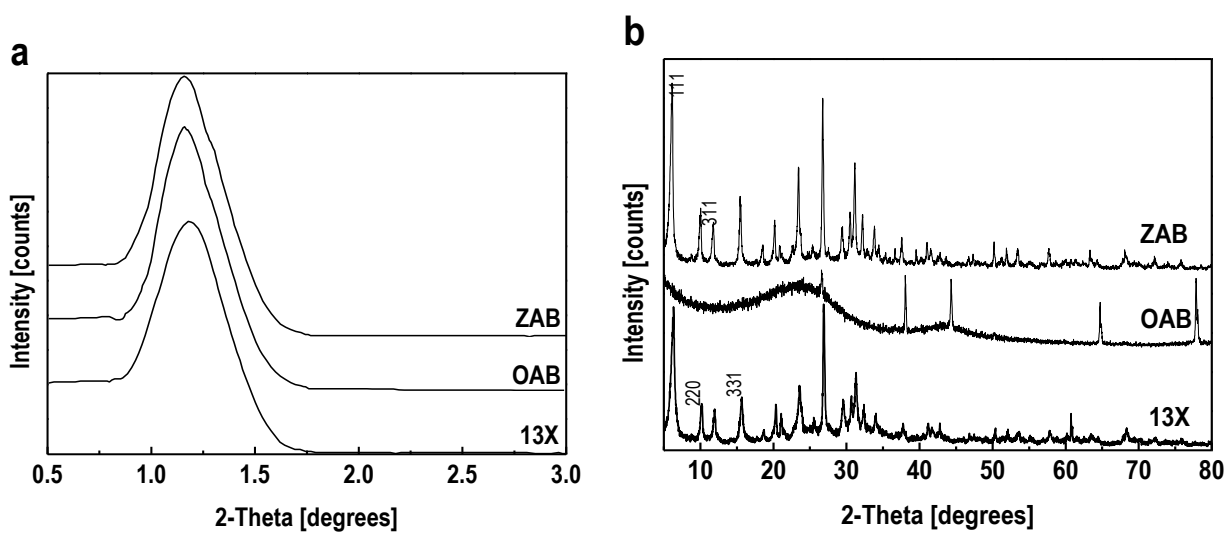


Figure 8.15. SEM micrograph of 13X zeolite and 13X-OAB composite membrane.

XRD

Even if geopolymers are X-ray amorphous, XRD analysis is usually carried out to check the presence of any undesired crystalline phases developed during curing that could affect mechanical properties, such as zeolites, or already present in the parent materials as impurities, like quartz or crystalline kaolinite. In particular, these last, having a non-centrosymmetric structure could contribute to the generation of electrical dipoles during mechanical stress Fig. 8.16 (a) shows the XRD patterns of metakaolin raw powder (lower curve) as well as that of the synthesized geopolymer (upper curve). Metakaolin exhibits a pronounced broad hump centered at approximately $22^\circ 2\theta$ with few peaks, indicating that it contains essentially amorphous silica and alumina and Quartz (PDF no 01-083-2468) and Muscovite (PDF no 00-002-0055) impurities as crystalline phases. No diffraction peaks of its parent material, kaolinite, were detected. After reaction with sodium silicate solution, XRD pattern shows a shift of the centre of the

original broad hump from $22^\circ 2\theta$ to approximately $28^\circ 2\theta$, that can be considered the typical distinguishing feature of the geopolymeric materials. All sharp peaks from crystalline phase in parent material are still present in the geopolymer diffraction pattern, thus confirming that they behave as inactive fillers in the geopolymer binder. Quartz could indeed contribute, even if unlikely to occur, since the crystal need to be cut and loaded along its symmetry directions, to the generation of electrical dipoles during mechanical stress, thus to piezoelectric activity. Fig. 8.16 b shows the FTIR spectra of OAB, bare 13X and 13X-OAB composites. Functional groups of OAB are masked with the functional groups of the composites. FTIR spectra of the composites show the same functional groups. The spectra show vibrational shoulder band at 1060 cm^{-1} which is associated with unreacted aluminosilicate; sharp peak at 955 cm^{-1} corresponds to Si-O-Si of geopolymer-13X network formed ; 3383 and 1642 cm^{-1} indicates the presence of -OH groups on the surface of NaX; 548 cm^{-1} are bands located at fingerprint region for faujasite zeolites.



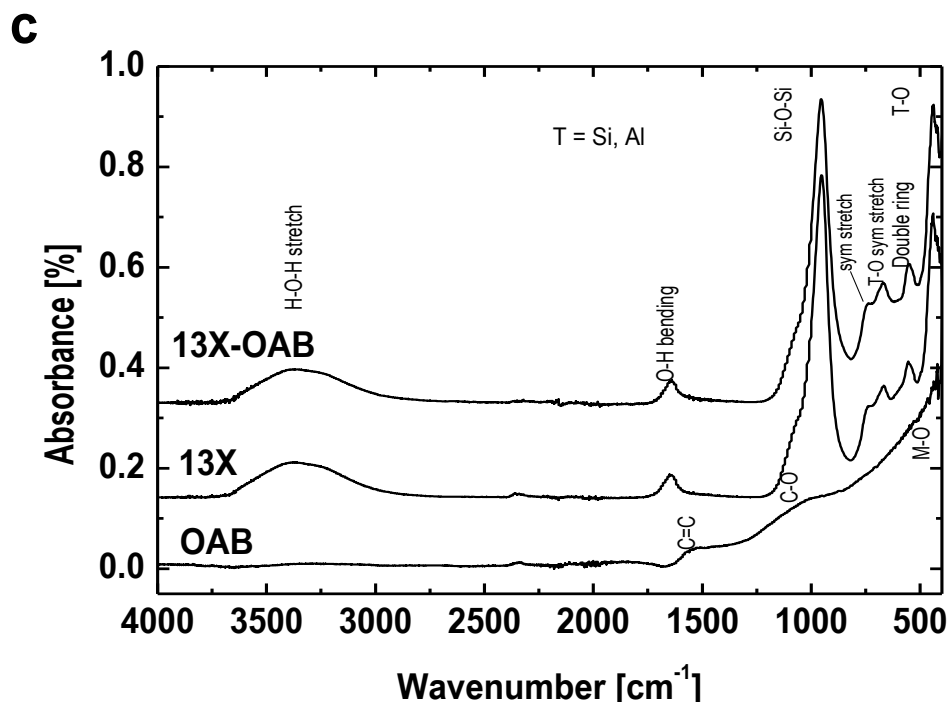
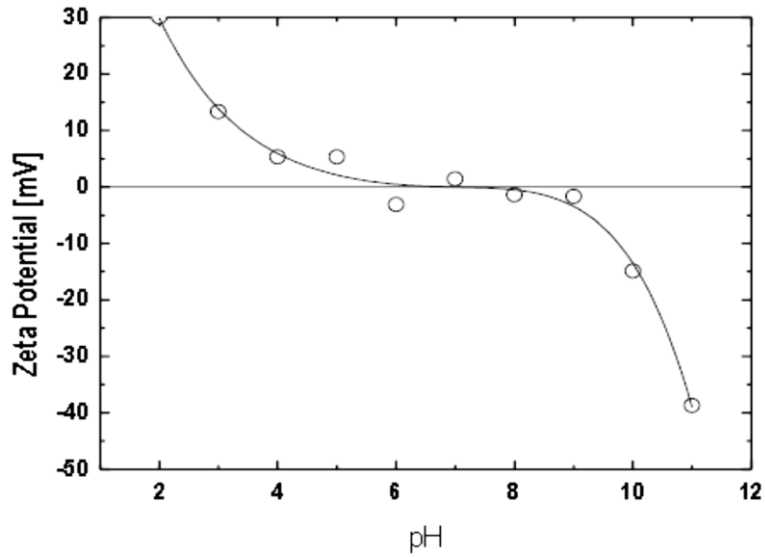


Figure 8.16 Diffractogram [(a) narrow and (b) wide angle] and (c) FTIR spectra of olive-based activated biochar, 13X zeolite and 13X-OAB composites.

The interpolated curve of zeta potential of suspended OAB is plotted as function of pH in Fig. 8.17. The zero point charge pHzpc of OAB is 6.63. This means that the OAB surface is positively charged if the pH is lower than pHzpc and negatively charged if the pH is higher than pHzpc . The linearly interpolated curve of zeta potential of suspended 13X and 13X-OAB composites are plotted as function of pH in Fig. 8.17. The zero point charge pHzpc of 13X and 13X-OAB 5.27 and 4.43, respectively. This means that the surface is positively charged if the pH is lower than pHzpc and negatively charged if the pH is higher than pHzpc . Cationic dyes are MB and RhB can be adsorbed by the composite materials because of the inherent negative charge of the surface, 13X-OAB being more negative than 13X makes it easier for cationic dyes to adsorb on its surface, in addition aluminosilicate materials greatly rely on electrostatic attraction for adsorption so addition of OAB to the geopolymer-13X matrix extends the adsorbing ability of material. MB adsorption is higher for both composites than with RhB; though both cationic dyes, RhB is slightly more negative ($\text{pKa}=3$) than MB ($\text{pKa}=3.8$), structurally bulkier and has more H-bond acceptor count (more lone pairs) than MB. Adsorption onto highly negative surface is expected to be low for RhB than with MB. In some cases we also see the desorption when a small amount of dye is passing on permeate side. Also we see the increase of dye concentration in feed tank after some time of treatment.



(a) Zeta potential of OAB as function of solution pH.

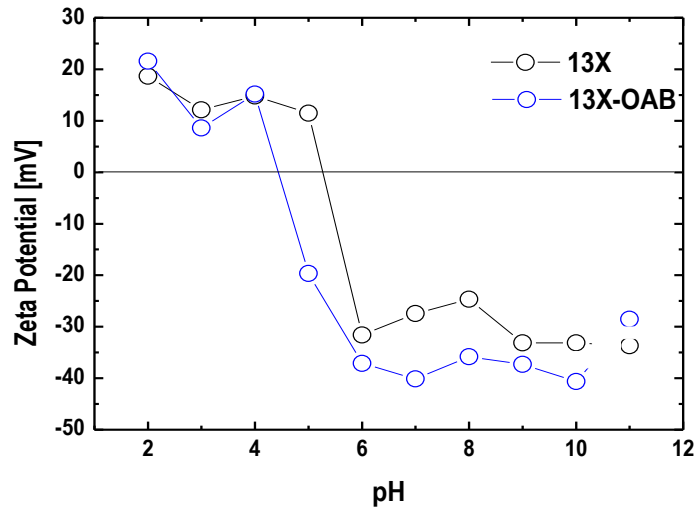


Figure 8.17 (b). Zeta potential of 13X and 13X-OAB as function of solution pH.

Permeation test

Fig. 8.18 shows the difference in permeability of 13X and 13X-OAB membranes. Addition of OAB into the geopolymer-13X matrix greatly enhanced the permeation of water through the ceramic membrane with measured permeability of 6.16 and 11.67 L m⁻² bar⁻¹ h⁻¹ for 13X and 13X-OAB, respectively. The permeability 13X composite is comparable to reported water flux of FAU membrane.

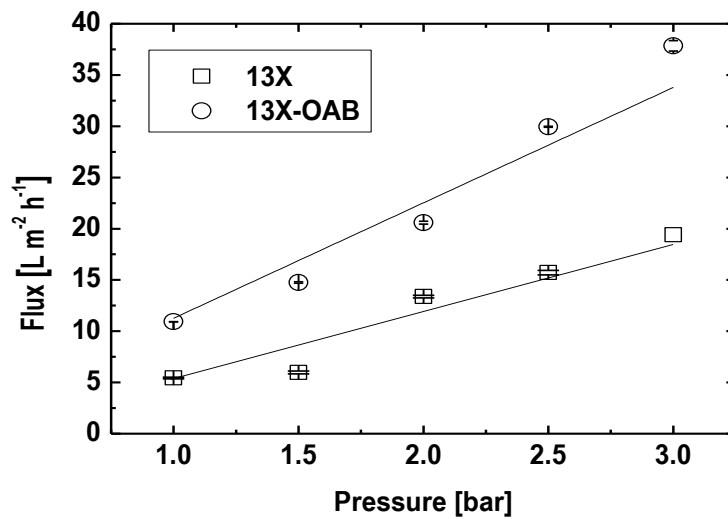


Figure 4-18. Permeability of 13X zeolite and 13X-OAB composite membrane.

Mechanical strength

The effect active carbon on the mechanical strength of the membranes was conducted to verify whether it does any compromise the mechanical integrity of the membrane. The effects were assessed by means of three indicators: a) the tensile strength, b) the maximum elongation that the membranes can endure before they are ruptured (elongation at break), and c) the membrane's Young Modulus. The maximum pressure at break and Young Modulus values are presented in Fig. 8.19

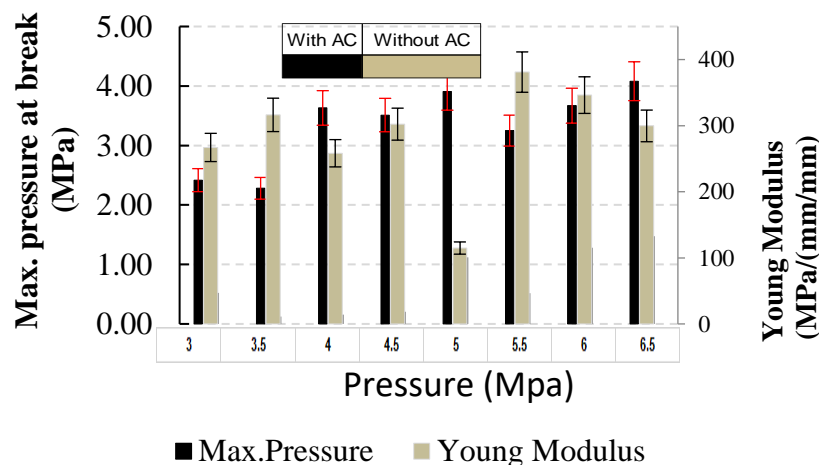


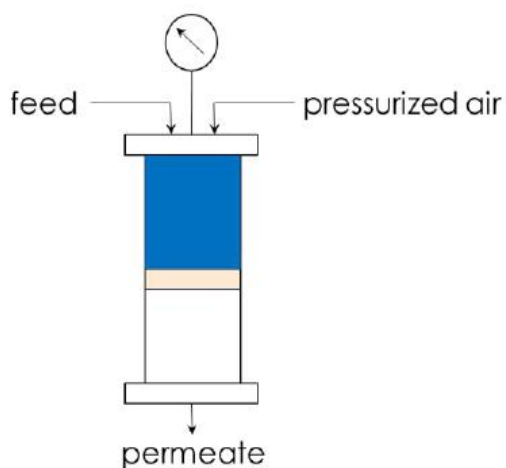
Fig 8.19 Mechanical strength of the membrane with and without AC

The mechanical strength results in Fig. 8.19 show that, though there are subtle differences in the maximum pressure at break of the membrane with and without AC, no clear trend can be confirmed. The overall stiffness of the membrane, as measured by the Young Modulus, increased when the membranes were exposed to the acidic medium. This effect is far more pronounced for geopolymeric membrane. When the membranes were mixed with AC, Young modulus values 3–20% lower than those

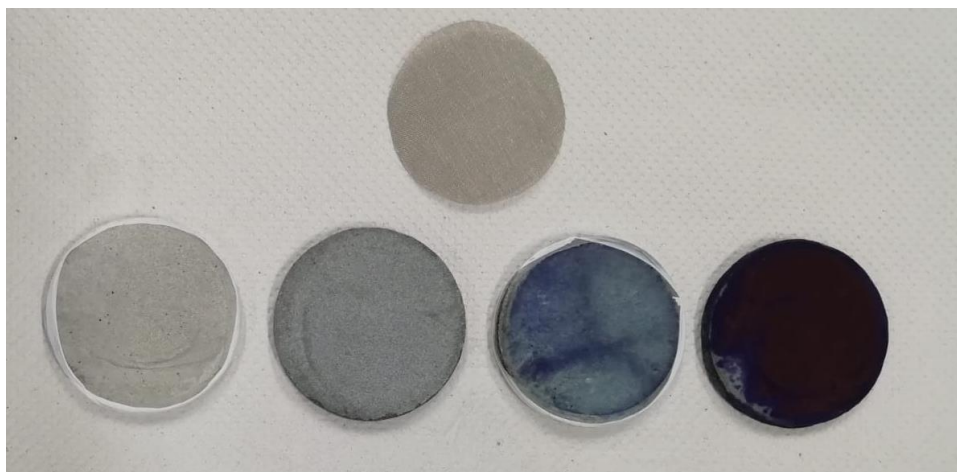
of the virgin samples which, indicating a slight decrease in stiffness. The mechanism by which the deposited coating caused such stiffness change is not clear.

8.8 Dead end membrane separation of MB

13X and 13X-OAB ceramic membranes were carefully placed O-rings in the Teflon membrane separation module (Fig. 8.19). The module is first filled with distilled water and permeation is measured at different operating pressure (1, 1.5, 2, 2.5 and 3 bar air pressure). The module is emptied and filled with 100 mg L⁻¹ MB. MB separation is performed at 2 bar pressure and permeate is collected at predetermined time interval. Initial data on MB separation were fitted with the kinetics models. The membrane before and after the MB adsorption is demonstrated here which also prove that the membrane is getting adsorbed with MB with respect to time.



(a)



(b)

Figure 8.19 (a) Experimental setup for dead-end membrane separation of MB.(b) membrane before and after the adsorption

8.9 Photodegradation studies

The AOB membrane is in fact a mixed matrix membrane that contains both organic (polymer) and inorganic components. Prior to the photo-degradation studies, a better understanding of the affinity between the membrane components (both organic and inorganic) and the feed solution in which the membrane will be used was asserted.

Upon establishing membrane/feed compatibility, the decomposition of MB, other model component for can be used for experimentally studied. The combined effect of light and effect of AC is clearly visible in Fig. 8.20. In the case of AC membranes, for two different runs reaction activity pattern was observed: After switching on the solar simulator, there was minor photodesorption of the MB (reflected by the permeate concentration spike, in the first 40 min) which was followed by a pronounced decrease of the permeate concentration in MB (resulting in more than 30% degradation). After almost 2 h of feed circulation under solar light, the MB concentration in permeate reached a steady state. On the other hand, for the PMR loaded with virgine membranes, the permeate concentration remained almost stable, confirming that the membrane with acive carbon (AC) was the determining factor for MB degradation. The degradation studies for MB feed solution was continuously recirculated through the membrane upper shell side for two periods: the dark and the light phase. Permeate concentration was monitored and measured at fixed time intervals. As shown, the same pattern as in the case of MB was observed. When the solar light was switched on, there was an almost immediate increase of permeate concentration in the permeation (during the first photodesorption period of 40 min) followed by an almost linear decline for 230 min. More than 80% MB was degraded by the end of this period..

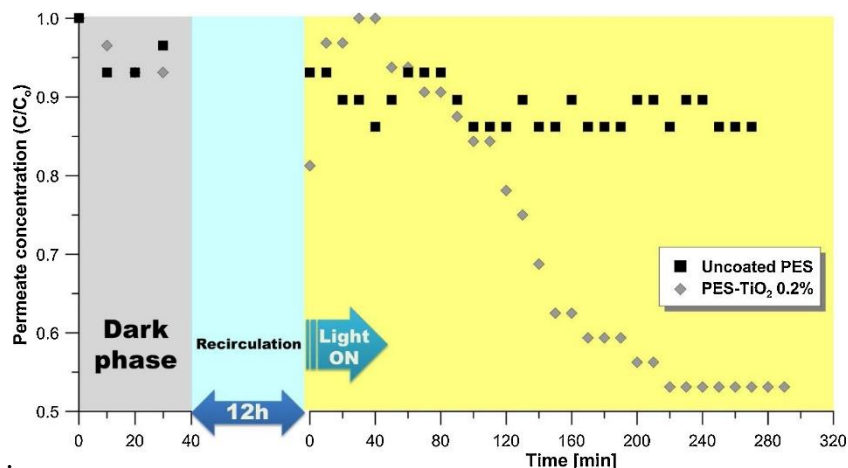


Fig 8.20. of MB concentration collected under the effect of simulated solar light

for a

The samples from the module runs with AC membranes were analyzed to probe the oxidative degradation of MB due to the photocatalytic effect in the membrane module. The first sample was extracted from the feed (pure MB aqueous solution) and the second sample was a permeate sample collected 140 min after switching on the solar simulator. The comparison of chromatograms obtained for both samples (not shown here) showed clear and distinct peaks for the permeate sample, which were attributed to degradation byproducts of MB in the permeate. Standard error of 6% has been observed in the degradation study with MB which indicate the stability of the coated films on the membrane surface. Though HPLC analysis confirmed the degradation of MB, a thorough identification of the particular byproducts was out of the scope of this work and thus investigation of the toxicological parameters of the degraded products is proposed as a future extension of this research.

8.10 Kinetics Study

The tests were carried out at room temperature, after the addition of the geopolymer a rise in the pH to 9.3 was noted. The adsorbent ratio is a very important parameter in the determination of the adsorption capacity, the optimization of the amount of adsorbent to be added plays a vital role in the MB adsorption process.

The quantity of granular solid was changed while maintaining the initial concentration of dye constant, in particular 15mg and 30mg of powdered geopolymer were used. The results obtained show how the percentage of dye removal increases with the increase in the amount of added adsorbent solid.

Figures 8.20 show, by way of example, the trend of removal efficiency during the immersion time in the solid 15mg, 30mg. It can be seen that as time increases, the solution tends to become clearer, demonstrating that the concentration of MB in solution decreases with time.

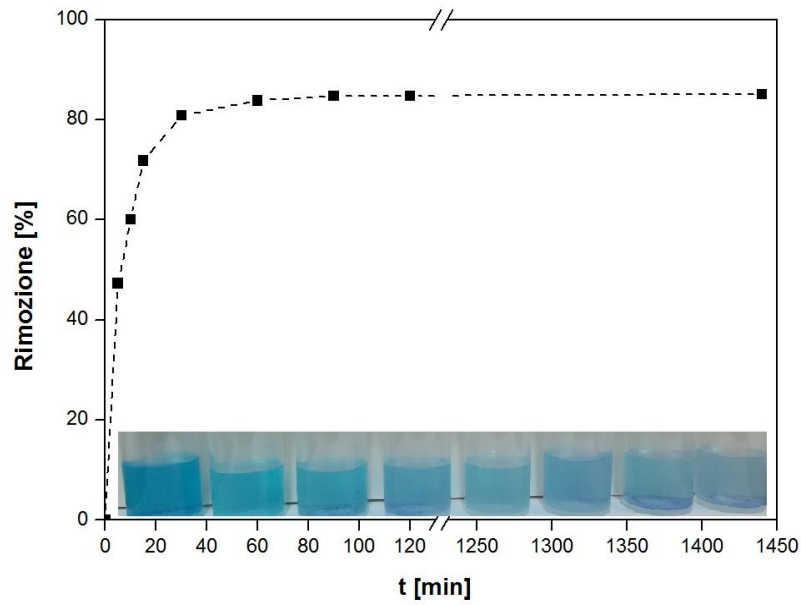


Figure 8.20 a - removal of the dye over time, 15mg solid

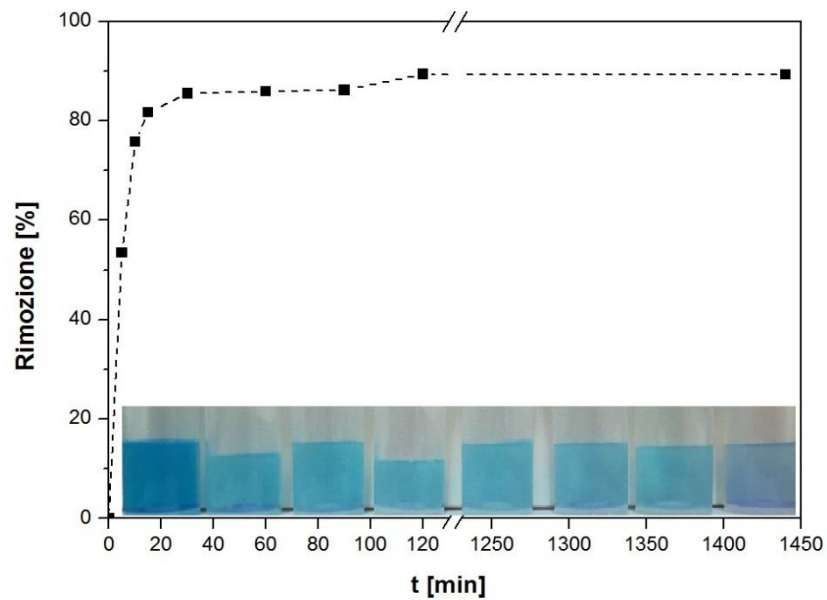
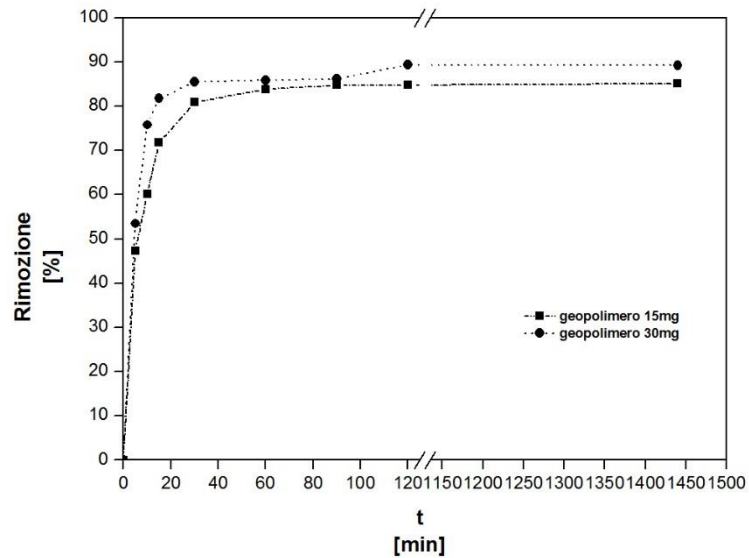


Figure 8.20 b removal of the dye over time, 30mg solid

Figure 8.20 c shows the trends of removal of samples containing 15 mg and 30 mg of geopolymer, after 120 minutes the stationary is reached. It should be noted that the doubling of the solid does not

greatly affect the removal of colorant index which already at 15 mg reaches the maximum level of



adsorption .

Figure 8.20 c-comparison removal when the added solid is changed

The impact of the initial concentration on the MB adsorption from an aqueous phase was studied at different time intervals in the range from 0 to 1440 min (24h). The result is shown in Fig.8.20 d. It can be seen that the removal due to adsorption decreases with decreasing concentration, in fact at 25 mg / L, the maximum adsorbed concentration is reached, which decreases for a concentration equal to 200 mg / L.

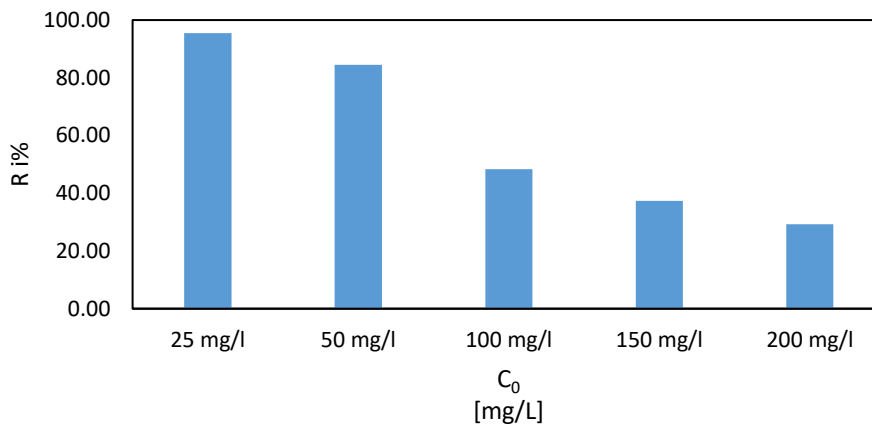
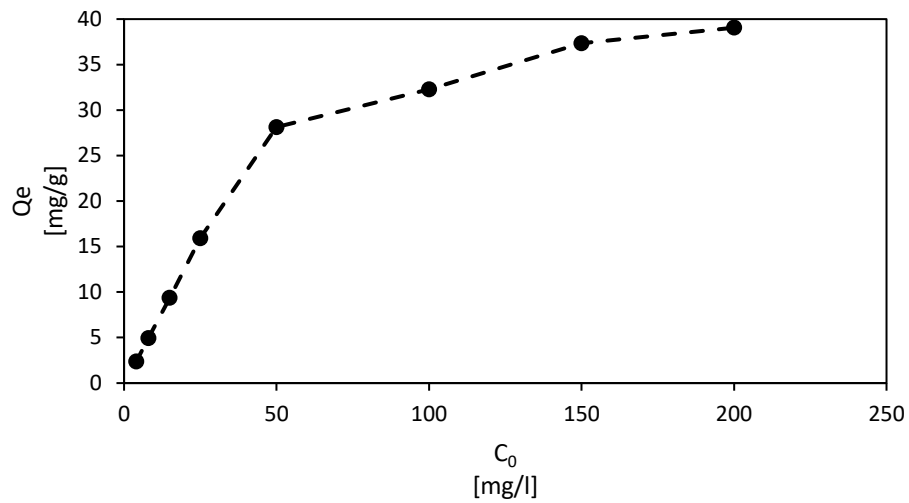


Figure 8.20d - Effect of the initial concentration on the percentage of colorant removed

The effect of the initial variation in the concentration of MB on the adsorption capacity of MB, Q_e , is shown in Fig.8.20 e. The results obtained for the adsorption capacity at equilibrium increase from 2.4 mg / g to 15.9 mg / g, with an increase in the initial concentration of dye from 4 to 200mg / L. After

maximum absorption, there are no free sites in the adsorbent , totally occupied by the dye molecules



(MB)

Figure 8.20 e - Effect of initial concentration on adsorption capacity

The data of the adsorption kinetics of MB using 15 mg of geopolymers as adsorbent were analyzed with kinetic models of pseudo-first order and of pseudo-second order. The following are examples of the graphs of interpolations, with the relative straight line used to derive the parameters K_n , where n is 1 or 2 based on the first or second order kinetics, and $Q_{modello}$, using the two kinetic models. Below are the graphs for the concentration at 25 mg / l.

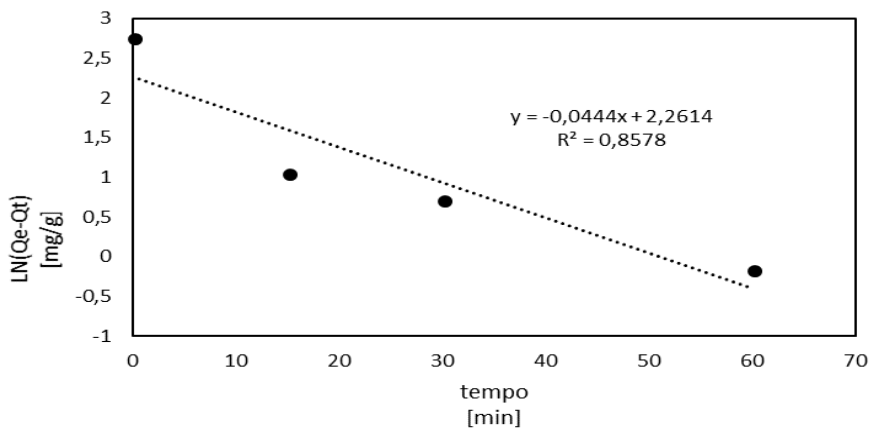


Figure 8.20 f-Pseudo first-order model $C_0 = 25\text{mg} / \text{l}$

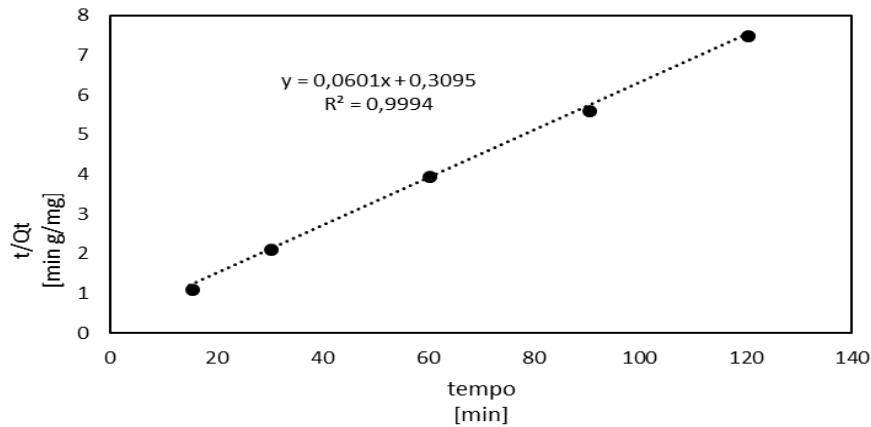


Figura 8.20 f-Pseudo secondo order model $C_0 = 25\text{mg/l}$

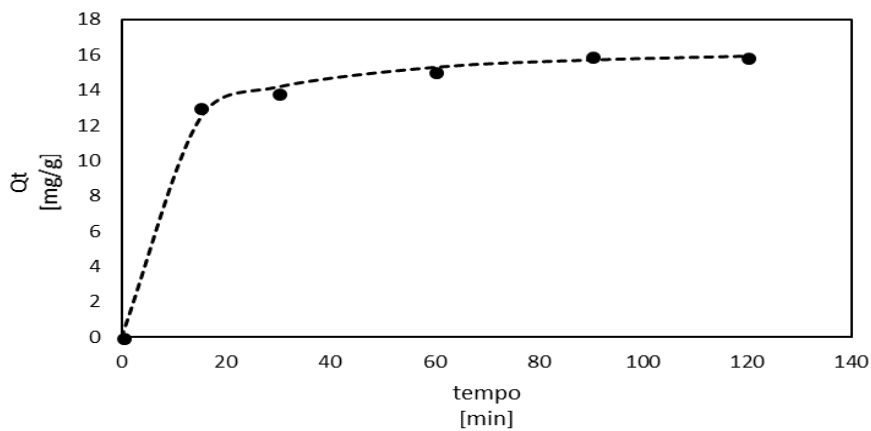


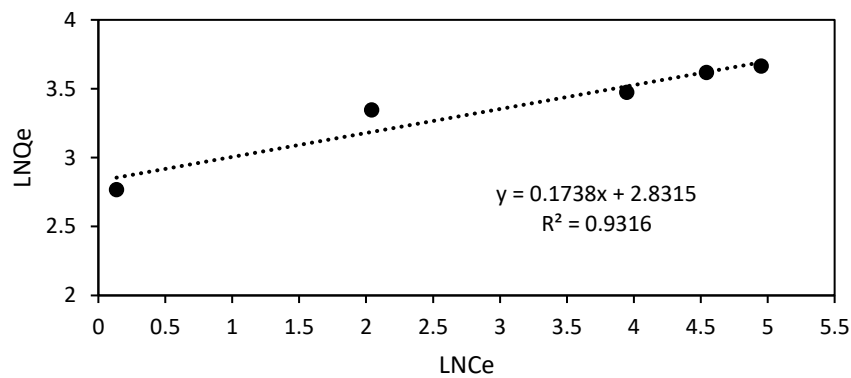
Figure 8.20 g Pseudo second order model (---), experimental data (●). $C_0 = 25\text{mg}$

As shown in the tables and graphs, the kinetics that best approximate the data is pseudo second order. In tab 8.6, in summary, the results of the simulations carried out with the two kinetic models are reported.

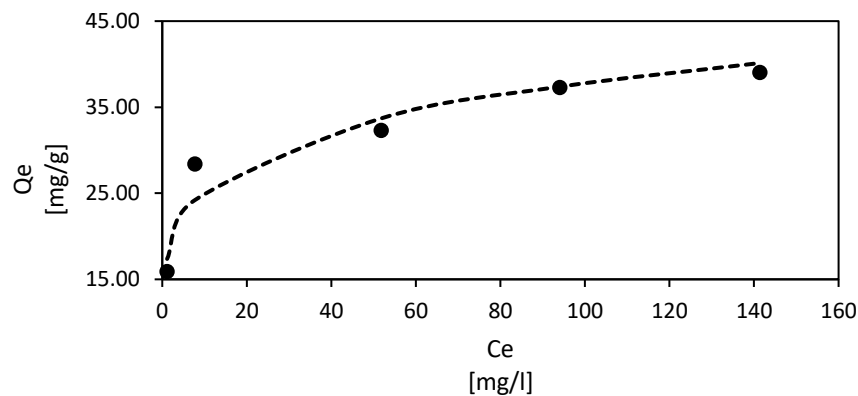
C_0 [mg/l]	Q_{exp} [mg/g]	Pseudo primo ordine			Pseudo secondo ordine		
		Q_{mod} [mg/g]	K_1 [1/min]	R^2	Q_{mod} [mg/g]	K_2 [g/mg min]	R^2
6	3.475	2.56	0.0805	0.9796	3.62	$6.8 \cdot 10^{-2}$	0.9996
8	4.93	3.38	0.0749	0.9712	5.23	$3.3 \cdot 10^{-2}$	0.997
10	6.33	4.13	0.0586	0.9523	6.56	$3.97 \cdot 10^{-2}$	0.9997
15	9.375	5.50	0.0455	0.9314	9.77	$2.06 \cdot 10^{-2}$	0.9997
25	15.2	9.59	0.0444	0.8578	15.95	$1.17 \cdot 10^{-2}$	0.9994
50	28.11	21.423	0.0032	92.32	30.33	$2.71 \cdot 10^{-4}$	0.9957
100	32.27	35.86	0.0046	99.6	39.64	$2.78 \cdot 10^{-5}$	0.9756
150	37.33	34.93	0.0023	98.933	46.08	$6.12 \cdot 10^{-5}$	0.9923
200	39.05	31.41	0.0017	85.33	45.04	$7.91 \cdot 10^{-5}$	0.9727

Adsorption isotherms were used to describe the mechanism of MB interaction on the adsorbent surface. In particular, two models, Langmuir and Freundlich, have been adapted to the experimental data, isothermal parameters and the values of the correlation coefficients (R²) are summarized in Table 8.6. The results show how the R² value obtained from the isotherm equation of Langmuir (0.9951) is greater than Freundlich (0.9316). From this it can be seen that the adsorption of the MB, with the geopolymer, can be adequately described with the Langmuir model and therefore consists of surface adsorption and homogeneous monolayer.

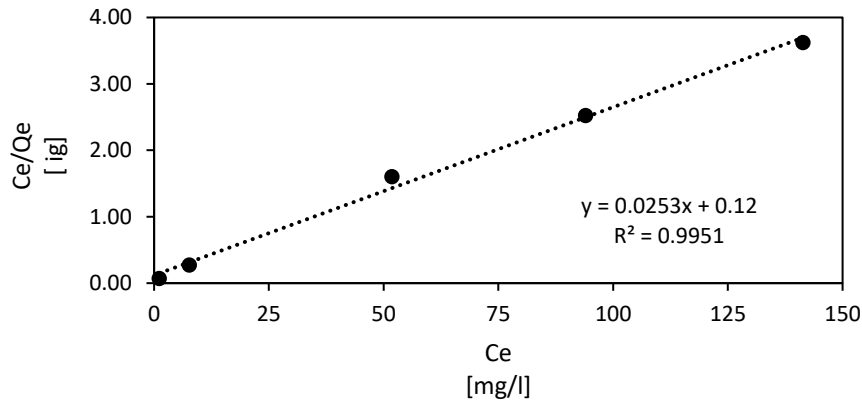
The maximum absorption capacity for the removal of MB, Q_m is equal to 39.52 mg / g, while the separation factor RL is in the range of 0.02 and 0.54, demonstrating that the absorption of MB with geopolymer is favorable. .



8.20 h- Linierization Freundlich model



8.20 i- Linierization Freundlich model (---), experimental data (●)



8.20 j- Linierization of Langmuir model

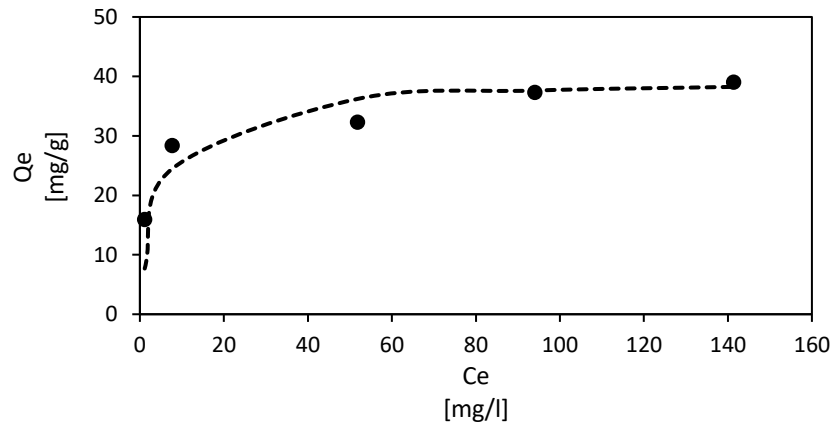


Figure 8.20k Linierization of Langmuir model(---), Exerimental data (●)

Adsorption isotherms were used to describe the mechanism of MB interaction on the adsorbent surface. In particular, two models, Langmuir and Freundlich, have been adapted to the experimental data, isothermal parameters and the values of the correlation coefficients (R2) are summarized in Table 8.6. The results show how the R2 value obtained from the isotherm equation of Langmuir (0.9951) is greater than Freundlich (0.9316). From this it can be seen that the adsorption of the MB, with the geopolymer, can be adequately described with the Langmuir model and therefore consists of surface adsorption and homogeneous monolayer.

The maximum absorption capacity for the removal of MB, Q_m is equal to 39.52 mg / g, while the separation factor RL is in the range of 0.02 and 0.54, demonstrating that the absorption of MB with geopolymer is favorable. .

Phase III

8.11 Membrane synthesis and characterization

The obtained membranes are very interesting since ultrafiltration active layers have been directly deposited on the zeolite support without the need of an intermediate MF layer, as it has been usually

considered. Synthesis without the intermediate MF layer could minimize the resistance against the mass transfer and thus improves the membrane filtration performance.

8.11.1 Morphology and pore size distribution

SEM images of the surface and the cross-section for the different zeolite ultrafiltration membranes sintered at 880°C for 3h are shown in Fig. 8.21 and Fig. 8.22. Fig. (8.21-a), Fig. (8.21-b) and Fig. (8.21-c) illustrate the surface morphology of ultrafiltration membranes DZ/Z, MZ/Z and Z42/Z, respectively. It is clearly observed that all samples have homogeneous and smooth surface with the absence of any macro-defects. The cross-section micrographs shown in Figs. (8.22-a,b,c), for DZ/Z, MZ/Z and Z42/Z, respectively, prove an excellent adhesion between the ultrafiltration layer and the support, confirming the efficacy of the slip casting technique for the synthesis of the membranes. For DZ/Z membrane, it was noticed that the used slip casting method allows an easy and sufficient flow of the suspension inside the membrane support without deep infiltration. After 7 minutes, an ultrafiltration layer of about 11.1 μm for DZ/Z membrane was obtained (see Fig. 8.22-a). Whereas, for the other membranes, MZ/Z and Z42/Z, there was a slight infiltration of the suspension into the pores of the membrane support, thereby causing the formation of an ultrafiltration layer with thickness of 2.4 μm and 10 μm for MZ/Z and Z42/Z, respectively (see Fig. 8.22-b for MZ/Z and Fig. 8.22-c for Z42/Z).

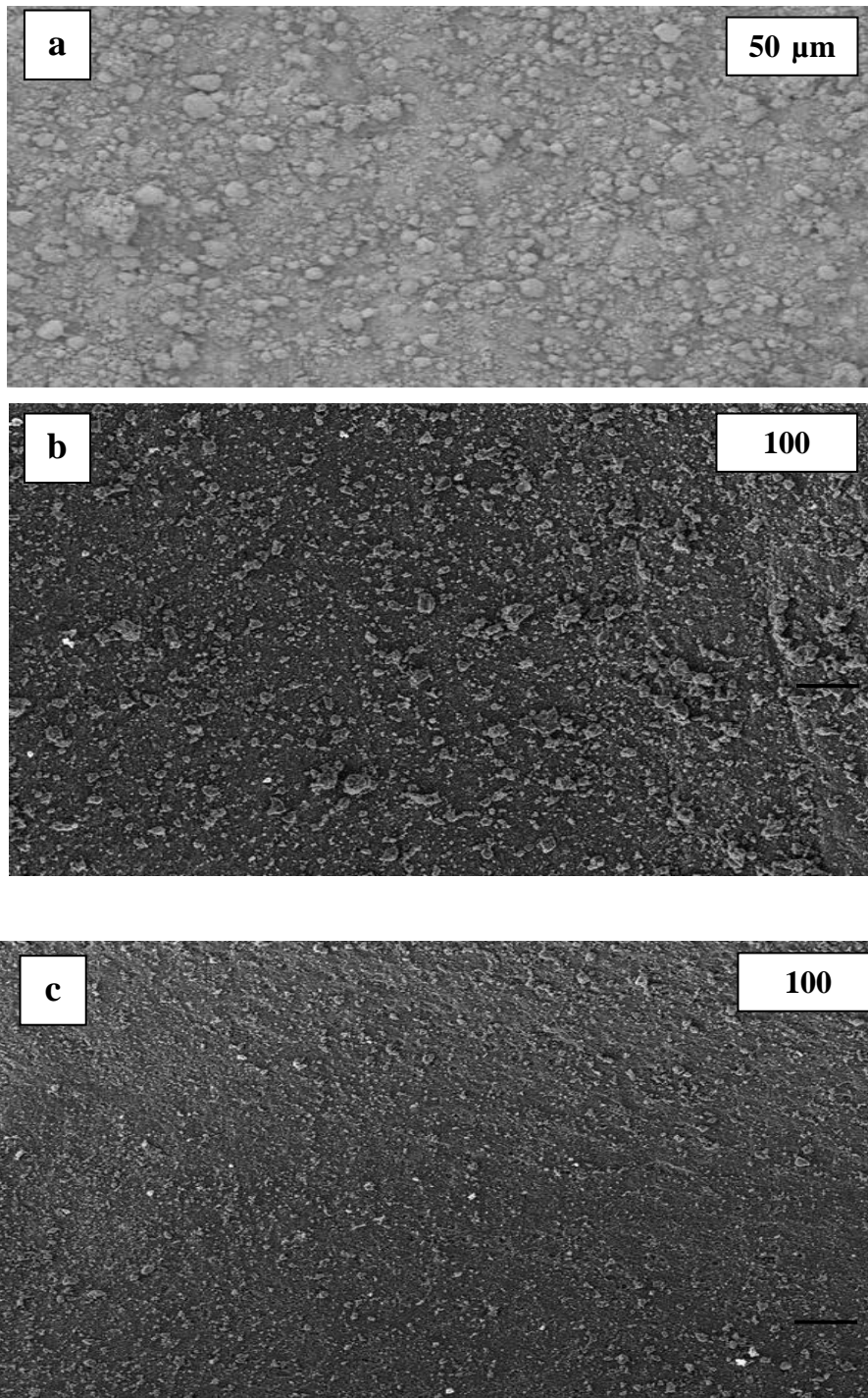


Figure 8.21 (a,b,c) SEM micrographs of zeolite ultrafiltration membranes surface: DZ/Z (a), MZ/Z (b) and ZA2/Z (c).

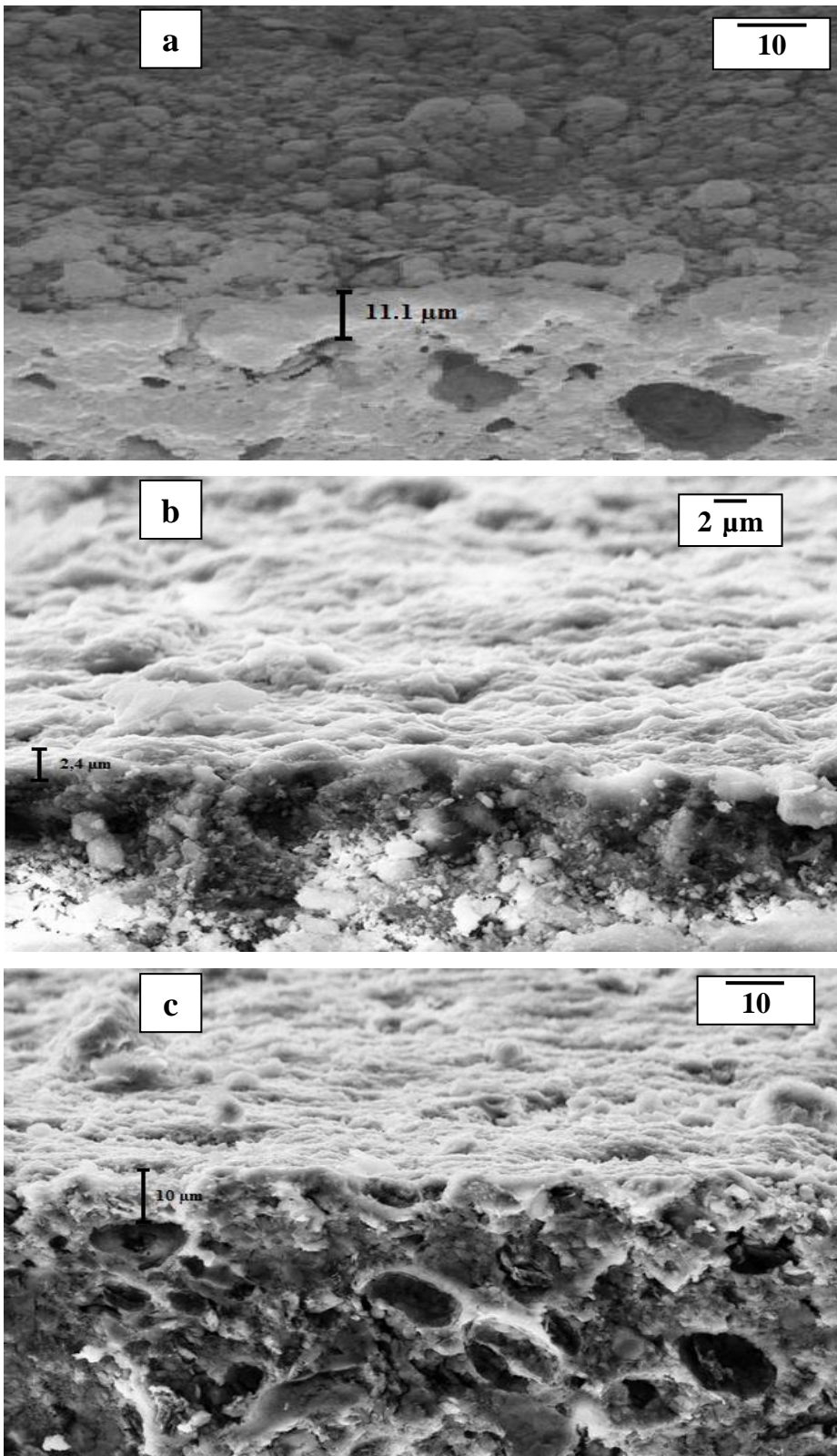


Figure 8.22: SEM micrographs of zeolite ultrafiltration membranes cross-section: DZ/Z (a), MZ/Z (b) and ZA2/Z (c).

The determination of UF pores size was done using adsorption/desorption isotherm of N_2 at 77 K (Figs. (8.23-a,b,c)). Results prove that all the elaborated UF membranes exhibit a type IV adsorption isotherm according to IUPAC, which is associated with mesoporous structure.

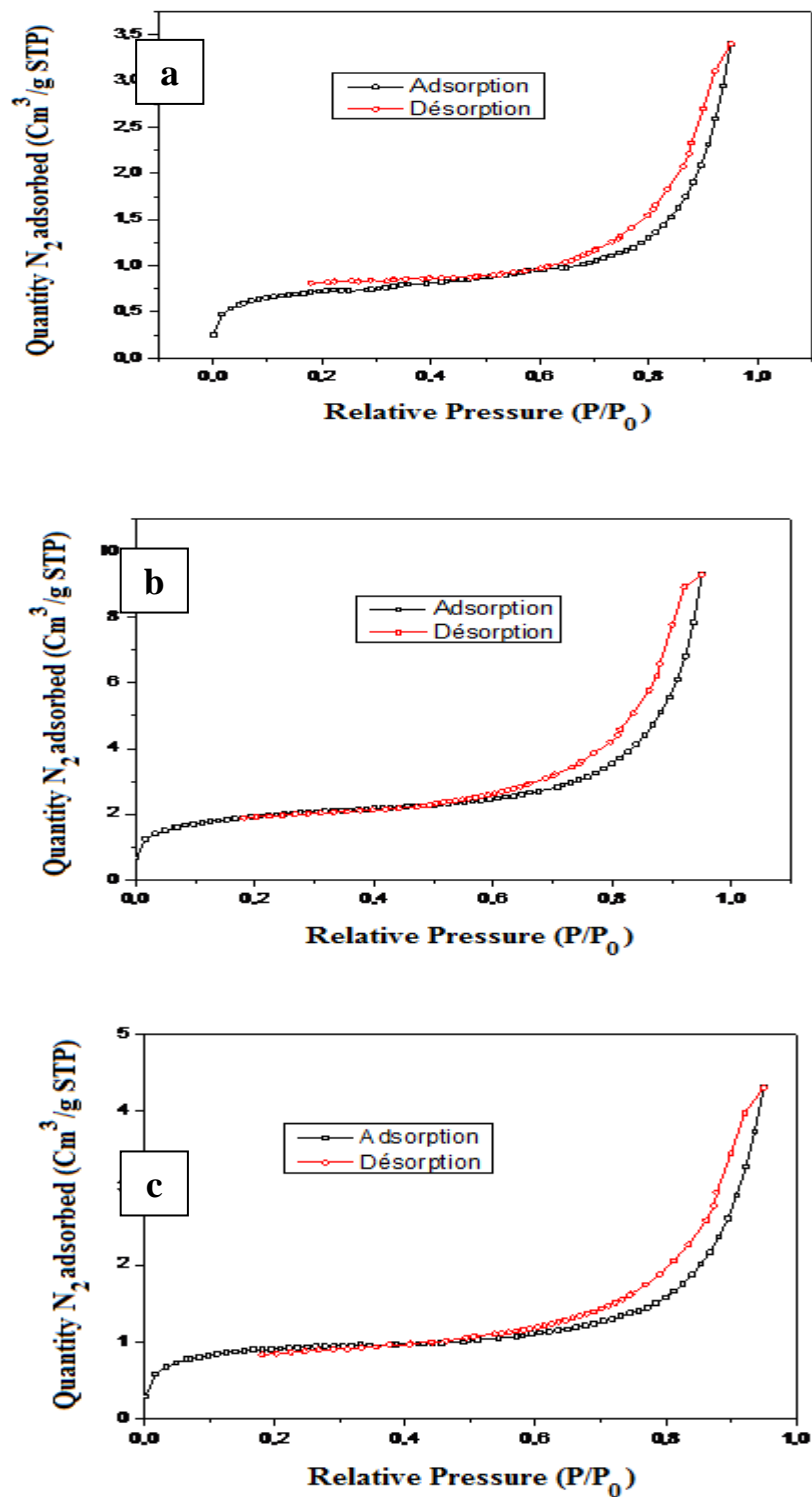


Figure 8.23 Nitrogen adsorption-desorption isotherm of zeolite ultrafiltration membranes: (a), MZ/Z (b) and Z42/Z (c).

Fig.8.24 shows the pore size distribution of the top layer of the three zeolite ultrafiltration membranes sintered at 880°C for 3h. The mean pore diameters for DZ/Z, MZ/Z and Z42/Z were 10.5 nm, 11nm and 8 nm, respectively. These values further strengthen the earlier speculation that the synthesized membranes are ultrafiltration membranes. In addition, all the curves relative to the three samples reveal the presence of an intense peak located between 15 and 16 nm. By comparing the pore size distribution of the zeolite support alone in the same conditions, these large and intense peaks correspond to the pore diameters of the upper layer relative to the membrane support which has absorbed the slip.

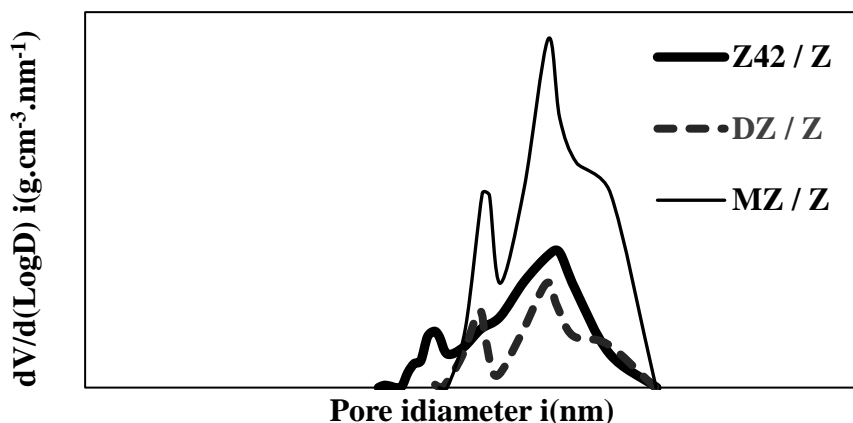


Fig 8.24 Nitrogen adsorption-desorption pore size distribution of DZ/Z, MZ/Z and Z42/Z sintered at 880°C / 3 h

8.11.2 Permeability tests

Results of the permeability tests of these membranes conducted using distilled water are depicted in Fig. 8.25. For all zeolite membranes, the water flux increased linearly with increasing feed pressure, obeying Darcy's law. The average water flux obtained for DZ/Z, MZ/Z and Z42/Z was 176, 125 and 118 L/h.m².bar, respectively.

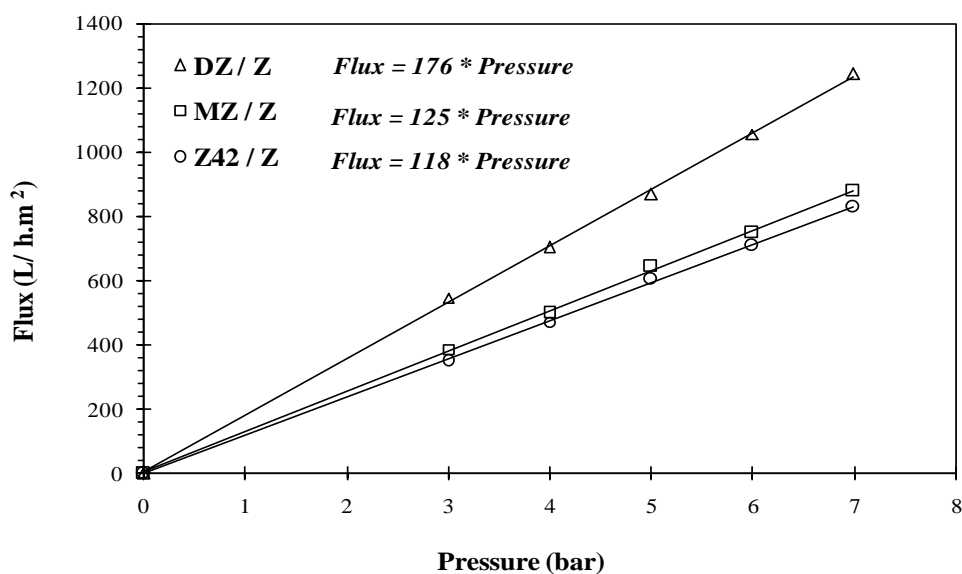


Figure 8.25 Permeability of ultrafiltration membranes.

8.11.3 Characterization of wastewater

The synthesized and characterized membranes were employed in the treatment of two wastewater sources namely: Cuttlefish effluent collected from a sea product-freezing factory located in Sfax (Tunisia) (EF1) and heavy metal-contaminated effluents from electroplating industry (SOPAL) located in Sfax, Tunisia (EF2). Results of the characterization of EF1 and EF2 are presented in Table 8.7.

Table 8.7: Main composition of the raw wastewater effluents.

Sample	pH	Conductivity (mS/cm)	Turbidity (NTU)	COD (mg/L)	Fe ³⁺ (mg/L)	Cl ⁻ (mg/L)
EF1	7.05	1.15	188	1350	-	-
EF2	2.90	3.34	-	1048	6.23	828

8.11.4 Ultrafiltration treatment

The filtration tests on the prepared zeolite membranes, DZ/Z, MZ/Z and Z42/Z, were conducted at room temperature and at transmembrane pressure ranged from 3 to 5 bar. The permeate flux as a function of time for the membranes is shown in Fig. 8.26. The results reveal that the permeate flux decreased slightly with time to obtain a stable value after 30 min of filtration. For EF1, the membrane flux increased from 103 to 115 L/h.m² for the DZ/Z; from 81 to 89 L/h.m² for MZ/Z; and from 74 to 85 L/h.m² for Z42/Z when the pressure increased from 3 to 5 bar. A similar behaviour was observed for the treatment of EF2 with flux increased from 460 to 663 L/h.m² for DZ/Z; from 251 to 420 L/h.m² for MZ/Z; and 204 to 398 L/h.m² for Z42/Z. The decrease of permeate flux with time is a typical behaviour of an ultrafiltration membrane, indicating presence of concentration polarization and fouling due to the interaction between membrane material and the feed solution.

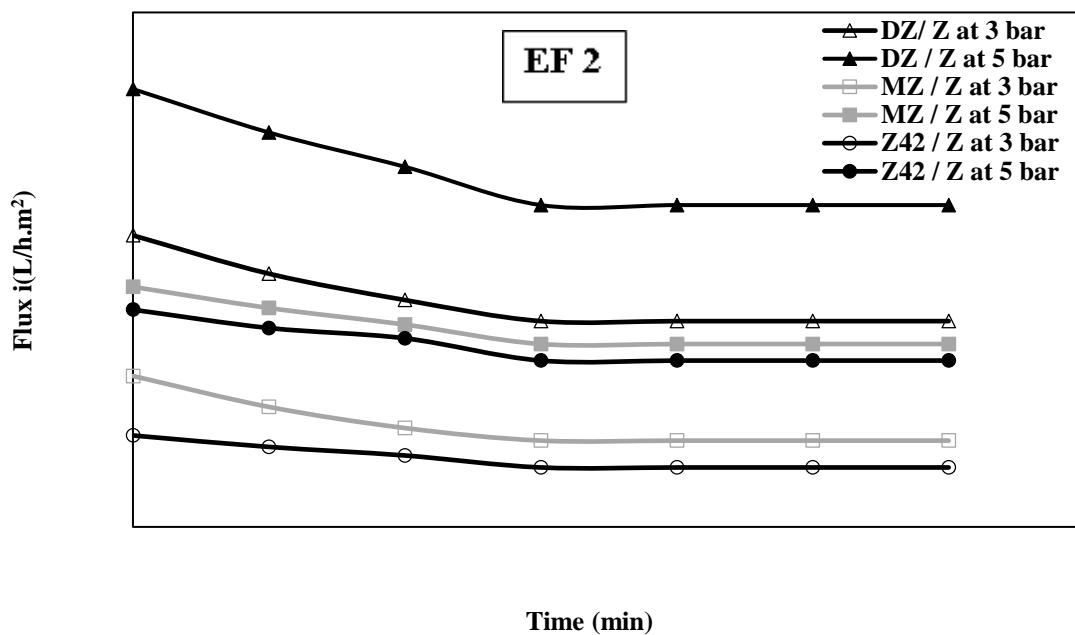
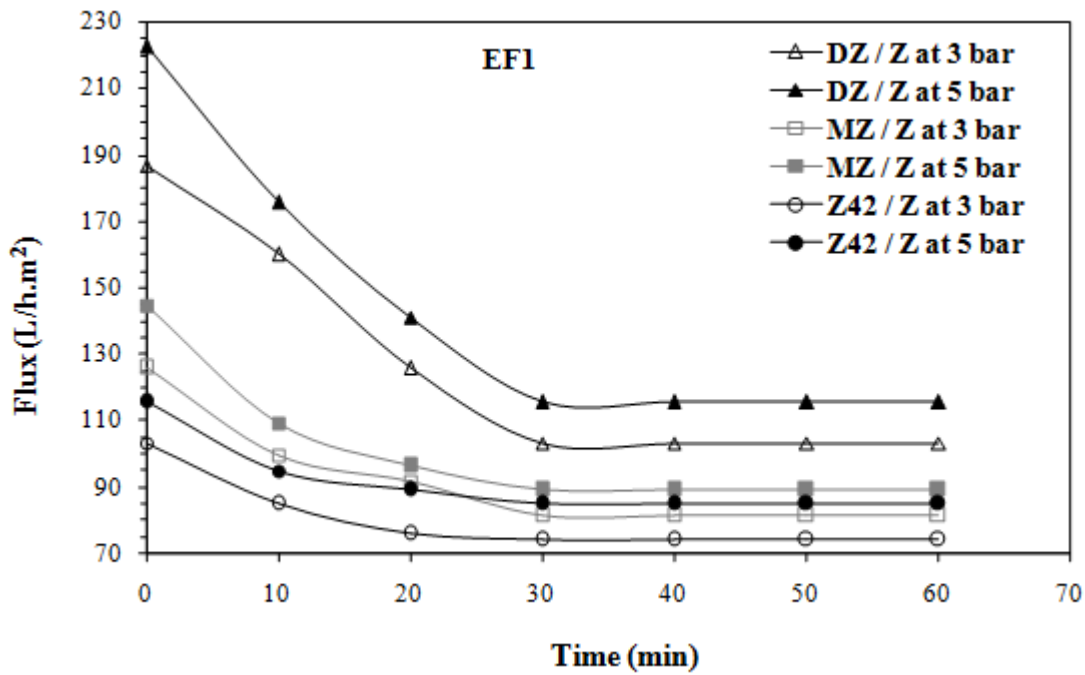


Figure 8.26 Permeate flux versus time at different TMP using different membranes: EF1 (a) and EF2 (b).

Zeta potential of modified (MZ) and unmodified (DZ and Z42) zeolite membranes was measured at pH range from 2 to 10 (Fig. 8.26) in order to explain the interaction with the effluent. The obtained values were -17 mV and + 37 mV for unmodified and modified membrane, respectively, at pH≈2 for EF2. Since the membrane with modified zeolite MZ/Z is positively charged, Fe³⁺ ions are repelled resulting to rejection rate of 90%. Subsequently Cl⁻ ions, present in the EF2, are also rejected (57%) to maintain the electroneutrality because cations and anions cannot act separately. In addition, it is noticed that the membranes with unmodified zeolite display lower rejection rate of Fe³⁺ and Cl⁻ than the rejection rate

displayed by MZ/Z. Furthermore, the negative charge on the surface of Z42/Z and DZ/Z membranes increases the intensity of the electrostatic repulsion between the Cl⁻ ions in the effluent and the membrane surface, resulting in the rejection of species. On the other hand, the pore size of the membrane also affects the rejection behaviour of the salts. The membrane Z42/Z has a lower average pore diameter (8 nm) than the membrane DZ/Z (10.5 nm), resulting in a higher rejection of Fe³⁺ and Cl⁻ (67% and 42% against 58% and 36% for Z42/Z and DZ/Z, respectively). These results confirm the efficiency of the synthesized membrane MZ/Z to separate trivalent ions from industrial effluents.

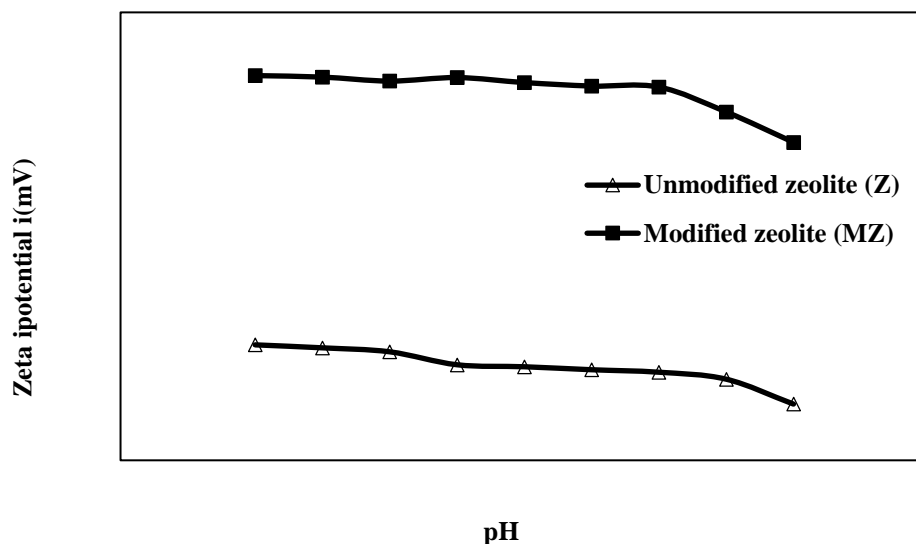


Figure 8.27 Zeta potential measurement of unmodified and modified zeolite powder.

In this study, new low cost UF membranes have been fabricated using Turkish natural zeolite powder via direct deposition of the active ultrafiltration layers on microporous zeolite supports by slip-casting method. The fabricated membranes (DZ/Z, MZ/Z and Z42/Z), which were sintered at low sintering temperature (880°C / 3 h), exhibited good adhesion between the support and the filtration layer with membrane thickness ranged from 2.4 μm to 11.1 μm. The performance of these membranes during the treatment of industrial wastewater was evaluated as well. The best performance was achieved at a TMP of 3 bar with relatively high permeate flux values and excellent quality of the treated water suitable for reuse or recycling. Especially, the MZ/Z membrane displayed a higher rejection for Fe³⁺ in comparison to the other prepared membranes. Our results suggest that the membrane fabricated with modified zeolite (MZ/Z) could be a promising candidate for the separation of trivalent metal ions from industrial effluents based on the interaction between the charged membrane and trivalent metal ions. Furthermore, comparison of our results with literature indicates that the fabricated membranes in this study out-perform those reported in literature.

Part II
CONCLUDING REMARKS AND FUTURE
DIRECTIONS

CHAPTER 9:

Concluding Remarks and future direction

The interrelationship between water and energy is intensifying significantly as a result of their ecological, regional and economic implications. The major challenges in this century for developing sustainable desalination technologies are: reducing energy consumption, lowering the environmental effect; and minimizing water production costs. Membrane and membrane-based technologies have been applied widely in various water purification and waste treatment applications, either individually or in combination with other processes. Currently, membrane processes such as RO, FO, UF, NF, MD are being used in seawater desalination, and waste water treatment applications. The effective utilization of membrane technologies as a sustainable solution for different applications requires novel membrane materials along with customized separation characteristics. Through this thesis improvement in the water treatment sector has been observed in terms of high permeation rate and salt rejection, membranes with controlled and distinct pores, tailored functionalities and defined passage channels for specific constituents could further lead to enhanced separation, purification and recovery of important products from various resources. Recent developments in polymeric materials and the emergence of nanomaterials have paved the way for more membrane-based processes for various applications with potential industrial use. However, the fabrication of new membrane materials with improved chemical and thermal stability for the treatment of industrial effluents needs to be explored in future. Depending on the requirements of specific applications, water quality could be monitored and alternative water treatments should be implemented, which remains an open challenge. Despite its advantages, huge effort is still required to mitigate some of the key concerns such as fouling, selectivity, polarization in case of membrane desalination process, and higher recovery with respect to the amount of feed treated. Membrane processes play a major role in both water purification and sustainable energy generation either individually or in combination with other membrane-based techniques, or by utilization of low-cost heat sources to make the process economic and viable for industrial applications. Membranes have started to play an important role in energy sectors, ranging from biofuel production to fuel cell application. Their performance in these sectors also depends on the quality and availability of the membrane components, hence it is important to achieve the synthesis of highly chemical, thermal and oxidative resistant materials. In summary, membrane-based approaches open up avenues for the development of a sustainable environment with respect to water treatment and energy generation, with ongoing challenges

for material scientists and membrane technologists to develop new, robust materials and economic hybrid processes.

This study consisted of the development and testing of new low cost membrane for water purification with the final aim to assess them for degradation of organic compounds commonly found in industrial wastewater. Functionalization of the membranes to impart utilization of renewable energy has been explored successfully:

Although a proof of concept was demonstrated, this needs further development. It is important to further optimize the fabrication protocol to minimize the impact on membrane permeability (e.g., by controlling the pore size distribution by adding active carbon or nanoparticles). It is also important to test the long term stability of the prepared ceramic membrane under various conditions (pH, interferences of other particles, solar radiation exposure etc.). Maximum degradation of pollutants and their separation in a single stage also need to be ensured. Developing a large-scale system design where a large number of surface area are adequately exposed to solar radiation and the testing of such system using real complex wastewater streams are also essential. These areas are all subjects of further development and future studies.

APPENDIX

Other Publications

Improving Cellulose Structure for Bioconversion: Sugarcane Bagasse Pretreatment Accompanied by Lignin Recovery and Ionic Liquid Recycle

Koel Saha, Jaya Sikder, Paulomi Diwedi, Ankita Ghosh, Sudip Chakraborty, Debolina Mukherjee, Stefano Curcio, and Vincenza Calabro

Keywords

Sugarcane bagasse • Pretreatment • Ionic liquid recycle • Lignin recovery • Enzymatic hydrolysis

1 Introduction

Bioethanol, derived from biomass has established itself as one of the leading biofuels in the global market (Sarkar et al. 2012). Lignocellulosic biomass has proved to be one of the most abundant and cost effective renewable resource which is non-polluting agricultural residue and potential to be converted into biofuel. The main components of lignocelluloses are lignin, and cross linked polysaccharides i.e. cellulose and hemicellulose. Cellulosic component which occurs in the highest percentage is used to synthesize biofuels such as ethanol. One of the most available lignocelluloses in tropical countries like India and Brazil is sugarcane bagasse as sugarcane is the most cultivated crops in these countries. Southern mediterranean countries mostly in Northern Africa are the center of origin and also a major producer of several cereals like sorghum, pearl millet, finger millet, rice etc. which contain lot of cellulosic materials as well. Hence, this part of the region has the potentiality for agriculture practiced by small farmers with higher yield but poor soils, amongst other constraints adding to the difficulties for sustainable farming and incomes. But conversion of lignocelluloses waste or agro industrial waste can add some value if new materials can also be produced from the waste (FAOSTAT 2014). Current study explored [EMIM]oAc

aided pretreatment of sugarcane bagasse to recover lignin and observe structural modification of bagasse and subsequently enzymatic hydrolysis of pretreated biomass. [EMIM]oAc was chosen as a solvent for bagasse pretreatment as the chemical structure of lignin is not altered during this [EMIM]oAc mediated pretreatment. Raw and pretreated bagasses were characterized by X-ray diffraction and Scanning electron microscopy to observe the effect of ionic liquid on bagasse. The lignin so regenerated is further characterized using Nuclear magnetic resonance analysis. [EMIM]oAc was recycled to check the reusability.

2 Materials and Methods

Sugarcane bagasse (SCB) was supplied by local juice mill of Durgapur, West Bengal, India. SCB was cleaned with water, sieved to a size of 1–3 cm, dried, grinded and screened to a size of 250–500 μm and stored in a sealed container at room temperature. Chemical composition of SCB was determined as: 30% cellulose, 24% hemicelluloses and 22.4% lignin as per the analytical procedure adopted from National Renewable Energy Laboratory (NREL) (Sluiter et al. 2012). Bagasse was pretreated at 140 °C, 120 min and 1:20 ionic liquid to bagasse ratio. Surface morphology of untreated and pretreated sugarcane bagasse was investigated by Scanning Electron Microscope (JEOL JSM-6360, JAPAN) and crystallinity was detected by X-ray diffractometer (X'pert PRO, PANalytical B.V., P.W 3040/60, Netherland). To assess the impact of pretreatment on enzymatic hydrolysis of bagasse, both untreated and pretreated bagasse was subjected to saccharification using commercial cellulase from *Trichoderma reesei*

K. Saha · J. Sikder · P. Diwedi · A. Ghosh
Department of Chemical Engineering, National Institute of Technology, Durgapur, West Bengal 713209, India

S. Chakraborty (✉) · D. Mukherjee · S. Curcio · V. Calabro
Department of Informatics, Modeling, Electronics and Systems Engineering (DIMES), University of Calabria, Via P. Bucci, Cubo—42a, 87036 Rende, CS, Italy
e-mail: sudip.chakraborty@unical.it; zsudip.c@gmail.com

(ATCC 26921) (Sigma Aldrich (USA). Both 1D (^{13}C and ^1H) and 2D (Heteronuclear single-quantum correlation (HSQC)) NMR spectra of lignin were obtained by Bruker ADVANCE 600 spectrometer (Bruker, Germany).

3 Results and Discussion

SEM analysis of raw sugarcane bagasse showed lamellar and smooth surface where cellulose is linked to lignin and hemicellulose. Ionic liquid aided pretreatment disrupted the cellular bond, cracked the surface layer and removed outer amorphous lignin and hemicellulose through depolymerization, thus formed conglomerate and irregular texture. The strong crystalline structure of cellulose as revealed by XRD analysis is formed due to the presence of van der Waals force and intermolecular hydrogen bonding between along-side cellulose molecule (Chirayil et al. 2014). In this study a less crystalline structure and larger amorphous region of pretreated sample was established from XRD pattern as it exhibits substantial reduction in peaks intensity as compared to untreated sample. The reason behind this phenomenon is the partial solubilization and distension of cellulose crystal with [EMIM]oAc due to complexity in cell wall component and structural diversity at moderate pretreatment temperature (Zhang et al. 2014). Crystallinity index (CrI) of untreated bagasse is 51.44 which decreased after pretreatment and the calculated value of CrI of pretreated bagasse is 36.74. Reduction of the CrI by 14.7% in pretreated biomass implies a rapid decline of crystalline structure and increase of amorphous region after pretreatment. After enzymatic hydrolysis, reducing sugar released from pretreated bagasse is much higher as compared to untreated bagasse. ^1H NMR spectrum of lignin shows the peak at 7.38 ppm which corresponds to *p*-coumaric and *p*-ferulic acid of lignin. The peak at 5.7 ppm signifies ether linkage (Cox and Ekerdt 2013). C NMR spectra detected peaks at 100–155 ppm, 60–86 ppm and 55–57 ppm which corresponds to the presence of aromatic carbon, aliphatic side chain and methoxy carbon respectively (Kim et al. 2011). No peak was observed in the region of 102–90 ppm. This signifies negligible presence of residual sugar in ionic liquid extracted lignin sample. Due to signal overlapping in C NMR, 2D HSQC NMR was performed to resolve resonance overlap and explore detailed structure. 2D NMR spectra can be divided in two regions. Side chain region: $\delta_{\text{C}}/\delta_{\text{H}}$ 50.0-90.0/2.50-6.00 and aromatic region: $\delta_{\text{C}}/\delta_{\text{H}}$ 100.0-135.0/5.50-8.50 (Moghaddam et al. 2014). Cross signals of side chain region correspond to details regarding inter unit linkage of lignin (Moghaddam et al. 2014) whereas aromatic region provides information

regarding guaiacyl (g), Syringyl (S) and *p*-hydroxyphenyl (H) unit and also substructures like spirodienone, *p*-hydroxycinnamyl alcohol and *p*-hydroxybenzoate substructure.

4 Conclusion

A preliminary study was executed on the impact of imidazolium ionic liquid pretreatment on sugarcane bagasse. Characterization of raw and pretreated bagasse revealed the physical and chemical changes in terms of lignin separation and lowering the crystallinity of cellulose. Further enzymatic saccharification corroborated an increase in reducing sugar yield after pretreatment process. The extracted low molecular weight lignin exhibited the presence of elemental functional group thus corroborated the recovery of lignin in almost pure form. Further investigation is necessary to study the fermentation of hydrolyzate to ethanol which determines overall efficiency of 1-ethyl-3-methylimidazolium acetate in processing of sugarcane bagasse to bioethanol.

Acknowledgements The authors acknowledge Department of Biotechnology, Government of India for the grant provided to carry out this research work under the bilateral collaboration between India and Brazil (DBT- India and MCTI-CNPq-Brazil) vide no. DBT/In-Bz/2013-16/06 and CNPq process no: 401361/2013-6.

References

- Chirayil CJ, Joy J, Mathew L, Mozetic M, Koetz J, Thomas S. Isolation and characterization of cellulose nanofibrils from *Helicteres isora* plant. *Ind Crop Prod.* 2014;59:27–34.
- Cox BJ, Ekerdt JG. Pretreatment of yellow pine in an acidic ionic liquid: extraction of hemicellulose and lignin to facilitate enzymatic digestion. *Bioresour Technol.* 2013;134:59–65.
- Kim J-Y, Shin E-J, Eom I-Y, Won K, Kim YH, Choi D, Choi I-G, Choi J-W. Structural features of lignin macromolecules extracted with ionic liquid from poplar wood. *Bioresour Technol.* 2011;102:9020–5.
- Moghaddam L, Zhang Z, Wellard RM, Bartley JP, O'Hara IM, Doherty WOS. Characterisation of lignins isolated from sugarcane bagasse pretreated with acidified ethylene glycol and ionic liquids. *Biomass Bioenerg.* 2014;70:498–512.
- FAOSTAT. <http://Faostat.fao.org>;2014.
- Sarkar N, Ghosh SK, Banarjee S, Aikat K. Bioethanol production from agricultural wastes: an overview. *Renew Energ.* 2012;19:19–27.
- Sluiter A, Hames B, Ruiz R, Scarlata C, Sluiter J, Templeton D, Crocker, D. Laboratory analytical procedure (LAP): determination of structural carbohydrates and lignin in biomass. Technical Report NREL/TP-510-42618. National Renewable Energy Laboratory, Golden, CO, USA; 2008, 2012. P. 18 (Revised in August 2012).
- Zhang J, Wang Y, Zhang L, Zhang R, Liu G, Cheng G. Understanding changes in cellulose crystalline structure of lignocellulosic biomass during ionic liquid pretreatment by XRD. *Bioresour Technol.* 2014;151:402–5.

Om V. Singh · Anuj K. Chandel *Editors*

Sustainable Biotechnology- Enzymatic Resources of Renewable Energy

 Springer

Chapter 5

Technological Aspects of Lignocellulose Conversion into Biofuels: Key Challenges and Practical Solutions



Catia Giovanna Lopresto, Alessandra Verardi, Cecilia Nicoletti, Debolina Mukherjee, Vincenza Calabro, Sudip Chakraborty and Stefano Curcio

Abstract Biofuels produced from crops have been the driving force in renewable energies since many years. In the first decade of the 21st century, there was a major focus on the debate of food versus fuel. Reports made by various national and international agencies, concluded that the food commodity prices were being impacted by consumption for the production of biofuels. Lignocellulosic biomass is an attractive renewable resource for future fuel. Efficiently and cost-effectively production of bioethanol from various lignocellulosic biomass, not only depends on the development of a suitable pretreatment system but also on other technological aspects with engineered feedstock. The aim of this chapter is to summarize and critically review on existing pretreatment method which is highly efficient due to engineering the feedstock as well as effectively using biocatalytic hydrolysis of various lignocellulosic biomass materials. The success behind this lignocellulosic bioethanol is depend on the modern technological development of pretreatment technologies as well as advanced conversion processes within the line of process intensification strategies.

keywords Lignocellulose · Biofuels · Fermentation · Heterogeneous catalysis Engineered biomass · Biorefinery

C. G. Lopresto · A. Verardi · C. Nicoletti · D. Mukherjee · V. Calabro · S. Chakraborty (✉)
S. Curcio
Department of Informatics, Modeling, Electronics and Systems Engineering (D.I.M.E.S.),
University of Calabria, 87036 Rende, Italy
e-mail: sudip.chakraborty@unical.it

© Springer International Publishing AG 2018
O. V. Singh and A. K. Chandel (eds.), *Sustainable Biotechnology- Enzymatic Resources of Renewable Energy*, https://doi.org/10.1007/978-3-319-95480-6_5

117

5.1 Lignocellulose Biomass Recalcitrance: Physico-Chemical Characteristics of the Plant Cell Wall

The lignocellulosic biomass is characterized by a natural resistance of the plant cell wall to microbial and enzymatic degradation, due to its rigid and compact structure, known as “biomass recalcitrance” (Himmel et al. 2007). This property is closely related to the chemical and physical features of the plant cell wall, which is a matrix of cross-linked polysaccharide networks, glycosylated proteins, and lignin. Several aspects contribute in building the lignocellulose’s recalcitrance, such as epidermal tissue and chemicals, chemical compositions, physical structure of the cell wall, cellulose structure, and pre-treatment-induced causes (Zhao et al. 2012). In particular, Himmel et al. have provided a list of the natural factors supposed to play a part in constructing the recalcitrance of lignocellulosic feedstocks to chemicals or enzymes, that includes: (i) the epidermal tissue of the plant body, particularly the cuticle and epicuticular waxes; (ii) the arrangement and density of the vascular bundles; (iii) the relative amount of sclerenchymatous (thick wall) tissue; (iv) the degree of lignification; (v) the structural heterogeneity and complexity of cell-wall constituents such as microfibrils and matrix polymers; (vi) the challenges for enzymes acting on an insoluble substrate; and (vii) the inhibitors to subsequent fermentations that exist naturally in cell walls or are generated during conversion processes (Himmel et al. 2007). These chemical and structural characteristics affect liquid penetration and/or enzymes accessibility and activity, resulting in increased conversion costs.

Lignocellulosic biomass is mainly composed of three polymers: cellulose, hemicellulose and lignin along with smaller amounts of pectin, protein, extractives and ash (Bajpai 2016), which do not participate significantly in forming the structure of the material (Harmsen et al. 2010).

Depending on the type of biomass, these polymers are organized in complex non-uniform three-dimensional structures to different degrees and varying relative compositions, as illustrated in Table 5.1, for various lignocellulosic feedstocks.

As can be seen from Table 5.1 cellulose is the major structural component of cell walls, and it provides mechanical strength and chemical stability to plants. Hemicellulose is a copolymer of different C5 and C6 sugars. Lignin is a polymer of aromatic compounds produced through a biosynthetic process that forms a protective layer for the plant walls (Harmsen et al. 2010). Their internal structures will be described in detail in the following paragraphs. From a structural point of view, the plant cell wall is a complex matrix typically composed of three types of layers, namely the middle lamella, the primary and the secondary wall (Fig. 5.1), that provide support and strength essential for plant cell survival. The main functions of the cell wall include the conferral of resistance, rigidity and protection to the cell against different biotic or abiotic stresses, but still allowing nutrients, gases and various intercellular signals to reach the plasma membrane (Ochoa-Villarreal et al. 2012).

Primary and secondary cell walls are microfibril-based nanocomposites that differ in the arrangement, mobility and structure of matrix polymers, the higher-order organization of microfibrils into bundles and discrete lamellae, their rheological and

Table 5.1 Composition of representative lignocellulosic feedstocks (Menon and Rao 2012)

Feedstocks	Carbohydrate composition (% dry wt)		
	Cellulose	Hemicellulose	Lignin
Barley hull	34	36	19
Barley straw	36–43	24–33	6.3–9.8
Bamboo	49–50	18–20	23
Banana waste	13	15	14
Corn cob	32.3–45.6	39.8	6.7–13.9
Corn stover	35.1–39.5	20.7–24.6	11.0–19.1
Cotton	85–95	5–15	0
Cotton stalk	31	11	30
Coffee pulp	33.7–36.9	44.2–47.5	15.6–19.1
Douglas fir	35–48	20–22	15–21
Hardwood stems	40–55	24–40	18–25
Rice straw	29.2–34.7	23–25.9	17–19
Rice husk	28.7–35.6	11.96–29.3	15.4–20
Wheat straw	35–39	22–30	12–16
Wheat bran	10.5–14.8	35.5–39.2	8.3–12.5
Grasses	25–40	25–50	10–30
Newspaper	40–55	24–39	18–30
Sugarcane bagasse	25–45	28–32	15–25
Sugarcane tops	35	32	14
Pine	42–49	13–25	23–29
Poplar wood	45–51	25–28	10–21
Olive tree biomass	25.2	15.8	19.1
Jute fibres	45–53	18–21	21–26
Switchgrass	35–40	25–30	15–20
Grasses	25–40	25–50	10–30
Winter rye	29–30	22–26	16.1
Oilseed rape	27.3	20.5	14.2
Softwood stem	45–50	24–40	18–25
Oat straw	31–35	20–26	10–15
Nut shells	25–30	22–28	30–40
Sorghum straw	32–35	24–27	15–21
Tamarind kernel powder	10–15	55–65	–
Water hyacinth	18.2–22.1	48.7–50.1	3.5–5.4

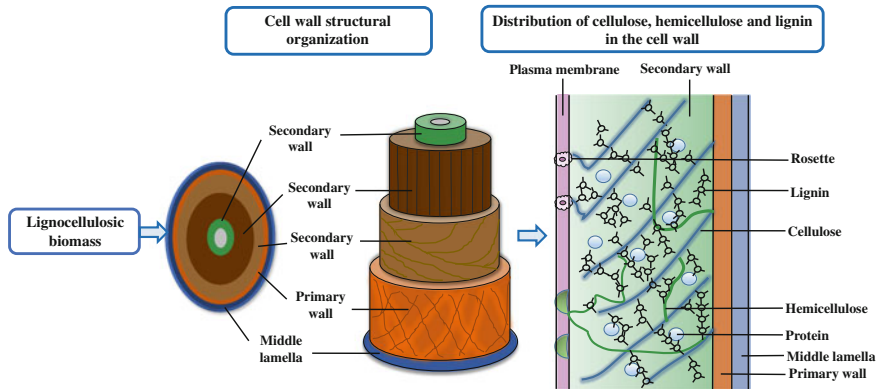


Fig. 5.1 Cell wall structure

mechanical properties, and their roles in the life of the plant (Cosgrove 2012). In the primary wall, the basic structure is a skeleton of cellulose cross-linked with glycans; according to the cross-link types present, there are two types of primary walls: (i) Type I walls that are found in dicotyledonous plants and consist of equal amounts of glucan and xyloglucan embedded in a matrix of pectin; (ii) Type II walls, present in cereals and other grasses, having glucuronoarabinoxylans as their cross-linking glucans, but lacking of pectin and structural proteins (Zhao et al. 2012). The secondary wall usually consists of three sub-layers, which are termed as S1 (outer), S2 (middle), and S3 (inner) lamellae, respectively. The cellulose microfibrils of secondary wall are embedded in lignin, being like steel rods embedded in concrete, but with less rigidity. Cellulose, hemicellulose, and lignin have different distribution in these layers. In wood fibers, it has been found that cellulose concentration is increased from middle lamella to the secondary wall. S2 and S3 lamellae have the highest cellulose concentration. Hemicellulose has a similar tendency of distribution in the cell wall to cellulose, and most of the hemicellulose distributes in the secondary wall. Lignin is found to be the dominant composition in the outer portion of the compound middle lamellae. The percentage of lignin in the lignocellulosic matrix decreases with increasing distance into the middle lamella; that means that the percentages of lignin in the primary wall and in the S1 layer of the secondary wall are much higher than those in the S2 and S3 sections (Zhao et al. 2012).

5.1.1 Cellulose

Cellulose is a linear homopolymer composed of D-glucopyranose units linked by β -1,4-glycosidic bonds. The chemical formula of cellulose is $(C_6H_{10}O_5)_n$; n , called the degree of polymerization (DP), represents the number of glucose groups, ranging from hundreds to thousands or even tens of thousands. In the twentieth century, it

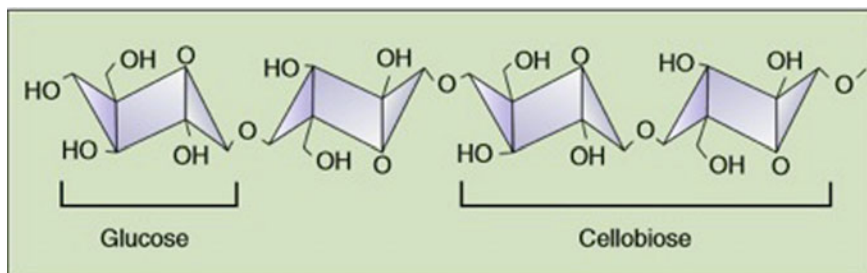


Fig. 5.2 Molecular chain structure of cellulose

was proved that cellulose consists of pure dehydrated repeating units of D-glucoses (as shown in Fig. 5.2), and the repeating unit of the cellulose is called cellobiose (Chen 2014).

The cellulose chains (20–300) are grouped together to form microfibrils, which are bundled together to form cellulose fibers. The long-chain cellulose polymers are linked together by hydrogen and van der Waals bonds, which cause the cellulose to be packed into microfibrils, that in most conditions, are covered by hemicellulose (dry matter accounting for 20–35%) and lignin (dry matter accounting for 5–30%) (Bajpai 2016). Natural cellulose has 10,000 glucose units and the fibril contains approximately 60–80 cellulose molecules. It is insoluble in water, dilute acidic solutions, and dilute alkaline solutions at normal temperatures and is found in both the crystalline and the non-crystalline structure (Harmsen et al. 2010). Indeed, study of the supramolecular structure of natural cellulose showed that the crystalline and non-crystalline phases intertwine to form the cellulose. The noncrystalline phase assumes an amorphous state when tested by X-ray diffraction because most hydroxyl groups on glucose are amorphous. However, large amounts of hydroxyl groups in the crystalline phase form many hydrogen bonds, and these hydrogen bonds construct a huge network that directly contributes the compact crystal structure.

5.1.2 Hemicellulose

The term hemicellulose is used to represent a family of polysaccharides such as arabino-xylans, gluco-mannans, galactans, etc. that are present in both the primary and the secondary cell walls, and in a small amount also the middle lamella region. They have different composition and structure depending on their source and the extraction method. The most common type of polymers that belongs to the hemicellulose family of polysaccharides is xylan (Harmsen et al. 2010). Xylans are a diverse group of polysaccharides with the common backbone of β -(1,4)-linked xylose residues, with side chains of α -(1,2) linked glucuronic acid and 4-O-methyl glucuronic acid residues. Composition and distribution of the substitutions is wide

variable according to the plant cell species. Xylans usually contain many arabinose residues attached to the backbone which are known as arabinoxylans and glucuronoarabinoxylans (Ochoa-Villarreal et al. 2012). The β -(1,4)-linked polysaccharides rich in mannose or with mannose and glucose in a nonrepeating pattern are the glucomannans and galactoglucomannans. Hemicellulose extracted from plants possesses a high degree of polydispersity, polydiversity and polymolecularity (a broad range of size, shape and mass characteristics). However, the degree of polymerization does not exceed the 200 units whereas the minimum limit can be around 150 monomers (Harmsen et al. 2010). Hemicellulose is insoluble in water at low temperature. However, its hydrolysis starts at a temperature lower than that of cellulose, which renders it soluble at elevated temperatures.

5.1.3 Lignin

Lignin is the most complex natural polymer. It is present in the primary cell wall and functions as the cellular glue which provides compressive strength to the plant tissue and the individual fibres, stiffness to the cell wall and resistance against insects and pathogens (Isikgor and Remzi 2015). It is an amorphous three-dimensional polymer with phenylpropane units nonlinearly and randomly linked as the predominant building blocks; the most commonly monomers encountered are p-coumaryl alcohol, coniferyl alcohol and sinapyl alcohol (Fig. 5.3).

The coupling modes between each basic unit include “ β -O-4, “ β -5, “ β -1, and so on. Ether bonds in lignin include phenol-ether bonds, alkyl-ether bonds, dialkyl bonds, diaryl ether bonds, and so on. About two thirds to three quarter phenylpropane units of lignin are linked to the adjacent structural units by ether bonds; only a small part is present in the form of free phenolic hydroxyl (Chen 2014).

Lignin is synthesized by polymerization of these components and their ratio varies between different plants, wood tissues and cell wall layers. Dividing higher plants into two categories, hardwood (angiosperm) and softwood (gymnosperm), it has been identified that lignin from softwood is made up of more than 90% of coniferyl alcohol with the remaining being mainly p-coumaryl alcohol units. Contrary to softwoods,

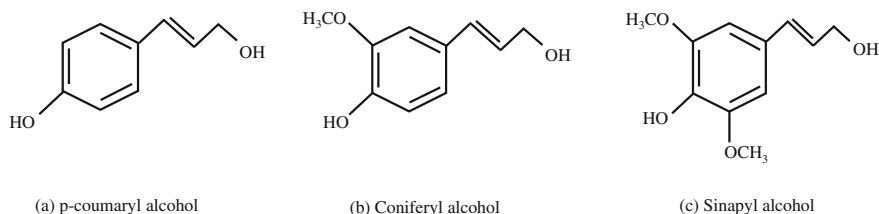


Fig. 5.3 Basic structural units of lignin (Srndovic 2011)

lignin contained in hardwood is made up of varying ratios of coniferyl and sinapyl alcohol type of units (Harmsen et al. 2010).

5.2 Chemical Interaction Between Components

The types of bonds identified within the lignocellulosic structure are four: ether, ester, carbon-to-carbon and hydrogen bonds. They can be divided into intrapolymer and interpolymer linkages (Table 5.2); the former refer to linkages within the individual components of the lignocellulose, while the latter to the connections among the different components to form complexes.

As shown in Table 5.2 the bonds types linking the molecules in the structure of the lignin are ether bonds and carbon-to-carbon bonds; the ether bonds may occur between allylic and aryl carbon atoms, or between aryl and aryl carbon atoms, or even between two allylic carbon atoms. The total fraction of ether type bonds in the lignin molecule is around 70% of the total bonds between the monomer units. The carbon-to-carbon linkages form the remaining 30% of the total bonds between the units. They can also appear between two aryl carbon atoms or two allylic carbon atoms or between one aryl and one allylic carbon atom (Harmsen et al. 2010). In the cellulose's polymer, the glucose units are connected together by a 1-4 β D-glucosidic bond, that can be considered as an ether bond, since it is in fact the connection of two carbon atoms with an elementary oxygen interfering. The other main type of bond present in the cellulose is the hydrogen bond that is responsible for its crystalline fibrous structure. In fact, every glucosyl ring of cellulose has three active hydroxyls: one primary hydroxyl group and two secondary hydroxyl groups. Thus, cellulose may have a series of chemical reactions related to hydroxyl. However, these hydroxyl groups also can form hydrogen bonds between molecules, which has a pro-

Table 5.2 Different types of bonds identified in the lignocellulose (Harmsen et al. 2010)

Bonds with different components (intrapolymer linkages)	
Ether bond	Lignin, (hemi)cellulose
Carbon to carbon	Lignin
Hydrogen bond	Cellulose
Ester bond	Hemicellulose
Bonds connecting different components (interpolymer linkages)	
Ether bond	Cellulose-lignin Hemicellulose lignin
Ester bond	Hemicellulose-lignin
Hydrogen bond	Cellulose-hemicellulose Hemicellulose-lignin Cellulose-lignin

found influence on the morphology and reactivity of cellulose chains, especially the intermolecular hydrogen bond formed by oxhydryl at C3 and oxygen at an adjacent molecule ring. These hydrogen bonds not only can enforce the linear integrity and rigidity of the cellulose molecule but also make molecule chains range closely to form a highly ordered crystalline region. The accessibility of cellulose refers to the difficulty of the reagents to arrive at the cellulose hydroxyl. In heterogeneous reactions, the accessibility is mainly affected by the ratio of the cellulose crystalline regions to the amorphous regions. The reactivity of cellulose is the reactive capability of the primary hydroxyl and the secondary hydroxyl at the cellulose ring. Generally, because of the smallest steric hindrance, the reactivity of the primary hydroxyl groups is higher than for the secondary hydroxyl groups, so the reactivity of hydroxyl at C6 with a bulky substituting group is higher (Chen 2014). In addition, it was noted that, carboxyl groups are also present in cellulose in a fraction of 1 carboxyl per 100 or 1000 monomer units of glucose. With respect to the structure of the hemicellulose, it can be stated that its molecule is formed mainly by the ether type bonds, such as the fructosic and glucosidic one. The main difference with cellulose is that the hydrogen bonds are absent and that there is significant amount of carboxyl groups. The carboxyl groups can be present as carboxyl or as esters or even as salts in the molecule (Harmsen et al. 2010).

The interpolymer linkages, namely those connecting the different polymers of the lignocellulose complex, can be determined by breaking down the lignocellulose and separating the individual components. Their separation is commonly achieved by methods that cause the alteration of their original structure. Therefore, the results obtained about the connecting linkages between the polymers are not definite. However, it has been identified that there are hydrogen bonds connecting lignin with cellulose and with hemicellulose, respectively and the existence of covalent bonds between lignin and polysaccharides. In particular, it is known that hemicellulose connects to lignin via ester bonds and that there are ether bonds between lignin and the polysaccharides. It is still not clear though whether the ether bonds are formed between lignin and cellulose, or hemicellulose (Harmsen et al. 2010).

5.3 Lignocelluloses Feedstock Biorefinery

Biorefinery represents the sustainable processing of biomass into a spectrum of marketable products and energy, as defined by International Energy Agency (IEA) Bioenergy Task 42 (Van Ree and Van Zeeland 2014; Morais and Bogel-Lukasik 2013). In biorefinery, all the types of biomass feedstocks can be exploited, including products, byproducts, residues and waste provided from different sectors: forestry (wood, logging residues, trees, shrubs and wood residues, sawdust, bark, etc.), agriculture (dedicated crops and residues), aquaculture (algae and seaweeds), industries (process residues and leftovers) and households (municipal solid waste and wastewaters) (De Jong and Jungmeier 2015). The biomass feedstock can be converted into dif-

ferent classes of bio-products, via combinations of different technologies, including mechanical/physical, (bio)chemical and thermochemical processes (de Wild 2015).

Among the possible biomass raw materials, the lignocellulose is one of the most promising feedstock for biorefineries, as the availability of the input material is relatively high and input material prices are low (Uihlein and Schebek 2009). The input material, used in lignocelluloses feedstock (LCF) biorefinery, can be obtained from: forestry residues and wood waste (including residues from harvest operations left in the forest after stem wood removal: branches, foliage, roots, etc.), agricultural residues (e.g. husks, chaff, cobs, bagasse), energy crops (crops specifically bred and cultivated at low-cost, on marginal land not suitable for food crops production), and municipal paper waste (Demirbas 2009).

The LCF biorefinery is classified as “phase III biorefinery”; three different types of biorefinery, known as phase I, II and III, have been described by Kamm and Kamm, and van Dyne et al. The phase I and II biorefinery use only one feedstock such as corn and wheat. The difference is that phase I biorefinery has the capability to produce a single major product by single process, while phase II biorefineries is capable of producing various end-products and has far more processing flexibility (Van Dyne et al. 1999). In Europe, there are many phase I biorefineries producing biodiesel from vegetable oil (rapeseed oil), through transesterification process. The Novamont plant in Italy is, indeed, an example of a phase II biorefinery that use corn starch to produce several chemical products, such as biodegradable polyesters (Origi-Bi) and starch derived thermoplastics (Master-Bi) (Clark and Deswarte 2015). The phase III biorefineries use various types of feedstocks and processing technologies to produce a variety of products (Van Dyne et al. 1999; Clark and Deswarte 2015). In LCF biorefinery, lignocellulosic feedstocks are fractioned into intermediate outputs (cellulose, hemicellulose and lignin) that are further processed into a multitude of products and bioenergy, (such as biofuels, fine chemicals, advanced polymer materials, steam/heat, and electricity), by jointly applying several technological processes (de Jong and Gosselink 2014). A number of commercial technologies are available today for the pretreatment of lignocelluloses all around the world. Some of these technologies have already been commercialized and are well known, whereas others are still at lab scale. The most relevant commercial technologies are given in following Table 5.3:

The general scheme for lignocellulose bioconversion involves multi-step processes. The first step, following feedstock selection, is the lignocellulosic biomass pretreatment that is a necessary upstream process to reduce the size of biomass and to fractionate, solubilize, hydrolyze and separate cellulose, hemicellulose, and lignin components (Capolupo and Faraco 2016). As described before pretreatments methods can be classified into different categories (Table 5.4): physical, physiochemical, chemical, biological, electrical, or a combination of these (Amelio et al. 2016).

Physical (mechanical) pretreatment increases the surface area by reducing the size of the biomass and improves the flow through biorefinery processes (Arens and Liu 2014). The physico-chemical methods requires high temperature and pressure; it is therefore necessary a high control of operating conditions. Steam explosion is the most commonly physico-chemical method used for pretreatment of lignocellulosic

Table 5.3 Pretreatment technologies commercially available

Process	Company	Characteristic
Steam explosion	Beta Renewables	Low xylose yield
		High enzyme loading
Single-stage dilute acid	Abengoa	High xylose yield
		Moderate enzyme loading
Two-stage dilute acid	Poet-DSM	High xylose yield
		Low enzyme loading
Ammonia & Steam	Dupont	Require high enzyme loading

biomass (Verardi et al. 2016). It combines mechanical forces and chemical effects. The mechanical effects cause separation of lignocellulose matrix in individual fibers (hemicelluloses, cellulose and lignin) with minimal loss of material. The chemical effects promote the hydrolysis of acetyl groups included in hemicellulose (Verardi et al. 2015).

Chemical methods remove and/or dislocate hemicelluloses and lignin, loosening the structural of lignocellulosic matrix (Capolupo and Faraco 2016). Biological pretreatment methods use cellulolytic, hemicellulolytic, and ligninolytic systems synthesized from microorganisms, such as fungi, bacteria, and actinomycetes, in order to degrade lignin, cellulose, and hemicellulose (Sindhu et al. 2016). Electrical method, such as pulsed-electric field (PEF) pretreatment, exposes the cellulose content in the biomass through the formation of pores in the cell membrane, allowing the entry of agents necessary to break the cellulose into constituent sugars (Kumar and Sharma 2017).

Following pretreatment, the biomass components (lignin, cellulose, hemicellulose and residues) are subject to a combination mainly of thermochemical and biochemical processes in order to convert lignocellulosic feedstock into valuable products (FitzPatrick et al. 2010). Thermochemical conversion includes processes as combustion, pyrolysis, gasification, and liquefaction. The combustion process, performed at 800–1000 °C, allows to transform biomass into energy by oxidation of carbon and hydrogen-rich biomass to CO₂ and H₂O. This method, used for the production of electricity and heat, is similar to fossil-fuel fired power plants and can produce high NO_x emission.

A variety of value-added chemicals can be obtain from main biomass constituents, hemicellulose, cellulose and lignin, by pyrolysis that consists of a thermal degradation, without oxidizing agent, of solid lignocellulosic biomass into gases and liquids (Table 5.5) This thermal decomposition starts at 350–550 °C and goes up to 700–800 °C (de Wild 2015).

Gasification means the conversion of lignocellulosic biomass into a combustible gas mixture, called producer gas, consisting of carbon monoxide (CO), hydrogen (H₂), and traces of methane (CH₄), at 700–1600 °C. After cleaning, producer gas can be used directly as an engine fuel or upgraded to liquid fuels or converted into chem-

Table 5.4 Methods for lignocellulosic biomass pretreatment

		Operating conditions	Advantages	Disadvantages
Physical	Chipping Grinding Milling	Room temperature Energy input <30Kw per ton biomass	Reduces cellulose crystallinity	Power consumption higher than inherent biomass energy
Physio-chemical	Steam pretreatment	160–260 °C (0,69–4,83 MPa) for several second (~15 min in the range 200–230 °C)	Causes hemicellulose auto hydrolysis and lignin transformation; cost-effective for hardwoods and agricultural residues	Destruction of a portion of the xylan fraction; incomplete disruption of the lignin-carbohydrate matrix; generation of compounds inhibitory; less effective for softwoods
	AFEX (Ammonia fiber explosion method)	90 °C for 30 min. 1–2 kg ammonia/kg dry biomass	Increases accessible surface area, removes lignin and hemicellulose;	Do not modify lignin neither hydrolyzes hemicellulose
	ARP (Ammonia recycle percolation method)	150–170 °C for 14 min Fluid velocity 1 cm/min	Increases accessible surface area, removes lignin and hemicellulose;	Do not modify lignin neither hydrolyzes hemicellulose;
	CO ₂ explosion	4 kg CO ₂ /kg fiber at 5.62 MPa 160 bar for 90 min at 50 °C under supercritical carbon dioxide	Do not produce inhibitor for downstream processes. Increases accessible surface area, does not cause formation of inhibitory compounds	It is not suitable for biomass with high lignin content (such as woods and nut shells) Does not modify lignin neither hydrolyze hemicelluloses
	Ozonolysis	Room temperature	Reduce lignin content; does not produce toxic residue	Expensive for the ozone required;

(continued)

Table 5.4 (continued)

		Operating conditions	Advantages	Disadvantages
	Wet oxidation	148–200 °C for 30 min	Efficient removal of lignin; Low formation of inhibitors; low energy demand	High cost of oxygen and alkaline catalyst
Chemical	Acid hydrolysis: dilute-acid pretreatment	Type I: T > 160°, continuous-flow process for low solid loading (5–10%);-Type II: T < 160 °C, batch process for high solid loadings (10–40%)	Hydrolyzes hemicellulose to xylose and other sugar; alters lignin structure	Equipment corrosion; formation of toxic substances
	Alkaline hydrolysis	low temperature; long time high; concentration of the base; For soybean straw: ammonia liquor (10%) for 24 h at room temperature	removes hemicelluloses and lignin; increases accessible surface area	Residual salts in biomass
	Organosolv	150–200 °C with or without addition of catalysts (oxalic, salicylic, acetylsalicylic acid)	Hydrolyzes lignin and hemicelluloses	High costs due to the solvents recovery
Biological		Several fungi (brown-, white- and soft-rot fungi)	Degrades lignin and hemicelluloses; low energy requirements	Slow hydrolysis rates
Electrical	Pulsed electrical field in the range of 5–20 kV/cm,	~2000 pulses of 8 kV/cm	Ambient conditions; disrupts plant cells; simple equipment	Process needs more research

Table 5.5 Main chemicals from lignocellulosic biomass pyrolysis (de Wild 2015)

Biomass constituent (thermal degradation range)	Pyrolysis products
Hemicellulose (150–300 °C)	Acetic acid; Furfural
Cellulose (200–400 °C)	Levoglucosan, Hydroxyacetaldehyde,
Lignin (150–600 °C)	2-Methoxyphenols (e.g. guaiacol), 2,6-Dimethoxyphenols (e.g., syringol), Catechols, Phenol, Alkyl phenols, Methanol,
Whole biomass (100–600 °C)	Extractives (e.g., terpenes), Charcoal, Pyrolysis oil, Gases (e.g., CO, CO ₂ , CH ₄)

ical feedstocks by several methods, as biological fermentation or catalytic upgrading through the Fischer-Tropsch process. Hydrothermal liquefaction is the thermochemical conversion of lignocellulosic biomass into liquid fuels, at 280–370 °C and 10–25 MPa, by processing in a hot, pressurized water environment (Rajvanshi 2014).

Biochemical conversion involves breaking down biomass into sugars, which can then be converted into potential fuel blend stocks and other bioproducts, including renewable gasoline, ethanol and other alcohols, and renewable chemical products, through the use of microorganisms and catalysts.

The most common types of biochemical processes are fermentation and anaerobic digestion (Zhao and Bai 2009). Fermentation is one of the oldest technologies in the world, mainly based on bioethanol synthesis from plant biomass. The fermentation process, in the presence of oxygen, is carried out by microorganisms, including bacteria, yeasts, and fungi. The most commonly used microbe is yeast, mainly *S. cerevisiae* (Zhao and Bai 2009). Several fungal species belonging to genera *Fusarium*, *Rhizopus* (Hahn-Hägerdal et al. 2007), *Monilia* (Gírio 2010), *Neurospora* (Xiros and Christakopoulos 2009), and *Paecilomyces* (Sommer et al. 2004) were able to ferment monomeric sugars. Bacteria used to produce bio-alcohols (ethanol) from fermentable sugars include *Zymomonas mobilis*, *Bacillus macerans*, *Bacillus polymyxa*, *Klebsiella pneumoniae*, *C. acetobutylicum*, *Aeromonas hydrophila*, *Aerobacter sp.*, *Erwinia sp.*, *Leuconostoc sp.*, and *Lactobacillus sp.* (Thatoi et al. 2014). Another bacterial resource is engineering *E. coli* (Srichuwong et al. 2009). Microbial culture types used in fermentation can be classified into five different categories: pure culture, consisting of only one type of organism developed from a single cell (e.g., *S. cerevisiae*); co-culture, containing growths from two distinct cell types (e.g., *Aspergillus niger* and *S. cerevisiae*); mixed culture, consisting of more than two organisms (*Paenibacillus sp.* and four strains of *Z. mobilis*); immobilized culture; and a co-immobilized culture made by entrapping microorganisms within a given matrix (Thatoi et al. 2014).

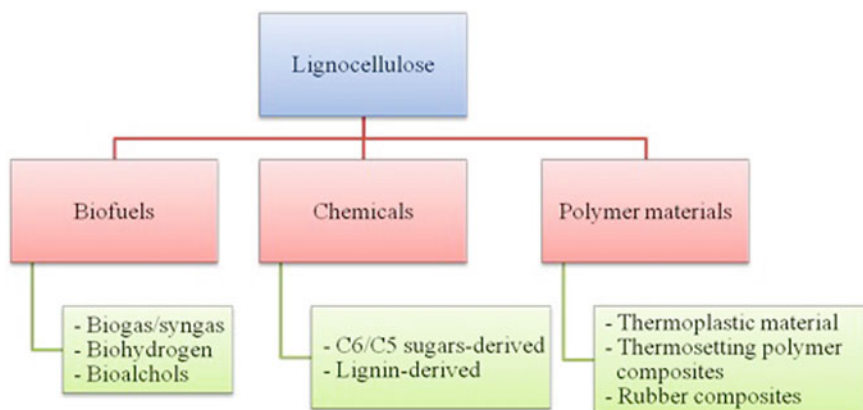


Fig. 5.4 High value bio-products from lignocellulose biomass

Lignocellulosic biomass can be also biochemically degraded by anaerobic digestion. The process is carried out from micro-organisms able to break down organic matter (liquid and solid) in the absence of oxygen and to produce biogas containing mostly methane and carbon dioxide for use as a source of renewable energy. Moreover, anaerobic digestion can be used as a biological pretreatment of lignocellulosic feedstocks, easing the subsequent fractionating of such biomass into its constituent sugars (glucose, galactose, xylose, arabinose, and mannose) and/or short chain fatty acids (acetic, propionic, and butyric acids), which can be further converted into valuable chemicals and biofuels (Surendra et al. 2015).

5.4 High Value Bio-products from Lignocelluloses Feedstock Biorefinery

The products derived from LCF biorefinery, such as biofuels, fine chemicals and advanced polymer materials (Fig. 5.4), might replace petroleum-based products (Cherubini 2010, Cheng and Zhu 2009) The progressive replacement of petroleum refinery oil with lignocellulosic feedstock biorefinery is generally regarded as necessary step for the development of a sustainable industrial society, energy independence, and for the effective management of greenhouse gas emissions (FitzPatrick et al. 2010).

5.5 Biofuels from Lignocelluloses

The conversion of lignocellulose material into several kinds of biofuel, such as biogas/syngas, biohydrogen, and bioalcohols, offers primarily a way to develop renewable and environmental friendly alternatives to substitute fossil fuel with net zero carbon dioxide (CO₂) emission; the CO₂ emitted during fuel combustion is indeed captured during the growth of the feedstock.

Biogas and syngas are complex mixtures composed mainly of methane (CH₄), carbon dioxide (CO₂), hydrogen (H₂), and carbon monoxide (CO) (Awe et al. 2017). The process used to produce the two gasses' mixtures is different: biogas is produced through anaerobic digestion which involves different groups of facultative or obligatory anaerobic microorganisms (Sárvári Horváth et al. 2016); syngas is created by gasification process that causes the partial combustion of biomass (Samiran et al. 2016).

Biohydrogen production can be obtained with low cost from biomass via hydrolysis and fermentation processes. During combustion process, hydrogen produces only water as its environment-friendly product, receiving widespread attention from researchers in the world (Jiang et al. 2016).

Bio-alcohols, such as bioethanol, biobutanol (or biogasoline), and propanol, can be obtained through the biomass fermentation by the action of aerobic and anaerobic micro-organisms. Today, biological ethanol and butanol are the most commonly produced alcohol fuels: in fact, they can be used directly as substitutes for gasoline, or mixed with gasoline in any ratio (Amelio et al. 2016). The bioconversion process of lignocellulose biomass to ethanol or butanol includes several stages: the pretreatment of feedstock, hydrolysis and fermentation steps, and recovery of products (Verardi et al. 2015). On the contrary, propanol, or isopropyl alcohol, is rarely used as alcohol fuel: it is produced through fermentation of carbohydrates from *Escherichia coli* to be commonly used as a solvent (Ibrahim 2013).

5.6 Chemicals from Lignocellulose

Besides biofuels production, the lignocellulose biomass holds a great potential for sustainable production of other value-added chemicals. Examples of some chemicals that have been obtained from lignocellulose biomass are given in Fig. 5.5.

The efficient cellulose and hemicellulose depolymerization in hexose (C₆) and pentose (C₅) sugars is of critical importance for the further development of valuable chemicals. Glucose is the only simple sugar produced by cellulose decomposition. On the other hand, the hemicellulose degradation results in formation of both C₆ (glucose, mannose, galactose, and rhamnose), as well as C₅ (xylose and arabinose) monosaccharides.

The glucose and xylose can be dehydrated, respectively, into 5-hydroxymethylfurfural (HMF) and furfural (2-furaldehyde), which can further

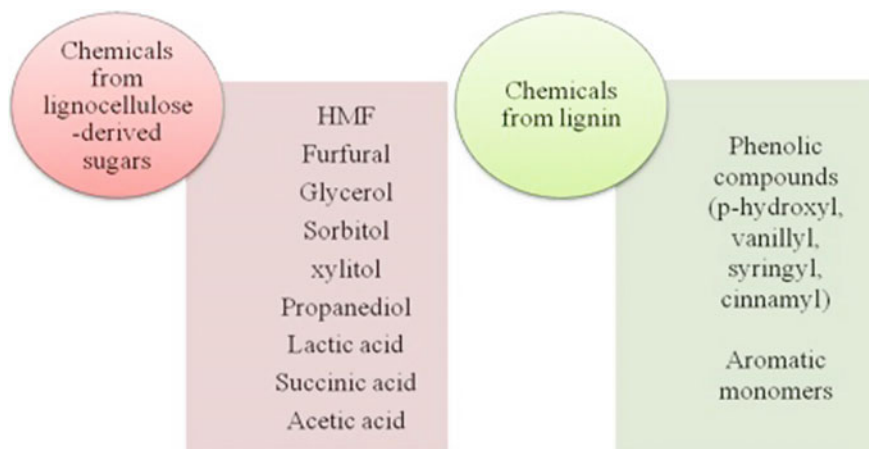


Fig. 5.5 Examples of Chemicals from lignocellulose biomass

be converted into various value-added compounds through feasible chemical transformations (Pereira et al. 2015).

The oxidation of HMF provides an efficient route to synthesis of 2,5-furandicarboxylic acid (FDCA), and 2,5 diformyl-furan (DFF). Currently, FDCA is the most famous HMF derivative: it has attracted much attention recently as potential substitute for terephthalic acid, a petroleum-derived monomer primarily used to produce poly-ethylene-terephthalate (PET) (Han et al. 2017).

Oxidation of HMF to FDCA is a multi-stages process which requires the primary oxidation of HMF to 2,5-diformylfuran (DFF) intermediate, and its sequential oxidation to 5-formyl-2-furancarboxylic acid (FFCA); therefore, FDCA is obtained by further oxidation of FFCA (Zheng et al. 2017).

HMF can also be reduced into 2,5-dihydroxymethylfuran (DHMF), 2,5-dihydroxymethyltetrahydrofuran (DHMTHF), and 2,5-dimethyltetrahydrofuran (DMTHF), or used as intermediate for the production of 2,5-dimethylfuran (DMF), a biofuel with high octane number and energy density that has the potential to replace gasoline directly. DMF is produced by hydrogenation of HMF and subsequent hydrogenolysis.

HMF is very useful also for the production of levulinic acid (LA) by acid rehydration reaction. LA is an important molecule that can be further upgraded in many sectors of industry such as fuel additives, polymer and resin (van Putten et al. 2013).

Furfural can be converted, by hydrogenation, to potential fuel components, such as furfuryl alcohol, 2-methylfuran (MF) and 2-methyltetrahydrofuran (MTHF), and to C4-C5 valuable chemicals, such as valerolactone, pentanediols, cyclopentanone, dicarboxylic acids, butanediol and butyrolactone, by oxidation, hydrogenolysis and decarboxylation processes (Li et al. 2016).

Other chemical compounds, in the form of acids and aldehydes, such as glycerol, sorbitol, xylitol, propanediol, lactic and succinic acid, acetoin or acetic acid, can be produced from lignocellulose biomass-derived sugars (Putro et al. 2016).

The value-added chemicals derived from lignin, via depolymerization or thermal degradation (e.g. oxidation, liquefaction, hydrolysis, hydrocracking, solvolysis and pyrolysis) are phenolic compounds, classified in p-hydroxyl, vanillyl, syringyl and cinnamyl, and aromatic monomers such as benzene, toluene, xylene and hydroxybenzoic acids (Thevenot et al. 2010; Kang et al. 2013; Ma et al. 2015).

5.7 Polymer Materials from Lignocellulose

Lignocellulose biomass can be also used in the preparation of polymer composites materials, using lignin as reinforcement in polymer matrix for making: thermoplastic material, thermosetting polymer composites, and rubber composites (Thakur et al. 2014).

Thermoplastic materials are polymeric materials that can be cooled and heated reversibly without affecting their inherent properties (Wang et al. 2016); several thermoplastic compounds was prepared using lignin as reinforcement, such as: lignin reinforced polystyrene (PS) composites (Barzegari et al. 2012), polydimethylsiloxane- α , ω -diol (PDMS) polymeric matrix-based composites (Thakur et al. 2014), poly(ethylene terephthalate) (PET) matrix-based composites reinforced with lignin (Canetti et al. 2009).

Thermosetting Polymer Composites are polymers that are cured into a solid form and cannot be returned to their original uncured form. Several thermosetting polymer matrix-based composites was prepared using lignin as the reinforcing material, such as: lignin-reinforced epoxy composites (Yin et al. 2012) and lignin-reinforced phenol formaldehyde (PF) polymer composites (Jagur-Grodzinski 2006). Different polymer composite systems were prepared by using rubber as the matrix and lignin as reinforcement, such as: lignin-reinforced styrene-butadiene rubber (SBR)/lignin-LDH (layered double hydroxide) composites (Frigerio et al. 2014), and polymer nanocomposites (Jiang et al. 2013).

Lignin has also been reported to be used as potential reinforcement in foam-based polymer composites, and as a compatibilizer in polymer composites (Thakur et al. 2014).

Finally, the lignin is a promising reinforcement in polymer composites, being biodegradable, CO₂ neutral, abundantly available as industrial waste, low in cost, and environmentally friendly, and having antioxidant, antimicrobial, and stabilizer properties.

5.8 Environmental Impact of Lignocellulose Feedstock Biorefineries

LCF biorefinery should be evaluated for the entire value chain of bio-based products by taking into account environmental, social and economic impacts. For biorefineries, the value chain is classified according to following characteristics: (i) feedstocks, including production and distribution activities; (ii) conversion processes; (iii) platforms (e.g. intermediate materials used for synthesis of more processed materials and chemicals); and (iv) products obtained after conversion processes from platforms. In particular, LCF biorefineries may play a major role in reduction of environmental impacts: in tackling climate change by reducing the demand on fossil fuel energy and providing sustainable energy, chemicals and materials. Then, LCF biorefineries are supposed to contribute to a reduction in greenhouse gas. However, biobased products and fuels may also be associated with environmental disadvantages due to, e.g. land use change/intensity or eutrophication of water. These effects also have an impact on biodiversity and ecosystem services. The environmental analysis can be done by life cycle assessment (LCA) methodology which takes into account all the input and output flows occurring along the production chain, from raw material acquisition, to production, use, and end-of-life (Cherubini 2010). This methodology is standardized in the ISO 14040 series by the International Organization of Standardization (ISO) (Mussatto 2016). From various literature data on the environmental impacts of LCF biorefineries, it can be concluded that LCF biorefinery system could be an effective option to mitigate climate change, reduce dependence on fossil fuels and improve cleaner production chains based on local and renewable resources, revitalizing rural areas (Cherubini 2010; Wertz and Bédué 2013; Valdivia et al. 2016; Cheali et al. 2015). The supply of biomass with sustainable practices is a key point to ensure a renewable energy supply to biorefineries. However, an careful environmental evaluation of LCF biorefinery should include several impact categories, for example: the potential consequences due to the competition for food and biomass resources; the impact on use and quality of water; the effects on land use change and soil carbon stocks and fertility of land; the net greenhouse gas balance; impacts on biodiversity and ecosystem services; potential toxicological risks and energy efficiency (De Jong and Jungmeier 2015). Therefore, the determining of all environmental impacts is complex and a certain degree of uncertainty is always present in the final results.

5.9 Conversion Processes

Various conversion processes of lignocelluloses biomass to biofuel are being summarized in following sections giving stress on the engineering of the lignocelluloses materials and mechanism.

5.9.1 *First Generation*

5.9.1.1 **Transesterification**

This reaction is used to produce biodiesel or vegetable oil based fatty acid methyl esters (FAME). The product of the reaction is glycerol which is a high value product derived from the oil (Kulkarni et al. 2006; Narwal and Gupta 2013). Transesterification is a reversible reaction and proceeds essentially by mixing the reactant in which the catalyst is a liquid acid or liquid base (called homogeneous catalysis), however in the cases of high free fatty acids (FFA) this process fails that is why solid catalyst is recommended. The reason is that the solid catalysts can simultaneously catalyze the Transesterification of triglycerides and FFA present in biomass to methyl esters (Kulkarni et al. 2006).

5.9.1.2 **Ethanol Conversion Process**

A wide variety of carbohydrates containing raw materials have been used for production of ethanol by fermentation process. The fermentation process refers to the metabolic conversion of organic substrate by the activity of enzymes secreted by micro-organisms. There are two basic kind of fermentation has been conceptualized, (a) aerobic and (b) anaerobic depending upon oxygen needed in the process or not. There are many micro-organisms capable of providing fermentative changes to both sugars and starches.

5.9.2 *Second Generation Biofuel*

There are two basic routes for conversion of biomass to liquid biofuels viz. thermo chemical processing and biochemical processing which is described in Fig. 5.6.

- Biochemical—in which enzymes and other micro-organisms are used to convert cellulose and hemicellulose components of the feedstock to sugars prior to their fermentation to produce ethanol;
- Thermochemical—(also known as biomass-to-liquids, BTL), where pyrolysis/gasification technologies produce a synthesis gas ($\text{CO} + \text{H}_2$) from which a wide range of long carbon chain biofuels, such as synthetic diesel, aviation fuel, or ethanol, can be reformed, based on the Fischer–Tropsch conversion

The clear advantage of thermo-chemical processing is that, it can essentially convert all the organic components of the biomass compared with biochemical processing which focuses mostly on the polysaccharides (Kyung Lee et al. 2015).

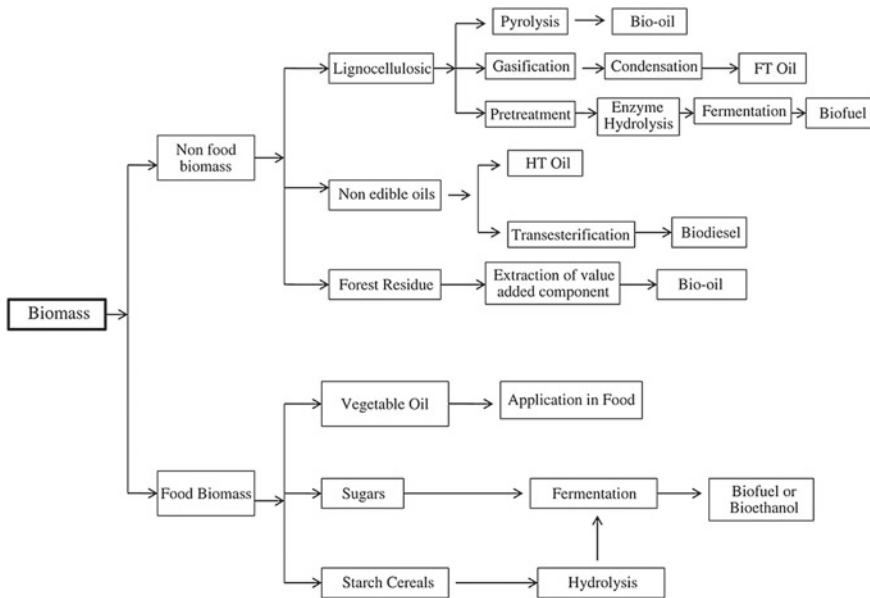


Fig. 5.6 Conversion of biomass to 2nd generation fuels (Chakraborty et al. 2012)

5.9.2.1 Bioethanol from Lignocellulosic Biomass

The ethanol that is produced from lignocelluloses biomass is called bioethanol, which is environmental friendly and renewable (Johnston 2008). It can be used directly in modified spark engines or can be blended with petrol. Ethanol also improves fuel combustion in vehicles hence reduction of emissions. In comparison to petrol ethanol contains only a trace amount of sulphur, so mixing ethanol with petrol helps reduce the sulphur content of fuel, simultaneously lowering the emission of sulphur oxide which is the major component of acid rain. Sugar and starch can also be fermented to alcohol. This is in-fact the least complex method used in producing ethanol (Kuhad et al. 2011; Chakraborty et al. 2012). With plant biomass it's a different story altogether. Plant biomass consists of cellulose microfibers embedded in hemicelluloses, pectin and lignin. The amount of each component varies among different plant species and parts. Following steps are involved in production of ethanol.

- pretreatment of substrates,
- Saccharification process to release the fermentable sugars from polysaccharides, fermentation of released sugars
- finally distillation step to separate ethanol.

Pretreatment is designed to facilitate in the separation of cellulose, hemicellulose and lignin, so that complex carbohydrate molecules constituting the cellulose and hemicellulose can be broken down by enzyme-catalysed hydrolysis into their constituent simple sugars. The complex structure of cellulose makes it difficult to depoly-

merise into simple sugars, but once the polymer structure has been broken down, the sugar molecules are simply fermented to ethanol using fermentative microorganisms (Elshaghabe et al. 2016).

Hemicellulose consists of 5-carbon sugars, which although are easily broken down into its constituent sugars such as xylose and pentose, the fermentation process is much more difficult, and requires efficient microorganisms that are able to ferment 5-carbon sugars to ethanol.

Lignin consists of phenols, and for practical purposes is not fermentable, although it can be recovered and utilized as a fuel, providing process heat and electricity for the alcohol (ethanol, butanol) production facility.

The hydrolysis is usually, catalyzed by cellulase enzymes and the fermentation are carried out by yeast or bacteria. The factors that affect the hydrolysis of cellulose include porosity, i.e., accessible surface area of the waste materials, cellulose fiber crystallinity and lignin and hemicellulose content (Kang et al. 2014). The presence of lignin and hemicellulose makes the access of cellulase enzymes to cellulose difficult. The lignin and hemicellulose removal, reduction of cellulose crystallinity and increase of porosity in pretreatment processes can significantly improve the hydrolysis. The cellulose crystallinity can be reduced by a combination of chipping, grinding and milling (Santos et al. 2011). Steam explosion is the most commonly used method for pretreatment of plant biomass (Kang et al. 2014).

Lignin biodegradation could be catalyzed by the peroxidase enzyme with the presence of H_2O_2 . Microorganisms such as brown, white and soft rot fungi are used in biological pretreatment processes to degrade lignin and hemicellulose (Cragg et al. 2015). Brown rots mainly attack cellulose, while white and soft rots attack both cellulose and lignin. The white rot fungus *Phanerochaete chrysosporium* produces lignin-degrading enzymes, lignin peroxidases and manganese-dependent peroxidases, during secondary metabolism in response to carbon or nitrogen limitation (Cragg et al. 2015). Other enzymes including polyphenol oxidases, laccases, H_2O_2 producing enzymes and quinone-reducing enzymes can also degrade lignin. The advantages of biological pretreatment include low energy requirement and mild environmental conditions, but the hydrolysis rate is very low (Santos et al. 2011).

Furfural is an important inhibitor of ethanol production from hemicellulose hydrolysate even at low concentrations. Various bacteria and yeast have been reported to partially transform furfural to either furfural alcohol or furoic acid, or a combination of both (Moysés et al. 2016). A few microbial species such as *Neurospora*, *Monilia*, *Paecilomyces* and *Fusarium* have been reported to hold the ability to ferment cellulose directly to ethanol by simultaneous saccharification and fermentation (SSF) (Singh et al. 2017). Consolidated bioprocessing (CBP) featuring cellulase production, cellulose hydrolysis and fermentation in one step, is an alternative approach with outstanding potential (Byadgi and Kalburgi 2016). The recombinant strain of *E. Coli* with the genes from *Z. mobilis* for the conversion of pyruvate into ethanol has been reported by Olson et al. (2015). A key challenge to commercializing production of fuels and chemicals from cellulosic biomass is higher processing costs (Manochio et al. 2017; Techaparin et al. 2017). Biological conversion opens such

low costs production path as it has the potential to achieve a higher yield and the modern tools of biotechnology can improve key process steps.

A range of residual substrates such as sugarcane bagasse, sugarcane molasses and starch has been found suitable for the bioconversion of available carbohydrates in these substrates to produce ethanol (Techaparin et al. 2017; Suryaningsih 2014). A variety of mesophilic and thermophilic microorganisms were employed to optimize the fermentation process, which could be practically viable in different climatic conditions, particularly to reduce the cost of temperature maintenance in large fermenters operating in warmer countries in summer months (Wu et al. 2016).

Sukumaran et al. have recently reported on bioethanol production from the saccharification of wheat bran, a ligno-cellulosic waste (Sukumaran et al. 2009). The cost of cellulase enzymes is a major factor in the enzymatic saccharification of agricultural biomass, which contains lignin. Production cost of cellulases and hence ultimately the cost of ethanol production may be brought down by multifaceted approaches. One important approach is the use of cheaper lignocellulosic substrates for the biosynthesis of the enzyme, and second strategy is the use of cost efficient fermentation process such as solid state or solid substrate fermentation at much cheaper cost.

Whilst bioethanol production has been greatly improved by development of new technologies but there are still challenges that need further improvements in the developed technology to bring forward to commercial scale. These challenges include maintaining a stable performance of the genetically engineered microorganisms and developing more efficient pretreatment technologies for the lignocellulosic biomass and integrating the optimal components into economic ethanol production systems.

5.9.3 *Third Generation Biofuel*

The conversion technologies for utilizing microalgae biomass can be separated into two basic categories of thermochemical and biochemical conversion (similar to terrestrial biomass). Thermochemical conversion covers the thermal decomposition of organic components to fuel products, such as direct combustion, gasification, thermochemical liquefaction and pyrolysis. The biological process of energy conversion of biomass into other fuels includes anaerobic digestion, alcoholic fermentation and photo biological hydrogen production (Slade and Bauen 2013).

5.10 Advancement in Different Fuels

As mentioned earlier the field of biofuels has seen meteoric change both in the techniques used and the quantities of biofuel produced. Use of food crops was supplemented by agricultural waste and residue and it was hypothesized that microscopic species can be used for further improvement. Transgenic has been used to improve the biofuel crops (Grant 2009). Efficient biotechnical methods to modify the struc-

ture of different algal species coupled with photonic techniques has been explored to give high yields. Different designs of bioreactors have been explored which aims at higher growth rate of algae. One such example is found in one of the recent work by Milano et al. 2016 but not only this there had been a thrust on developing different technologies to use biofuel in different forms. Bio-fuel cells both enzyme and microbe based to convert biofuels to electricity has been created and improved. One such advancement in the bio fuel cells is creation of organelle based biofuel cell (Marbelia et al. 2014) which uses mitochondria immobilized on paper instead of complete cells. This kind of fuel cell is more efficient than enzymatic fuel cell and has the efficiency of microbial fuel cell. These and many such other developments have propagated the hope that these biofuels can be used competitively with petroleum based products as well as production of hydrogen in recent days (Sharma 2017).

5.11 Progress in Processing of Lignocellulosics to Biofuels

5.11.1 Pre-treatment

Due to the nonfermentable nature of lignin, biomass is pretreated to separate cellulose, hemicellulose and lignin. Pretreatment is the major step in the successful production of valuable products from lignocellulosic biomass. A suitable pretreatment of biomass is necessary to ensure good yields of sugars from the polysaccharides. Pretreatment disrupts the plant cell wall and improves enzymatic access to the polysaccharides as raw and untreated biomass is usually resistant to enzymatic degradation. A number of biomass pretreatment technologies are available today (Nanda et al. 2014; Putro et al. 2016; Menon and Rao 2012), such as **physical** (comminution by chipping, grinding and milling to reduce biomass particle size; ozonolysis; gamma rays; pulsed electrical field; electron beam; ultrasound and microwave digestion), **chemical** (use of acids, bases and organic solvent in biomass hydrolysis), **thermo-physical** (liquid hot water, steam explosion, supercritical water), **thermochemical** (wet oxidation, ammonia recycle percolation, ammonia fiber explosion, supercritical CO₂) and **biological** (enzymatic hydrolysis).

As regard chemical pre-treatments, hydrolysis of lignocellulosic biomass result in undesirable components found in biomass hydrolysates that are inhibitory to fermentation include sugar degradation products (e.g. hydroxymethyl furfural or HMF and levulinic acid), hemicellulose degradation products (e.g. acetic acid, ferulic acid, glucuronic acid and p-coumaric acid) and lignin breakdown products (e.g. syringaldehyde and syringic acid). New pretreatment methods were proposed to be highly efficient and effective for downstream biocatalytic hydrolysis of various lignocellulosic biomass materials, which can accelerate bioethanol commercialization, such as the hydrogen peroxide–acetic acid pretreatment (Wi et al. 2015). Recent advances included acidic treatments to deconstruct biomass in combination with organic solvents in a biphasic system, in order to increase the concentrations of products and

the efficiency of downstream processing options (Wettstein et al. 2012). It would be highly desirable if these organic solvents could be produced from biomass, thereby eliminating the need to transport solvents derived from petroleum to the biomass refining site. Recently, ionic liquids are gaining interest in biomass hydrolysis and being attractive alternatives to volatile and unstable organic solvents due to their high thermal stability and nearly absolute nonvolatility (Vancov et al. 2012). Nevertheless, there are several core issues that stand in the way of commercialization, including the relative high cost of the ionic liquids, a lack of knowledge in terms of process considerations for a biorefinery based on these solvents, and scarce information on the co-products of this pre-treatment technology (Klein-Marcuschamer et al. 2011).

Thermophysical and thermochemical pretreatments often result in the generation of inhibitory byproducts such as furfural, HMF and acetic acid. They have adverse effects on enzymatic hydrolysis and fermentation, consequently several post-treatment steps such as detoxification, neutralization and nutrient supplementation to the hydrolysate medium could curb the inhibitory effects (Nanda et al. 2014).

As regard biological pre-treatments, lignocellulose polysaccharides are hydrolyzed to provide the mono-saccharides used by microbial biocatalysts in fermentation processes.

Synergistic interaction between different enzymes have been investigated in order to design optimal combinations and ratios of enzymes for different lignocellulosic substrates subjected to various pretreatments (Van Dyk and Pletschke 2012). Bio-conversion using enzyme synergy has generally opted for two approaches, individual enzyme combinations or combinations of commercial mixtures. Based on the substrate analysis and identification of sugars, enzymes are selected for hydrolysis of bonds relating to those sugars. Enzymes required for glucose and xylose release are considered the main enzymes, while accessory enzymes are added should those sugars be present. These enzymes are then evaluated for optimal yield and synergy. Once enzyme ratios are optimized, further accessory enzymes can be evaluated for total release of all sugars (see Fig. 5.7a). Finally, commercial mixtures must be selected and characterized to identify the presence of relevant enzyme activities. Ratios of commercial mixtures are optimized based on yield of glucose and xylose. Enzyme activities that are not present in the commercial mixtures must then be added in the form of additional enzymes and evaluated for improved hydrolysis (Fig. 5.7b).

5.11.2 Cellulose and Hemicelluloses Conversion

After biomass pretreatment, cellulose and hemicellulose fractions of the lignocellulosic biomass are converted to various biofuels, while the residue fraction (lignine) is converted via combustion. Hydrothermal, thermochemical, biochemical and chemocatalytic processes are typically studied to produce biofuels from lignocellulosic biomass. Along with bio-oil, ethanol, butanol and syngas, various value-added co-products including biochar, organic acids, solvents, phenols, aromatic compounds, etc. are also obtained. The most used platform molecules include: (a) levulinic acid

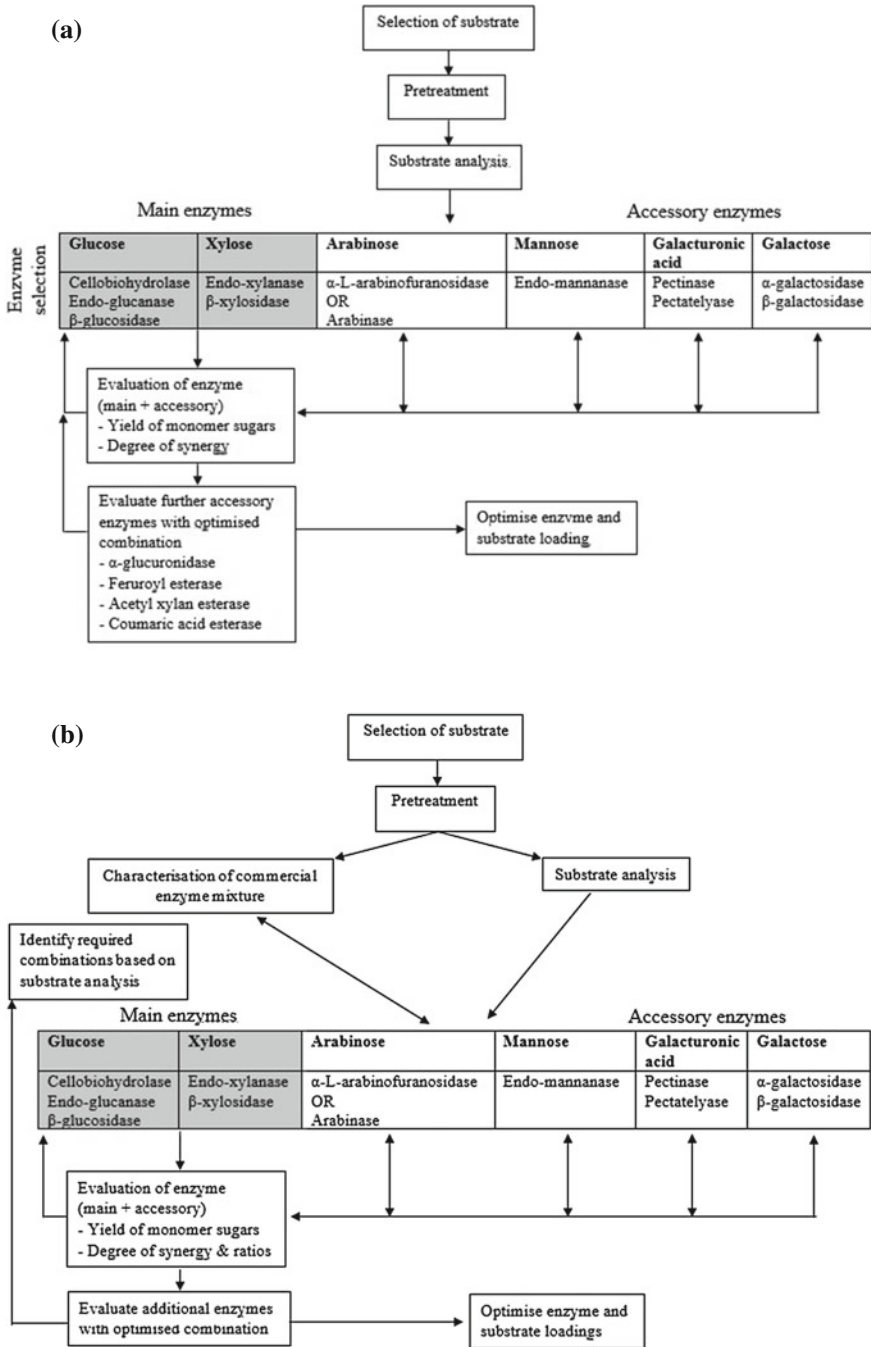


Fig. 5.7 a Model for developing optimal combinations with individual enzymes and b optimal synergistic combinations with commercial mixtures of enzymes (Van Dyk and Pletschke 2012)

that can be transformed to produce either fuels or additives for fuels; (b) furan derivatives that can also be transformed into fuels and fuel additives; (c) polyols to produce liquid fuels as well as oxygenated additives; (d) fatty acids for producing diesel and lubricants (Climent et al. 2014).

In **hydrothermal** processes, supercritical water acts as a medium in the biomass conversion to fermentable sugars and H₂-rich syngas. This technology has been found to be promising for the production of H₂ from biomass over last few years, but it has a few limitations for industrial applications (Nanda 2012). **Thermochemical** processes do not require enzymes or microorganisms, they are applicable over a wide range of feedstocks, and they are generally compatible with conventional petroleum processing technologies. However, pre-treatment of the biomass and physical feeding into thermal processing units are challenging. The thermochemical conversion of biomass includes gasification, pyrolysis and liquefaction.

Gasification produces syngas and tar (condensable high molecular weight hydrocarbons produced by incomplete biomass gasification). Syngas is converted to biofuels by using chemical catalysts known as FT process or by using microbial catalysts known as syngas fermentation (Munasinghe and Khanal 2011). The syngas fermentation into ethanol and other bioproducts is considered to be more attractive due to several inherent merits over the biochemical approach and the FT process. In gasification, challenges include minimization of tar formation, syngas cleanup, development of effective catalysts, and integration with Fischer–Tropsch (FT) process. The direct integration of biomass gasification and FT synthesis requires an intermediate gas-cleaning system, because the gaseous stream delivered from the gasifier typically contains a number of contaminants that need to be removed before the FT unit, which is highly sensitive to impurities (Serrano-Ruiz and Dumesic 2011). The utilization of pure oxygen atmosphere, small particle sizes (lower than 1 mm diameter), and a combination of high temperatures, high pressures and low residence times favors the production of syngas versus producer gas (a mixture of CO, H₂, CO₂, CH₄, and N₂ used for heat and electricity production) (Serrano-Ruiz and Dumesic 2011).

Pyrolysis produce bio-oil, gas and char and major challenges include cleanup of the bio-oil and sufficient stabilization of it for practical delivery and use in a petroleum refinery (Hoekman 2009). A new controlled conversion of lignocellulose biomass to bio-jet and diesel fuels by catalytic pyrolysis of biomass into low carbon hydrocarbons coupled with alkylation of aromatics was recently proposed (Zhang et al. 2015).

Finally, liquefaction gives bio-oil and gas as products. Bio-oil results in a complex mixture of volatile organic acids, alcohols, aldehydes, ethers, esters, ketones, and non volatile components. This oil could be upgraded catalytically to yield an organic distillate product which is rich in hydrocarbons and useful chemicals (Naik et al. 2010).

The **biochemical** conversion involves biomass hydrolysis with dilute acids and enzymes to produce monomeric sugars followed by microbial fermentation of the sugars to fuel ethanol and butanol (Balat 2011). Recent studies have aimed to better characterize and understand the mechanisms of cellulase/hemicellulase reactions to design high performance cellulosomes/hemicellulosomes (Gao et al. 2013).

Recent articles reported the identification and characterization of novel xylanases (GH10-XA) and α -glucuronidase (GH67-GA) from *Alicyclobacillus* and *Caldicellulosiruptor* (GH67-GC) (Cobucci-Ponzano et al. 2015). Several authors focused on the current status and advances in cellulase and hemicellulase improvement (Dumon et al. 2012, Behera and Ray 2016, Gao et al. 2011). Recent developments include engineered strains for consolidated bioprocessing for cost-effective production: hydrolytic strains with a recombinant biofuel pathway and engineering of a natural ethanologenic strain by inserting cellulolytic and/or hemicellulolytic potentialities (Amore and Faraco 2012). Although the actual consolidated bioprocessing yields are lower than those of wild fermenting microorganisms on lignocellulose hydrolysates, the concept is promising. The biomass hydrolysates containing monomeric sugars (glucose and xylose) were fermented using *Saccharomyces cerevisiae* and *Clostridium beijerinckii* for ethanol and butanol production, respectively (Nanda et al. 2014). New strains and process intensification are being investigated, including the use of a pervaporation system in order to remove the produced alcohol continuously and increase the yield (Amelio et al. 2016).

Solid-state fermentation technology is expanding with increasing importance for the production of high value-added products, by involving the growth of microorganisms on moist solid substrates in the absence of free flowing water. It has gained considerable attention due to several advantages over submerged fermentation (Behera and Ray 2016). Other authors investigated the rapid bioconversion of lignocellulosic sugars into ethanol using high cell density fermentations with cell recycle by using nine different engineered microbial strains: the results showed that acceptable performance is largely correlated to the specific xylose consumption rate (Sarks et al. 2014).

Bioconversion of lignocellulose by microbial fermentation is typically preceded by an acidic thermochemical pretreatment step designed to facilitate enzymatic hydrolysis of cellulose. Substances formed during the pretreatment of the lignocellulosic feedstock inhibit enzymatic hydrolysis as well as microbial fermentation steps. Conditioning of slurries and hydrolysates can be used to alleviate inhibition problems connected with hydrolytic enzymes and the yeast *Saccharomyces cerevisiae*. Novel developments in the area include chemical in situ detoxification by using reducing agents, and methods that improve the performance of both enzymatic and microbial biocatalysts, such as fermentation technology and microbial resistance to inhibitors (Amelio et al. 2016).

Since lignocellulose conversions carried out at <50 °C have several limitations, thermophilic bacteria and thermostable enzymes were also investigated to overcome the limitations of existing lignocellulosic biomass conversion processes to biofuels (Amelio et al. 2016; Bhalla et al. 2013).

Alternatively, an integrated system including anaerobic digestion and aerobic fungal fermentation was investigated to convert corn stover, animal manure and food wastes into microbial lipids for biodiesel and methane production (Zhong et al. 2015). This novel self-sustaining advanced lignocellulosic biofuel production is based on a combined hydrolysis treating synergistically solid digestate and corn stover (see

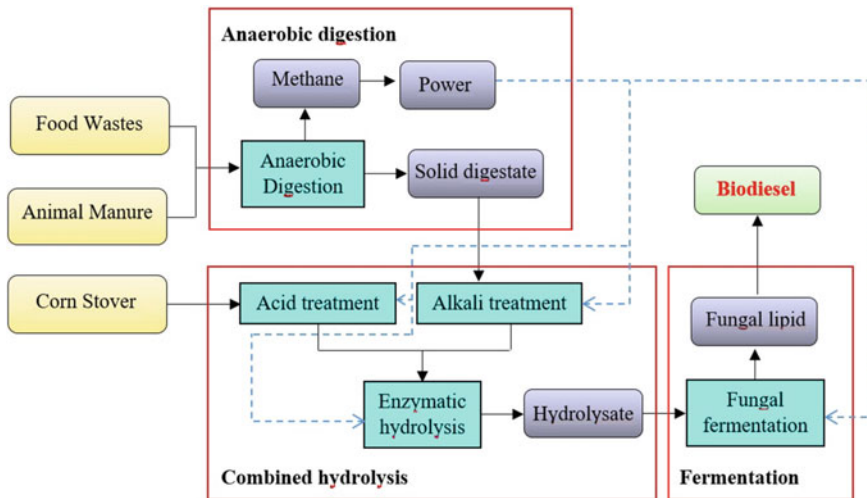


Fig. 5.8 Flowchart of a self-sustaining advanced lignocellulosic biofuel production (Zhong et al. 2015)

Fig. 5.8). Some authors also proposed to link anaerobic digestion and pyrolysis in order to convert lignocellulosic biomass more efficiently (Fabbri and Torri 2016).

In metabolic engineering, significant progress has been made using physical and chemical mutagens to increase production of lignocellulolytic enzymes (Behera and Ray 2016; Chandel and Singh 2011). A wide range of microorganisms are being engineered reflecting the effectiveness of today's gene technology. Successful metabolic engineering strategies are being applied with emphasis on xylose catabolism, inhibitor tolerance, synthetic microbial consortium, and cellulosic oligomer assimilation (Chen and Dou 2016).

In the **chemical or chemo-catalytic** approach, the cellulosic biomass undergoes catalytic hydrolysis, using acids either in aqueous solution or heterogeneous phase. Continued research is necessary to address the use and separation of mineral acids, increase the concentration of product streams, and improve product separations. Mineral acids can be eliminated by the identification of solid acid catalysts easily recoverable from the reaction mixture and recyclable for biomass deconstruction and for upgrading the resulting sugars. Alternatively, effective management and recycle of the mineral acid must be achieved to reduce costs and environmental impact.

Direct transformation of lignocellulosic biomass into 5-hydroxymethylfurfural (HMF)—emerging platform for the next generation plastics and biofuels (Wang et al. 2014)—was carried out using single or combined metal chloride catalysts in DMA–LiCl solvent under microwave-assisted heating or using Sn-Mont catalyst in a tetrahydrofuran (THF)/H₂O–NaCl biphasic system under mild conditions (Wang et al. 2014).

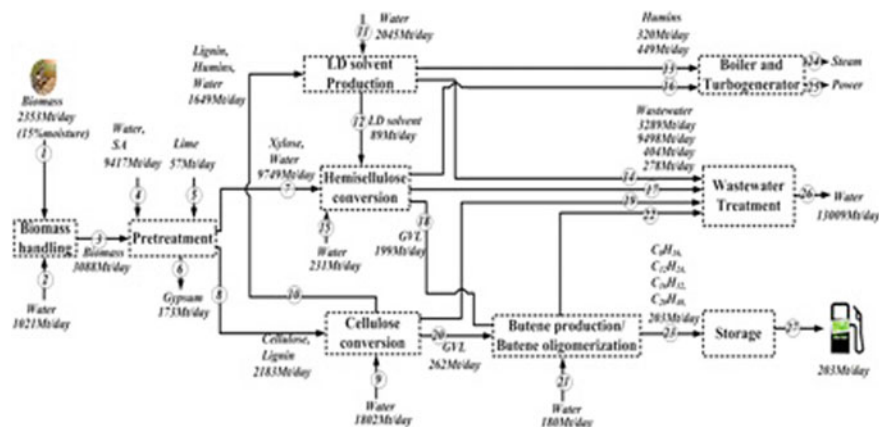


Fig. 5.9 Integrated catalytic process for monophasic conversion of cellulose to butene oligomers (using SBP solvent), biphasic conversion of hemicellulose to butene oligomers (using LD solvent), and monophasic conversion of lignin to LD solvent (Kim and Han 2016)

A novel controllable transformation of lignin into C8–C15 cycloparaffins and aromatics in the jet and diesel fuel range by catalytic depolymerization of lignin using ionic liquid was demonstrated. Ionic liquids may play a role in catalysis, in addition to their role in facilitating the dissolution of cellulose (Zhang and Zhao 2010). However, ionic liquids were not suitable for large scale applications due to their high cost and deactivation by small amounts of water, and their separation from the reaction mixture was still a problem.

An integrated process (see Fig. 5.9) based on a new alkylphenols-based biomass conversion technology was recently developed by Kim and Han (2016) as an economically competitive alternative to current biofuel production approaches. This catalytic production strategy involves separate conversion of hemicellulose and cellulose using 2-sec-butylphenol (SBP) and lignin-derived (LD) alkylphenol solvents, in order to produce liquid hydrocarbon fuels (butane oligomers). Firstly, raw biomass is fractionated by dilute sulfuric acid (SA)-catalyzed pretreatment into cellulose and hemicellulose-derived xylose. These two fractions are then converted separately to levulinic acid (LA) using SBP and LD alkylphenol solvents, respectively. Finally, LA is upgraded catalytically to butene oligomers via *c*-valerolactone (GVL) and butene intermediates.

The proposed strategy has a high biomass-to-fuels yield (34.8 mol%) at low solids concentrations using large volumes of solvents, which are mostly recovered (99%). Energy integration reduced the total heating requirements by 72%.

Hemicellulose and cellulose can be also simultaneously converted in a single reactor, thus eliminating pre-treatments steps to fractionate biomass and simplifying product separation. This process uses gamma-valerolactone (GVL) as a solvent, that is also one of the reaction products, over different catalysts (Climent et al. 2014).

Commercial processes for the conversion of biomass to fuels are now based mainly on the production of bioethanol, biodiesel and renewable fuels from gasification and pyrolysis of biomass and hydroprocessing of triglycerides, but there are few commercial processes based on the catalytic approaches. A catalytic process was developed by Avantium (Netherlands) in order to produce furan derivatives such as ethoxymethylfurfural as alternatives to petroleum-derived hydrocarbons. In 2010 Shell and Virent announced the first biogasoline demonstration plant based on Virent's Bioforming[®] process converting aqueous carbohydrate solutions into mixtures of hydrocarbons by combining aqueous phase reforming using heterogeneous catalysts (Virent modified ZSM-5 zeolite) (Climent et al. 2014).

5.12 Conclusions and Future Trends

Biofuels are a promising short term alternative to petroleum-derived fuels and can be derived from renewable carbon sources to mitigate greenhouse gas emissions. The applicability of biomass as a renewable resource for transportation fuels has been demonstrated by the successful integration of first generation bioethanol and biodiesel into the current infrastructure. However, first generation technologies have drawbacks related to their consequent ethic question food *vs* fuel. A more sustainable biofuels strategy would utilize widely available biomass feedstocks to the largest extent possible, drawing upon non-edible lignocellulosic biomass. A successful lignocellulosic biorefinery can be realized through a combination of different technologies and biomass processing strategies for the flexible production of varied fuel and chemical products.

There are many challenges which need to be addressed to make the syngas fermentation commercially viable in producing biofuels and other value-added products. The yields of the products from syngas fermentation are usually low; hence new recombinant microorganisms with high yields of ethanol are essential for industrial scale fermentation of syngas. Genetic manipulation of microorganisms to amplify solvent production over acetic acid can be considered as a possible option (Nanda et al. 2014).

Bioconversion using enzyme synergy is generally based on two useful approaches, individual enzyme combinations or combinations of commercial mixtures. The use of individual enzymes can lead to a greater understanding of synergy and cooperation between enzymes to degrade a complex substrate, but there is no commercial availability of pure enzymes (mostly the lesser known accessory enzymes) to study interactions between enzymes, as well as there is no characterization of the available enzymes in terms of activity on complex substrates, stability and inhibition in the bioreactor environment. New enzymes and protein engineering are necessary to improve characteristics of enzymes and to provide suitable enzymes for the future.

Instead, the use of commercial enzymes may be a quicker route to commercialization, but it is important that production of these mixtures should be optimised for different substrates with different pretreatments.

In order to perform the biocatalytic conversion of lignocellulose at industrial scale, further aspects need to be addressed. At first, the biocatalysts have to be improved so that higher yields and productivities can be achieved. Moreover, product recovery and the recycling of water as well as biocatalysts have to be considered, since both aspects are essential for industrial processes. Ultimately, the evaluation and model-based synthesis of the complete process chain needs to be performed, since pretreatment, hydrolysis, fermentation, product recovery as well as recycling steps are strongly associated and need to be harmonized (Jäger and Büchs 2012). Further research should be done with respect to hemicellulases and their contribution to lignocellulose degradation, particularly the role of enzymes such as pectinases, mannanases and other accessory enzymes. The role of other proteins and non-hydrolytic enzymes to achieve and enhance complete degradation of lignocellulose requires further investigation (Van Dyk and Pletschke 2012).

New trends in engineering synthetic microbial consortia and direct use of cellulosic or hemicellulosic oligomers are promising potential future directions for research and development. Strain improvement for enhanced cellulases biosynthesis using mutagenesis, metabolic engineering and genomics approaches, should be used for the lignocellulosic bioconversion processes. Recombinant DNA technology and protein engineering are also being used as a powerful modern approach for efficient lignocellulosic bioconversion by improving various aspects of lignocellulolytic enzymes such as production, specific activity, pH and temperature stability, or by producing novel proteins/enzymes with altered properties (Kumar et al. 2008).

Moreover, degrading the recalcitrant part of the lignocellulosic biomass (chitin for example) remains a challenge. Further challenges concern the combination of pretreatment and hydrolysis at high solids loadings to make energetic molecule production economically viable. However, efforts need to be continued to overcome biological bottlenecks and transfer limitations, crucial steps to optimize processes with high solids lignocellulosic materials (Alfenore and Molina-Jouve 2016).

In order to compete with the cost of petroleum fuels, the cost of biofuel processing should be kept as low as possible using energy efficient technologies and using less water. Producing as many co-products as possible in a biorefinery will help to reduce the cost of biofuel production. It is important that a biorefinery should be established in an appropriate location that has good water resources, access to feedstocks, and energy that is needed to process the feedstock. Several studies are in progress to enhance carbohydrate release from lignocellulose by combinations of physical and physicochemical pretreatments; combine pretreatments and hydrolysis to improve yields at high solids loadings; maximize and accelerate the conversion of sugar monomers into the final products by improving enzyme activities for separate hydrolysis and fermentation processes; improve the fermentation performances by ensuring nutritional complementation of both liquid and gaseous media, optimizing mass transfer with new configurations of bioreactor, and developing engineered strains to better understand the metabolic pathways involved in biofuel synthesis to develop over-producing engineered strains with increased inhibitor resistance; develop a cleanup system to remove inhibitors present in both the substrate (liquid or gas) and the fermented broth for purifying energetic molecules.

In conclusion, the success of a biorefinery concept depends on the development of energetically efficient processes to convert lignocellulosic biomass directly into biofuels. For this reason, the research should focus on:

- in-depth understanding of the mechanism of conversion of lignocellulosic biomass by heterogeneous catalysis and of the interrelationship among the feedstock, the catalyst, the reaction conditions and the product distribution;
- design and preparation of multifunctional catalysts for highly active and selective conversion of lignocellulosic biomass;
- development in biological and genetic fields;
- development of strategies for the production of flexible chemical platform molecules, such as levulinic acid and γ -valerolactone;
- applications for the production of speciality chemicals and hydrocarbon fuels;
- technologies for biomass deconstruction, such as fast pyrolysis;
- methods for the synergistic coupling of hydrolytic and thermochemical processes into an integrated biorefinery;
- strategies for lignin utilization.

References

- Alfenore S, Molina-Jouve C (2016) Current status and future prospects of conversion of lignocellulosic resources to biofuels using yeasts and bacteria. *Process Biochem* 51:1747–1756. <https://doi.org/10.1016/j.procbio.2016.07.028>
- Amelio A, Van der Bruggen B, Lopresto C, Verardi A, Calabro V, Luis P (2016) Pervaporation membrane reactors: biomass conversion into alcohols. <https://doi.org/10.1016/b978-0-08-100451-7.00014-1>
- Amore A, Faraco V (2012) Potential of fungi as category i consolidated bioprocessing organisms for cellulosic ethanol production. *Renew Sustain Energy Rev* 16:3286–3301. <https://doi.org/10.1016/j.rser.2012.02.050>
- Arens K, Liu S (2014) Lignocellulosic feedstock biorefinery. In: Sustainable bioenergy production. pp 477–500. <https://doi.org/10.1201/b16764-28>
- Awe OW, Zhao Y, Nzihou A, Minh DP, Lyczko N (2017) A review of biogas utilisation. *Purif Upgrading Technol Waste Biomass Valorization* 8:267–283. <https://doi.org/10.1007/s12649-016-9826-4>
- Bajpai P (2016) Pretreatment of lignocellulosic biomass for biofuel production. *Springer Briefs Green Chem Sustain* 34:86. <https://doi.org/10.1007/978-981-10-0687-6>
- Balat M (2011) Production of bioethanol from lignocellulosic materials via the biochemical pathway: a review. *Energy Convers Manag* 52:858–875. <https://doi.org/10.1016/j.enconman.2010.08.013>
- Barzegari MR, Alemdar A, Zhang Y, Rodrigue D (2012) Mechanical and rheological behavior of highly filled polystyrene with lignin. <https://doi.org/10.1002/pc.22154>
- Behera SS, Ray RC (2016) Solid state fermentation for production of microbial cellulases: recent advances and improvement strategies. *Int J Biol Macromol* 86:656–669. <https://doi.org/10.1016/j.ijbiomac.2015.10.090>
- Bhalla A, Bansal N, Kumar S, Bischoff KM, Sani RK (2013) Improved lignocellulose conversion to biofuels with thermophilic bacteria and thermostable enzymes. *Bioresour Technol* 128:751–759. <https://doi.org/10.1016/j.biortech.2012.10.145>

- Byadgi SA, Kalburgi PB (2016) Production of bioethanol from waste newspaper. *Proc Environ Sci* 35:555–562
- Canetti M, Bertini F, Bassini CNRV (2009) Influence of the lignin on thermal degradation and melting behaviour of poly (ethylene terephthalate) based composites, 1–10
- Capolupo L, Faraco V (2016) Green methods of lignocellulose pretreatment for biorefinery development. *Appl Microbiol Biotechnol* 100:9451–9467. <https://doi.org/10.1007/s00253-016-7884-y>
- Chakraborty S, Aggarwal V, Mukherjee D, Andras K (2012) Biomass to biofuel: a review on production technology. *Asia-Pac J Chem Eng* 7:S254–S262
- Chandel AK, Singh OV (2011) Weedy lignocellulosic feedstock and microbial metabolic engineering: advancing the generation of “Biofuel”. *Appl Microbiol Biotechnol* 89:1289–1303. <https://doi.org/10.1007/s00253-010-3057-6>
- Cheali P, Posada JA, Gernaey KV, Sin G (2015) Upgrading of lignocellulosic biorefinery to value-added chemicals: Sustainability and economics of bioethanol-derivatives. *Biomass Bioenerg* 75:282–300. <https://doi.org/10.1016/j.biombioe.2015.02.030>
- Chen H (2014) Biotechnology of lignocellulose: theory and practice. https://doi.org/10.1007/978-94-007-6898-7_2. © Chemical Industry Press, Beijing. Springer Science+Business Media, Dordrecht
- Chen R, Dou J (2016) Biofuels and bio-based chemicals from lignocellulose: metabolic engineering strategies in strain development. *Biotechnol Lett* 38:213–221. <https://doi.org/10.1007/s10529-015-1976-0>
- Cheng S, Zhu S (2009) Lignocellulosic feedstock biorefinery-the future of the chemical and energy industry. *BioResources* 4:456–457
- Cherubini F (2010) The biorefinery concept: Using biomass instead of oil for producing energy and chemicals. *Energy Convers Manag* 51:1412–1421. <https://doi.org/10.1016/j.enconman.2010.01.015>
- Clark J, Deswarte F (2015) Introduction to chemicals from biomass, 2nd edn. <https://doi.org/10.1002/9781118714478>
- Climent MJ, Corma A, Iborra S (2014) Conversion of biomass platform molecules into fuel additives and liquid hydrocarbon fuels. *Green Chem* 16:516. <https://doi.org/10.1039/c3gc41492b>
- Cobucci-Ponzano B, Strazzulli A, Iacono R, Masturzo G, Giglio R, Rossi M, Moracci M (2015) Novel thermophilic hemicellulases for the conversion of lignocellulose for second generation biorefineries. *Enzyme Microb Technol* 78:63–73. <https://doi.org/10.1016/j.enzmictec.2015.06.014>
- Cosgrove D, Jarvis M (2012) Comparative structure and biomechanics of plant primary and secondary cell walls. *Front Plant Sci* 204. <https://doi.org/10.3389/fpls.2012.00204>
- Cragg SM, Beckham GT, Bruce NC, Bugg TDH, Distel DL, Dupree P, Etxabe AG, Goodell BS, Jellison J, McGeehan JE, McQueen-Mason SJ, Schnorr K, Walton PH, Watts JEM, Zimmer M (2015) Lignocellulose degradation mechanisms across the tree of life. *Curr Opin Chem Biol* 29:108–119
- de Jong E, Gosselink RJA (2014) Chapter 17—Lignocellulose-based chemical products. In: *Bioenergy research: advances and applications*. pp 277–313. <https://doi.org/10.1016/b978-0-444-59561-4.00017-6>
- De Jong E, Jungmeier G (2015) Biorefinery concepts in comparison to petrochemical refineries. <https://doi.org/10.1016/B978-0-444-63453-5.00001-X>
- de Wild PJ (2015) Biomass pyrolysis for hybrid biorefineries. <https://doi.org/10.1016/b978-0-444-63453-5.00010-0>
- Demirbas A (2009) Biofuels securing the planet’s future energy needs. *Energy Convers Manag* 50:2239–2249. <https://doi.org/10.1016/j.enconman.2009.05.010>
- Dumon C, Song L, Bozonnet S, Fauré R, O’Donohue MJ (2012) Progress and future prospects for pentose-specific biocatalysts in biorefining. *Process Biochem* 47:346–357. <https://doi.org/10.1016/j.procbio.2011.06.017>
- Elshagabee FMF, Bockelmann W, Meske D, de Vrese M, Walte H-G, Schrezenmeir J, Heller KJ (2016) Ethanol production by selected intestinal microorganisms and lactic acid bacteria

- growing under different nutritional conditions. *Front Microbiol* 7:47. <https://doi.org/10.3389/fmicb.2016.00047>
- Fabbri D, Torri C (2016) Linking pyrolysis and anaerobic digestion (Py-AD) for the conversion of lignocellulosic biomass. *Curr Opin Biotechnol* 38:167–173. <https://doi.org/10.1016/j.copbio.2016.02.004>
- FitzPatrick M, Champagne P, Cunningham MF, Whitney RA (2010) A biorefinery processing perspective: treatment of lignocellulosic materials for the production of value-added products. *Bioresour Technol* 101:8915–8922. <https://doi.org/10.1016/j.biortech.2010.06.125>
- Frigerio P, Zoia L, Orlandi M, Hanel T, Castellani L (2014) Application of sulphur-free lignins as a filler for elastomers: effect of hexamethylenetetramine treatment. *BioResources* 9:1387–1400. <https://doi.org/10.1002/app.39311>
- Gao D, Uppugundla N, Chundawat SP, Yu X, Hermanson S, Gowda K, Brumm P, Mead D, Balan V, Dale BE (2011) Hemicellulases and auxiliary enzymes for improved conversion of lignocellulosic biomass to monosaccharides. *Biotechnol Biofuels* 4:5. <https://doi.org/10.1186/1754-6834-4-5>
- Gao D, Chundawat SPS, Sethi A, Balan V, Gnanakaran S, Dale BE (2013) Increased enzyme binding to substrate is not necessary for more efficient cellulose hydrolysis. *Proc Natl Acad Sci* 110:10922–10927. <https://doi.org/10.1073/pnas.1213426110>
- Girio FM, Fonseca C, Carvalheiro F, Duarte LC, Marques S, Bogel-Lukasik R (2010) Hemicelluloses for fuel ethanol: a review. *Bioresour Technol* 101:4775–4800. <https://doi.org/10.1016/j.biortech.2010.01.088>
- Grant B (2009). Biofuels made from algae are the next big thing on alternative energy horizon. *Scientist* 37–41
- Hahn-Hägerdal B, Karhumaa K, Fonseca C, Spencer-Martins I, Gorwa-Grauslund MF (2007) Towards industrial pentose-fermenting yeast strains. *Appl Microbiol Biotechnol* 74:937–953. <https://doi.org/10.1007/s00253-006-0827-2>
- Han X, Li C, Liu X, Xia Q, Wang Y (2017) Selective oxidation of 5-hydroxymethylfurfural to 2,5-furandicarboxylic acid over MnO_x-CeO₂ composite catalysts. *Green Chem* 19:996–1004. <https://doi.org/10.1039/C6GC03304K>
- Harmsen PFH, Huijgen WJJ, Bermúdez López LM, Bakker RRC (2010) Literature review of physical and chemical pretreatment processes for lignocellulosic biomass. Energy Research Centre of the Netherlands, 1–49. <http://www.ecn.nl/docs/library/report/2010/e10013.pdf>
- Himmel ME, Ding SY, Johnson DK, Adney WS, Nimlos MR, Brady JW, Foust TD (2007) Biomass recalcitrance: engineering plants and enzymes for biofuels production. *Science* 315:804–807
- Hoekman SK (2009) Biofuels in the U.S.—challenges and opportunities. *Renew Energy* 34:14–22. <https://doi.org/10.1016/j.renene.2008.04.030>
- Ibrahim H (2013) Biofuel for sustainable (and eco-friendly) energy development. *Int J Eng Comput Sci* 2:1584–1594
- Isikgor FH, Remzi Becer C (2015) Lignocellulosic biomass: a sustainable platform for production of bio-based chemicals and polymers. *Polym Chem* 2015(6):4497–4559
- Jäger G, Büchs J (2012) Biocatalytic conversion of lignocellulose to platform chemicals. *Biotechnol J* 7:1122–1136. <https://doi.org/10.1002/biot.201200033>
- Jagur-Grodzinski J (2006) Nanostructured polyolefins/clay composites: role of the molecular interaction at the interface. *Polym Adv Technol* 17:395–418. <https://doi.org/10.1002/pat>
- Jiang C, He H, Jiang H, Ma L, Jia DM (2013) Nano-lignin filled natural rubber composites: preparation and characterization. *Express Polym Lett* 7:480–493. <https://doi.org/10.3144/expresspolymlett.2013.44>
- Jiang D, Fang Z, Chin S, Tian X, Su T (2016) Biohydrogen production from hydrolysates of selected tropical biomass wastes with *Clostridium butyricum*. *Sci Rep* 6:27205. <https://doi.org/10.1038/srep27205>
- Johnston J (2008) New world for biofuels. *Energy Law* 86:10–14
- Kang S, Li X, Fan J, Chang J (2013) Hydrothermal conversion of lignin: a review. *Renew Sustain Energy Rev* 27:546–558. <https://doi.org/10.1016/j.rser.2013.07.013>

- Kang Q, Appels L, Tan T, Dewil R (2014) Bioethanol from lignocellulosic biomass: current findings determine research priorities. *Sci World J*. <https://doi.org/10.1155/2014/298153>
- Kim S, Han J (2016) A catalytic biofuel production strategy involving separate conversion of hemicellulose and cellulose using 2-sec-butylphenol (SBP) and lignin-derived (LD) alkylphenol solvents. *Bioresour Technol* 204:1–8. <https://doi.org/10.1016/j.biortech.2015.12.075>
- Klein-Marcuschamer D, Simmons BA, Blanch HW (2011) Techno-economic analysis of a lignocellulosic ethanol biorefinery with ionic liquid pre-treatment. *Biofuels*. *Bioprod Biorefining* 5:562–569. <https://doi.org/10.1002/bbb.303>
- Kuhad RC, Gupta R, Khasa YP, Singh A, Percival Zhang Y-H (2011) Bioethanol production from pentose sugars: current status and future prospects. *Renew Sus Energ Rev* 15:4950–4962
- Kulkarni M, Gopinath R, Meher LC, Dalai AK (2006) Solid acid catalyzed biodiesel production by simultaneous esterification and transesterification. *Green Chem* 8:1056–1062
- Kumar AK, Sharma S (2017) Recent updates on different methods of pretreatment of lignocellulosic feedstocks: a review. *Bioresour Bioprocess* 4:7. <https://doi.org/10.1186/s40643-017-0137-9>
- Kumar R, Singh S, Singh OV (2008) Bioconversion of lignocellulosic biomass: biochemical and molecular perspectives. *J Ind Microbiol Biotechnol* 35:377–391. <https://doi.org/10.1007/s10295-008-0327-8>
- Kyung Lee OK, Seong DH, Lee CG, Lee EY (2015) Sustainable production of liquid biofuels from renewable microalgae biomass. *J Ind Eng Chem* 29:24–31
- Li X, Jia P, Wang T (2016) Furfural: a promising platform compound for sustainable production of C4 and C5 chemicals. *ACS Catal* 6:7621–7640. <https://doi.org/10.1021/acscatal.6b01838>
- Ma Z, Custodis V, Hemberger P, Bährle C, Vogel F, Jeschk GD et al (2015) Chemicals from lignin by catalytic fast pyrolysis, from product control to reaction mechanism. *Chim Int J Chem* 69:597–602. <https://doi.org/10.2533/chimia.2015.597>
- Manochio C, Andrade BR, Rodriguez RP, Moraes BS (2017) Ethanol from biomass: a comparative overview. *Renew Sustain Energy Rev* 80:743–755
- Marbelia L, Bilad MR, Passaris I, Discart V, Vandamme D, Beuckels A, Muylaert K, Vankelecom Ivo FJ (2014) Membrane photobioreactors for integrated microalgae cultivation and nutrient remediation of membrane bioreactors effluent. *Bioresour Technol* 163:228–235
- Menon V, Rao M (2012) Trends in bioconversion of lignocellulose: biofuels, platform chemicals & biorefinery concept. *Prog Energy Combust Sci* 38(2012):522–550
- Milano J, Ong HC, Masjuki HH, Chong WT, Lam MK, Loh PK, Vellayan V (2016) Microalgae biofuels as an alternative to fossil fuel for power generation. *Renew Sustain Energy Rev* 58:180–197
- Morais AR, Bogel-Lukasik R (2013) Green chemistry and the biorefinery concept. *Sustain Chem Process* 1:18. <https://doi.org/10.1186/2043-7129-1-18>
- Moysés DN, Reis VCB, Almeida JRM, Moraes LMP, Torres FAG (2016) Xylose fermentation by *Saccharomyces cerevisiae*: challenges and prospects. *Int J Mol Sci* 17:207
- Munasinghe PC, Khanal SK (2011) Biomass-derived syngas fermentation into biofuels. *Biofuels* 101:79–98. <https://doi.org/10.1016/B978-0-12-385099-7.00004-8>
- Mussatto SI (2016) Biomass fractionation technologies for a lignocellulosic feedstock based biorefinery. <https://doi.org/10.1016/c2014-0-01890-4>
- Naik SN, Goud VV, Rout PK, Dalai AK (2010) Production of first and second generation biofuels: a comprehensive review. *Renew Sustain Energy Rev* 14:578–597. <https://doi.org/10.1016/j.rser.2009.10.003>
- Nanda S, Dalai AK, Kozinski JA (2014) Butanol and ethanol production from lignocellulosic feedstock: biomass pretreatment and bioconversion. *Energy Sci Eng* 2:138–148. <https://doi.org/10.1002/ese3.41>
- Narwal SK, Gupta R (2013) Biodiesel production by transesterification using immobilized lipase. *Biotechnol Lett* 35:479–490
- Ochoa-Villarreal M, Aispuro-Hernández E, Vargas-Arispuro I, Martínez-Téllez MÁ (2012) Plant cell wall polymers: function, structure and biological activity of their derivatives. *IntechOpen science open minds*. <http://dx.doi.org/10.5772/46094>

- Olson DG, Sparling R, Lynd LR (2015) Olson. Ethanol production by engineered thermophiles, *Curr Opin Biotechnol* 33:130–141
- Pereira SC, Maehara L, Machado CMM, Farinas CS (2015) 2G ethanol from the whole sugarcane lignocellulosic biomass. *Biotechnol Biofuels* 8:1–16. <https://doi.org/10.1186/s13068-015-0224-0>
- Putro JN, Soetaredjo FE, Lin S-Y, Ju Y-H, Ismadji S (2016) Pretreatment and conversion of lignocellulose biomass into valuable chemicals. *RSC Adv* 6:46834–46852. <https://doi.org/10.1039/C6RA09851G>
- Rajvanshi AK (2014) Biomass gasification. *Altern Energy Agric* II:1–21
- Samiran NA, Jaafar MNM, Ng JH, Lam SS, Chong CT (2016) Progress in biomass gasification technique—with focus on Malaysian palm biomass for syngas production. *Renew Sustain Energy Rev* 62:1047–1062. <https://doi.org/10.1016/j.rser.2016.04.049>
- Santos ALF, Kawase KYF, Coelho GLV (2011) Enzymatic saccharification of lignocellulosic materials after treatment with supercritical carbon dioxide. *J Supercrit Fluid* 56:277–282
- Sarks C, Jin M, Sato TK, Balan V, Dale BE (2014) Studying the rapid bioconversion of lignocellulosic sugars into ethanol using high cell density fermentations with cell recycle. *Biotechnol Biofuels* 7:73. <https://doi.org/10.1186/1754-6834-7-73>
- Sárvári Horváth I, Tabatabaei M, Karimi K, Kumar R (2016) Recent updates on biogas production—a review. *Biofuel Res J* 3:394–402. <https://doi.org/10.18331/BRJ2016.3.2.4>
- Serrano-Ruiz JC, Dumesic JA (2011) Catalytic routes for the conversion of biomass into liquid hydrocarbon transportation fuels. *Energy Environ Sci* 4:83–99. <https://doi.org/10.1039/c0ee00436g>
- Sharma A, Arya SK (2017) Hydrogen from algal biomass: a review of production process. *Biotechnol Rep* 15:63–69
- Sindhu R, Gnansounou E, Binod P, Pandey A (2016) Bioconversion of sugarcane crop residue for value added products??? An overview. *Renew Energy* 98:203–215. <https://doi.org/10.1016/j.renene.2016.02.057>
- Singh N, Mathur AS, Tuli DK, Gupta RP, Barrow CJ, Puri M (2017) Cellulosic ethanol production via consolidated bioprocessing by a novel thermophilic anaerobic bacterium isolated from a Himalayan hot spring. *Biotechnol Biofuels* 10:73. <https://doi.org/10.1186/s13068-017-0756-6>
- Slade R, Bauen A (2013) Micro-algae cultivation for biofuels: cost, energy balance, environmental impacts and future prospects. *Biomass Bioenergy* 53:29–38
- Sommer P, Georgieva T, Ahring BK (2004) Potential for using thermophilic anaerobic bacteria for bioethanol production from hemicellulose. *Biochem Soc Trans* 32:283–289
- Srichuwong S, Fujiwara M, Wang X, Seyama T, Shiroma R, Arakane M et al (2009) Simultaneous saccharification and fermentation (SSF) of very high gravity (VHG) potato mash for the production of ethanol. *Biomass Bioenerg* 33:890–898. <https://doi.org/10.1016/j.biombioe.2009.01.012>
- Srnđovic JS (2011) Interactions between wood polymers in wood cell walls and cellulose/hemicellulose biocomposites. Doktorsavhandlingar vid Chalmers Tekniska Högskola Chalmers Reproservice, Thesis for the degree of doctor of philosophy
- Sukumaran RK, Singhania RR, Mathew GM, Pandey A (2009) Cellulase production using biomass feed stock and its application in lignocellulose saccharification for bioethanol production. *Renew Energy* 34:421–424
- Surendra KC, Sawatdeenarunat C, Shrestha S, Sung S, Khanal SK (2015) Anaerobic digestion-based biorefinery for bioenergy and biobased products. *Ind Biotechnol* 11:103–112. <https://doi.org/10.1089/ind.2015.0001>
- Suryaningsih R (2014) Bioenergy plants in Indonesia: sorghum for producing bioethanol as an alternative energy substitute of fossil fuels. *Energy Procedia* 47:211–216
- Techaparin Atiya, Thanonkeo Pornthap, Klanrit Preekamol (2017) High-temperature ethanol production using thermotolerant yeast newly isolated from Greater Mekong subregion. *Braz J Microbiol* 48:461–475
- Thakur VK, Thakur MK, Raghavan P, Kessler MR (2014) Progress in green polymer composites from lignin for multifunctional applications: a review. *ACS Sustain Chem Eng* 2:1072–1092. <https://doi.org/10.1021/sc500087z>

- Thatoi H, Dash PK, Mohapatra S, Swain MR (2014) Bioethanol production from tuber crops using fermentation technology: a review. *Int J Sustain Energy* 1–26. <https://doi.org/10.1080/14786451.2014.918616>
- Thevenot M, Dignac MF, Rumpel C (2010) Fate of lignins in soils: a review. *Soil Biol Biochem* 42:1200–1211. <https://doi.org/10.1016/j.soilbio.2010.03.017>
- Uihlein A, Schebek L (2009) Environmental impacts of a lignocellulose feedstock biorefinery system: an assessment. *Biomass Bioenerg* 33:793–802. <https://doi.org/10.1016/j.biombioe.2008.12.001>
- Valdivia M, Galan JL, Laffarga J, Ramos JL (2016) Biofuels 2020: biorefineries based on lignocellulosic materials. *Microb Biotechnol* 9:585–594. <https://doi.org/10.1111/1751-7915.12387>
- Van Dyk JS, Pletschke BI (2012) A review of lignocellulose bioconversion using enzymatic hydrolysis and synergistic cooperation between enzymes—Factors affecting enzymes, conversion and synergy. *Biotechnol Adv* 30:1458–1480. <https://doi.org/10.1016/j.biotechadv.2012.03.002>
- Van Dyne DL, Blase MG, Davis Clements L (1999) A strategy for returning agriculture and rural America to long-term full employment using biomass refineries. In: *Perspectives on new crops and new uses*. pp 114–123
- van Putten R-J, van der Waal JC, de Jong E, Rasrendra CB, Heeres HJ, de Vries JG et al (2013) Hydroxymethylfurfural, a versatile platform chemical made from renewable resources. *Chem Rev* 113:1499–1597. <https://doi.org/10.1021/cr300182k>
- Van Ree R, Van Zeeland A (2014) IEA bioenergy: Task42 biorefining, pp 1–66. http://www.ieabioenergy.com/wp-content/uploads/2014/09/IEA-Bioenergy-Task42-Biorefining-Brochure-SEP2014_LR.pdf
- Vancov T, Alston AS, Brown T, McIntosh S (2012) Use of ionic liquids in converting lignocellulosic material to biofuels. *Renew Energy* 45:1–6. <https://doi.org/10.1016/j.renene.2012.02.033>
- Verardi A, Blasi A, De Bari I, Calabrò V (2015) Steam pretreatment of *Saccharum officinarum* L. bagasse by adding of impregnating agents for advanced bioethanol production. *Ecotoxicol Environ Saf* 1–8. <https://doi.org/10.1016/j.ecoenv.2015.07.034>
- Verardi A, Blasi A, Molino A, Albo L, Calabrò V (2016) Improving the enzymatic hydrolysis of *Saccharum officinarum* L. bagasse by optimizing mixing in a stirred tank reactor: quantitative analysis of biomass conversion. *Fuel Process Technol* 149. <https://doi.org/10.1016/j.fuproc.2016.03.025>
- Wang J, Liu X, Hu B, Lu G, Wang Y (2014) Efficient catalytic conversion of lignocellulosic biomass into renewable liquid biofuels via furan derivatives. *RSC Adv* 4:31101. <https://doi.org/10.1039/C4RA04900D>
- Wang C, Kelley SS, Venditti RA (2016) Lignin-based thermoplastic materials. *Chemsuschem* 9:770–783. <https://doi.org/10.1002/cssc.201501531>
- Wertz J-L, Bédoué O (2013) Features of first generation biorefineries. In: *Lignocellulosic biorefineries*, pp 13–19, 83. <https://doi.org/10.1201/b15443-4>
- Wettstein SG, Martin Alonso D, Gurbuz EI, Dumesic JA (2012) A roadmap for conversion of lignocellulosic biomass to chemicals and fuels. *Curr Opin Chem Eng* 1:218–224. <https://doi.org/10.1016/j.coche.2012.04.002>
- Wi SG, Cho EJ, Lee D-S, Lee SJ, Lee YJ, Bae H-J (2015) Lignocellulose conversion for biofuel: a new pretreatment greatly improves downstream biocatalytic hydrolysis of various lignocellulosic materials. *Biotechnol Biofuels* 8:228. <https://doi.org/10.1186/s13068-015-0419-4>
- Wu X, Zhang J, Xu E, Liu Y, Cheng Y, Addy M, Zhou W, Griffith R, Chen P, Ruan R (2016) Microbial hydrolysis and fermentation of rice straw for ethanol production. *Fuel* 180:679–686
- Xiros C, Christakopoulos P (2009) Enhanced ethanol production from brewer's spent grain by a *Fusarium oxysporum* consolidated system. *Biotechnol Biofuels* 2:4. <https://doi.org/10.1186/1754-6834-2-4>
- Yin Q, Yang W, Sun C, Di M (2012) Preparation and properties of lignin epoxy resin composite. *BioResources* 7:5737–5748. <https://doi.org/10.15376/biores.7.4.5737-5748>
- Zhang Z, Zhao ZK (2010) Microwave-assisted conversion of lignocellulosic biomass into furans in ionic liquid. *Bioresour Technol* 101:1111–1114. <https://doi.org/10.1016/j.biortech.2009.09.010>

- Zhang Y, Bi P, Wang J, Jiang P, Wu X, Xue H, Liu J, Zhou X, Li Q (2015) Production of jet and diesel biofuels from renewable lignocellulosic biomass. *Appl Energy* 150:128–137. <https://doi.org/10.1016/j.apenergy.2015.04.023>
- Zhao XQ, Bai FW (2009) Yeast flocculation: new story in fuel ethanol production. *Biotechnol Adv* 27:849–856. <https://doi.org/10.1016/j.biotechadv.2009.06.006>
- Zhao X, Zhang L, Liu D (2012) Biomass Recalcitrance. Part I: The Chemical Compositions and Physical Structures Affecting the Enzymatic Hydrolysis of Lignocellulose. *Biofuels Bioprod Biorefin* 6:465–482. <https://doi.org/10.1002/bbb.1331>
- Zheng L, Zhao J, Du Z, Zong B, Liu H (2017) Efficient aerobic oxidation of 5-hydroxymethylfurfural to 2, 5-furandicarboxylic acid on Ru/C catalysts. <https://doi.org/10.1007/s11426-016-0489-3>
- Zhong Y, Ruan Z, Zhong Y, Archer S, Liu Y, Liao W (2015) A self-sustaining advanced lignocellulosic biofuel production by integration of anaerobic digestion and aerobic fungal fermentation. *Bioresour Technol* 179:173–179. <https://doi.org/10.1016/j.biortech.2014.12.013>

Manuscript Details

Manuscript number	ETI_2020_603
Title	Membrane processes: Innovation and perspective in dairy industry
Short title	Membrane in dairy industry
Article type	Review Article

Abstract

As the dairy industry is renowned to be one of the most wide sectors of industry in terms of worldwide spread production and vastity of products and byproducts, a great attention to its technology development has been paid through out the decades, resulting in a constant improvement in technology for environmental remediation. A crucial focal point in dairy industry has always been the separation of milk components (fats, proteins) and its fractionation which has been carried out by a number of unit operations that have been replaced over time by membrane filtration, thus eliminating the side effects of more invasive proceedings like thermal operations, resulting in higher quality and more valuable products. Membrane filtration in dairy industries has developed to be used in the most dairy operations like: fractionation, bacteria removal, whey purification, proteins isolation and more. Main membrane applications in dairy industry are taken in account in this article as well as some instances of their development as patented plant unit processes.

Keywords	Membrane processes, Dairy industrial waste, byproduct recovery, Innovation, Industrial processes
Manuscript region of origin	Europe
Corresponding Author	Sudip Chakraborty
Corresponding Author's Institution	University of Calabria
Order of Authors	Debolina Mukherjee, Gerardo Coppola, Maria Teresa Gaudio, Stefano Curcio, Vincenza Calabro, Sudip Chakraborty
Suggested reviewers	Urmila Ukil, Jaya Sikder, raja Ben Amar

Submission Files Included in this PDF

File Name [File Type]

Cover Letter.doc [Cover Letter]

Research Highlight.docx [Highlights]

graphical abstract.JPG [Graphical Abstract]

State of the art reviews on membrane engineering - DAIRY PROCESSES 121119.docx [Manuscript File]

Conflict of Interest.pdf [Conflict of Interest]

declaration-of-competing-interests.pdf [Author Statement]

To view all the submission files, including those not included in the PDF, click on the manuscript title on your EVISE Homepage, then click 'Download zip file'.

Research Data Related to this Submission

There are no linked research data sets for this submission. The following reason is given:
No data was used for the research described in the article

Sub: Submission of a new manuscript to Environmental Technology & Innovation

Dear Prof. Nghiem
Editor in Chief
Environmental Technology & Innovation

Dear Dr. Nghiem,

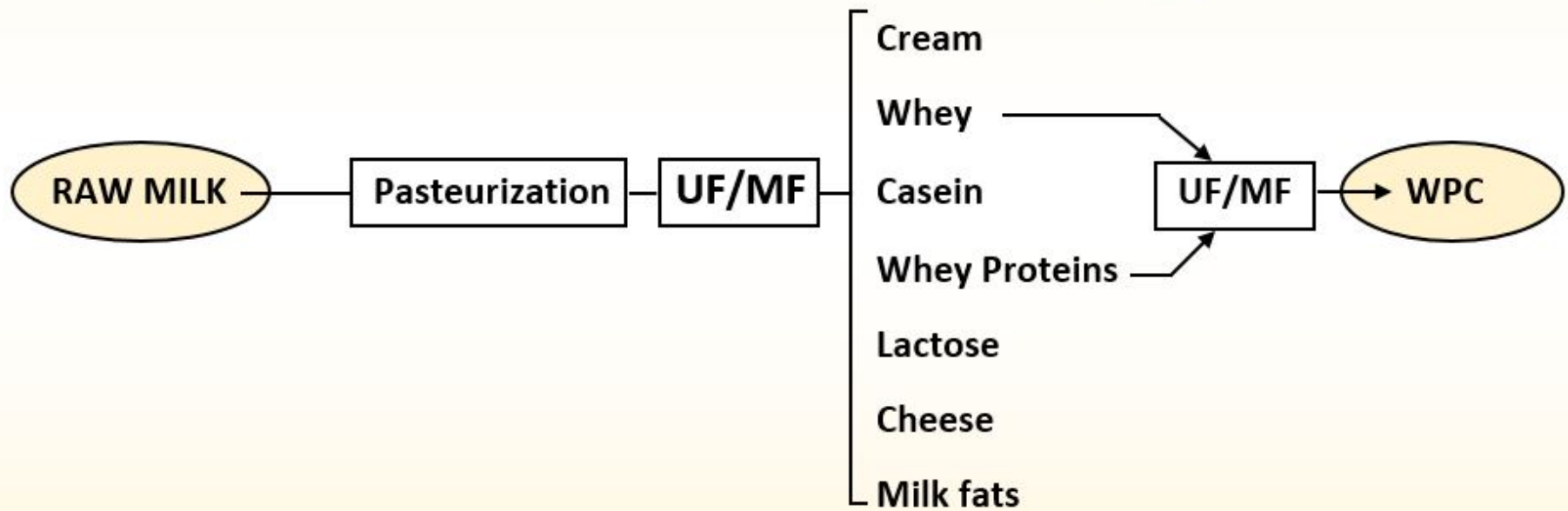
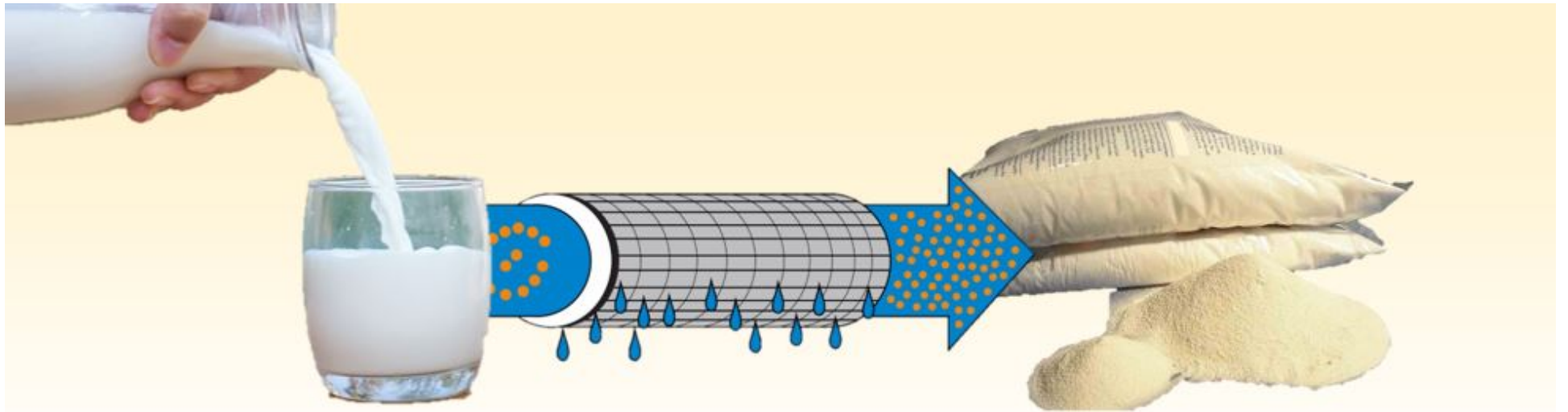
Kindly find attached the manuscript entitled “Membrane processes: Innovation and perspective in dairy industry” for consideration for possible publication in your esteemed journal. I would like to state that all the authors mutually agree that it should be submitted to ETI. We also acknowledge that it is the original work of the authors and that the manuscript was not previously submitted to another journal.

I look forward to hearing from you.
Thanking you in advance.

Sincerely Yours,

Research Highlight:

- Treatment of Milk Industry waste
- Recovery of value added component from Milk industry waste
- Membrane based separation of the treatment of milk waste
- Membrane based separation of undesirable product from milk.
- Membrane based Process intensification in milk industry.



1
2
3
4
5
6
7
8
9
10
11
12
13
14
15
16
17
18
19
20
21
22
23
24
25
26
27
28
29
30
31
32
33
34
35
36
37
38
39
40
41
42
43
44
45
46
47
48
49
50
51
52
53
54
55
56
57
58
59

Membrane processes: Innovation and perspective in dairy industry

Debolina Mukherjee¹, Gerardo Coppola¹, Maria Teresa Gaudio¹, Stefano Curcio¹, Vincenza Calabro¹, Sudip Chakraborty^{1*}

¹ University of Calabria, Laboratory of Transport Phenomena and Biotechnology, Department of DIMES, Cubo-42a, 87036 Rende (CS), Italy

Corresponding author: sudip.chakraborty@unical.it

Abstract:

As the dairy industry is renewed to be one of the most wide sectors of industry in terms of worldwide spread production and vastity of products and byproducts, a great attention to its technology development has been paid through out the decades, resulting in a constant improvement in technology for environmental remediation. A crucial focal point in dairy industry has always been the separation of milk components (fats, proteins) and its fractionation which has been carried out by a number of unit operations that have been replaced over time by membrane filtration, thus eliminating the side effects of more invasive proceedings like thermal operations, resulting in higher quality and more valuable products. Membrane filtration in dairy industries has developed to be used in the most dairy operations like: fractionation, bacteria removal, whey purification, proteins isolation and more. Main membrane applications in dairy industry are taken in account in this article as well as some instances of their development as patented plant unit processes.

Keywords: Membrane processes, Dairy industrial waste, byproduct recovery, Innovation, Industrial processes

Introduction:

Membrane separation technology is a well-established process not only in dairy industry but also other industrial processes. Applications of membrane in dairy processing include the isolation of whey as well as serum proteins, separation of fats from whole milk (skimming), removal of microbial cells from the milk and more applications, as shown in the following table 1 [Cheyran and Alvarez, 1995, Pouliot, 2008, Brans et al., 2004;].

60
61
62
63 **A. Alternatives to unit operations**

- Centrifugation: separation and fractionation of milk fat
- Cold pasteurization: removal of bacteria and spores
- Evaporation: concentration of casein micelles from skim milk
- Electrodialysis: demineralization of whey

70 **B. Fractionation of milk/ whey**

- Isolate individual serum proteins: α -lactalbumin, β -lactoglobulin, bovine serum albumin, immunoglobulins, lactoferrin, transferrin, and peptides

74 **C. Formulating new products**

- UF cheeses, MF cheeses
- Whey-based beverages

78 **D. Standardization of milk products**

80 **E. On-farm ultrafiltration of milk:** to reduce transportation and refrigeration costs

81
82
83 Table 1: Membrane applications in dairy processing industry [Modified from Cheyran and Alvarez, 1995; Pouliot, 2008; Brans et al., 2004]

84
85 **2.1 Microfiltration:**

86
87 Microfiltration is one of the first kinds of membrane technology ever used. As other kinds of membrane technologies, MF is a pressure driven separation process and it's applied on relatively big particle separations.

88
89 MF membranes are made of organic, mainly polymers, or inorganic materials as ceramics.

90
91 An example of widely used membrane casting material are PTFE (polytetrafluoroethylene) and PVDF (polyvinylidene fluoride). The latter are two hydrophobic membrane examples, hydrophilic materials are widely used based on the needs of the process. It has to be said that some hydrophobic materials can turn to hydrophilic by surface modification.

92
93 MF can be operated in two different ways: dead-end or cross-flow filtration. In dead-end filtration the driving force (pressure) is applied pushing the inlet flow towards the membrane in a perpendicular manner, while during the cross-flow separation the feed stream drifts in a tangential way on the membrane surface (figure 1). Dead-end leads to a more pronounced fouling and pore inaccessibility, so that is more feasible to be applied to diluted streams.

94
95
96
97
98
99
100
101
102
103
104
105
106
107
108
109
110
111
112
113
114
115
116
117
118

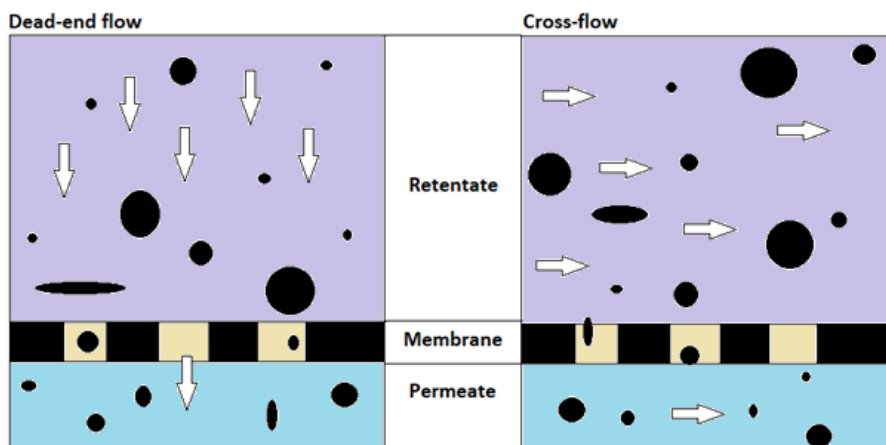


Figure 1: Dead-end filtration and cross flow filtration schemes.

The application of MF in food beverage, mainly operated in a cross-flow scheme, includes fluid sterilisation, clarification and water potabilization. In dairy business MF is common used for bacterial and spores removal from milk and in process water treatment. MF has the ability of prolonging milk shelf-life by microbial removal without altering its taste. In figure 2 the MF effect on skim milk components is reported: microfiltration leads to the removal of the microbial cells, but allows smaller components such as proteins, lactose, minerals and water to pass through the permeate producing a “bacterial free” skim milk.

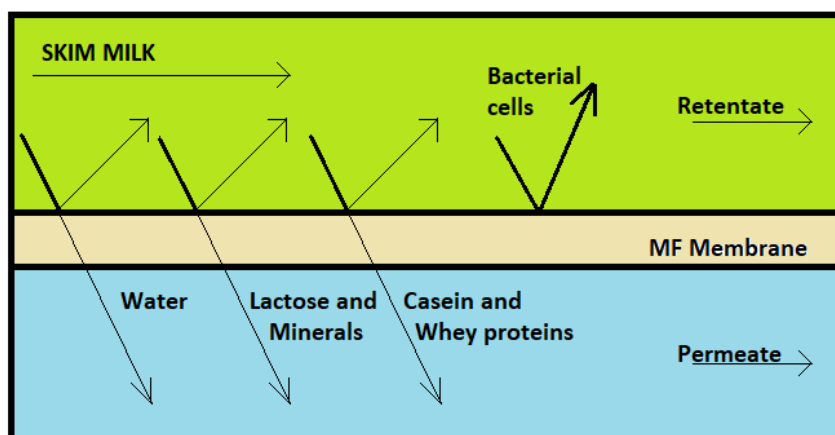


Figure 2: Effect of MF on skim milk components.

Bovine milk contains about 3.2% w/w proteins. These are casein proteins and whey proteins (around 18% w/w of total proteins). Whey proteins are commonly used in the food supplement industry and commercialized as concentrates (WPCs, whey proteins concentrates) or isolate (WPI, whey protein isolate).

MF can be applied to separate WPs without any chemical change in the product: casein proteins after MF are found in the retentate side while WPs which are permissible to pass over the membrane and drift in the permeate side to be recovered.

Whey/casein protein separation is possible due to the physical and chemical differences between the two. The following Table 2 [Saha K 2017; Nath A 2015; Fox and McSweeney, 2003] reports the concentration and the molecular weight of the major proteins in milk.

Proteins	Conc. (g/L)	Molecular weight, D
α 1-Casein	10.0	24 000
α 2-Casein	2.6	25 000
β -Casein	9.3	24 000
??-Casein	3.3	19 000
γ -Casein	0.8	12 000–20 000
β -Lactoglobulin	3.2	18 000*
α -Lactalbumin	1.2	14 000
BSA	0.4	66 000
Immunoglobulins	0.7	150 000–900 000
*Normally present as a dimer in milk solution with MW of 36 000.		

Table 2: Concentrations and MW of major proteins in milk [Fox and McSweeney, 2003].

2.2 Ultrafiltration mechanism:

Ultrafiltration (UF) is a pressure-driven process (usually 2 to 10 bars), it works by size-exclusion and is a process capable to concentrate macromolecules in the feed side of the solution such as proteins or lipids.

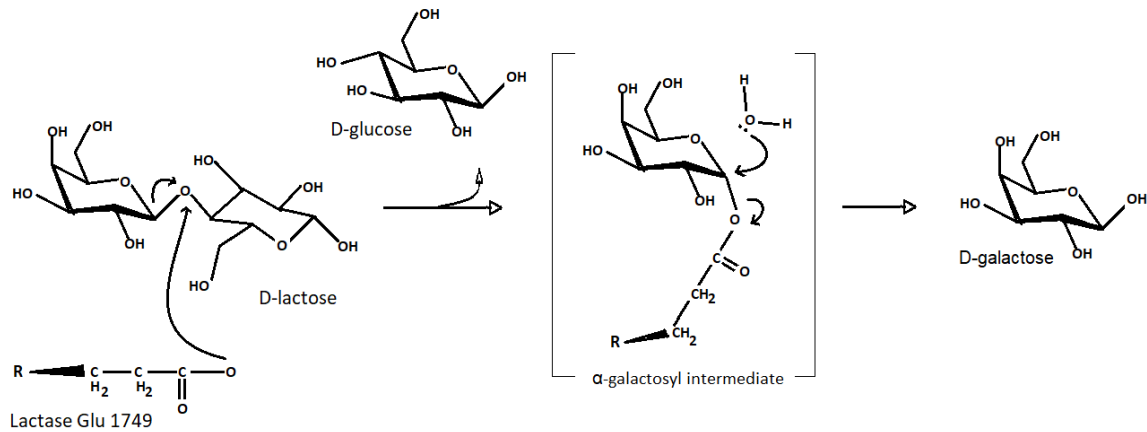
UF is consistently used for solutions clarification, concentration or fractionation.

UF membranes are typically casted starting from polymeric materials, like polysulfone or cellulose acetate, or inorganic materials like γ -alumina/ α -alumina or pyrolyzed carbons.

Cow's milk composition includes lactose as its main carbohydrate with a concentration of 4.5-5% while nearly 70% of world population is lactose intolerant [Hu and Dickson, 2015].

These two data well justify the interest of dairy industry in lactose-free milk.

Lactose can be separated by hydrolysis, in which lactase is used as enzyme to hydrolyze D-galactosyl molecules (Fig.3), by chromatographic separation [Harju, 1989] in which a column is packed with a cation exchange resin allowing separation while milk is pumped through the column.



253 Figure 3: Lactose enzymatic hydrolysis to D-galactose.

254
255 A third method is membrane separation: UF is a reasonably good method for lactose reduction in
256 milks. UF allows to retain fats and proteins in the retentate side while lactose, salts and other minerals
257 permeate through the membrane.

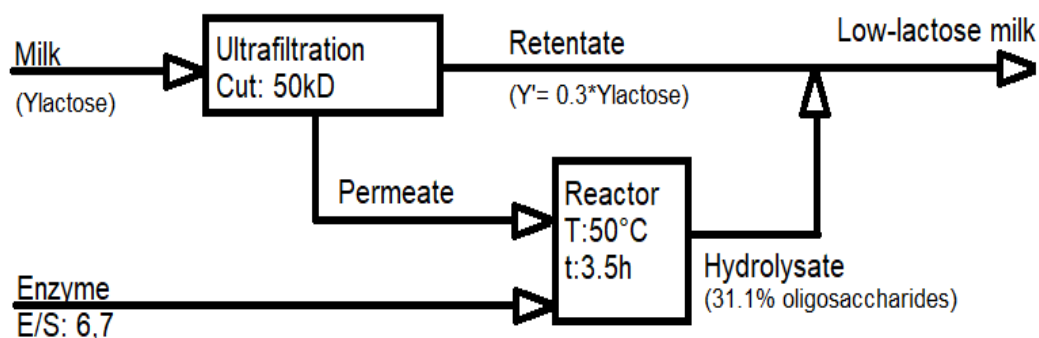
258
259 A comparison between two processes was made [Chen, Hsu, Chiang, 2002] by research to obtain
260 low-lactose milk: a catalyst driven and a membrane separation.

261
262 The first of the two methods included the use of *Aspergillus oryzae* β -galactosidase as a catalyst to
263 convert milk lactose into oligosaccharides, while for the second method a hollow fiber UF membrane
264 with a 50 kD molecular weight cut-off was used.

265
266 The whole process scheme and variables are reported in figure 4.

267
268 At first UF was applied to a skim milk feed where a 30% lactose has been retained. The resulting
269 permeate was treated with the first method where lactose was further converted into oligosaccharides.
270 Highest yield of 31% total oligosaccharides content has been obtained by the conversion of 25.5% of
271 lactose in the permeate with a ratio E/S (enzyme to substrate) of 6.8% at 50°C for more than 3 hours.
272 Whereas the hydrolysate stream is then mixed with UF retentate to get a final low or minimal lactose
273 milk.

274
275 This process is able to provide a really good low-lactose milk quality because milk proteins and milk
276 natural flavours were not in straight interaction with the enzyme.



290 Figure 4: Scheme of the low-lactose milk production proposed by Chen, Hsu and Chiang.

291 **Nanofiltration (NF) and Reverse osmosis (RO) in dairy sector:**

292
293
294
295

Nanofiltration and Reverse osmosis has vastly used in dairy industry not only to whey and permeates reduction but also to decrease the inorganic components— particularly sodium and potassium chlorides. Since both whey and permeates are essential to pass over a membrane prior to further processing, hence NF becomes a very important technology, as its cartels volume decrease with partial demineralization in the same step. Production of Lactose is based on whey. NF plays a significant role in modern lactose production processes. During production of demineralized or non-hygroscopic whey powder, NF can be useful as a cost-effective enhancement to electrodialysis and ion-exchange technologies.

On the other hand, reverse osmosis can be applied as a supplement to evaporation in dairy industry. Huge savings can be attained by Process intensification strategies. Reverse osmosis (RO) is a very effective way of eliminating water from the milk or whey before the evaporation step. By mounting a reverse osmosis plant in upstream process, the dimensions of the evaporator can be improved considerably. Reverse osmosis can be implemented to concentrate skimmed milk or whole milk in order to increase the total solids component. By this way industry is able to meet the demands – both economic and environmental in terms of waste and energy recovery.

3. Lactose-free milk production:

There are a number of patented processes for lactose-free milk production, here some of them are presented.

Lange [Callegari A 2018; Lange, 2005] along with The Agropur Cooperative, Canada, patented a process (figure 5) that is able to remove 99% of lactose from skim milk. Cow milk with an average lactose content of 4.8% was standardized and then thermally treated at 72.8°C for 16 seconds to eliminate the bacterial content. A temperature rise has also the effect of speed up the permeation in the UF processing step by reducing deposition on the membrane itself. After thermal treatment milk is pumped into a diafiltration system. The patent includes the use of a Romicon™ PM50 membrane (operating variables in table 3) as the core of the diafiltration step while adding water with same velocity as the permeate flux leaving the UF membrane.

Permeate flux	30 L/m ² h
Temperature	≥ 50°C
TMP	1.0 bar
Cross-flow velocity	≥ 7m/s

Table 3: Process conditions of Romicon™ PM0 membrane units in Lange process.

The permeate coming from the UF step is subjected to an enzymatic hydrolysis for lactose conversion and to a thermal treatment. After these steps homogenization is applied to disperse fat molecules thus preventing a phase split between the lipids and the aqueous phase.

355
 356
 357
 358
 359
 360
 361
 362
 363
 364
 365
 366
 367
 368
 369
 370
 371
 372
 373
 374
 375
 376
 377
 378
 379
 380
 381
 382
 383
 384
 385
 386
 387
 388
 389
 390
 391
 392
 393
 394
 395
 396
 397
 398
 399
 400
 401
 402
 403
 404
 405
 406
 407
 408
 409
 410
 411
 412
 413

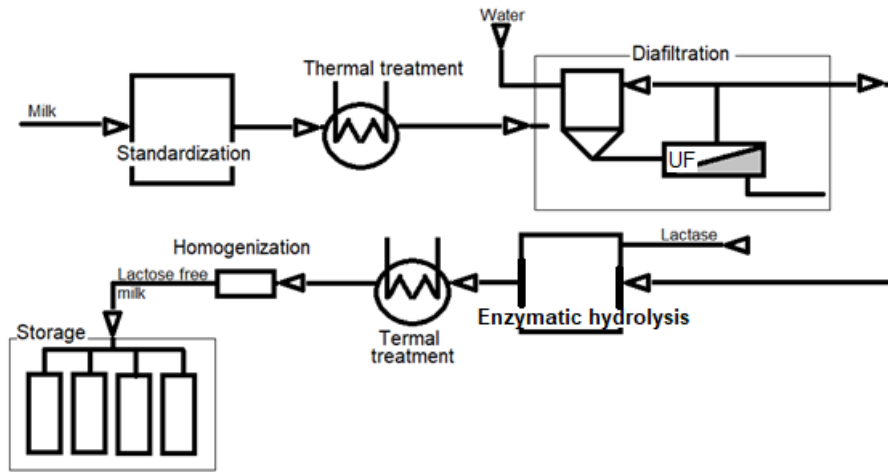


Figure 5: Scheme of the Lactose-free milk production plant patented by Lange.

A different approach has been presented and patented by Wang [Abdelkader, 2019 Wang, 2005]. This process is based upon a series of sequential membrane processings (figure 6). The UF operates by diafiltration (as better explained below) on membranes with a MWCO of 900 daltons under conditions listed in table 4. Large molecular weight components as fats and proteins are found in the UF retentate while water lactose and some of the minerals pass into the permeate side of the membrane.

Feed flow velocity	22 gpm
Temperature	10°C
TMP	45 psi

Table 4: Process conditions UF membrane units in Wang process.

The UF permeate is sent to a nanofiltration with a 150-300 daltons MWCO. NF operative variables are listed in table 5.

Feed flow velocity	4 gpm
Temperature	10°C
TMP	220 psi

Table 5: Process conditions NF membrane units in Wang process.

NF permeate results in a stream containing water and part of the minerals. This stream is used as diafiltration media in the previous UF step so it is pumped to the UF step retentate tank.

The whole process can reach a lactose content of 0.07% in the UF retentate stream so that the 99% of lactose is removed from the incoming skim milk and the protein content in the lactose-free product is higher than the unprocessed skim milk (nearly 30% more than the feedstock).

Final milk compositions are reported in the following table 6.

Total nitrogen proteins	4.44%
Lactose	0.07%
Fats	0.31%
Ca	136 mg/100g
Na	45 mg/100g
K	147 mg/100g
Mg	16 mg/100g
P	110 mg/100g

Table 6: Final milk composition in Wang process.

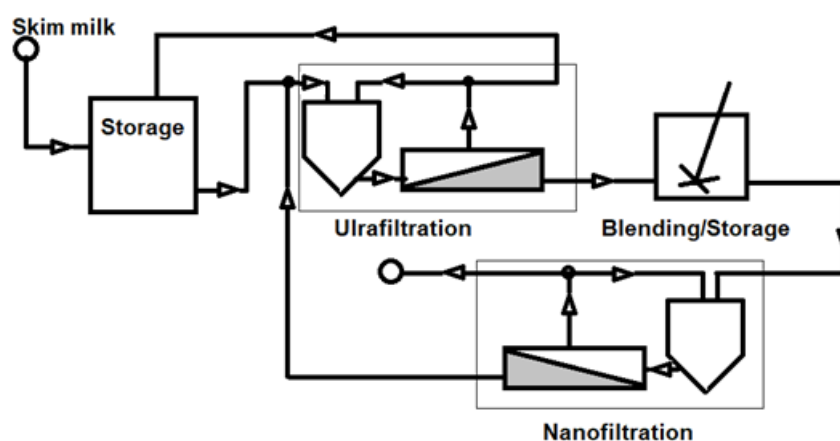


Figure 6: Scheme of the Lactose-free milk production plant patented by Wang.

In 2013 Tossavainen and Sahlstein patented a process (figure 7) for lactose-free milk production and milk concentration based upon UF, NF and RO (reverse osmosis). This kind of process allows the milk to retain its organoleptic characteristics. A standardized milk with a fixed protein and fat content is at first pasteurized at 72°C for 15 seconds, then UF is applied at 50°C using GR61PP membranes with a MWCO of 20kD. The resulting UF permeate, mainly containing water and minerals is sent to a NF step on a Nanomax-50NF membrane at room temperature. Nanofiltration is carried out until the retentate reaches the volume of $\frac{1}{4}$ in respect to the original feed. In this NF step lactose is retained in the retentate.

The NF permeate is then concentrated using a RO membrane until the retentate reaches $\frac{1}{10}$ of the volume of the previous NF permeate fed into the RO. In the reverse osmosis step minerals are concentrated in the retentate.

UF retentate is then mixed with RO retentate, water and β -D-galactosidase so that a hydrolysis reaction takes place at 10°C for 24h. The final milk has a lactose content of less than 0.01% so that the final composition results similar to a semi-skimmed milk as shown in table 7.

Proteins	3.35%
Lactose	<0.01%
Glucose/Galactose	3%
Fats	1.5%
Ash	0.79%
Dry matter	8.84%

Table 7: Final milk composition in Tossavainen and Sahlstein process.

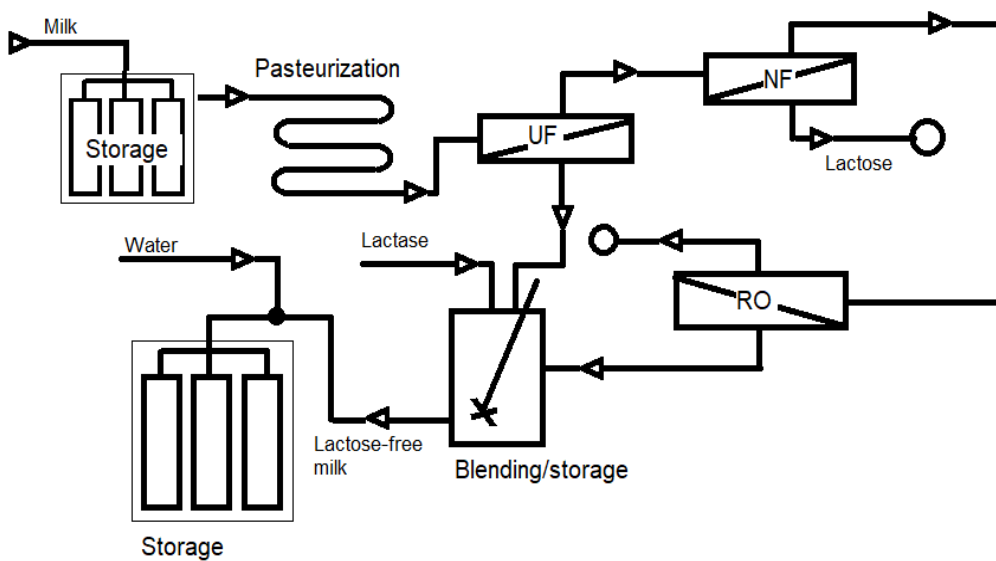


Figure 7: Scheme of the Lactose-free milk production plant patented by Tossavainen and Sahlstein.

4. Whey production:

Whey is a liquid formed in the cheese manufacturing processes, it contains proteins, lactose, vitamins, minerals and growth factors. Usually 8 to 9 litres of whey per kg of cheese products are formed.

Whey is richer in proteins and fat than milk. Its energy value corresponds to 27 kcal per 100 grams of product; it is composed by water about 93% of the total and other components are: sugars (5.14 grams), proteins (0.85 grams), fats (0.36 grams) and vitamins and mineral salts, such as sodium (54 grams), calcium, phosphorus and potassium.

Whey components as whey proteins and lactose can be recovered by membrane filtrations.

A patented process made by Cloldt and Lehman [Cloldt and Lehman, 2007] uses UF to separate whey proteins from a whey stream, then the UF permeate, which is rich in lactose, is sent to RO to help water evaporation and consequential lactose crystallization [Souza et al., 2010].

Souza et al. presented four processes for the recovery of purified lactose from whey. This processes include two consequential UF steps (diafiltration) for lactose separation and a RO step for its purification. In the fourth of the presented processes a microfiltration step is followed by UF, ion exchange and RO and it appears to produce the purest lactose.

Lactose fractionation is heavily conditioned by three main factors [Hu and Dickson, 2015].

As the operating pressure of the membrane steps increases the permeate flux increases. His until a critical TMP is reached, so that a further increase in pressure causes no more changes in permeate flux.

As operating temperature increase the permeate flux increases because of the diminution of milk viscosity but the operating temperature should anyway not exceed the denaturation temperature of milk proteins and the temperature range applicable on the specific membrane used.

In the following table 8, the thermal denaturation temperatures T_d of major whey proteins are shown:

Table 8: Thermal denaturation of whey protein

Whey Protein	T_d [°C]
α -lactalbumin	63
α -lactalbumin (Ca depleted)	41
β -lactoglobulin	78
Bovine Serum Albumin	63

An increase in feed flow velocity causes a decrease of the concentration polarization so that [Kessler,2002; Atra et al., 2005] the pressure independence mentioned before occurs at higher TMPs. In addition, a higher mass transfer trough the boundary layer is reported because of the lower hydraulic resistance of the fouling layer.

4.1 MBR applications:

In more recent periods the use of biocatalytic membrane reactors has been put under great attention and it can be used in lactose removal from milk or whey [Giorno and Drioli, 2000; Jochems et al., 2011].

Biocatalysts can be operated, as shown in figure 8, as a free suspension in a reacting solution in the retentate side of the membrane or immobilized inside the membrane matrix or on its surface.

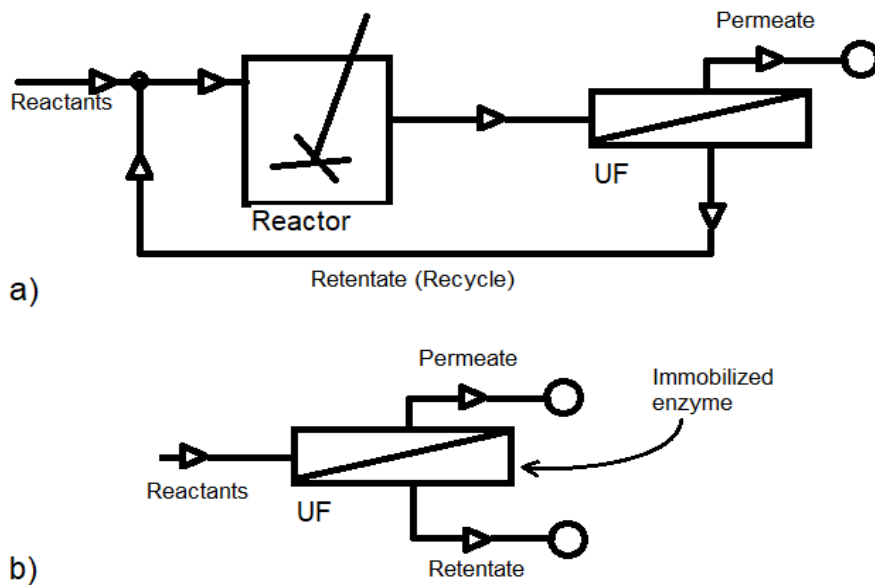


Figure 8: Schemes for MBR: a) Coupling of a reactor and a membrane unit; b) Integrated membrane bioreactor.

In the following table 8 are listed the advantages and the disadvantages of the integrated membrane bioreactor as mentioned in the works of Garcia et al. and Rias et al. [Garcia et al., 1999; Rios et al., 2004; Gésan-Guiziu, G. 2019

].

The configuration with a reactor and a membrane separation unit is preferred when the catalyst distribution is the main concern of the process, so that the membrane is used as a retention medium for large enzyme molecules like for the hydrolysis process on starch, pectin, k-casein and collagen [Wang 2020; Giorno and Drioli, 2000].

ADVANTAGES	DISADVANTAGES
Retention and reuse of biocatalysts	Heterogeneous of reaction conditions between the bulk solution and membrane surface
Minimize processing time	Decrease of enzyme activity as a function of time
Integrated process (simultaneous reaction and separation)	Concentration polarization and membrane fouling
Reduce substrate or product inhibition continuously	Difficulty in maintaining aseptic conditions (in the case of the cell membrane bioreactor)
Economical and high productivity	
Easy to control product properties by enzyme (specificity) and/or membrane (selectivity)	

650
651
652 Table 8: Advantages and disadvantages of the integrated membrane [Garcia et al., 1999; Rios et al.,
653 2004].
654

655 Integrated membrane bioreactors applications in dairy processes can be found in lactose hydrolysis:
656 the use of a MBR allows the simultaneous removal of monosaccharides and the hydrolysis of lactose
657 while the process can be operated in continuous and with low pressures and high enzyme
658 concentrations, but it has to be said that high enzyme concentrations can lead to microbial
659 contaminations which can consequentially cause a loss of enzyme activity. This issue can be avoided
660 by UV irradiation of the enzyme solution.
661

662
663 When using hollow fibers membranes in this process a loss of enzyme is encountered because of its
664 adsorption on the membrane surface. A method to avoid this loss is to cover the shell side of the
665 membrane with proteins obtained by UF of skim milk.
666

667
668 Another MBR application can be found in regards to the market of functional foods. Galacto-
669 oligosaccharides (GOS) are the main prebiotic used in the dairy industry. By prebiotic is intended a
670 nondigestible food component that, once ingested, has beneficial effects on health by helping the
671 growth of good bacteria in the digestive system of the body [Gibson and Roberfroid, 1995; Wen-
672 qiong 2019].
673

674
675 GOS can be found in many natural products as garlic, onions and honey and also are associated with
676 low sweetness, low caloric values and even low cariogenicity [Sako, Matsumoto and Tanaka, 1999;
677 Park and Ho, 2010] while maintaining high stability to high temperatures in low pH conditions.
678

679
680 A major issue in GOS production is the formation of monosaccharides that inhibit enzyme activity.
681 A study by Boon, Riet and Janssen [Zhu B 2018; Boon, Riet and Janssen, 2000] showed an
682 improvement of 23% in GOS yield with a continuous product removal on activated carbons.
683

684
685 Enzyme immobilization can help the separation of monosaccharides during the process, also allowing
686 the reusage of the enzyme and a higher temperature and pH stability [Bhattacharyya et al. 1996].
687

688 **5. Conclusions and Future developments:**

689
690 The application of membrane technologies in the dairy industry at present day is limited but still
691 improving. One technique that is worth mentioning and it's still under optimization studies is
692 membrane chromatography: a bio separation process which involves membranes as chromatographic
693 media; this technique advantage over column chromatography is the higher speed of separation. Other
694 field of studies that are active at present day can be found in membrane processes: the optimum
695 combination of membrane operations and enzymatic hydrolysis with the development of new
696 materials and techniques to minimize operational issues such as membrane fouling and poor enzyme
697 stability could enhance membrane applications in dairy processes and lead to better products in terms
698 of sensory and nutritional properties. All this research fields are leading to better techniques and more
699 reliable and sustainable processes while obtaining higher quality products so that they can be easily
700 seen as well promising fields of research.
701
702
703
704
705
706
707
708

709
710
711 **References**
712

713 Atra, R., Vatai, G., Bekassy-Molnar, E., et al. (2005) Investigation of ultra- and nanofiltration for
714 utilization of whey protein and lactose. *Journal of Food Engineering*, **67**, 325–332.
715

716 Abdelkader, S., Gross, F., Winter, D., Went, J., Koschikowski, J., Geissen, S.U., Bousselmi,
717 L.(2019); Application of direct contact membrane distillation for saline dairy effluent treatment:
718 performance and fouling analysis; 26 (19), 18979-18992.
719

720 Bhattacharyya, D., Ganapathi, S., Vishwanath, S., et al. (1996) Immobilized enzyme reactions on
721 beads and membranes, in *Biofunctional Membrane* (ed. D.A. Butterfield), Platinum Press, New
722 York, pp. 117–129.
723

724 Boon, M.A., Riet, K.V., and Janssen, A.E. (2000) Enzymatic synthesis of oligosaccharides: product
725 removal during a kinetically controlled reaction. *Biotechnology and Bioengineering*, **70**, 411–420.
726

727 Brans, G., Schroen, C.G.P.H., Sman, R.G.M., et al. (2004) Membrane fractionation of milk state of
728 the art and challenges. *Journal of Membrane Science*, **243**, 263–272. Pouliot, 2008.
729

730
731 Callegari, A., Cecconet, D., Molognoni, D., Capodaglio, A.G.(2018); Sustainable processing of
732 dairy wastewater: Long-term pilot application of a bio-electrochemical system; 189,563-569.
733

734
735 Chen, C.-S., Hsu, C.-K., and Chiang, B.-H. (2002) Optimization of the enzymatic process for
736 manufacturing low-lactose milk containing oligosaccharides. *Process Biochemistry*, **38**, 801–808.
737

738 Cheryan, M., and Alvarez, J.R. (1995) Food and beverage industry applications, in *Membrane*
739 *Separation Technology. Principles and Applications* (eds. R.D. Noble and S.A. Stern), Elsevier
740 Science, pp. 415–465. Rosenberg, 1995
741

742 Cloidt, R. and Lehmann, H. (2007) Process for the preparation of lactose from whey. EP patent
743 **1,869,984-A1**.
744

745 Fox, P.F. and McSweeney, P.L.H. (eds.) (2003) *Advanced Dairy Chemistry, Vol. 1, Proteins*, third
746 edition, Kluwer Academic/Plenum Publishers, New York.
747

748 Garcia, A.A., Bonen, M.R., Ramirez-Vick, J., et al. (1999) *Bioseparation Process Science*,
749 Blackwell Science, Massachusetts, p. 423.
750

751 Gibson, G.R. and Roberfroid, M.B. (1995) Dietary modulation of the human colonic microbiota:
752 introducing the concept of prebiotics. *Journal of Nutrition*, **125**, 1401–1412.
753

754
755 Giorno, L. and Drioli, E. (2000) Biocatalytic membrane reactors: applications and perspectives.
756 *Trends in Biotechnology*, **18**, 339–349.
757

758 Gésan-Guiziu, G., Sobańska, A.P., Omont, S., Froelich, D., Rabiller-Baudry, M., Thueux, F.,
759 Beudon, D., Tregret, L., Buson, C., Auffret, D. Life Cycle Assessment of a milk protein
760 fractionation process: Contribution of the production and the cleaning stages at unit process level
761 (2019) *Separation and Purification Technology*, 224,591-610.
762
763
764
765
766
767

- 768
769
770 Jochems, P., Satyawali, Y., Roy, S.V., et al. (2011) Characterization and optimization of β -
771 galactosidase immobilization process on a mixed-matrix membrane. *Enzyme and Microbial*
772 *Technology*, **49**, 580–588.
773
774 Harju, M. (1989) Process for the specific separation of lactose from milk. US patent 4,820,348.
775
776 Hu K. and Dickson J.M. (2015) Membrane processing for dairy ingredient separation. IFT Press –
777 Wiley Blackwell
778
779
780 Kessler, H.G. (2002) Food and Bioprocess Engineering, Dairy Technology, Verlag A. Kessler,
781 Munich, Germany, pp. 56–96.
782
783 Lange, M. (2005) Process for making a lactose-free milk and milk so processed. US Patent
784 6,881,428 B2.
785
786 Nath, A., Chakraborty, S., Bhattacharjee, C., Chowdhury, R.; (2015); Studies on the separation of
787 proteins and lactose from casein whey by cross-flow ultrafiltration; 54 (2), 481-501.
788
789 Nath, A., Mondal, S., Kanjilal, T., Chakraborty, S., Curcio, S., Bhattacharjee, C. (2015); Synthesis
790 and functionality of proteinacious nutraceuticals from casein whey-A clean and safe route of
791 valorization of dairy waste, 97, 192-207.
792
793
794 Pouliot, Y. (2008) Membrane processes in dairy technology – From a simple idea to worldwide
795 panacea. *International Dairy Journal*, **18**, 735–740.
796
797 Rios, G.M., Belleville, M.P., Paolucci, D., et al. (2004) Progress in enzymatic membrane reactors –
798 a review. *Journal of Membrane Science*, **242**, 189–196.
799
800 Rosenberg, M. (1995) Current and future applications for membrane processes in the dairy industry.
801 *Trends in Food Science and Technology*, **6**, 12–19.
802
803 Sako, T., Matsumoto, K., and Tanaka, R. (1999) Recent progress on research and applications of
804 non-digestible galacto-oligosaccharides. *International Dairy Journal*, **9**, 69–80.
805
806 Saha, K., R, U.M., Sikder, J., Chakraborty, S., da Silva, S.S., dos Santos, J.C. (2017); Membranes as
807 a tool to support biorefineries: Applications in enzymatic hydrolysis, fermentation and dehydration
808 for bioethanol production; 74, 873-890.
809
810 Souza, R.R., Bergamasco, R., Costa, S.C., et al. (2010) Recovery and purification of lactose from
811 whey.
812
813
814 Tossavainen, O. and Sahlstein, J. (2013) Lactose-free milk product and processes for producing the
815 same. US patent 8,449,938 B2.
816
817 Wang, J. (2005) Lactose-removed milk product and process for the preparation thereof. US patent
818 2005/0196508 A1.
819
820 Wen-qiong, W., Yun-chao, W., Xiao-feng, Z., Rui-xia, G., Mao-lin, L. Whey protein membrane
821 processing methods and membrane fouling mechanism analysis; (2019) 289, 468-481.
822
823
824
825
826

827
828
829
830
831
832
833
834
835
836
837
838
839
840
841
842
843
844
845
846
847
848
849
850
851
852
853
854
855
856
857
858
859
860
861
862
863
864
865
866
867
868
869
870
871
872
873
874
875
876
877
878
879
880
881
882
883
884
885

Wang, Q., Chen, G.Q., Kentish, S.E.:(2020) Isolation of lactoferrin and immunoglobulins from dairy whey by an electro dialysis with filtration membrane process;233, art. no. 115987, .

Zhu, B., Duke, M., Dumée, L.F., Merenda, A., des Ligneris, E., Kong, L., Hodgson, P.D., Gray, S.(2018); Short review on porous metal membranes—Fabrication, commercial products, and applications;8 (3), art. no. 83

Declaration of interests

The authors declare that they have no known competing financial interests or personal relationships that could have appeared to influence the work reported in this paper.

The authors declare the following financial interests/personal relationships which may be considered as potential competing interests: